The Role of WFDC1/ps20 in Prostate Cancer

Hickman, Oliver

Awarding institution:
King's College London

The Role of WFDC1/ps20 in Prostate Cancer

Oliver J. Hickman

Submitted for the degree of Doctor of Philosophy in the School of Medicine at King's College London

January 2015

King's College London
Guy's, King's and St Thomas' School of Medicine
MRC Centre for Transplantation
Guy's Hospital, 5th Floor Tower Wing
London SE1 9RT

Abstract

In prostate cancer (PCa), stromal tissues co-evolve through reciprocal interactions with the tumour to support tumour growth and suppress the immune response. WFDC1/ps20 is a secreted whey acid protein (WAP) four-disulphide core (WFDC) family member highly expressed within the prostate stroma. Ps20 expression has been frequently observed to be down-regulated or lost in cancers including in prostate cancer, and numerous lines of evidence suggest that ps20 has intrinsic growth suppressive function in numerous tumour model systems. However, ps20 remains biochemically uncharacterised and the mechanisms by which it functions are unknown.

WFDC1/ps20 is expressed in numerous mRNA and protein isoforms some of which result from proteolytic cleavage. These post-translational modifications affect the ability of the protein to inhibit the proliferation of PCa cells. We demonstrated that ps20 undergoes oligomerisation by transglutaminase, and crosslinking to fibronectin. We show that ps20 is cleaved by cathepsin L, which while failing to abrogate function of the protein, does liberate cross-linked ps20 from solid phase fibronectin. We show that ps20 binds to glycosaminoglycans (GAG) and interacts with cell surfaces in a GAG dependent manner.

To further investigate the cellular effects of ps20 we overexpressed ps20 in PCa cell lines. Transgenic overexpression of WFDC1/ps20 reduced proliferation in WPMY-1 cells, and conditioned media (CM) from these cells had potent pro-apoptotic effects on a range of PCa cell lines. Whole genome differential transcriptome analysis of WPMY-1-EV v WPMY-1-ps20FL/WPMY-1-ps20TR cells identified numerous factors, including IL-8, IL-32, COX2, and SerpinF1 to be upregulated in WPMY-1 cells. Addition of a COX2 inhibitor reversed the suppressive effect of WPMY-1-ps20 CM, suggesting that expression of ps20 in the prostate stroma can regulate growth of epithelial and other tissues through the prostaglandin synthase pathway.

Lastly, using ps20 overexpression in WPMY-1 prostate stromal cells, we demonstrated that CM from ps20 expressing cells inhibits proliferation of CD4 and CD8 T cells. Using depletion of ps20 from CM we show that suppression is indirectly mediated. We show that ps20 expression in WPMY-1 cell CM inhibits both anti-CD3/28 and IL-7/15 dependent T cell. However no effect on the secretion of IFNγ or expression of common T cell activation markers is observed. We demonstrate that the suppression of T cell proliferation is partly due to enhanced COX-2 activity.

Acknowledgements

I'd like to thank my supervisors for putting up with me and my unorthodox approach to time-keeping for four years. I'm grateful to you all for providing me with a thoroughly stimulating, if sometimes frustrating, PhD project - I think it turned out ok in the end. For your excellent supervision and mentoring throughout, Anna, Christine, Richard and Prokar, I thank you sincerely.

Thank you to the members of my thesis committee for feedback and support, especially Stuart Neil who made it clear at the outset that it was his job to 'get me a PhD', and hasn't let me down. Anne Ridley I'd like to thank for the extra discussions and for the invaluable feedback throughout the final stages of the project.

I'd like to thank Christina and Dorota from the protein therapeutics lab, not least for making sure my orders always made it as far as the freezer, and generally for just being excellent lab mates who didn't berate me too much for leaving the place a mess again or never learning where anything was kept. As for the AV lab contingent, past and present, I couldn't have done it without you.

Thanks to my wonderful Mother and Father who since I was about as small as I've ever been have provided love and support despite me making all sorts of frankly baffling choices.

Lastly - and by any metric worth counting - most importantly, I'd like to thank the ladies and gents of DIIID who are kind, and wonderful company, and who made it all worth the long hours and headaches. You've made my time here basically the best five years of my life. Anyone who's ever joined me at the Miller gets a shout out, but especially members of the pentagon and any mermaids, honorary or actual, still floating around the place (Sangmi Kim, James Reading, Terry Bryan, Tom Hayday, Max Handley, Vicky Martin and Das Martin), cheers!

As for all the rest that came and went - I've got more friends for life than would generally be considered convenient for a person to have. So thanks for that.

Contents

List of Figures

List of Tables.

Abbreviations

AA	-	Amino acids
APC	-	Antigen presenting cell
AR	-	Androgen receptor
BSA	-	Bovine Serum Albumen
CD	-	Cluster of differentiation
CFSE	-	Carboxyfluorescein succinimidyl ester
CM	-	Conditioned media
COX	-	Cyclooxygenase
CRPC	-	Castration resistant prostate cancer
CTL	-	Cytotoxic T lymphocyte
CTLA-4	-	Cytotoxic T-lymphocyte-associated protein 4
DAMPs	-	Damage associated molecular patterns
DC	-	Dendritic cell
DMEM	-	Dulbecco's modified eagle medium
DMSO	-	Dimethyl sulfoxide
ECM	-	Extracellular matrix
EDTA	-	Ethylenediaminetetraacetic acid
eGFP	-	Enhanced green fluorescent protein
ELISA	-	Enzyme linked immunosorbant assay
EMT	-	Epithelial-to-mesenchymal transition
ERG	-	ETS-related gene
ETS	-	E26 transformation specific
EV	-	Empty Vector
FACS	-	Fluorescence activated cell sorting
FAP-	-	Fibroblast activation protein
FCS	-	Fetal Calf Serum
FL	-	Full length
FOXP3	-	Forkhead box P3
HRP	-	Horseradish peroxidase
ICAM	-	Intercellular Adhesion Molecule
IDO	-	Indoleamine 2,3-dioxydase
lFNγ	-	Interferon-gamma
IG	-	Immunoglobulin
IL	-	Interleukin
KO	-	Knockout

L-PGDS	-	Lipocalin-type prostaglandin D synthase
LIF	-	Leukaemia inhibitory factor
LPS	-	Lipopolysaccharide
МΦ	-	Macrophage
MDSC	-	Myeloid derived suppressor cells
MHC	-	Major histocompatibility complex
MMP	-	Matrix-metalloproteinase
mTOR	-	Mechanistic target of Rapamycin
NFиB	-	Nuclear factor kappa-light-chain-enhancer of activated B cells
NK	-	Natural killer
p53	-	Tumour protein p53
PAMPS	-	Pathogen associated molecular pathogens
PBMC	-	peripheral blood mononuclear cells
PBS	-	Phosphate buffered saline
PCa	-	Prostate Cancer
PCR	-	Polymerase chain reaction
PE	-	Phycoerythrin
PE-Cy7	-	Phycoerythrin conjugated with cyanine 7
PerCP	-	Peridin-chorophyll-protein complex
PGE_2	-	Prostaglandin E_2
PGD_2	-	Prostaglandin D_2
PGH_2	-	Prostaglandin H_2
PGH_2	-	Prostaglandin H_2
PGJ_2	-	Prostaglandin J_2
PIN	-	prostate intraepithelial neoplasia
pRB	-	Retinoblastoma Protein
PRR	-	Pattern recognition receptor
Ps20	-	prostate stromal 20
PTEN	-	Phosphatase and tensin homolog
PTGS2	-	Prostaglandin-endoperoxide synthase 2
qPCR	-	Quantitative-PCR
RAG	-	Recombination activating gene
RORγ	-	RAR-related orphan receptor gamma
RPMI	-	Roswell Park Memorial Institute medium
RT	-	Room temperature
RT-PCR	-	Reverse Transcription-PCR
SDS-PAGE	-	Sodium dodecyl sulphate polyacrylimide gel electrophoresis

SLPI	-	Secretory leukocyte protease inhibitor
SV40	-	Simian vacuolating virus 40
TAA	-	Tumour associated antigen
T bet	-	T-box transcription factor TBX21
TCR	-	T cell receptor
TG	-	Transglutaminase
TGFβ	-	Transforming growth factor-β
T_H1	-	T Helper 1 cell
T_H2	-	T helper 2 cell
T_H17	-	T helper 17 cell
TIL	-	Tumour infiltrating lymphocytes
TNFα	-	Tumour necrosis factor-α
TR	-	Truncated
TRAIL	-	TNF-related apoptosis-inducing ligand
TRAMP	-	Transgenic adenocarcinoma of the mouse prostate
Treg	-	T regulatory cell
WAP	-	whey acidic protein
WB	-	Western Blot
WFDC	-	WAP-four disulphide core
WHO	-	World health organisation
x-gal	-	β-galactosidase

Chapter 1. Introduction

Humans have had knowledge of cancer since at least the ancient Egyptians, with the first known references being to an untreatable tumour of the breast found in the Edwin Smith Papyrus, dated between 3000-2500BC. Later, the 4th century BC Greek physician Hippocrates coined the term carcinoma, referring to the finger like projections that tumours manifest, resembling a crab. Our modern English word for the disease stems from Celsus, a Roman physician who used the Latin word for crab; cancer (Hajdu, 2011).

In high-income countries cancer is the second leading cause of death after cardiovascular disease, and represents a significant economic and health burden. Cancer is primarily a disease caused by dysregulation of cellular growth, leading to uncontrolled proliferation of cells, invasion into surrounding tissues, and the dispersal of secondary tumour metastases to sites around the body, which is ultimately fatal. The transformation of cells from healthy to neoplastic involves the accumulation of genetic lesions and mutations in genes which regulate and suppress growth, or which control cellular survival. These can arise from spontaneous mutations, germ line inheritance/viral-transmission of oncogenes, or from exposure to DNA-toxic carcinogens and radiation. Studies reveal that people carrying specific germ line mutations will not all develop the tumours they are predisposed toward. Similarly people exposed to comparable quantities of radiation, or mutagenic toxins will not all develop cancer, demonstrating that ultimately there are several checkpoints which a cell must overcome before it can proceed to unrestrained, or transformed growth. The immune system also plays a significant role in preventing the outgrowth of neoplasms by surveillance of tissues and eradicating transformed cells.

1.1 Ps20, SLPI, and elafin – WFDC family proteins with important roles in cancer.

Whey-acidic protein (WAP) family members prostate stromal 20 (ps20), secretory leukocyte protease inhibitor (SLPI), elafin and are small secreted factors containing highly conserved WAP-four-disulphide-core (WFDC) domains. The main physiological role of this protein family seems to be as mucosal anti-microbials and serine-protease inhibitors, which assist in wound healing, suppression of tissue damage following injury, and as regulators of innate immunity (Clauss et al., 2005). However, it is being increasingly recognised that these factors have important roles in cancer and there is now abundant data linking ps20, SLPI, and elafin, to numerous human cancers in both protective and deleterious roles. It is becoming clear that the pleiotropic nature of these factors, including their anti-inflammatory, growth regulatory and more recently immunoregulatory functions may have overlapping or conflicting roles in the development and progression of tumours.

1.1.1 Evolution of WFDC family proteins.

The WFDC domain, with its characteristic 8 cysteine residues forming 4 disulphide bonds, has been highly conserved from mammals down to cnidarians and urochordates (Smith, 2011). There are 18 WFDC domain containing proteins in man (fig. 1.1), most of which have not been characterized beyond the gene level (Bingle and Vyakarnam, 2008). Due predominantly to studies of the function and expression of SLPI and elafin, WFDC domain containing proteins have become associated with the homeostatic regulation of inflammation (Sallenave et al., 1994) through a well-characterized serine protease inhibitor function (Sallenave, 2010). However both SLPI and elafin possess well characterised anti-microbial functions, including anti-bacterial, anti-viral and anti-fungal activity (Williams et al., 2006). Both SLPI and elafin therefore are proposed to protect tissues from protease induced damage,

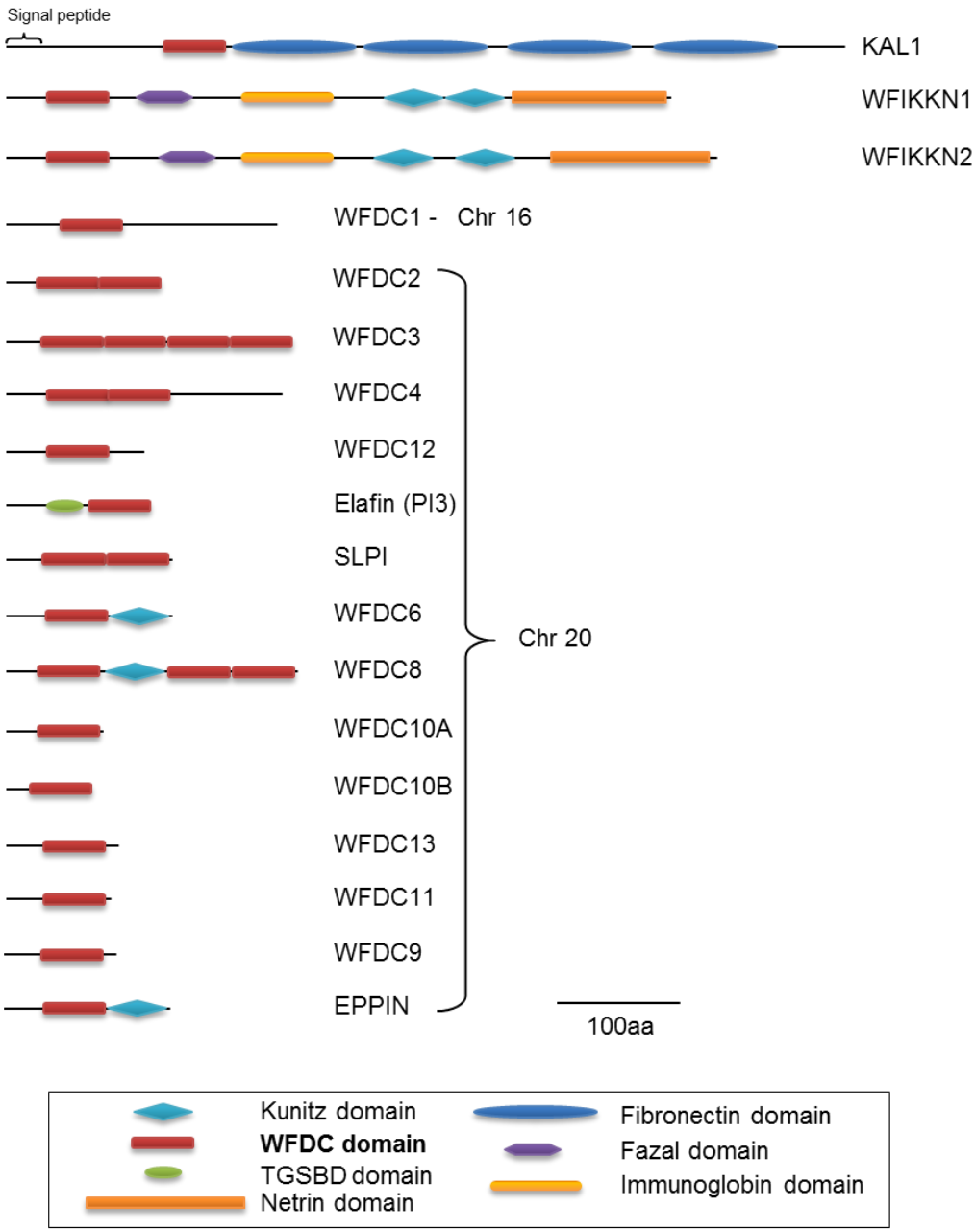

Fig1.1 Schematic representation of WFDC domain containing proteins in man. The human genome contains 18 proteins containing the WFDC domain. 14 are on chromosome 20. WFDC1 is the only member on chromosome 16. All proteins contain a signal peptide for secretion. The position of the characterised domains is shown respective to each proteins primary structure. Figure adapted from (Bingle and Vyakarnam, 2008).

especially by neutrophil elastases, and have demonstrated specificity for inhibition of diverse proteases including neutrophil elastase, cathepsin-G and proteinase-3 amongst other factors produced during the inflammatory response (Wilkinson et al., 2011, Moreau et al., 2008). Ps20 was first characterised by its ability to inhibit growth of PC-3 prostate cancer cells and to date has no characterized protease inhibitory function (Rowley et al., 1995). Various studies have suggested pleiotropic functions, including regulation of ICAM-1 (Alvarez et al., 2011), induction of senescence (Madar et al., 2009), and induction of angiogenesis (McAlhany et al., 2003), though the predominant physiological function is still a subject of investigation (Larsen et al., 1998).

Of the 18 WFDC proteins in man, 14 are encoded on a single region on chromosome 20, while the others are distributed throughout the genome. It has been noted that the genetic locus at chromosome 20 where the majority of human WFDC containing proteins are encoded is undergoing rapid divergence between humans and chimpanzees, a hallmark of proteins with innate immune functions (Hurle et al., 2007, Emes et al., 2003). Conversely, however, the ps20 aa sequence shows a remarkable level of conservation, with certain protein regions such as exon 3 being 100% conserved between human, chimpanzees chickens, all the way down to fish (fig 1.2A). This lack of evolutionary divergence suggests that ps20 may possess a unique functional history, distinct from other WFDC family members which appear to be evolving rapidly (Bingle and Vyakarnam, 2008). Notably, WFDC1 is encoded on the 16q23 locus, which was shown to be frequently under-expressed or down-regulated in prostate cancer relative to healthy controls, indicating a role as a potential tumour suppressor gene (Watson et al., 2004a).

With the regards to the function of the WFDC domain itself, only the WFDC domain of elafin, and the second the two WFDC domains in SLPI have reported protease

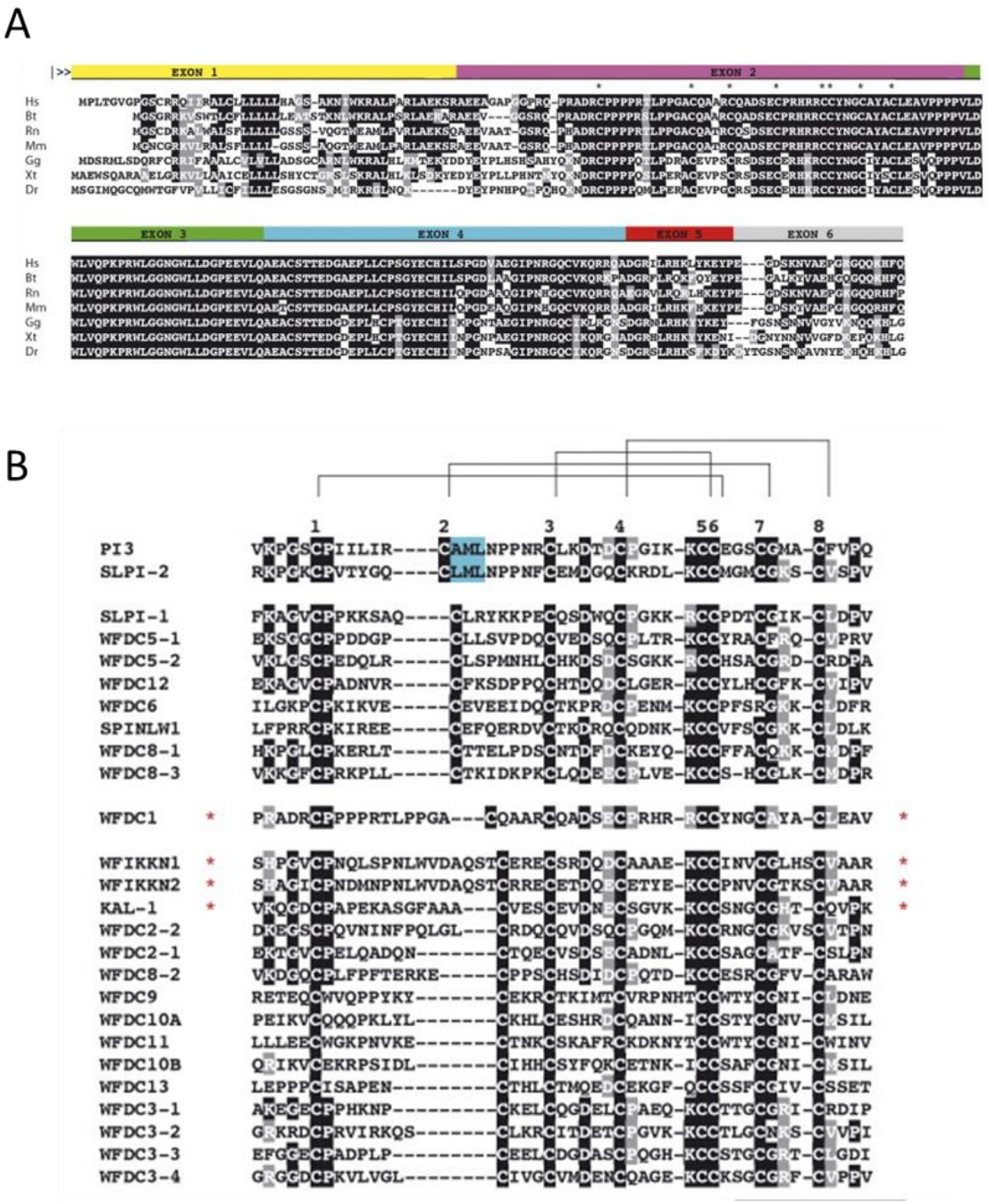

Figure 1.2 Amino acid sequence of ps20 and the WFDC domains of WFDC family proteins. A, The aligned AA sequence of ps20 in 6 species. Identical residues are presented as white on black, and conserved residues as white on grey. The 8 conserved cysteines of the WFDC domain are indicated by asterisks. B, A comparison of the AA sequences of the WFDC domain in all 18 human family members. The domain in SLPI and elafin blue) contains a three AA sequence which confers anti-proteinase activity. Figure taken from (Bingle and Vyakarnam, 2008).

inhibitory function, and this has been attributed to a three AA sequence between the second and third cysteine residue of the WFDC region (Fig. 1.2B) (Bingle and Vyakarnam, 2008). As such despite a relatively high level of conservation in the spacing of the cysteines of WFDC domains throughout the family, it is unlikely that other WFDC proteins possess this anti-protease function.

1.1.2 Expression of WFDC proteins.

The first study looking at WFDC1 expression was performed on rat tissues, as ps20 was originally purified as a growth inhibitory factor from rat urogenital sinus mesenchymal cells. This study also showed high expression of ps20 in the heart, with detectable but low expression in testis and prostate. However, immunohistochemical analysis of rat prostate tissue, revealed strong staining in smooth muscle in the stroma and vasculature (Larsen et al., 1998). This was the first suggestion that ps20 is a stromally expressed protein. In a later study reporting cloning of the human WFDC1 gene, expression was shown in lung, cervix, prostate and uterus, with the highest being in the lung and prostate (Larsen et al., 1998). Subsequent reports including immunohistochemical analysis have also suggested that stromal smooth muscle is a key site of ps20 expression (McAlhany et al., 2003), and global BioPGS data largely support previous sites of WFDC1 expression, with the highest being in the prostate, placenta, lung, gut, retina and brain (fig. 1.3).

More recently, one key function of WFDC1 has been uncovered by a study identifying the gene mutation causing multiple ocular defects (MOD) in cattle to the WFDC1 locus. This condition comprises several developmental abnormalities in the eyes of Japanese cattle, revealing a significant role for WFDC1 in the development of these tissues (Abbasi et al., 2009). In the same report by Abbassi *et al* situ hybridization revealed significant expression of WFDC1 mRNA in the ocular tissues of cattle and

mice, and this was confirmed in mouse eyes using immunohistochemical analysis of ps20 expression. Ps20 was also present at the embryonic stages of development, suggesting a role during development of these tissues in animals other than cattle (Abbasi et al., 2009). Interestingly, SLPI is also highly expressed in the retina (fig 1.3) and has recently been reported to be a regulator of neuron repair following upregulation in response to cAMP signalling. Furthermore, exogenous SLPI was shown to enhance axonal regeneration (Hannila et al., 2013). Taken alongside the report citing WFDC1 mutations as the cause of MOD, it seems reasonable to conclude that expression of WFDC family proteins in nervous tissues may play an important role in either development, and/or neuronal repair mechanisms, in keeping with a broader role in wound repair, which has been previously characterised for both WFDC1 and SLPI (Ressler et al., 2014, Zhu et al., 2002).

Another report demonstrated high levels of WFDC1 expression in the hind quarters of developing murine embryos, supporting a broader role for WFDC1 in development (Jukkola et al., 2006). However, WFDC1 null mice have been produced on the C57BL/6 background, and utilized in two reports to date (Ressler et al., 2014, Rogers et al., 2012). Authors of both studies report that the mice breed successfully and appear healthy, suggesting that WFDC1/ps20 is not a vital component of successful development, at least in mice. Curiously, in light of the reports of WFDC1 expression being crucial for successful bovine eye development, the mice do not appear to have reported abnormalities in the development of their eyes, or in their vision (Ressler et al., 2014). Our lab have recently taken receipt of WFDC1 null mice, kept in standard animal house conditions rather than the sterile environs utilised in previous reports. Early indications show that the WFDC1 null mice are not doing well in this non-sterile

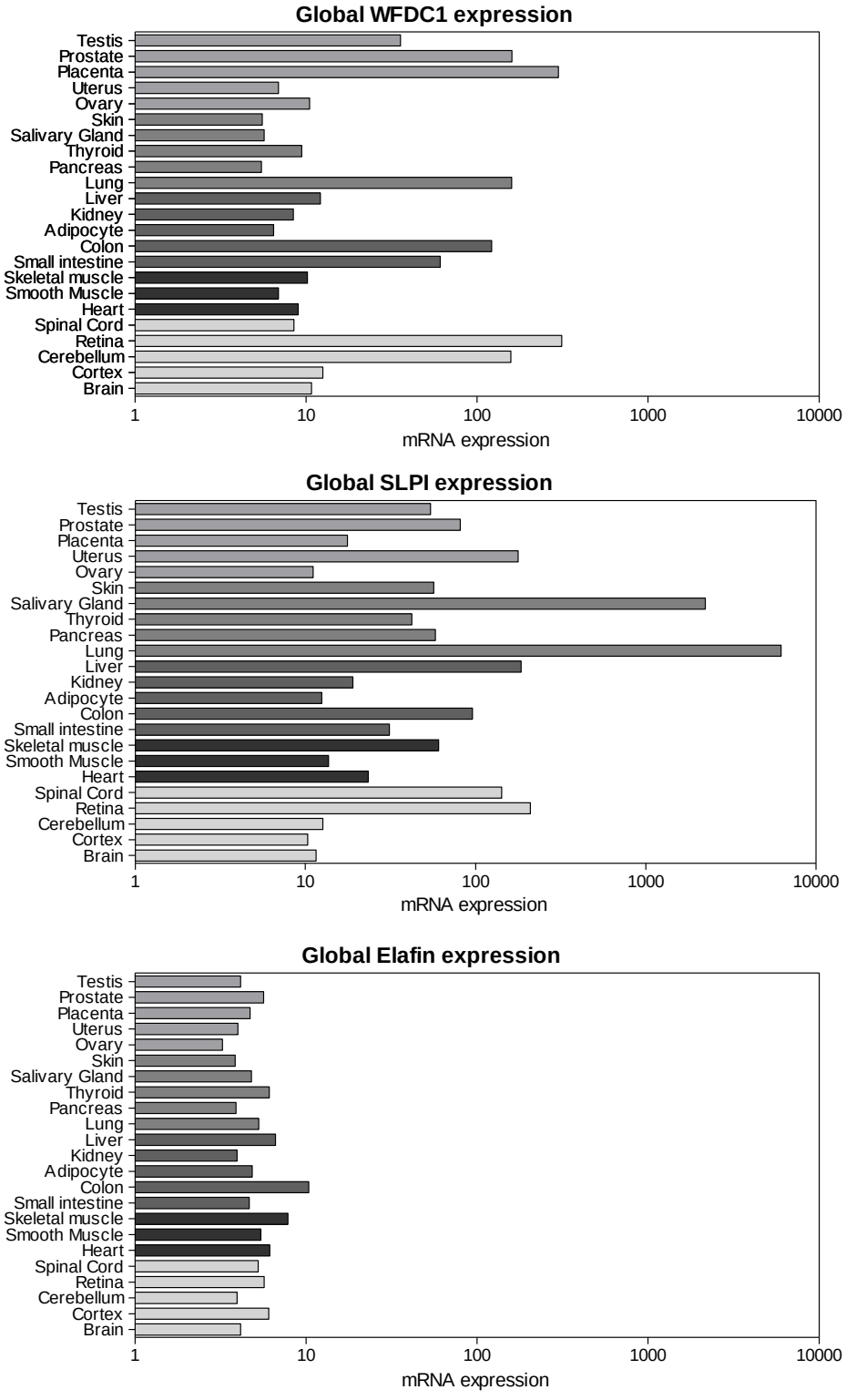

Figure 1.3 BioGPS expression pattern of WFDC1, SLPI, and elafin in human tissues.
Data representing 79 samples taken from (Su et al., 2002).

environment, have broad lack of wellbeing, and are not breeding (Vyakarnam. A, unpublished observation). Given the reported roles of SLPI, elafin and more recently WFDC1/ps20 in regulation of immunity, it is tempting to speculate that the lack of wellbeing in WFDC1 null mice is due to a higher propensity to infection in the non-sterile conditions, however, there is currently no data to support this.

Another notable site of WFDC1 expression is in CD4 T cells. Using qPCR to assess the level of WFDC1 expression, CD4 T cells were shown to express both the full-length WFDC1 mRNA transcript and a novel species in which a region of exon 2 is absent (Alvarez et al., 2008). This report, published previously by the author's laboratory, showed that the level of ps20 expression positively correlated with the ability of CD4 T cells to become infected with HIV and that this was linked to increased ICAM-1 expression. A subsequent report demonstrated conclusively that WFDC1 expression regulates the adhesion characteristics of T cells, increasing the number of cell-to-cell conjugates formed and thereby the levels of HIV intercellular transmission (Alvarez et al., 2011). While these reports show no direct functional consequence of WFDC1 expression in CD4 T cells beyond the ICAM-1 dependent increase in permissiveness to HIV infection, unpublished data has shown that anti-CD3/28 stimulation induced lower levels of IFNγ and IL-2 expression and reduced proliferation in WFDC1 expressing CD4 T cells relative to WFDC1 low/neg cells (Vyakarnam *et al* unpublished data), suggesting that WFDC1/ps20 may have effects on activation of CD4 T cells.

Unlike WFDC1/ps20, the key sites of SLPI and elafin, appear to be epithelial rather than stromal, with significant protein secretion observed in inflammatory cells and mucosal surfaces, especially in the respiratory tract (Schalkwijk et al., 1999, Bingle et al., 2006, Sallenave et al., 1994). Elafin exhibits notably low baseline expression by measurement of global mRNA expression (fig.1.3), though studies have found

detectable elafin protein in cervico-vaginal lavage (Iqbal et al., 2009), and in bronchial lavage samples in health people (Tremblay et al., 1996, Sallenave and Silva, 1993) indicating a detectable level of constitutive expression in specific tissues. However, it is established that like SLPI, elafin is highly inducible and expression is increased in response to inflammatory stimulus. Epithelial cells have been shown to secrete elafin following stimulation with IL-1β and TNFα *in vitro* (Sallenave et al., 1994). The target of elafin's protease inhibitory activity, neutrophil elastase, was shown to induce expression of elafin mRNA, suggesting a feedback mechanism to regulate tissue damage by this inflammation associated protease (Williams et al., 2006). Notably, it was observed that bronchial alveolar cells in culture secreted negligible amounts of elafin until stimulation with inflammatory factors, which lend agreement to the low baseline expression levels presented here (fig 1.3). The inducible nature of elafin expression supports a role in the control of inflammation and infection in direct response to inflammation related stimuli, while the lack of constitutive expression implies that the molecule serves little homeostatic or regulatory role in normal conditions.

This is in stark contrast to WFDC1 and SLPI which have highly levels of baseline expression in several tissues (fig 1.3). Moreover, there is a notable degree of overlap between the tissues which express both molecules; lung, colon, retina, testis and prostate are notable venues of WFDC1 expression which also express higher than average levels of SLPI. Notably, lung and colon are mucosal surfaces and the testis and prostate are secretory organs, which is in line with the proposed role of SLPI as a guardian against inflammation (Williams et al., 2006). However, with a far less clearly defined role for ps20, it is unknown what the function of ps20 is in these tissues. Unlike elafin and SLPI, work in our lab and others has to date not found any protease inhibitory function nor any anti-microbial activity for ps20 (Fish and Vyakarnam, unpublished data).

Despite having high baseline expression in many tissues (fig 1.3) SLPI, like elafin has been shown to be induced in response to epidermal growth factor (EGF), neutrophil elastase, and α-defensins (Sallenave et al., 1994). However, SLPI induction in macrophages is more nuanced. SLPI is expressed in response to LPS stimulation, but not TNFα or IL-1β. Interestingly, it is induced with slow kinetics in response to IL-6 and IL-10, suggesting it may in certain contexts be a component of an induced immunoregulatory response (Jin et al., 1998). However, it has been observed that SLPI expression can be inhibited in bronchial epithelial cells following TGFβ stimulation, again indicating that SLPI may have context and tissue specific immunoregulatory functions (Fleming et al., 2003).

Unlike SLPI and elafin, there is no evidence to date that WFDC1 is induced, nor that ps20 is expressed in tissues in response to inflammation or inflammatory cytokines. It has been observed that WFDC1 was upregulated in placentas from women suffering pre-eclampsia, a hypertensive condition whose aetiology is little understood but during which global inflammation is enhanced (Rajakumar et al., 2011). In the named study no functional insights were drawn from this observation. However, in line with expression traits of SLPI and elafin, it is interesting to speculate that WFDC1/ps20 may be induced under certain inflammatory contexts, though to date the only observed induction of WFDC1 was shown in response to TGFβ stimulation in the PS-1 prostate stromal cell line, where northern blotting showed significantly increased mRNA signal following 50pM TGFβ stimulation (McAlhany et al., 2003).

1.1.3 Biochemistry of ps20 and WFDC family proteins SLPI and elafin

No studies to date have explored the biochemical characteristics of ps20. Indeed, beyond resolving ps20 on a western blot, no further *in vitro* elucidation of its

biochemical properties has been undertaken. However, numerous biochemical properties of other WAP family proteins are well elucidated, and these may provide an insight into characteristics common to the WFDC protein family.

Ps20, SLPI, and elafin all contain a signal peptide and are secreted into the extracellular milieu, where SLPI and elafin have been shown to interact with transglutaminase (TG) and become cross-linked to extracellular matrix factors (Baranger et al., 2011, Guyot et al., 2005b). In addition to this there are a number of well characterized processing events involved in the functional regulation of WFDC proteins. The elafin precursor pre-elafin (also called Trappin-2) is secreted as an ≈11kDa protein with an N-terminal cementoin domain containing a repeated transglutaminase motif (this motif is absent in SLPI and ps20). Pre-elafin is then cleaved to release a functional 6kDa elafin C-terminal region. The physiological protease responsible for this cleavage is unknown, but *in vitro* cathepsin L, cathepsin K, trypsin, tryptase and plasmin are able to cleave between Lys38 – Ala39 (Guyot et al., 2005a). SLPI is secreted as a 12kDa protein and has similarly been shown to be a substrate for cleavage by cathepsins, specifically L, B and S, yielding a 7.5kDa N-terminal and a 4.5kDa C-terminal fragment (Taggart et al., 2001). Interestingly, pre-elafin and cleaved-elafin have comparable serine protease inhibitory function, while the serine-protease inhibitory function of SLPI is inactivated by cathepsin cleavage which takes place within the active site of the C-terminal WFDC domain (Taggart et al., 2001). In contrast to SLPI and elafin, ps20 has no known serine-protease substrate and no protease capable of cleaving it has yet been identified. However, it is clear that there are multiple ps20 species present in ps20 CM (Alvarez et al., 2008, Larsen et al., 1998) and the ps20 species demonstrated to inhibit cellular proliferation of PC-3 cells resolved at a molecular weight well below the predicted 24kDa of the full length protein, which would suggest a cleavage of the full-length, or pre-protein, may be taking place (Rowley et al., 1995). Given the pluripotent functions of these

three molecules, it may be the case that the cleavage of these proteins is an important regulatory step; activating/abrogating the activity of their protease inhibitory functions and/or their other non-protease inhibitory functions in a cell and context specific manner, and allowing these proteins to function with a high degree of specificity in reaction to dynamic events such as immune activation, wound healing, angiogenesis, and tumourigenesis. Likewise, given that WFDC proteins can become cross-linked to ECM components such as Fibronectin (Guyot et al., 2005b, Baranger et al., 2011), it may also be the case that proteolytic cleavage of regions of the peptide chain may serve to liberate WFDC proteins, or WFDC protein fragments from the ECM, creating soluble mediators. In this respect, cathepsins have been shown to have an important role in cancer invasion and metastasis and are frequently upregulated in cancer (Turk et al., 2012). Cathepsins B and L specifically are responsible for ECM degradation and remodelling in the tumour microenvironment, leading to increased invasion by a number of tumour cell types (Turk et al., 2012).

It is likely therefore that the biochemical regulation of WFDC protein functions is complex and tissue specific and involves a number of post-secretion processing events involving cleavage by various proteases and interactions with extracellular matrix components such as transglutaminase and fibronectin. As both SLPI and elafin are subjects of extensive translational research, it seems germane that a full understanding of how post-secretion processing of WFDC family proteins impacts the diverse functionalities of these molecules be an aim of WFDC focused studies.

1.2 Prostate Cancer

More than 1.1 million cases of prostate cancer were recorded in 2012, accounting for around 8 per cent of all new cancer cases and 15 per cent in men (Ferlay et al., 2015). Despite this, it remains the second leading cause of death in men. The vast majority of prostate tumours arise from epithelial tissues, resulting in adenocarcinomas. The accepted paradigm is that prostate carcinoma usually arises from lesions termed prostate intraepithelial neoplasia (PIN). This condition is characterised by many features reminiscent of early stage cancer, including loss of cellular polarity, nuclear atypia, and focal dysplasia, resulting in displaced cells lining the acinar and luminal spaces (Epstein, 2009).

1.2.1 Anatomy of the prostate

The prostate is a gland located at the base of the bladder, surrounding the urethra, with the average being slightly larger than a walnut, weighing between 11 and 16 grams. The human prostate has been divided anatomically into different zones (fig. 1.4A) which have discreet embryologic origins and manifest different histologies and biological functions (Lee et al., 2011). Most prostate cancers have been shown to arise in the peripheral zone, with some in the transitional zone, and almost none from the central zone (Lee et al., 2011, De Marzo et al., 2007). The prostate is a gland composed mainly of two tissue types; i) Epithelial tissue containing secretory glandular cells, non-secretory basal cells -- which are thought to be stem cells --, and neuroendocrine cells; and ii) the stromal compartment, which includes diverse cell

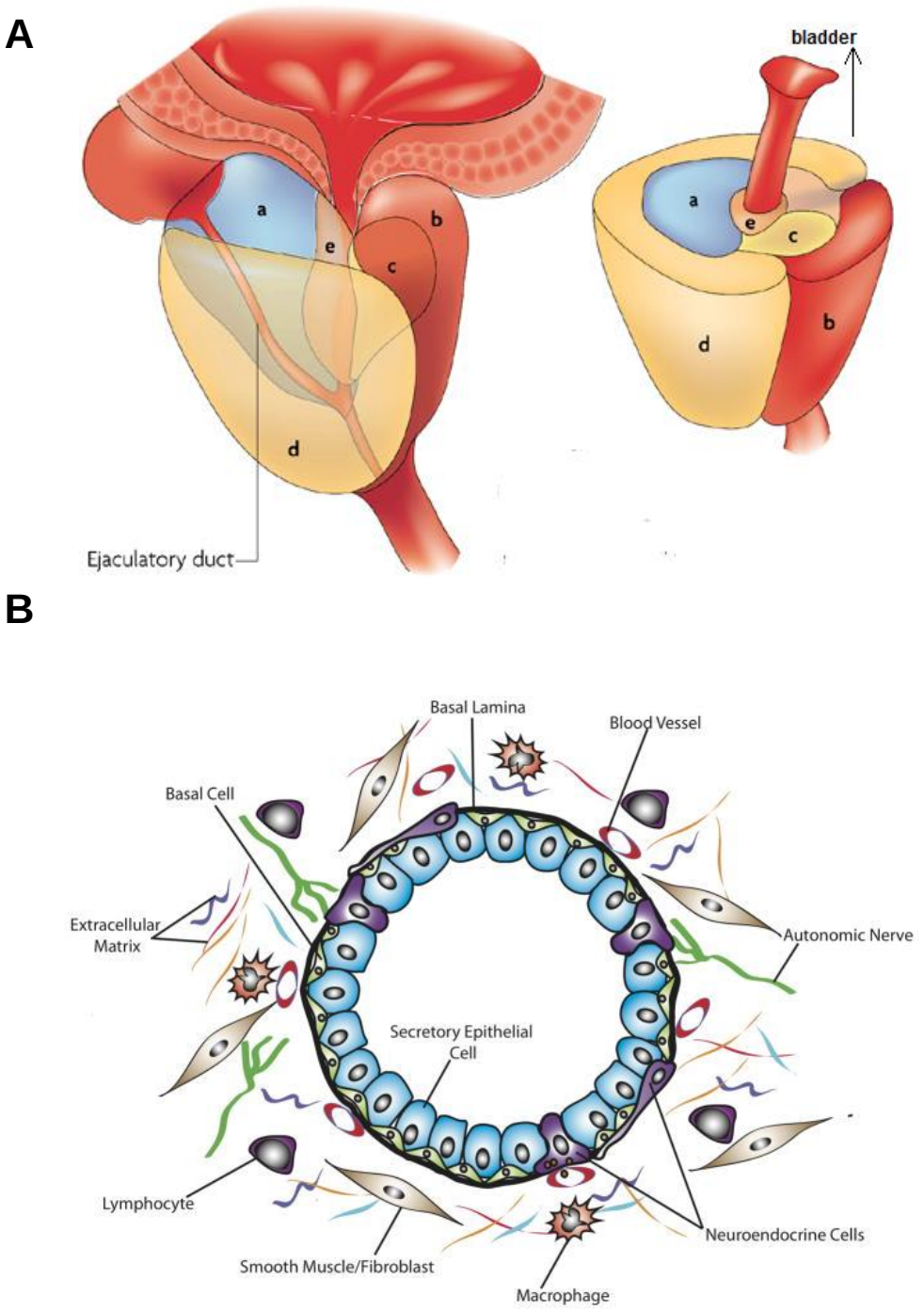

Figure 1.4 Anatomy of the prostate. A) Schematic illustration of the prostate showing the zones of the prostate. a) Central zone, b) Fibromuscular zone, c) Transitional Zone, d) Peripheral Zone, and e) Periurethral gland region. Adapted from (De Marzo et al., 2007). B) Outlines the cell types present in the human prostate gland, adapted from (Barron and Rowley, 2012).

types including fibroblasts, myofibroblasts, lymphocytes, smooth muscle cells, neuro-muscular cells and a complex network of extracellular-matrix (fig. 1.4B). The cellular origins of prostate adenocarcinomas have long been thought to be luminal, i.e. secretory glandular epithelial cells. This is largely due to immunohistochemical diagnostic tests, wherein loss of basal epithelial tissue is a prognostic indicator of invasive cancer (Hameed and Humphrey, 2005). Despite this however, recent experiments - in which individual basal and luminal cell populations were isolated from human prostectomy samples by expression of different keratins and cell-type specific surface markers - have shown that only cells of basal origin were able to form tumours following grafting onto mice alongside stromal tissue. Luminal tissue, despite being subjected to oncogenic transformations, showed no tumour formation, and biopsies were indiscernible to those from mice grafted with stromal tissue alone (Goldstein et al., 2010).

1.2.2 Molecular biology of prostate cancer.

Since the sixties, it has been understood that prostate cancer growth is dependent on steroid hormones termed androgens, such as testosterone, and its major metabolite dihydrotestosterone. This is evident by the regression of prostate tumours in animals deprived of androgen (Heinlein and Chang, 2002a). Androgens signal through the androgen receptor, a large intracellular hormone-activated transcription factor. Androgen receptor signalling regulates the growth and development of the prostate and maintains prostate homeostasis (Heinlein and Chang, 2002b). Both stromal and epithelial compartments rely on androgen signalling; stromal tissues respond to androgen signalling to modulate epithelial growth, survival and differentiation in a paracrine manner (Cunha et al., 2004), while epithelial tissues respond to androgen signalling to regulate production of secreted proteins (Yu et al., 2009). It is now accepted that prostate tumours commonly result from outgrowth of

PIN legions, and are frequently characterised by disruption of a number of key signalling pathways. Studies have shown that 40% of primary prostate tumours, and 70% of metastatic cases have genomic aberrations in the PI3K/Akt pathway. A significant proportion of these feature the loss or mutation of phosphatase and tensin homologue (PTEN), a tumour suppressor protein which limits AKT activation (El Sheikh et al., 2008, Reid et al., 2010). Indeed, homozygous PTEN deletion is sufficient to induce progressive, metastasising tumours in mice (Wang et al., 2003). Another genetic abnormality associated with large numbers of prostate cancers are chromosomal translocations between coding regions of ETS (E26 transformation specific) family transcription factors (typically ERG, and less commonly ETV1), and the promoter of the androgen responsive gene TMPRSS2 (Tomlins et al., 2005). Indeed, two recent studies have proposed that this genetic lesion is sufficient to induce PIN in otherwise healthy prostate epithelia, and can contribute to progression of neoplasias to invasive cancers (Carver et al., 2009, Tomlins et al., 2007). A number of studies have indicated that this gene rearrangement may be induced as a direct result of AR signalling (Lin et al., 2009). As well as ETS recombinations and PTEN mutations, more generic oncogenic alterations are also found in prostate cancer. For example, c-MYC overexpression is frequently observed (Taylor et al., 2010), and as with most cancer types p53 and pRb are frequently mutated or absent, though these are more common in metastatic cancer than in local disease (Taylor et al., 2010), corroborating the commonly held assumption that increasing genetic instability facilitates the progression and metastasis of tumours.

Local prostate cancer is usually treated using radical prostectomy, or with radiation treatment. However, given the reliance of prostate tissue on AR signalling for growth, initial treatment of metastatic or recurrent disease, or where recurrence is predicted, patients are treated with androgen depravation therapy, which usually restrains growth of the cancer. However, in most cases PCa will progress to androgen

independence, a condition called castration resistant prostate cancer (CRPC), whereby tumours, through a variety of biological mechanisms still being elucidated, acquire the ability to grow unrestrained by the availability of androgen (Shafi et al., 2013). Androgen independence can emerge through a number of known mechanisms. Androgen receptor mutations have been found in 20 to 50% of CRPCs (Gottlieb et al., 2004) and are reported broaden the ligand binding specificity of AR to non-androgynous ligands leading to more frequent AR activation (Shafi et al., 2013). Another cause of androgen independence is amplification of the *AR* gene, leading to overexpression of the AR. This has been observed in up to 80% of CRPC cases (Liu et al., 2008b), and is rarely seen in non-castration resistant cases (Bubendorf et al., 1999). Alternatively, many studies have cited alternative splicing of the *AR* gene as the catalyst event for CRPC. While the relevance in clinical cases is controversial and difficult to study given the lack of available antibodies, it has been established that alternatively spliced forms of AR are extant which lack the ligand binding domain, and are thus constitutively active and growth inducing (Hu et al., 2009). In addition to obtaining androgen independence, as tumours progress and become increasingly genetically unstable, multiple signalling pathways become dysregulated, leading to synergy between different pathways responding to androgens, growth factors and cytokines, adding extra levels of complexity to the causes of both tumour growth the and processes leading to androgen independence.

1.2.3 Stromal-epithelial interactions: the Reactive Stroma in PCa.

Cell-intrinsic changes in biochemistry are fundamentally important in the emergence of neoplastic cells, but it is now generally accepted that the reciprocal interactions between neoplastic epithelia and the surrounding stroma are critical in supporting growth and progression of emerging neoplasms. The stromal compartment within the

prostate surrounds the secretory epithelium and is separated from the luminal and basal epithelial layer by a robust matrix named the basal lamina (fig 1.4B). In health, the stromal response to androgen signalling is the expression of paracrine factors which regulate the growth, survival of the epithelium, as well as maintaining tissue differentiation (Lai et al., 2012). The stroma itself is a plastic tissue whose components vary temporally and spatially in response to micro-environmental cues. For example, stroma will respond to insult and injury with the appropriate wound healing response; or to the presence of microorganisms in the lumen of the prostate, with the appropriate inflammatory response. This coordinated mobilisation of stromal components, including the genotypic and phenotypic changes that accompany it, have been termed the reactive stroma (Tuxhorn et al., 2001). There is now a well-established etiological link between chronic prostatic inflammation and the development of PCa (De Marzo et al., 2007), and the accepted paradigm is that the changes in the stroma which accompany the onset and development/resolution of inflammation are important in supporting prostate carcinogenesis. Indeed, it is thought that any response by the stroma to a damaged or disrupted epithelium, be it to chronic inflammation, wounding, benign prostatic hyperplasia, or the early stages of neoplastic growth, can induce a reactive stromal phenotype (Barron and Rowley, 2012).

Perhaps the main constituent of tissue stroma, including in the prostate, and a critical mediator of a reactive stromal phenotype are fibroblasts. These cells exhibit a phenotypic diversity depending on their micro-environmental stimuli, and are characterized by the expression of numerous factors, described in fig. 1.5. It is

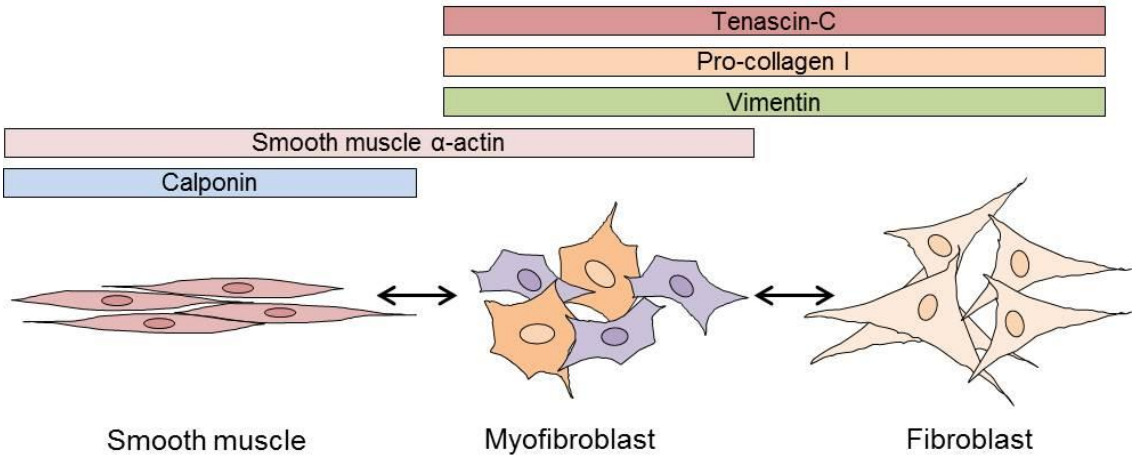

Figure 1.5 Stromal cell phenotypes are characterized by their expression of a series of stromally associated factors. Smooth muscle cells are defined by expression of Calponin and Smooth muscle actin. Fibroblasts express vimentin, Pro-collagen I and Tenascin-C. Myofibroblasts are considered to be plastic representing an intermediate phenotype with an expression prolife which includes factors specific to both smooth muscle and fibroblasts (Barron and Rowley, 2012).

well documented that fibroblasts are phenotypically different when associated with prostate tumours than in healthy tissue. These cancer associated fibroblasts (CAF) or myofibroblasts show expression of both smooth muscle α-actin fibroblast associated factors, suggesting a shift toward a myofibroblast type phenotype (Tuxhorn et al., 2002). It's commonly understood that myofibroblasts represent an activated fibroblast cell type; increasingly synthetic, contractile, with increased deposition of ECM, and have been shown to secrete growth factors which induce a microenvironment favourable to the survival of other cell types (Powell et al., 1999). The particular characteristics of myofibroblasts lend themselves to a wound healing environment where they can encourage tissue regeneration, and use their contractile properties and ECM deposition to suture the wound. However their dysregulation in the context of tumours, leads to enhanced tumour growth and the induction of a pro-angiogenic microenvironment (Powell et al., 1999).

Experimentally it has been shown that tumours can actively change the surrounding stroma to support their own survival and growth. Using a mouse model of prostate cancer it was shown that the tumours can impose a p53 dependent growth suppression on the surrounding stroma. This results in a selection pressure from which emerges a p53 null stromal compartment, which manifests high proliferative potential and supports the growth of the surrounding stroma (Hill et al., 2005). A more recent study has suggested a role for p62 in the reprogramming of fibroblastic stroma to support tumour growth. p62 was found to be reduced in the reactive stroma of numerous tumour types, including prostate tumours, and a p62 KO mouse had increased tumour volumes relative to controls. It subsequently emerged that the loss of p62 from the murine prostate stroma induces metabolic reprograming, altered mTOR signalling, and an increase in IL-6 which induces PIN, and leads to the induction of carcinogenesis. p62 was shown to be reduced in stromal tissues of human tumours of the breast and prostate and this was shown to be linked to altered mTOR signalling (Valencia et al., 2014).

Other studies have focused on the soluble mediators of CAF/myofibroblast biology, amongst the most important of which is transforming growth factor-β (TGFβ). The TGFβ family members have been shown to regulate a wide range of biological functions of relevance to prostate homeostasis, including i) the chemotaxis of immune cells into the organ, ii) regulation of the deposition of ECM, and iii) maintenance of tissue integrity by regulating the expression of matrix-metalloproteases and their respective inhibitors (Stover et al., 2007). TGFβ family members signal through type I and II trans membrane serine kinases (TGFβ receptors I-III), and signal transduction is followed by activation the SMAD family transcription factors, resulting in activation and repression of series of target genes (Massague, 2008). While the role of TGFβ family members is likely highly complex,

the commonly accepted function of stromally derived TGFβ is anti-proliferative and pro-apoptotic with respect to prostate epithelia (Siegel and Massague, 2003). During early stage prostate cancer, evidence suggests that TGFβ signalling through SMAD4 transcription factor restrains tumour growth and prevents progression and metastasis. Indeed, in PTEN *null* mice, which develop poorly progressive tumours, deletion of SMAD4 was sufficient to induce lethal metastatic cancer in 100% of the mice (Ding et al., 2011). It was subsequently shown that the expression of transcription factor NR2F2, a member of the nuclear receptor superfamily, was sufficient to overcome the SMAD4 dependent barrier in PTEN KO induced tumour growth. NR2F2 is highly overexpressed in human and mouse prostate tumours, further supporting the evidence that TGFβ signalling is fundamental in restraining the progression and development of PCa (Qin et al., 2013). However there are numerous lines of evidence that TGFβ can also lead to PCa progression through SMAD4 independent signalling pathways. Transformed PCa cells respond to TGFβ signalling by increased entry to the cell cycle and induction of epithelial-to-mesenchymal transition (EMT), a process where cells loose epithelial polarity and appropriate a mesenchymal morphology. This suggests that once the SMAD4 barrier has been overcome, TGFβ may signal through different pathways to mediate pro-tumourigenic functions (Ao et al., 2006).

1.2.4 Role of ps20 in cancer

Unlike elafin and SLPI the primary physiological function of ps20 has yet to be definitively elucidated. However, work published to date has implicated ps20 in range of processes including wound healing (Bouchard et al., 2006), ocular development (Abbasi et al., 2009), pre-eclampsia (Rajakumar et al., 2011), tumour suppression (Gratias et al., 2007), cellular senescence (Madar et al., 2009) and an increase in susceptibility of CD4 T cells to HIV through regulation of adhesion molecule ICAM-1

(Alvarez et al., 2011, Alvarez et al., 2008). However, the biochemical complexities of ps20 and the lack of known binding partners continue to significantly hamper efforts understand this protein's physiological significance in health and disease.

ps20 was originally purified as a 20kDa factor from the culture media of rat urogenital sinus cells and was shown to potently inhibit proliferation of the PC-3 Prostate cancer cell line (Rowley et al., 1995). Later, the same group cloned the WFDC1 gene (Larsen et al., 1998) and located it to chromosome 16q24, a region which is subject to frequent mutation and loss in various cancers (Larsen et al., 2000) (Harkonen et al., 2005). This protein is strikingly well conserved which suggests an important physiological role, but what this is exactly remains elusive. Further investigation into the biology of ps20 in prostate cancer demonstrated two important but contradictory phenomena. In a mouse xenograft model of prostate cancer, tumours formed from PC-3 cells engineered to overexpress rat-ps20 showed significant increase in size, dry weight, and micro-vascular density compared to control tumours (McAlhany et al., 2003). Immunohistochemical analysis of this data showed significantly increased neo-vascularization in the ps20 tumour, suggesting a role in angiogenesis. Other experiments corroborated this, demonstrating that ps20 acts as a chemo-attractant, though not a growth factor, for endothelial cells and that ps20 expression was induced in prostate stromal cells by TGFβ (McAlhany et al., 2003), a known angiogenic factor. This evidence suggests that despite being associated with a region of the chromosome often absent or mutated in tumours, that ps20 may also exert pro-tumourigenic characteristics under certain physiological conditions.

In contrast, a subsequent study by the same group looked at ps20 expression in cancerous-prostate stromal and epithelial tissues from clinical samples using immunohistochemical analysis (McAlhany et al., 2004). Interestingly, a strong association was observed between increased gleason score and decreased stromal

expression of ps20, suggesting that tissue specific loss of expression was beneficial to tumour growth. Accompanying this however, was a highly localized increase in ps20 staining in the epithelial compartment, and this staining significantly correlated with reduced recurrence-free survival of patients with PCa (McAlhany et al., 2004). It is likely therefore that ps20 has both pro-tumourigenic and tumour-suppressive roles that are cell and tissue specific, which may be exhibited at different temporal and spatial points.

A number of other studies have looked at ps20 expression in cancers and it has been shown to be down regulated in a number of tumour types (table 1.1) including bladder, brain, lung (Madar et al., 2009), melanoma (Liu et al., 2009), and prostate cancer (Madar et al., 2009, Watson et al., 2004b). However, no difference of expression was seen in either retinoblastoma or hepatic cancer (table 1.1) (Saffroy et al., 2002, Gratias et al., 2007) suggesting that its proposed tumour suppressive functions are restricted to specific tissues. In another study latexin was over expressed in gastric cancer cells and shown to induce ps20 expression. Subsequently, the growth of the gastric tumour cells was inhibited, which is consistent with data in other cancers and cell types (Li et al., 2011). However, in contrast to studies focusing on SLPI and elafin, no evidence of ps20 over expression in cancer has been observed, suggesting that it has predominantly anti-tumourigenic functions incompatible with the growth of tumours.

One study observed that the WFDC1 locus was frequently subject to methylation in melanoma (Liu et al., 2009). To investigate the function of ps20 in melanoma, the group then overexpressed ps20 in melanoma cell lines, and observed reduced xenograft tumour growth *in vivo.* Interestingly, ps20 expressing cells were not growth inhibited *in vitro* suggesting the anti-tumourigenic properties were not related to cellular proliferation *per se*. It was observed that secreted factor Dickkopf1 was

upregulated in ps20 expressing cells, indicating that ps20's growth inhibitory functions may be associated with indirect inhibition of the Wnt signalling pathway, which is important for growth in many tumour types (Katoh, 2005). Further mechanist insights have been garnered from a more recent study in melanoma where it was shown that experimental knockdown of membrane bound protein ABCB5 upregulated WFDC1 gene expression. It was subsequently shown that IL-8 was directly down-regulated by ectopic expression of ps20, as were numerous proteins of the WNT family (Wilson et al., 2014). These two studies then, provide evidence that ps20 may have growth regulatory properties which are mediated through regulation of the WNT pathway, and other cytokines.

The body of WFDC1/ps20 focused studies to date largely suggest a growth inhibitory role, where stromal ps20 expression is incompatible with tumour growth. However, it seems that when expression of WFDC1/ps20 is dysregulated, it may conform to pro-tumourigenic phenotypes, involving increased epithelial expression and the promotion of angiogenesis.

1.2.5 Role of SLPI in Cancer

A number of studies have investigated the role of SLPI in cancer, both at the level of expression, and, more recently a number of studies addressing function have been published. SLPI expression is shown to be both up and down-regulated depending on tumour type (table.1.1). In many cases elevated SLPI expression has been reported, such as in lung cancers (Ameshima et al., 2000, Bild et al., 2006), ovarian cancer (Israeli et al., 2005, Hough et al., 2001, Schwartz et al., 2002), pancreatic cancer (Iacobuzio-Donahue et al., 2003, Ryu et al., 2002) and in one report, breast cancer, showing an overexpression (>2.5 fold) expression of SLPI in a highly metastatic breast cancer line compared to a poorly metastatic line (Kluger et al., 2005). These data are suggestive that in certain contexts SLPI may be advantageous to tumour growth. However, there are an almost equal number of cancers where decreased SLPI expression has been observed, such as in nasopharengeal carcinoma (Huang et al., 2012, Tse et al., 2012, Sriuranpong et al., 2004), melanoma (Jaeger et al., 2007, Martins et al., 2011), and prostate (Thompson et al., 2008), which is indicative of a potential tumour suppressor role in those tissues. In breast cancer, SLPI expression was shown to be down-regulated in one study (Hu et al., 2004) and in another its expression was linked to increased survival from disease (Cimino et al., 2008). A further study showed that SLPI overexpression in breast cancer cell lines, increased apoptosis, and that intra-tumoural administration of SLPI in mice reduced tumour growth (Amiano et al., 2012). In addition, inoculation of mice with mammary tumour cells over expressing SLPI reduced subsequent tumour growth (Amiano et al., 2011). This contrasts with another study which shows mouse mammary tumour cells overexpressing SLPI have increased growth *in vivo*, but reduced invasiveness (Sugino et al., 2007). This study also highlighted a potential role for SLPI in enhancing blood borne metastasis, though it provided no mechanistic insight as to how this metastatic advantage was mediated.

Table 1.1 Expression of ps20, SLPI and elafin in cancer

Ps20	**mRNA/protein**	**Expression**	**References**
Prostate	mRNA	Downregulated	(Madar et al., 2009)
	protein	Downregulated	(Watson et al., 2004b, McAlhany et al., 2004)
Melanoma/ Brain/ Lung/Stomach	mRNA	Downregulated	(Madar et al., 2009)
Melanoma	mRNA	Downregulated	(Liu et al., 2009)
Hepatic	mRNA	Not regulated	(Saffroy et al., 2002)
SLPI	**mRNA/protein**	**Expression**	**References**
Thyroid, Stomach, Prostate, Kidney	mRNA	Not regulated	(Devoogdt et al., 2004)
Intestinal tract	mRNA	Upregulated	(Devoogdt et al., 2004)
Prostate	mRNA/protein	Downregulated	(Thompson et al., 2008)
Pancreas	mRNA	Not regulated	(Devoogdt et al., 2004)
	mRNA	Upregulated	(Iacobuzio-Donahue et al., 2003, Ryu et al., 2002)
Lung	mRNA	Not regulated	(Devoogdt et al., 2004)
	mRNA	Upregulated	(Bild et al., 2006, Ameshima et al., 2000)
Breast	mRNA	Not regulated	(Devoogdt et al., 2004)
	mRNA	Downregulated	(Hu et al., 2004)
	mRNA	Upregulated	(Bertucci et al., 2004, Kluger et al., 2005)
Ovarian	mRNA	Upregulated	(Israeli et al., 2005, Hough et al., 2001, Schwartz et al., 2002, Clauss et al., 2010)
	protein	Upregulated	(Tsukishiro et al., 2005)
Cervix Uteri	mRNA	Upregulated	(Devoogdt et al., 2004)
	promoter	Upregulated	(Rein et al., 2004)
Uterus	mRNA	Upregulated	(Devoogdt et al., 2004)
	mRNA	Downregulated	(Tian et al., 2004)
Nasopharyanx	mRNA	Downregulated	(Sriuranpong et al., 2004)
	mRNA/Protein	Downregulated	(Tse et al., 2012)
		Downregulated	(Huang et al., 2012)
Endometrial epithelial carcinoma	mRNA	Upregulated	(Zhang et al., 2002)
Bladder	mRNA	Downregulated	(Liang et al., 2002)
Gastric Cancer	mRNA/protein	Upregulated	(Cheng et al., 2008)
elafin	**mRNA/protein**	**Expression**	**References**
Urothelium	mRNA	Upregulated	(Smith et al., 2001)
Skin	mRNA/protein	Upregulated	(Alkemade et al., 1994)
Oesophagus	protein	Upregulated	(Alkemade et al., 1994)
Head and Neck	protein	Upregulated	(Westin et al., 2002)
Bladder	mRNA	Downregulated	(Liang et al., 2002)
	mRNA	Upregulated	(Blaveri et al., 2005)
Mouth	protein	Upregulated	(Robinson et al., 1996)
Lung	protein	Upregulated	(Yoshida et al., 2002)
Prostate	mRNA	Downregulated	(Li and Sarkar, 2002)
Breast	mRNA	Downregulated	(Clauss et al., 2010, Zhang et al., 1995)
Ovarian	protein	Upregulated	(Clauss et al., 2010)
Glioblastoma	mRNA/protein	Upregulated	(Saidi et al., 2008)

Interestingly, SLPI was highly upregulated in a study looking at a rare and aggressive form of disease called inflammatory breast cancer which fits with the concept of SLPI as a molecule induced under inflammatory conditions. However this study does not indicate whether SLPI itself contributes directly to the development/growth of the breast tumours under these inflammatory conditions (Bertucci et al., 2004). SLPI expression has also been shown to correlate with more aggressive, metastatic gastric carcinoma, and experimental overexpression of SLPI in two gastric carcinoma cell lines enhanced cell growth, migration and invasion, once again demonstrating SLPI's tumourigenic properties (Cheng et al., 2008). These studies taken together suggest that SLPI has a context dependent function in cancer, which is dependent on the specific micro-environmental conditions within tumours.

A number of studies have investigated the role of SLPI in ovarian cancer, and up-regulation of SLPI in this tumour type is well established (Israeli et al., 2005, Hough et al., 2001, Schwartz et al., 2002, Tsukishiro et al., 2005) leading to investigations as to its efficacy as a diagnostic biomarker (Havrilesky et al., 2008, Jacob et al., 2009). Functional studies suggest that SLPI possesses direct tumourigenic effects: overexpression of different SLPI isoforms in ovarian cancer cells increased growth, colony formation and *in vivo* xenograft growth, and this function was shown to be independent of SLPIs protease inhibitor function (Devoogdt et al., 2009). A subsequent study by the same group showed that SLPI dependent enhancement of ovarian cancer cell growth is dependent on binding to progranulin, which protects the molecule from degradation by elastase (Simpkins et al., 2008). SLPI can also antagonize the effects of paclitaxel suggesting that under certain cellular conditions the presence of SLPI inhibits apoptosis (Rasool et al., 2010). It has also been observed that SLPI possesses a net pro-invasive effect *in vivo* in ovarian cancer xenografts by up-regulation of the collagenase MMP-9. This is despite the fact that SLPI's protease inhibition activity has been demonstrated to antagonise the release

of MMP9 from the cell surface (Hoskins et al., 2011). Taken together these studies suggest that in ovarian cancer SLPI is clearly tumourigenic. However, its growth enhancing functions seem to be predominantly mediated indirectly through processing events upstream of other proteases or growth factors rather than in a cell-intrinsic manner. It remains to be conclusively demonstrated that SLPI has direct cell-intrinsic effects on signalling or transcription which could mediate pro- or anti-tumourigenic functions, or whether its functional effects are mediated solely by regulation of the extracellular environment.

The role of SLPI as a protease inhibitor and guardian against inflammatory damage by elastases in the lung is well characterized (Moreau et al., 2008). However, the function of SLPI in lung cancer remains poorly understood. SLPI is over expressed both in adenocarcinomas and in squamous cell carcinomas of the lung. Urethane induced tumour development in mice was abrogated in SLPI knockout animals (Nukiwa et al., 2008). Similarly, overexpression of SLPI in lewis lung carcinoma cells increased sub-cutaneous tumour growth without increasing proliferation of cells *in vitro* (Devoogdt et al., 2003), suggesting that this function relies on altered tumourigenic processes mediated by secondary factors, rather than direct increases in tumour cell proliferation and/or survival. Devoogdt et al showed that TNFα can promote tumour development *in vivo* by inducing SLPI expression. Knockdown of SLPI in 3LL lung carcinoma cells completely abrogated tumour formation (Devoogdt et al., 2006). However, in contrast to these studies, SLPI was elevated in non-metastatic lung carcinoma lines relative to liver-metastatic lines, and SLPI expression in tumour cells curbed TNFα and NFκB signalling and led to 80% fewer metastases *in vivo* (Wang et al., 2006a). This is strong evidence that SLPI can have a directly protective role in preventing tumour metastasis and serves to reinforce the pervading view that SLPI's role in tumourigenesis is complex and not yet well understood.

To date then, numerous studies suggest SLPI is capable of acting as a tumourigenic factor in certain tumour cell types, corroborating expression data showing SLPI up-regulation in various solid tumours. However somewhat disparate evidence shows that SLPI is down-regulated in certain tumour types indicating that its role is complex and probably tissue and/or cell type specific. Interestingly, SLPI is involved in antimicrobial responses and the dampening of inflammatory processes at mucosal sites, especially in the lower respiratory tract and it is thought to perform similar functions in the stomach and intestinal mucosae (Taha et al., 2005). Development of cancer in the lungs and gastro intestinal tract is etiologically linked to chronic inflammation of these tissues (Hannelien et al., 2012). It is of note that SLPI expression was also upregulated in inflammatory breast cancer (Bertucci et al., 2004). The enhanced expression of SLPI in these particular cancers may suggest that there are reciprocal effects of SLPI expression on increased tumour growth, and of the inflamed tumour microenvironment on SLPI expression, which may require interpretation through the complicated nexus of the inflammatory response. It has been clearly demonstrated that overexpressing SLPI can drive tumourigenesis (Simpkins et al., 2008, Devoogdt et al., 2009) and it may therefore be the case in tumours, especially at mucosal surfaces, that SLPI expression is induced as a result of local inflammatory signalling and subsequently has deleterious effects on tumour growth. Or alternatively it may be that the tumours themselves drive SLPI expression for their own growth advantage, and this induces subsequent effects on local inflammation, possibly contributing to immune evasion by the tumour (discussed further below).

1.2.6 Role of elafin in cancer.

Like SLPI, elafin has been shown to be upregulated in numerous tumour types including mouth (Robinson et al., 1996), urothelium (Smith et al., 2001), breast (Larramendy et al., 2000) bladder (Blaveri et al., 2005), glioblastomas (Saidi et al., 2008) and ovarian cancers (Tanner et al., 2000, Clauss et al., 2010) and it was shown to be over expressed specifically in highly differentiated squamous cell carcinomas of the lung (Yoshida et al., 2002), skin (Alkemade et al., 1994), and upper respiratory tract (Westin et al., 2002) (Table 1.1). However there is conflicting evidence from other tumour types where decreases in elafin expression have been observed, as in cancers of the breast (Clauss et al., 2010, Zhang et al., 1995) and in primary samples from numerous squamous cell carcinomas (Clauss et al., 2010, Larramendy et al., 2000). In one study of ovarian cancer, researchers found genomic gains of elafin's chromosomal locus in various cell lines suggesting that elafin expression may provide an advantage in cellular growth. In addition, elafin expression in these cells was shown to be specifically induced by inflammatory conditions and NFκB activation, suggesting that inflammatory conditions are conducive to elafin expression in ovarian tumour tissues (Clauss et al., 2010). In addition to being upregulated in ovarian cancer, a subsequent study showed knockdown of elafin in ovarian cancer cell lines *in vitro* increases the sensitivity to apoptosis induced by a number of commonly used agents including cisplatin, carboplatin, cyclophosphamide and 5-fluorouracil, which is further suggestive of a potentially advantageous role in tumour growth (Wei et al., 2012). In contrast however, elafin was shown to be transcriptionally silenced in melanoma cells. Epigenetic suppression of the Foxa2 transcription factor was responsible for regulating elafin in melanoma cell lines and this could be reversed by a DNA methylation inhibitor which subsequently induced elafin specific growth suppression and apoptosis (Yu et al., 2011). Similarly, in a separate study, over expression of elafin in melanoma cell lines induced p53 dependent apoptosis (Yu et

al., 2010). Another study showed that elafin overexpression can supress breast cancer cell proliferation by halting the cells in G_0-G_1 phase of the cell cycle. However, in the absence of functional Rb protein elafin induces caspase3 dependent apoptosis (Caruso et al., 2010). So it seems elafin can function upstream of at least two pathways (p53 and Rb) to control cell death and function as a tumour suppressor protein when expressed in certain tumour cell types.

Data suggests that the highest expression of elafin is seen in well differentiated tumours, and despite expression being elevated in cancer compared to healthy tissues, the expression does not seem to be associated with aggressive or invasive tumour types (Bouchard et al., 2006). This may be because elafin is capable of inhibiting various proteases within the tumour microenvironment which assist in tumour invasion. Lastly, in glioblastomas, elafin expression was increased and appears from histochemical analysis to be expressed at sites undergoing necrosis (Saidi et al., 2008). Subsequently, the same study showed elafin to be upregulated by hypoxia which supports a role for WFDC family proteins as potential regulators of angiogenesis during tumour development , as has been shown in a study of ps20 (McAlhany et al., 2003). These contrasting data paint a familiar picture, wherein elafin expression, like SLPI, appears to have both advantageous and deleterious roles on tumour growth depending on the tumour type and cellular origin. Dissection of elafin's function at the molecular level will likely be required to elucidate further the overall stage-by-stage role in tumourigenesis and the potentiality of utilizing or targeting elafin therapeutically in cancer.

1.3 Cancer and the Immune system

Of fundamental importance to health is the ability of the body to recognise and eliminate cells as they become genetically unstable and begin to replicate uncontrollably. Myriad biological mechanisms service this end; intracellular proteins which recognise genetic lesions and induce cell-death, extracellular factors which regulate cellular growth and survival, and manipulate the extracellular environment; and the immune system, facets of which surveil tissues and eradicate cells which have begun to deviate from routine immune presentation. These systems, while highly effective, can malfunction, leading to outgrowth of transformed cells, neoplasms, and ultimately invasive tumours. Once cells have become transformed, the growth and persistence of tumours results from a failure of anti-tumour immunity at three key stages: (i) Immunosurveillance, (ii) activation of anti-tumour immunity and lastly, (iii) the failure of adaptive anti-tumour immunity to clear the tumour burden.

Numerous lines of evidence both *in vitro* and *in vivo* suggest ps20 and WFDC family proteins SLPI and elafin possess immunomodulatory functions which may impact their effect within tumourous tissues, either when over-expressed, or when their expression is lost. In this section I will outline the facets of tumour immunobiology relevant to this study before reviewing the literature pertaining to the role immunoregulatory role of ps20, SLPI and elafin, and how this may impact tumourigenesis.

1.3.1 Immunosurveillance

The term immunosurveillance refers to a series of processes whereby the immune system spontaneously patrols for, recognises, and eradicates neoplastic cells before they become tumours. This phenomenon has been clearly demonstrated through

evidence of increased numbers of tumours in immune-deficient humans and mice (Dunn et al., 2004). Immunosurveillance is thought to be the principle function of an innate immune cell type called natural killer (NK) cells. Like certain T cells types, these cells are activated by the cytokines IL-2, IL-12, IL-15 and type 1 interferons, and migrate into tumourigenic environments in response to chemokines CCL2 and CCL5 (Bernardini et al., 2012, Zwirner and Domaica, 2010). NK cells are able to mediate cellular killing through i) the release of cytotoxic granules containing perforin and granzyme, ii) the ligation of death receptors such as TNF, FasL and TRAIL, to induce apoptosis, or iii) the expression of IFNγ, which halts tumour growth and induces the activation of other immune compartments (Zwirner and Domaica, 2010). Key to the function of NK cells is their ability to distinguish transformed cells from healthy cells. They do this through the recognition of a number of stress induced molecules on the surface of tumour cells which bind and activate a highly redundant series of receptors on the NK surface, most notably NKG2D (Long et al., 2013). NK cells require ligation of the inhibitory KIR receptor (Ly49 in mice) by MHC class 1 on the target cell surface to provide a 'do not kill' signal. In the presence of other stimulatory signals from the target cell, the failure to detect MHC class 1 leads to the activation of second pathway, and the tumour cell is perceived as non-self, and subsequently destroyed (Long et al., 2013).

An increasing body of evidence in mice supports the concept of NK cells as the natural mediators of immunosurveillance. For example, RAG-/- mice, which lack adaptive immunity, developed far fewer tumours than RAG-/- and γc-/- mice, which lack both adaptive immunity and NK cells (O'Sullivan et al., 2012). Further evidence comes from the transgenic adenocarcinoma of the mouse prostate (TRAMP) model of prostate cancer. TRAMP mice spontaneously develop prostate adenocarcinoma at puberty due to the transgenic expression of the SV40 large T antigen under control of the prostate specific probasin promoter (Hurwitz et al., 2001). Augmented tumour

growth was observed in TRAMP mice which were also deficient for the NK cell activating NKG2D receptor, suggesting activation of NK cells restrains TRAMP tumour growth (Guerra et al., 2008). In humans, evidence for the role of NK cells in immune surveillance comes from a longitudinal study in which the blood of a large cohort of 3625 subjects was investigated for its natural cytotoxicity against the cancerous K562 myeloid progenitor cell line. Over the 11 years of follow up, those subjects whose blood exhibited low natural cytotoxicity had a statistically increased risk of developing tumours. Certain haplotypes of the NKG2D gene were found to be a key risk factor in subjects developing cancer, and were associated with the level of NK cell cytotoxicity observed in the original study (Hayashi et al., 2006, Imai et al., 2000), again highlighting the importance of NK cell recognition of transformed cells in defence against neoplasms.

The concept of immunosurveillance logically leads to the concept of immunoediting. Simply stated, this is the process whereby neoplastic cells are constantly eradicated, placing nascent neoplasms under a selective pressure to escape recognition by the immune system. It is described in three stages, i) elimination, where immunogenic tumour cells are cleared, ii) equilibrium, where surviving tumour cells remain dormant and coexist with the active machinery of immune surveillance (Koebel et al., 2007), ultimately progressing to, iii), immune escape, whereby the surviving malignancy has become poorly immunogenic and is no longer recognised by the immune system (Dunn et al., 2002).

1.3.2 Induction of anti-tumour immune response.

Once a tumour has escaped immune surveillance, other physiological mechanisms are required to recognise the neoplasm and instigate an immune response against it. However, the immune system has evolved primarily to protect the host from

infectious pathogens. Innate immune cells which patrol tissues such as macrophages (MΦ) and dendritic cells (DCs), are activated through a broad family of cellular receptors known as pattern recognition receptors (PRRs). These PPRs, are activated by highly conserved pathogen-associated molecular patterns (PAMPs) associated with viruses, bacteria, fungi and other pathogens (Reis e Sousa, 2001). Once activated MΦ, and DCs act as antigen presenting cells (APCs), presenting self and foreign peptides to the adaptive arm of the immune system to invoke a specific and robust response against the pathogen. Because tumours are sterile and derived from host cells, these PAMPs are not present, and despite the presence of APCs and other leukocytes in the tumour microenvironment, PRRs do not become activated and there is a failure to illicit an adaptive immune response.

APCs express high levels of MHC class II, which when loaded with pathogen derived antigen (e.g. from phagocytosis) can interact with the CD4 receptor and the cognate T cell Receptor (TCR) on CD4 T cells. When combined with the appropriate secondary activation signal, this interaction results in the activation of the CD4 T cell. Alternatively, endogenous antigen resulting from viral infection, or (via cross presentation) exogenous antigen, can be presented in the context of the MHC class I molecule, which interacts with CD8 and the cognate TCR on a CD8 T cell. This results in the activation of CD8+ cytotoxic T cells (CTL). As host cells bear MHC class I at their surface, activated CTLs are highly specialised to bind to and kill infected self-cells in an antigen specific manner (Berke, 1994).

In the context of cancer, immunity has to be initiated against cells expressing tumour-associated antigens (TAA); peptides derived from self-proteins commonly associated with specific tumour types, and which are presented in the context of MHC class 1 molecules at the surface of tumour cells. As in the case of a viral infection, a robust response by CTLs is desirable to destroy tumour cells (Savage et al., 2002, Ikuta et

al., 2000). However, due to the lack of PAMPs and therefore of immune activation of APCs, there is frequently a failure to elicit robust TAA-specific CTL immunity.

There are however mechanisms through which sterile inflammation, i.e. in the absence of pathogens, can result in anti-tumour adaptive immunity. These rely on the presence of danger-associated molecule patterns (DAMPs), a series of molecular signals, including inflammatory mediators, nucleotides such as ATP, and lipids, which are shed or purposefully released from dying cells (Ghiringhelli et al., 2009). Though these processes are still not well understood, it has been shown that DAMPs attract and signal to innate immune cells, predominantly MΦ. During tumourigenesis numerous cell-intrinsic processes such as oncogenic stress and oxidative stress can lead to cell death, either by apoptosis or necrosis. These highly conserved processes can result in the production of DAMPs which interact with MΦ as they scavenge apoptotic cell corpses and other cellular debris. The recognition of DAMPs results in the activation of the MΦ and the release of IL-1β, resulting in further downstream immune activation (Ghiringhelli et al., 2009). The presence of ATP in the milieu of cellular debris has also been shown to result in the activation of the NLRP3 inflammosome in DC cells and the secretion of IL-1β which in turn lead to the priming and activation of tumour specific, IFNγ secreting CTLs, and activation of γδ T cells, essentially turning the dying tumour cells into an anti-tumour vaccine (Eisenbarth and Flavell, 2009).

How the recognition of tumours and activation of immune pathways leading to adaptive responses occurs *in vivo* is still not well understood, but the existence of such processes is clear by the existence of adaptive responses which have been observed toward tumours of diverse origins (Willimsky et al., 2008).

1.3.3. Stromal suppression of anti-tumour immunity.

As we have seen, the growth of tumours, including in the prostate, is accompanied by reciprocal cellular and molecular changes within the surrounding stroma, which facilitate and support the growth of the tumour. It is now known that as well as supporting the growth of the tumour through reciprocal interactions which facilitate cellular proliferation and vascularization of the tumour, the tumour stroma also mediates potent immune suppression, preventing established anti-tumour adaptive immunity from taking effect. Kraman *et al* have recently demonstrated that expression of the fibroblast activation protein (FAP) on the surface of cancer-associated fibroblasts delineated a highly immune-suppressive tumour-stromal cell compartment. Coupling the expression of FAP to the transgenic expression of the diphtheria toxin receptor in mice, they demonstrate that elimination of the FAP^+ cell compartment throughout the animal is sufficient to restore robust T cell mediated anti-tumour immunity and instigate regression of the tumour (Kraman et al., 2010). FAP^+ fibroblasts mediate suppression through expression of immunosuppressive proteins such as stromal derived factor-1 (SDF-1) and transforming growth factor-β (TGF-β). Such cytokines prevent the activation of effector T cells and facilitate the development and function of T regulatory cells (Tregs) which themselves suppress immune responses.

There are however myriad ways in which the tumour can co-opt extant immune suppressive mechanisms to escape and inhibit anti-tumour immunity. For example, the recruitment of MMP9 expressing neutrophils has been shown to have similar suppressive effect to FAP^+ fibroblasts, by liberating cell associated TGFβ, and contributing to fibroblast activation (Seung et al., 1995). There is also evidence from a number of studies that tumours can recruit myeloid-derived suppressor cells to the stroma which are potently suppressive of T cell responses through numerous

mechanisms including production of IDO (Meyer et al., 2011, Prendergast et al., 2014), and tumour cells and cancer associated fibroblasts secrete high levels of chemokines such as CCL2, CCL5, which have been shown to induce T_H17 cell migration into the tumour, a T cell subset which evidence shows are likely pro-tumourigenic and deleterious to anti-tumour immunity (discussed below) (Su et al., 2010). So while there is accumulating evidence that the immune system recognises and attacks tumours, it is now accepted that tumours are able to survive, in part at least, by regulating tumour the microenvironment to suppress these immune responses directed against them.

1.3.4 T cells in cancer.

T cells are the fundamental mediators of adaptive, specific immune responses, and it has been shown in animal models that T cell mediated anti-tumour responses can mediate the eradication of solid tumours (Kraman et al., 2010). It has been demonstrated that the frequency and location of tumour infiltrating T cells within tumours can be a better predictor of progression and survival than established histopathological methods used for tumour staging (Galon et al., 2006), suggesting an active role for T cells in the restriction of tumour growth.

T cells are characterized by the expression of a unique T cell receptor (TCR) that recognises specific molecular targets through interaction between their TCR and target cell surface MHC-cognate antigen complexes. Following migration from the bone marrow, T cells mature in the thymus, where their unique TCR interacts with self-antigen. The T cell clone is then selected for survival or deletion based on the affinity with which its TCR-recognises self-derived peptides. Each surviving T cell will bear one of either CD4 or the CD8, the co-stimulatory molecules which will delineate

the cells ability to interact with MHC class II or MHC class I molecules respectively (Lo and Allen, 2014).

Following the priming and co-stimulation of T cells by APCs in the spleen or lymph node, naïve T cells will undergo expansion and differentiation to become antigen specific effector cells. Depending on the innate response elicited, CD4 T cells will be induced to become T_H1, T_H2, T_H17 or T regulatory cells (Raphael et al., 2014). These subsets are primarily delineated by the cytokines they produce and the functional effects they elicit. CD8 T cells will become activated to become CTLs. Besides CTLs, T_H1 cells are the cells of primary interest in anti-tumour responses as their predominant role is the co-stimulation and activation of CTLs, and their activation and recruitment leads to more effective target cell lysis, and the production of cytokines IFNγ and TNFα, which is desirable during infection with intracellular pathogens, or in cancer (Shankaran et al., 2001).

Though the mechanisms are not well elucidated, tumours do induce specific T cell responses. These can be to i) self-antigens restricted to highly specific tissues, e.g. the testis, and which have become expressed on the tumour, ii) self-antigens associated with specific differentiated tissues, such as prostate acid phosphatase in the prostate (Westdorp et al., 2014), iii) or self-antigens that have been highly upregulated by tumours. However, there are also examples of specific T cell responses to neo-antigens resulting from mutations within the tumour, or from tumour-induced changes to the post-translational modifications of certain proteins (Vigneron et al., 2013). Early evidence of MHC restricted tumour specific CD8 T cells came when it was demonstrated that tumour infiltrating lymphocytes (TILs) from resected melanomas could specifically lyse autologous melanoma cells (Yee et al., 1999). CTLs capable of lysing tumour cells had high avidity for specific MHC-tumour associated antigen (TAA) complexes, while those cells with low avidity could not (Yee

et al., 1999) demonstrating the importance of MHC-TAA complexes in the induction of CTL responses. However, while a number of studies have demonstrated the presence of infiltrating TAA specific CTLs within tumours, other studies have suggested that the proportion of these cells within tumours may be very low, in the region of 1-5% (Savage et al., 2008, van Rooij et al., 2013, Andersen et al., 2012). Indeed, that these cells were derived from growing tumours demonstrates that they are not having the desired effects of lysing tumour cells *in vivo*. Toward elucidating what T cells make up the other 95% of TIL, studies have suggested that it includes T regulatory cells (Tregs)(both thymically and locally induced), CD8 T suppressor cells, derived from tolerized CTLs, and non-specific T cells migrating to inflammatory cues (Savage et al., 2014).

Numerous studies have investigated the role of Tregs in cancer, and it is now established that tumours are frequently infiltrated by tumour specific Tregs which actively suppress immune responses and induce tolerance (Wang et al., 2005a). Tregs are CD4 T cells characterized by high levels of CD25 expression and expression of the FoxP3 transcription factor, and are able to mediate suppression of effector T cell responses through cell-to-cell contact and through secretion of soluble mediators such as IL-10 and TGFβ. Increased proportions of Treg in the total CD4 T cell populations have been observed in lung, breast and ovarian tumours (Woo et al., 2001, Wang et al., 2006b). These cells present a significant challenge to anti-cancer therapies, and understanding the mechanisms which drive suppressive immunity within tumours is one of the fundamental aims of tumour-immunological research.

Pertinent to the concept of Treg function are the concepts of recessive and dominant immune tolerance. Recessive tolerance stems from the thymic deletion of auto-reactive CD4 and CD8 T cells. While fundamental in preventing autoimmunity, this mechanism leaves the T cell repertoire devoid of T cells which strongly recognise

self-antigen, from which tumour associated antigens ultimately derive (Rizzuto et al., 2009). Dominant tolerance is more local to the tumour. Tumours employ numerous mechanisms, including the co-opting of regulatory T cells, to suppress tumour specific T cell responses and in this way tolerizes the adaptive immune system to its presence (Savage et al., 2014). Numerous lines of evidence suggest that natural Tregs (nTregs) arise in the thymus in response to recognition of self-antigen, though none of these antigens have been elucidated (Jordan et al., 2001, Apostolou et al., 2002). Induced Tregs (iTregs), in contrast are thought to be naïve T cells which differentiate in extra-thymic sites in response to antigens present in commensal bacteria and food. It has also been proposed that iTregs may be conditioned in tumours in response to neo-antigens (Yang et al., 2010) and there is evidence to suggest the antigen specific CD4 T cells within tumours up-regulate FoxP3 upon transfer into tumours (Getnet et al., 2009). However, other studies looking at the TCR repertoire of Tregs found in prostate and other tumour types concluded that the contribution of locally induced Tregs to immune suppression was negligible (Malchow et al., 2013, Hindley et al., 2011). They demonstrated repeated recruitment of distinct Treg specificities, supporting the hypothesis that thymic selection of tolerogenic Tregs results in specific clones which become expanded within tumours, and mediate suppression which contributes to suppressing TAA specific effector T cells.

There is now a great deal of evidence supporting the notion that infiltrating Tregs, actively suppress anti-tumour response. Specifically, Yu *et al* demonstrated that CD4+ CD25+ Tregs within the tumour inhibited proliferation and activation of anti-tumour CTL and blocked the production of IFNγ. Subsequently, blockade of Treg derived immunosuppressive cytokines IL-10 and TGFβ partially restored anti-tumour immunity, however depletion of Tregs from the tumour was necessary and sufficient to mitigate the complete eradication of well established, highly aggressive tumours

(Yu et al., 2005). Further evidence has come from studies focused on prostate tumours and will be discussed in the following section.

The discovery of IL-17 producing T_H17 cells changed the classical T_H1/T_H2 dichotomy of T helper cell differentiation (Harrington et al., 2005, Park et al., 2005). These cells differentiate from naïve CD4 T cells activated in the presence of IL-1, IL-6 and IL-23 (Wilson et al., 2007). While these cells are classically thought to be pro-inflammatory, their physiological roles are still being characterized. It has however emerged that T_H17 cells are abundant in most common cancers (Ye et al., 2013), including prostate cancer (Sfanos et al., 2008, Derhovanessian et al., 2009). Indeed, many tumour microenvironments produce IL-1, IL-6, IL-23 and TGFβ, providing optimal conditions for the differentiation and expansion of T_H17 cells (Su et al., 2010, Kryczek et al., 2009, Miyahara et al., 2008). It has also been shown that chronic inflammation within tumours can lead to activation of NOD2 and TLR signalling, which stimulated IL-1β, IL-6, IL-23 and TGFβ expression and induced T_H17 differentiation (Su et al., 2010). It seems likely then, that the induction of T_H17 cells is in part due to inflammation associated with tumours, but also that the presence of T_H17 within tumours contributes to and prevents the resolution of that self-same inflammation. The pro-tumourigenic function of T_H17 cells has been demonstrated in mice and numerous human studies and have shown IL-17 to be pro-tumourigenic, most likely through its pro-angiogenic functions (Tartour et al., 1999, Numasaki et al., 2003). However, studies disagree on the prognostic value of T_H17 cells in prostate cancer. One found increased T_H17 number to correlate with slower PCa progression (Sfanos et al., 2008), whereas these results were contradicted by another group investigating castration resistant cancer (Derhovanessian et al., 2009) indicating that these cells may have variable context specific roles. The function of T_H17 in tumours remains controversial, and elucidating this will rely on understanding the origin of these cells within tumours. T_H17 cells, unlike T_H1 and T_H2 cells, are in their nature highly plastic

and can differentiate into T_H1 or iTreg cells (Koenen et al., 2008). It is not yet understood whether tumour associated T_H17 cells are i) induced *de novo* within the tumour from naïve cells, ii) recruited to the tumour site, or iii) arise as a result of reprogrammed Treg cells (Alizadeh et al., 2013). Determining the origin of these cells is important in helping to understand their role with in the microenvironment.

Adding another layer of complexity to the activity of T cells within tumours, is the recently discovered subset of CTL, termed suppressors of regulatory T cells (srT cells). These are naturally occurring thymically selected CD8 T cells which have specificity for antigens expressed by regulatory components of the immune system, such as Tregs or other suppressive facets of the tumour microenvironments. CTLs have been isolated in cancer patients and from healthy donors which have specificity for FoxP3 expressing Tregs, through recognition of HLA-A2 restricted FoxP3 derived antigen (Larsen et al., 2013); cells expressing the regulatory receptor PD-L1 (Munir et al., 2013b, Munir et al., 2013a); and cells expressing the tryptophan depleting immune-suppressive enzyme IDO (Sorensen et al., 2011b, Sorensen et al., 2011a). These CTLs target the cell baring the relevant cognate antigen and eliminate them, thereby reducing the suppressive component within the tissue. The role of these cells in health, and their effectiveness in targeting suppressive elements during disease is not yet established, but they represent an interesting immunological subset, which may be of use therapeutically.

While T cells are likely fundamental to any successful anti-tumour immune response, tumours employ various mechanisms to overcome active anti-tumour immunity, and to skew the immune milieu away from a CTL and T_H1 response, towards a pro-angiogenic T_H17 cell based infiltrate. Equally, the predisposition for TAAs to restrict nTregs results in a suppressive regulatory infiltrate which further abrogates any active anti-tumour immunity.

1.3.5 Immunity of Prostate cancer

As we have seen, innate immune activation during tumourigenesis can result in the generation of anti-tumour immune responses. These responses are then suppressed by immune and stromal components associated with the tumour. Despite this standard narrative, immune responses are context specific, and as such, have unique characteristics in different tumour types. The failure of the immune system to prevent and eradicate prostate tumours suggests that one of two things has occurred, i) anti-tumour adaptive immunity has not been induced, or ii) the adaptive immunity is being modulated by the prostate tumour microenvironment to adopt a regulatory/suppressive phenotype. Here I will discuss the literature pertaining to immunity within the prostate, and to prostate tumours.

A number of studies have tried to define the immune infiltrate of prostate tumours. Both CD4 and CD8 T cells have been shown to be present within the organ, including IFNγ producing T_H1, IL-4 producing T_H2 cells, IL-17 producing T_H17 cells and FoxP3 positive Tregs. (Kiniwa et al., 2007, Sfanos et al., 2008). It has also been observed that IFNγ positive cells were increased in prostates with a gleason score of 7-9 (with increased gleason score reflecting the severity of the tumour) compared to those with scores <6. Conversely, numbers of IL-17 producing cells showed an inverse correlation with severity. No difference in numbers of T_H2 or Tregs was observed (Sfanos et al., 2008). Another recent study has provided evidence of TAA specific T cells in patients with PCa. Peripheral blood derived T cells from PCa patients had significantly higher reactivity to prostate specific antigens than patients with either benign prostate hyperplasia, or healthy patients. These cells responded with far higher frequency once Tregs had been depleted (Hadaschik et al., 2012). The induction of a tolerogenic T cell phenotype has also been demonstrated in the

TRAMP mouse modal of PCa. TRAMP tumours were shown to induce large T-antigen (TAG) specific T cell and B cell responses, but TAG specific CTLs were unable to kill target tumour cells, demonstrating that while the tumours do not escape immune recognition by CTLs, these cells are subject to suppressive mechanisms which prevent them from killing target cells (Willimsky et al., 2008, Willimsky and Blankenstein, 2005).

One study investigated both CD4 and CD8 Regulatory cells in prostate cancer. The study demonstrated proportionally high numbers of CD4CD25+ Tregs in prostate tumours, suggesting a potential skewing of the immune infiltrate towards a regulatory phenotype. However, it was also found that both CD4 and CD8 T cells derived from tumours were potent suppressors of naïve T cell responses ex-vivo, suggesting that prostate tumours are capable of inducing potent immune suppressive phenotypes in infiltrating lymphocytes including the induction of $FoxP3^{+}$ regulatory CD8 cells, often called T suppressor cells (Kiniwa et al., 2007). Other studies have also demonstrated the presence and function of this cell type (Arruvito et al., 2014). Like CD4 Tregs these cells feature a FoxP3 regulated transcription programme, and can suppress T-effector responses through contact dependent and independent mechanisms. Indeed, Olsen et al showed CD8+ Tregs elicited antigen specific suppression of T cell responses, and that this suppression was mediated through both surface CTLA-4 expression, and through the secretion of IL-35. Experimental blockade of either mechanism relieved the suppressive phenotype (Olson et al., 2012). In a different study, CTLA-4 and PD-L1 blockade abrogated CD4 Treg and CD8 Treg suppression of IL-15 induced CTL immunity against TRAMP tumours in mice (Yu et al., 2012).

Despite T cell mediated immune-suppression being clearly pertinent to the suppression of anti-tumour immunity, another study has suggested that tumour suppression of CTL killing of PCa is dependent on intra-tumoural TGFβ signalling.

The authors demonstrated that transfer of CD8 T cells specific for the tumour, but deficient of TGFβ signalling, induced elimination of the tumour, in contrast to the transfer of CD8 cells in which TGFβ signalling was intact, which were suppressed (Zhang et al., 2006). Supporting this was evidence that tumour specific CTLs adoptively transferred to tumour bearing mice became tolerogenic upon infiltration into the tumour. Blocking TGFβ in these mice partially reversed the tolerogenic phenotype of these cells, providing further evidence that processes mediating suppression of T cell responses are based on the presence of secreted factors local to the tumour microenvironment (Shafer-Weaver et al., 2009). Interestingly, one study has proposed a role for T-effector cell-intrinsic TGFβ signalling in the generation of tolerogenic immune responses in the TRAMP mouse. Inhibition of SMAD signalling in T cells induced CTL activity against TRAMP tumours leading to tumour regression. However, inhibition of SMAD signalling in Treg cells had no effect, highlighting, i) that it is possible to reverse tolerogenic phenotype through inhibition of specific signalling pathways and ii) that there are numerous different mechanisms by which tumours can induce immune tolerance (Donkor et al., 2011).

1.3.6 Role of WFDC family proteins in immunity.

The above observation that TGFβ can directly induce tolerance in anti-tumour immune contexts is pertinent to the hypothesis that soluble mediators within tumours are capable of enhancing or abrogating vital anti-tumour immune responses. There is amassing evidence that WFDC family proteins especially SLPI, elafin, and ps20 possess immuno-modulatory functions which may have important implications within the tumour microenvironment. It is now well understood that tumours and the associated stromal tissues manipulate their environment to suppress the host anti-tumour immune response leading to a failure of anti-tumour immunity and progressive disease (Ganss and Hanahan, 1998, Yigit et al., 2010, Belladonna et al.,

2008). Furthermore we have seen that ps20 and WFDC proteins are indeed commonly dysregulated in tumours. Here we will discuss the known immunomodulatory functions of SLPI, elafin and ps20 and the possible implications in the context of tumours.

There is emerging evidence that ps20 may possess intrinsic immuno-modulatory properties. In man, ps20 is expressed in CD4 T cells and increased ps20 expression correlates with ICAM-1 expression and increased propensity to form cell-to-cell conjugates (Alvarez et al., 2008). Observations from our laboratory also suggest that ps20 expression In CD4 T cell clones is inversely correlated with the ability of those cells to produce IFNγ upon CD3/CD28 induced IFNγ expression (Reading and Vyakarnam, unpublished data), which is suggestive that ps20 it may possess adaptive immune modulatory properties and may be a T cell-intrinsic regulator of immune activation. Further insights have been gleaned from the development of the WFDC1 null mouse. It was shown that ps20$^{-/-}$ animals were more susceptible to neutrophil invasion into the lung upon challenge by Murine Hepatitis Virus, and these mice showed significantly elevated chemokines CXCL1 and CXCL2 (Rogers et al., 2012). Ultimately, the infected ps20 null mice displayed higher titres of virus than did the control animals. In contrast, ps20 null mice subjected to influenza virus infection showed significantly increased viral titres at day 4 and macrophage infiltration into the lung was greatly increased (Ressler et al., 2014). In addition, this study demonstrated that embryonic fibroblasts taken from ps20 null mice expressed higher levels of the pro-inflammatory proteins MMP9 and Osteopontin. This response indicates that ps20 may play a protective role in some viral infections, possibly through the induction of certain inflammatory factors. Taken together then, these two studies suggest that ps20 has innate immune functions which can act in a context specific manner to regulate responses to viral responses, including the regulation of chemokines and the infiltration of immune cells. However, to date there is not enough

evidence to suggest a role for ps20 in modulating anti-tumour immunity. But it seems reasonable to speculate that ps20 has specific innate and possibly adaptive immune regulatory functions which may be pertinent to tumour biology.

Two recent papers have indicated that SLPI possesses the ability to modulate adoptive immune functions in the maintenance of mucosal tolerance (Samsom et al., 2007, Xu et al., 2007). Specifically, DCs from SLPI$^{-/-}$ knockout mice released more inflammatory cytokines and directed increased T cell proliferation following stimulation with LPS. Importantly, NFκB activation was lower in SLPI positive DCs. This is pertinent given the control the NFκB transcriptional program has on the innate immune response and subsequent adaptive immune interactions (Doyle and O'Neill, 2006). Suppression of an inflammatory program may have knock-on effects on natural killer cell and T cell activation and consequently the killing of tumour cells. Therefore SLPI expression at cancer sites may suppress immune activation as it does at mucosal surfaces, and contribute to immune tolerance of the tumour. It is understood that factors produced by the tumour can affect the maturation of antigen presenting cells, resulting in poor T cell activation and proliferation (Gabrilovich et al., 1996, Zou et al., 2001). In one study, CM from SLPI treated monocytes was shown to inhibit CD4 T cell proliferation. Interestingly, a cohort of Columbian HIV-1 controllers who showed reduced expression of immune activation markers and higher T cell count also produced more SLPI, suggesting a correlation of SLPI expression with reduced adaptive immune activation (Taborda et al., 2012). Consequently, it holds that SLPI may contribute to the immunosuppressive milieu within the tumour microenvironment, and which may be advantageous for tumour growth in certain tumour types.

The role of elafin in innate and adaptive immunity is somewhat harder to dissect. Contrary to the proposed anti-inflammatory role of SLPI, a number of studies have

shown an increased inflammatory response; increased recruitment of neutrophils and other immune cell types; and increased clearance of infectious agents when human elafin is over expressed in murine models. But these studies are extremely difficult to interpret given the lack of an elafin gene in mice (Simpson et al., 2001a, Simpson et al., 2001b, Sallenave et al., 1994, Roghanian et al., 2006, Wilkinson et al., 2009). Evidence in man shows that elafin expression is correlated with inflammatory cell numbers and is increased in suffers of farmers lung and psoriasis, two conditions which provoke an inflammatory T_H1 skewed immune responses (Tremblay et al., 1996, Schalkwijk et al., 1993). It is not clear however whether the increased elafin levels in these contexts serves to augment the T_H1 response or is simply concomitant with the inflammatory response, perhaps induced as a homeostatic mechanism. There is recent evidence to suggest that elafin may regulate NFκB signalling in similar ways to SLPI. One recent study showed that adenoviral elafin transduction reduced NFκB activation and the subsequent activation of downstream intracellular pathogen recognition factors (Drannik et al., 2012). This manipulation of NFκB activation may have effects in the tumour environment as we have discussed, however, until direct evidence in man of an immune modulatory function for elafin is demonstrated its potential to regulate anti-tumour immune responses when expressed in that context remains ambiguous.

To date then, work has shown that WFDC family proteins have the ability to regulate and inhibit facets of the innate and adaptive immune response which may be pertinent in the context of intra-tumoural immune-suppression and immune escape. Therefore it seems at the very least plausible that the expression of WFDC family proteins within the tumour microenvironment may be contributing to the immunosuppressive phenotype observed in many cancerous tissues, and that the pro-tumourigenic role exerted by WFDC proteins in the tumours discussed in the previous paragraphs may be linked to these immune modulatory functions.

Consequently, further studies to assess the contribution of these factors to the immune response in tumour systems are warranted.

1.4 Conclusions/Perspectives

Many studies have now shown that WFDC family proteins SLPI, elafin and ps20 are differently expressed in cancers relative to healthy tissue, and that in some cases, have tumourigenic functions which can lead to enhanced tumour growth, invasiveness and metastasis. However the biochemical regulation of these proteins is complex and their interactions with proteases and the ECM within tissues is likely to add a further level of complexity to the function of these proteins in health and disease. In addition, it has also become apparent that the WFDC family of protein are capable of manipulating innate-immune signalling processes and cellular immune responses, suggesting that within tumours they may have deleterious roles which lead to enhanced intra-tumoural immune suppression and evasion. If this is the case, WFDC family proteins may be targets for therapeutic intervention. Given the highly specific properties of individual tumours and tissues, the next generation of cancer therapies will likely be targeted at the molecular level to molecules of known detriment to host clearance of the tumour challenge. In certain tumours, blockade of WFDC family molecules may serve a dual purpose, to abrogate the directly tumourigenic functions of the protein, and to block the anti-immune functions, which potentially act upon innate and adaptive immune cell types within the tumour microenvironment. As such, a better understanding of these complicated but important molecules may shed light on aspects of tumour growth regulation, tumour-stromal interactions, and tumour immune escape.

1.5 Aims

Work undertaken in this thesis intends to examine and elucidate the properties and functions of ps20, with particular focus on the role of ps20 in the prostate, such that its frequent down regulation in tumours of that organ may be better understood. The use of ps20 as a component of a locally delivered cytotopic therapy has been suggested due to its previously described growth inhibitory properties on prostate cancer cells (Larsen et al., 1998). However a far greater understanding of the biochemical properties of ps20 is required before this molecule could be utilized therapeutically. Previous attempts to purify ps20 have relied on the production of large volumes of conditioned media (CM) from urogenital sinus mesenchyme cells, followed by a complex and laborious protocol involving numerous fast protein liquid chromatography, and high pressure liquid chromatography steps. In addition, the use of C-terminal tags (e.g. HIS tag purification by Nickel chelate) has resulted in pure but non-functional protein.

As such our first aim is to investigate the use of immune-affinity chromatography using an anti-ps20 antibody-conjugated column to purify ps20 as it is expressed both natively, for example by HeLa cells, and from a recombinant plasmid. These studies will use the range of ps20 specific antibodies available to us to perform a series of western blotting and ELISA based assays to characterise the protein produced by purification studies and to assay the results of subsequent downstream investigation. We will then undertake a characterization of the biochemical characteristics of ps20, with special focus on characteristics previously observed in fellow WFDC family proteins. For example, interactions with ECM proteins, transglutaminase, glycosaminoglycans and cathepsin family proteases will be investigated and we will interrogate the functional consequences of such interactions. Using CM and purified

ps20 protein, we will investigate the binding of ps20 to heparin and physiologically relevant glycosaminoglycans heparin sulphate, and chondroitin sulphate A and C.
In the second part of this thesis we will attempt to further elucidate the function of ps20 using models of ps20 expression *in vitro*. Using commonly studied healthy and tumour derived prostate cell lines we aim to follow the work of Rowley et al and others in studying the effect of ps20 expression on the growth of these cell lines. We will clone and express WFDC1 mRNA species in numerous prostate cancer cell lines of both epithelial tumour, and prostate stromal origin. Subsequently we aim to characterize the effects of ps20 and attempt to investigate the mechanisms of ps20 dependent effects.

Subsequently we aim to study the effect of ps20 expression on gene expression in the aforementioned cells. Using a combination of transcriptome microarray and multiplex ELISA technology we can interrogate ps20 induced changes in the expression of cellular and secreted factors. Further to this, we will investigate the effect of ps20 expression *in trans*, using CM from ps20 expressing cells as a model of stromally expressed ps20, and its effect on neighbouring epithelial/tumour tissues.

Lastly, this thesis will attempt to use a cellular *in vitro* model of stromally expressed ps20 to investigate the role of ps20 expression on immunity within the tumour. The rational for this experimental approach is twofold: i) SLPI has been shown to have potent anti-proliferative effects on T cells, and ii) T cell responses are required for effective anti-tumour immunity. Our aim therefore is to assay the effect of ps20 expression in prostate stromal cells on T cell responses, using readouts of T cell proliferation, activation and cytokine secretion to characterize the immune regulatory function of ps20.

Our overall aim is to investigate and clarify the biochemical properties and functional effects of ps20 when expressed in the prostate in order guide future studies which may seek to utilise ps20 therapeutically for its growth suppressive and immunomodulatory effects.

Chapter 2. Materials and Methods

2.1 Materials and reagents

2.1.1 Plasticware

6, 12, 24, 48, 96 -well tissue culture plate (Costar corning).

96-well U-bottom tissue culture plate (Costar corning).

25cm^2 / 75cm^2 tissue culture flasks (Costar corning).

10cm culture dishes (Costar corning).

1.5ml Cyrovials™ (Costar corning).

5ml, 10ml and 25ml serological pipettes (Costar corning).

5ml FACs tubes (Beckton Dickenson).

Syringe filters 0.22μm/0.4μm (Triple Red).

ART filter tips, 1000, 250, 20ul (Thermo scientific).

Glasstic Slides (Hycor KOVA, distributed by Fisher Scientific, USA).

Vacutainer™ tubes (BD, Biosciences, San Jose, CA).

1.5ml micro-centrifuge (Eppendorf) tubes (VWR, UK).

15ml and 50ml Falcon tubes (Costar corning).

96-well flat bottom ELISA NUNC-IMMUNO PLATE F96 MAXISORP (NUNC, Thermo Fischer Scientific, USA).

2.1.2 Molecular Biology Reagents

Agarose (molecular biology grade) (Sigma-Aldrich).

Ampicillin (Sigma-Aldrich).

Dimethyl sulfoxide (Sigma-Aldrich).

Ethanol (Sigma-Aldrich).

Methanol (Sigma-Aldrich).

DNA ladder 100bp-1000bp (New England Biolabs).

Ethidium Bromide (Sigma-Aldrich).

LB broth (Sigma-Aldrich).

LB agar (Sigma-Aldrich).

Nuclease Free water (Qiagen).

All Primers (MWG Biotech).

RNeasy RNA isolation kit (Qiagen).

T4 DNA Ligase (New England Biolabs).

EDTA (Sigma-Aldrich).

Tris-(hydroxymethyl)-aminomethane (TRIS) (Sigma-Aldrich).

Agarose (Invitrogen Life Technologies).

E.coli stain JM109 competent cells (Promega).

SOP media (Life Technologies).

XhoI Restriction Enzyme (New England Biosciences).

EcoRI Restriction Enzyme (New England Biosciences).

RNeasy Extraction Kit (Qiagen).

Gel Extraction Kit (Qiagen).

One-step RT-PCR kit (Qiagen).

Taqman PCR mix (Applied Biosystems, Life Technologies).

High-Capacity cDNA Reverse Transcription Kit (Applied Biosystems).

2.0 mil polyester sealing film, non-sterile (Elkay).

Ethydium Bromide (Sigma Aldrich).

2.1.3 Tissue Culture and cell biology reagents

Dulbeco's modified eagle medium (DMEM) + GlutaMAX™(Gibco, Invitrogen Life Technologies, Paisley)

RPMI1640 GlutaMAX™ + 1.25mM HEPES (Gibco, Invitrogen Life Technologies, Paisley)

X-vivo™ 15 medium (Lonza, Walkersville, MD, USA)

Gentomycin (Sigma-Aldrich).

Fungazone™ (Gibco, Invitrogen Life Technologies).

Phosphate Buffered Saline (Gibco, Invitrogen Life Technologies).

Optimem™ (Gibco, Invitrogen Life technologies)

Trypan Blue (Sigma-Aldrich).

TrypLE express (Gibco, Invitrogen Life Technologies).

Foetal Calf Serum (Gibco, Invitrogen Life Technologies).

Human Serum (Lonza)

BD Matrigel™ Basement Membrane Matrix (BD Biosciences)

Cell Proliferation Dye eFluor® 670 (eBioscience)

CellTrace™ CFSE Cell Proliferation Kit (Invitrogen Life Technologies).

Lipofectamine 2000 (Invitrogen Life Technologies)

Celltitre96® Aqueous One step solution cell proliferation reagent (Promega).

Dynabeads® Untouched™ Human CD4 T Cells Kit (Invitrogen, Life Technologies).

Propidium Iodide (Sigma Aldrich).

RNase A (Applichem GmbH, distributed by VWR. UK).

CD3/CD28 T cell activator Dynabeads (Life Technologies)

Brefeldin A (Sigma-Aldrich)

Formalin (37% Formaldehyde), (Sigma-Aldrich).

GeneIn® Transfection Reagent (AMS Biotechnology Ltd, Europe)

β-galactosidase activity staining kit (Millipore)

2.1.4 Antibodies and Proteins

Human ps20-GST fusion protein (Proteintech).

Tissue Transglutaminase from Guinea Pig Liver (Sigma-Aldrich).

Human Cathepsin L (R&D Systems).

Human Cathepsin B (R&D Systems).

Anti-V5-HRP antibody (Invitrogen Life Technologies).

AnnexinV-PE (eBiosceince).

Neutralising anti-SerpinF1/PEDF Clone H-125 (Santa Cruz Biotechnology).

Neutralising anti-Human IL-6 MAb Clone 1936 (R&D Systems Europe).

Neutralising anti-TGFβ (R&D Systems Europe).

Fibronectin from human plasma (Sigma-Aldrich).

Polyclonal antibody, anti-rabbit IgG HRP-conjugated, host goat (AbD Serotec).

Polyclonal antibody, anti-mouse IgG HRP-conjugated, host rabbit (AbD Serotec).

Monoclonal antibody, Mouse IgG1, clone NCG01 (Fisher Scientific).

Antibodies used in fluorescence-associated cell sorting (FACS) experiments are listed in Table 2.1.

Anti-ps20 antibodies 650, 651, 5B9, 1G7, and 254.

Table 2.1 Antibodies used for FACS staining experiments

Antigen	Fluorophore	Clone	Manufacturer
CD3	PE	HIT3α	Biolegend
CD8	PE-CY7	OKT8	Biolegend
CD3	FITC	HIT3α	SCBT
CD4	APC	RPA-T4	Biolegend
IL-2	PERCP-CY5.5	MQ1-17H12	Biolegend
IFNγ	PE-CY7	48.B3	Biolegend
CD69	PE-CY7	FN50	Biolegend
CD25	APC	M-A251	Biolegend
CD8	PERCP	OKT8	Biolegend

2.1.5 Biochemistry reagents

Phosphate buffered saline x 1 sterile (PBS) Gibco, Invitrogen Life Technologies)

Phosphate buffered saline x 10 sterile (PBS) Gibco, Invitrogen Life Technologies)

NHS activated columns (GE healthcare)

HiTrap Heparin columns 1ml (GE Healthcare).

Glycine (Sigma-Aldrich).

Heparan-sulphate from shark cartilage (Sigma Aldrich).

Chondroitin sulfate C sodium salt from shark cartilage (Sigma Aldrich).

Chondroitin sulfate A sodium salt from bovine trachea (Sigma Aldrich)

Calcium chloride ($CaCl_2$) (Sigma Aldrich).

Dithiothreitol (DTT) (Sigma Aldrich).

Lumitein protein stain (Biotium, UK)

NuPage protein gels, Bis-Tris 12%, 1.5mm thickness 10/12 and 15 well formats (Life Technologies).

Tween20 (Sigma-Aldrich)

Bovine Serum Albumin (BSA) (Sigma-Aldrich).

NuPage LDS reducing buffer (Invitrogen Life Technologies).

1-Step Ultra TMB-Blotting Solution (HRP substrate) (Thermo-Fisher, UK)

1-Step Ultra TMB-ELISA Substrate Solution (HRP substrate) (Thermo Fisher, UK)

Sodium Chloride (NaCl) (Sigma-Aldrich).

Sulphuric acid (Sigma-Aldrich).

NuPage MOPS buffer x 20 (Invitrogen, Life Technologies)

Bench Mark pre-stained protein ladder (Invitrogen, Life Technologies).

Protran nitrocellulose membranes (Whatman, GE Healthcare)

Millicoat™ ECM Screening Kit (Millipore)

2.1.6 Plasmids

pBK-CMV expression vector.

Expresses the native untagged cDNA of WFDC1 in mammalian cells (A kind gift of David Rowley, Stratagene, USA)

pMIGR1-eGFP

Retroviral plasmid pMIGR1-eGFP encodes a multiple cloning site (MCS) upstream of enhanced green fluorescent protein (eGFP) separated by an internal ribosome entry site (IRES). The gene of interest is cloned into the MCS and the IRES ensures bicistronic expression of the eGFP reporter gene independently of the gene of interest.

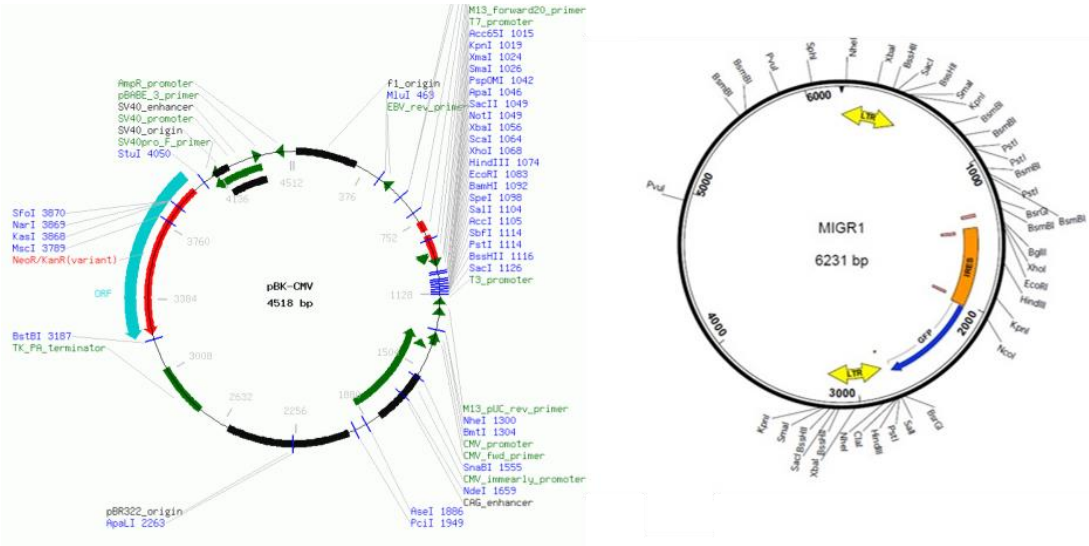

Figure 2.1 plasmid maps of pBK-CMV and MIGR1

2.1.7 Commercial Kits

QIAquick™ gel extraction kit (Qiagen)

Miniprep™ kit (Qiagen)

Endofree Maxiprep™ kit (Qiagen)

Quantitect™ RT-PCR kit (Qiagen)

RNeasy™ extraction kit (Qiagen)

One-step RT-PCR kit (Qiagen)

IL-6 duoset™ ELISA kit (Rnd Systems)

Multiplex (eBiosciences).

SilverXpress® Silver Staining Kit (Invitrogen Life Technologies).

Untouched CD4 T cell isolation kit (Life Technologies).

FoxP3 intracellular staining kit (eBiosciences)

2.1.8 Buffers

The composition of buffers used in this thesis that are not part of a commercial kit are described below.

SDS-PAGE/Western Blot

Running Buffer - 1x NuPage MOPs buffer (2.5mM MOPS, 2.5mM TRIS base, 0.01% SDS, 0.05mM EDTA in ddH_2O, pH 7.7)

Transfer Buffer - 200mM Glycine, 25mM Tris Base, 10% Methanol, 0.1% SDS in ddH_2O.

Wash Buffer - 1% BSA W/V, 0.2% Tween 20 W/V in PBS.

Ps20 ELISA

Wash buffer - 0.2% Tween in PBS

Blocking buffer - 1% BSA W/V in PBS

Antibody binding buffer - 0.4% Tween in PBS + 1% BSA

FACS staining

Cell staining buffer +2% FCS, 2mM EDTA, +0.01 NaN_3 in PBS.

Fixing Buffer - 4% v/v formalin in PBS.

Agarose Gel running buffer

40mM Tris acetate, 1mM EDTA in ddH_2O, pH 8.3

Affinity chromatography

Binding buffer - 50mM Tris in ddH_2O

Heparin column elution buffer - 50mM Tris, 1M NaCl in ddH_2O.

1G7 column elution buffer - 50mM Tris, 200mM Glycine in ddH_2O, pH 2.

2.1.9 Cell Culture Media and Serum

Media used in day-to-day culture of cell lines and primary human cells are described below and specific ingredients are prepared as described. Components are expressed either as a percentage (v/v) or by concentration (e.g. µg/ml).

Foetal Calf Serum (FCS): Fetal Calf Serum was heat inactivated (HI) by agitated incubation at 56^0C for 1h in a water bath followed by storage in appropriately sized aliquots at -20^0C.

Human AB serum: Serum was purchased from PAA laboratories (Yeovil), heat inactivated by agitated incubation at 56^0C for 1h in a water bath followed by storage in appropriately sized aliquots at -20^0C. Human serum is abbreviated to HS henceforth.

DMEM complete medium: Dulbeco's modified eagle medium + GlutaMAX™ containing 4.5g/L D-glucose and pyruvate was supplemented with 250µg/ml Gentomycin and 10% HI FCS.

RPMI complete medium: RPMI1640 GlutaMAX™ containing 1.25mM HEPES, (Invitrogen Life Technologies) supplemented with 250µg/ml Gentomycin and 10% HI FCS.

X-vivo medium: X-vivo™ 15 medium was supplemented with 250µg/ml Gentomycin.

2.1.10 Immortalised/Established Cell lines.

PC-3 A cell line derived from bone metastases of a 62yr old male with grade IV prostate adenocarcinoma. This cell line is used in studies relating to prostate tumourigenesis. This androgen independent cell line was first established in 1979 and is one of the most commonly used cell lines for in studies relating to prostate tumourigenesis (Kaighn et al., 1979). PC-3 cells were grown in 10cm dishes in ≈12mls of RPMI complete media with 10% (v/v) FCS. Cells were frozen and thawed as described and cultured for 3-4 days up to a maximum of 10 passages. Obtained from ATCC.

LNCaP Cells were originally isolated from the left supraclavicular lymph node of a 50 year old caucasian male with prostate carcinoma. This is an androgen dependent cell line established in 1977 is a standard tool for studies relating to prostate tumourigenesis and growth (Horoszewicz et al., 1980). LNCaP cells were grown in 10cm dishes in ≈12mls of RPMI complete media with 10% (v/v) FCS. Cells were frozen and thawed as described and cultured for 3-5 days up to a maximum of 10 passages. Obtained from ATCC.

WPMY-1 A prostate stromal myofibroblast cell line isolated from a histologically normal 54 year old man and immortalised with SV40 (Webber et al., 1999). This cells

line is taken from the peripheral zone of the prostate and is useful in studying paracrine stromal-epithelial interactions. WPMY-1 cells are cultured in 10cm dishes in ≈12mls DMEM complete media + 10% (v/v) FCS. Cells are frozen and thawed as described, cultured for 3-4 days up to a maximum of 10 passages. Obtained from ATCC.

PNT2 Established by immortalisation of normal adult prostatic epithelial cells by transfection with a plasmid containing SV40 genome with a defective replication origin. The primary culture was obtained from a prostate of a 33 year old male at post mortem. PNT2 cells contain the SV40 genome and express large T protein. Obtained from ATCC.

HeLa A commonly used cell line and the first cell line successfully grown in the laboratory. Originally isolated in the 1951 (Scherer et al., 1953) from an unusually aggressive cervical carcinoma. This cell line is used as model in a number of branches of cellular biology due to their rapid proliferation rate and ease of culture and transfection efficiency. They display a strange morphology. A kind gift of Professor Michael Malim.

293T An immortalised Human embryonic kidney cell line stably expressing the SV40 Large T antigen. This cell line is commonly used experiments involving transient expression of transfected cDNAs due to the cells high transfection efficiency. A kind gift of Professor Mike Malim.

2.2 Methods

2.2.1 Cell culture

2.2.1.1 Thawing of cryopreserved cells.

Vials were taken from -80^{0}C freezer or liquid nitrogen and transferred to a 37^{0}C water bath until defrosted. Cells were then taken into 5-10mls of appropriate complete media+10% FCS in a 15ml falcon tube to dilute out DMSO, and centrifuged at 200xg for 5 mins to pellet cells. Cells were then resuspended in complete media and transferred to culture vessels. Cells were cultured for at least 48h before being used in assays.

2.2.1.2 Culture of adherent cell lines.

All adherent cell lines were grown routinely in 10cm dishes or 75cm^2 flasks depending on the number of cells needed for a given series of experiments. Cells were usually seeded at 10^6 cells in 12mls or 25mls of complete media+10% FCS depending on the culture vessel. Cells were grown at 37^{0}C in a 5% CO2 humidified incubator (hereon referred to as 37^{0}C/5%) for the indicated time or until 90-100% confluent. If cultured from a low density for an extended period (such as following thawing of limited number of cells) culture medium was changed every 3-4 days. Once cells reached an appropriately level of confluency they were passaged by removing media and incubating cells with 2-5mls of TrypLE™ express detachment reagent (preheated to 37^{0}C) for ≈5 mins or until cells were detached. Cells were then washed in complete media to neutralise the trypsin analogue reagent. Following centrifugation cells were counted, resuspended in the appropriate volume of complete media, and seeded as described.

2.2.1.3 Cryopreservation of cell lines.

For long term storage, cells were resuspended in ice-cold FCS + 10% dimethyl sulfoxide (DMSO) at a cell density between 10^6-10^7/ml. The resulting cell suspension (0.5ml-1ml) was transferred to cryovials™ (Corning) which were immediately placed on ice until transferred to the -80^{0}C freezer. Vials were then stored at -80^{0}C or for extended periods >6 months in liquid nitrogen.

2.2.1.4 Peripheral blood mononuclear cell (PBMC) isolation.

Blood samples were drawn from healthy donors from within KCL into 9ml heparinised Vacutainer™ tubes. Samples were diluted 1:1 with Hanks Balanced Salt solution (HBSS, GIbco, Invitrogen Life Sciences). PBMCs were isolated using high speed density centrifugation. Blood /HBSS was then layered gently on top of Lymphoprep™ (d=1077g/cm3), at a 1:2 Lymphoprep to Blood/HBSS ratio. Tubes were then centrifuged for 20 mins at 1000G with a minimal rate of deceleration. PBMCs were extracted from the resulting interphase buffy coat using a 5ml Pasteur pipette and washed 1:3 in RPMI complete media +10% human serum to dilute remaining lymphoprep. Washing was performed twice (i) at 200xg for 5 mins to remove low weight platelets and (ii) at 300xg to remove all remove remaining traces of lymphoprep™. Cells were resuspended in RPMI complete media+10% human serum and used immediately (within 4 h) or cryopreserved as described. All steps were performed in sterile conditions at room temperature.

2.2.1.5 CD4+ T cell isolation

CD4+ T cells were negatively isolated from whole PBMCs using the Dynabeads® Untouched™ Human CD4 T Cells isolation kit (Invitrogen Life Sciences). This

process uses supermagnetic polymer beads (1µm diameter) coated with human anti-mouse IgG Fc-specific antibodies. PBMCs are ligated to a mixture of mouse IgG antibodies: CD8, CD14, CD16 (for CD16a and CD16b) CD19, CD36, CD56, CDw123, and CD235a, which bind to target cells expressing these antigens. These cells are then removed from the milieu by incubation with the magnetic beads. The supernatant remaining therefore contains only CD4+ T cells, which lack the specific cellular markers listed.

Prior to the isolation procedure all reagents with the exception of the PBMCs were chilled on ice. Freshly isolated PBMCs are resuspended in PBS+1% HS, 500µl for every 10^7 PBMCs used and transferred to 15ml falcon tube. 100µl of antibody mix and 100µl of HS are then added for every 10^7 PBMCs and the mixture is incubated with gentle rotation for 20-30 mins at 4^0C to allow the antibodies to ligate to their respective cell surface antigens. Following ligation of the antibody mixture, cells are washed once with 5mls of ice cold PBS+1%HS and pelleted by centrifugation in order to remove un-ligated antibodies. Cells were resuspended in 1ml PBS+1%HS for every 10^7 cells. 1ml Dynabeads® were washed twice by adding 5 volumes of PBS+1%HS and holding against a magnet for 2 mins until beads had adhered to the tube wall. The remaining supernatant was and following removal of the magnet washing was repeated. Washed beads were then resuspended to the original volume with PBS+1%HS. These beads are then added to the washed and resuspended PBMC/ligated antibody mix and incubated at room temperature for 20 mins with gentle rotation to allow antibody-bead ligation to take place. Following the ligation of the beads to the antibody coated cell surface, negative isolation of CD4 T cells was performed by holding the resulting solution to a magnet for 5 mins. Once the beads and adjoining cell mixture was adhered to the side of the tube the supernatant was removed. This resulting suspension was counted and resuspended in RPMI complete

media+10% HS. Staining for purity of CD4+ve T cells was subsequently performed and consistently found to be ≈95%.

2.2.1.6 Harvesting conditioned media from WPMY-1 cells.

Batches of WPMY-1 transduced cell CM were collected from cells seeded in 75cm^2 flasks in a volume of 25mls of complete media. 10^6 cells were seeded, and CM was collected 72h after seeding. Where CM was required in multiple conditions, e.g. developed in the presence of a COX-2 inhibitor, cells seeded in multiwell plates and the ratios of cell number seeded, surface area and volume of media were kept the same as with 75cm^2 flasks. Following collection of CM, media was clarified by centrifugation at 1000g for 10 mins, aliquoted in 1.5 ml Eppendorf tubes and stored at -80ºC.

2.2.2 Cellular Assays

2.2.2.1 Viability/MTS assay.

Proliferation and cell viability can be measured by using reagents which undergo a colourimetric catalysis through cell-metabolic processes. MTS is one such reagent. The Celltitre96® Aqueous One step solution cell proliferation reagent (Promega) contains a tetrazolium compound [3-(4,5-dimethylthiazol-2-yl)-5-(3-carboxymethoxyphenyl)-2-(4-sulfophenyl)-2H-tetrazolium, inner salt; MTS] and an electron coupling reagent (phenazine ethosulfate; PES) which when cultured with metabolically active cells results in the generation of a formazan product which absorbs light at a wavelength of 490nm. The absorbance in any given well following incubation with the reagent is directly proportional to the number of living cells in culture. The reagent was thawed and aliquoted into 1ml aliquots to reduce the

number of freeze thaw cycles the reagent would be subjected to. Before each experiment an aliquot was thawed in a 37^{0}C water bath and kept in the dark at RT until use.

For individual experiments, cells were seeded at 2000-5000 cells/well in 100µl of complete media +/-FCS in 96 wells plates for the indicated time period. After this time 15µl of Celltitre® reagent was added and the plate was incubated at 37^{0}C/5% and readings were taken at specific time points, usually 1, 2 or 4h, using a colorimetric plate reader (Biorad, USA).

2.2.2.2 Cell Cycle Staining/Analysis.

Propidium iodide (PI) staining of nuclear chromatin was used to quantify the number of cells from a given population in each respective phase of the cell cycle. 5x10^4 cells were seeded in 12 well plates usually in triplicate. After treatment cells were cultured for 48/72h as indicated and harvested with TrypLE™. Cells were transferred to FACs tubes containing PBS+2% FCS to neutralise the TrypLE™ and centrifuged at 1000xg for 5 mins. Media was removed by flicking and cells were resuspended by running individual FACS tubes across a draining board grate. Tubes were then individually vortexed as 400µl of 70% ethanol in ddH_2O was added to prevent cell clumping. Cell fixing was for 30 mins at RT or for <1 week at 4^{0}C.

For staining cells were once again centrifuged at 1000xg for 5 mins and fixing buffer was flicked off. Cells were resuspended as described. Staining solution was 0.05% Triton-X in PBS + 50µg/ml PI+100µglml RNase A (Both Sigma-Aldrich). 500µl of staining solution was added to each tube and incubated in the dark at 37^{0}C for 45 mins. In this time RNaseA digests the cells' RNA content which is necessary as PI binds to both DNA and RNA and intact RNA remaining in the sample will invalidate

the result. Following staining cells are centrifuged once more and remaining staining buffer flicked off and cells resuspended. Cells are then acquired using the FACS canto II. Data was analysed using the 1D cell cycle analysis feature in FlowJo 7.6.4.

2.2.2.3 Annexin V staining for apoptosis.

Induction of apoptosis was investigated using annexin V conjugated to FITC. 3-6x10^4 cells were seeded in 12 well plates in complete medium + 10% FCS. Cells were treated for the appropriate time (e.g. 24-72h) and harvested with trypsin as discussed. Cells were transferred to 5ml polystyrene tubes (BD biosciences) and centrifuged at 2000xg for 5 mins. Media was poured away and cells were washed once in 500µl Annexin V binding buffer (BD Biosciences) and again centrifuged. Excess buffer was poured off, and cells were resuspended in remaining buffer (≈100µl). 2µl of Annexin V-FITC were added and 4µl of PI solution (50mg/ml stock) and cells were incubated for 20 mins on ice in the dark before adding a further 100ul of PBS and acquiring using a FACS Canto II.

2.2.2.4 Purified T cell CFSE proliferation assay.

Purified CD4 T cells were purified as described and resuspended in 10^7 cells/ml in PBS. CFSE was added at 5µM and incubated for 5-10 mins at 37ºC. Cells were then washed in complete RPMI media and resuspended at 2x10^6 cells/ml in x-vivo. Cells were plated at 10^5/well in 96 well U-bottom plates in the relevant conditions and stimulated with 0.06µl of anti-CD3/28 dynobeads™ (Invitrogen Life Sciences). Following 6 days of proliferation cells were transferred to FACS tubes and assayed for CFSE dilution in the FITC channel of a FACS CantoII.

2.2.2.5 T cell proliferation assay using whole PBMCs.

PBMCs were purified as described and resuspended in 10^7 cells/ml in PBS. Either CFSE or eFluor605 reagent (eBioscience, UK) was added at 5µM and incubated for 5-10 mins at 37ºC. Cells were then washed in complete RPMI media and resuspended at $2x10^6$ cells/ml in x-vivo. Cells were plated at $5x10^4$/well in 96 well U-bottom plates in the relevant conditions and stimulated with a variable concentration of anti-CD3/28 dynobeads™ (Invitrogen Life Sciences). Following 6 days of proliferation cells were stained for CD3 and CD8 as described and transferred to FACS tubes and assayed for CFSE dilution in the FITC channel of a FACS CantoII.

2.2.2.6 Analysis of T cell activation

Whole PBMCs were purified and seeded $2x10^5$ cells in round well 96 well plates. Conditioned media or purified protein was added and the final volume made to 200µl with x-vivo media. Cells were incubated for the indicated time and then stimulated with anti-CD3/28 beads at a bead to cell ratio of 1 bead to 5 cells. Cells were then stained for CD3, CD8, CD69 and CD25 and fixed as described and analysed on the FACS canto II.

2.2.2.7 Cell staining.

Cells were transferred to FACS tubes and washed with 2mls of wash buffer (PBS + 2% FCS + 0.05% sodium azide) and centrifuged (5 mins at 1000g). Cells were resuspended by agitation and the relevant Ab cocktail was added from the list given in table 2.1. Cells were incubated in the dark for 30 mins and washed and centrifuged again. Excess buffer was removed and cells were resuspended by agitation. Cells

were then acquired by FACS or fixed by addition of an equal volume of 4% paraformaldehyde and stored in the dark at 4ºC until acquisition.

2.2.2.8 Intracellular FACS staining.

IC staining was performed using the FoxP3 staining kit (eBiosciences). Whole PBMCs were isolated and seeded at $5x10^5$ in 48 well plates in x vivo media and 50% WPMY-1 CM. Cells were treated with 1:2 anti-CD3/28 dynabeads™ (Life technologies) for 48h and 5µg/ml brefeldin A (Sigma Aldrich) was added 16h prior to harvesting. Cells were washed with FACS wash buffer and stained with CD3 and either CD4 or CD8 antibody. Cells were washed and then fixed. Cells were washed in permeabilisation buffer and the excess removed. Antibodies to the relevant cytokines were added and incubated at room temperature for 30 mins. Cells were again washed with FACS buffer and 200µls of fix buffer was added. Cells were stored at 4ºC in the dark until acquisition on a FACS canto II (BD biosciences).

2.2.2.9 Cell Transfection.

For ps20 purification:

Transfection of 293F cells in 30ml conical flasks 1µg of pBK-WFDC1 was combined with 1ug of PEI or Lipofectamine in 100µl of optimum™ and incubated for 20mins. 1µg of DNA was used per 10^6 cells. The mixture was added to cells drop wise and cells were cultured for different time points to express protein as required.

Alternatively, 293T cells were transfected in $72cm^2$ plates. 1ug DNA /10^6 cells was used and media was changed to DMEM/F-12 after 6 hrs. Cells were cultured to

express protein for maximum 48h as 293T cell viability decreases rapidly in serum free media.

For the transient expression of ps20 protein species in 293T cells to generate conditioned media (CM) a multiwell transfection assay was optimised using the GeneIn® reagent. The afternoon prior to the day of transfection cells were seeded in 6 well plates at $4x10^5$/well. The following day, media was replaced. The transfection reagents were prepared for each well according to the schema presented in table 2.2 and incubated together at room temperature for 15 mins. 200µl of each mixture was then added dropwise to 293T cells. CM was collected after 48h, clarified, filtered and stored at -80ºC. Where cells where transfected in larger vessels all experimental components including, volume of media added, number of cells seeded, and quantities of transfection agents used, were scaled up in proportion to the surface area of the vessel used.

Table 2.2 Preparation of GeneIn™ for transfection

optimum	to 200µl
plasmid DNA	2µg
Blue reagent	8µl
Red reagent	4µl

2.2.2.10 β-galactosidase activity staining

Cells seeded in 24 well plates were first fixed using 4% PA. The x-gal substrate is then added for 24h at 37ºC without CO_2 before photographing cells using a camera positioned to the eye piece of a light microscope.

2.2.3 Assays using bacterial cells

2.2.3.1 Transformation of Competent Bacteria

Bacteria were thawed on ice and 20µl per condition was added to pre-chilled tubes. 1-100ng of DNA was added and incubated on ice for 30 mins. Tubes were heat shocked for 1 minute at 37ºC and returned to ice for a further 5 mins. 200µl of SOC media was added and bacteria were incubated with agitation at 37ºC for 1 hour before spreading onto agar plates.

2.2.3.2 Bacterial culture

Transformed bacteria were selected by overnight growth on agar plates. Agar plates were produced by adding 0.035% (w/v) LB agar to $_{dd}H2O$ water in sterile bottles, followed by autoclaving. While still warm, ampicillin was added to a final concentration of 100µg/ml. 25mls of molten agar was then added to 10cm dishes, left to solidify, and stored at 4ºC for no more than 2 weeks. Streaking bacteria was performed by adding 200ml of bacteria in SOP media to the centre of an agar plate and then spreading evenly across the surface using a glass rod. These plates were then inverted and incubated over night at 37ºC. Individual colonies were picked by touching with a sterile pipette tip and then placing into a 30ml universal tube containing 5mls of LB broth containing 100µg/ml ampicillin. Clones were cultured for 4-6hours at 37ºC in a shaker, and then 1ml of selected cultures was transferred to a sterile culture flask containing 200mls of LB broth +100µg/ml ampicillin. These flasks were cultured overnight. Bacteria was pelleted by centrifugation at 1000g for 20 mins and then processed immediately or frozen at -20ºC for no more than two weeks.

2.2.4 Molecular Biology techniques

2.2.4.1 RNA purification

Total RNA was isolated from cell cultures using Qiagen™ RNeasy mini (1x105<5x106) kit. Pelleted cells were resuspended in 350ul RLT lysis buffer and homogenised using the Qiashredder™ spin column (Qiagen) and DNA removed by use of the RNAse-free DNAse set (Qiagen) according to the manufacturer's instructions. Eluted RNA was quantified using a Nanodrop™ spectrophotometer and protein contamination determined via the 230:280nm ratio. RNA was either reverse transcribed immediately or stored at -80ºC.

2.2.4.2 One step RT-PCR

Following RNA isolation, RT-PCR was performed using the one-step RT-PCR kit (Qiagen, UK). The assay used 0.2µg of template RNA and 0.6µM of the relevant primer (WFDC1 or GAPDH, MWG Biotech, UK). Q solution supplied with the kit was added (10% of total volume) to remove secondary structure in the GC-rich target sequence. Primers used to amplify WFDC1 or GAPGH control sequences are shown in Table 2.3. Reactions were made up to 50µl with nuclease free water. Amplification was performed in an Eppendorf gradient thermocycler (Eppendorf, UK) as follows Hotstar Taq initiation at 95ºC for 15 mins, denaturation at 94ºC for 30 sec, annealing at 56ºC for 30 sec and extension at 72ºC for 1 min for 35 cycles, followed by final extension at 72ºC for 10 min. Products were stored at -20ºC until needed or visualised on an agarose gel as described.

Table 2.3 Primers used in RT-PCR

WFDC1 Fwd	5’ CGACCTTGACCATCTTTGGA 3’
WFDC1 Rev	5’ GCTTACTGAAAGTGCTTCTG 3’
GAPDH Fwd	5’ AGGTCGGAGTCAACGGATTTG 3’
GAPDH Rev	5’ GTGATGGCATGGACTGTGGT 3’

2.2.4.3 Agarose Gel Electrophoresis

Agarose gels were prepared by adding powdered agarose to distilled water, usually 2% (w/v), and heating for 1min in the microwave. Once melted, 5µl ethidium bromide was added per 100mls, and a gel was poured and left at room temperature to solidify. Samples were prepared with loading buffer (1:5 ratio) and added to wells. Gels were run at 100V until an adequate separation had been achieved and the relevant band were excised using a scalpel and a flat UV lamp.

2.2.4.4 Taqman qPCR

200ng-1µg of RNA was reverse transcribed in an Eppendorf™ Mastercycler Gradient thermocycler using the High capacity reverse transcription Kit (Applied Biosystems) according to the manufacturer’s instructions (RT was primed by random hexamers supplied) in a nuclease-free 96-well low profile PCR plate (Thermo, Fischer Scientific). cDNA was diluted in 3 volumes of nuclease free H2O (optimal dilution determined previously by Dr James Reading) and stored at -20ºC or used directly in a qRT-PCR assay. Relative gene expression was performed using commercially available Taqman™ gene expression hydrolysis probe sets. The WFDC1 Taqman™ gene expression assay was custom designed by submission of a 3’ based amplicon (exons 4-6) to the Applied Biosystems Assays-by-Design™ service, using the Filebuilder 3.0™ software (Applied Biosystems) with the resulting assay spanning

exon boundaries (>1Kb intronic sequence) to avoid genomic DNA contamination and showed results matching previous qRT-PCR and RT-PCR assays described previously(Alvarez et al., 2008). Assay sequences FWD: 5' TCGCCCATCTGCTTGC 3', probe 5' FAM- GAGTCACCTTCTGGATATTCTTTGTAAAGT -NFQ 3', REV: 5' GTGGGCAGTGCGTCAAG 3'. GAPDH was employed as a reference gene. Previous members of the laboratory had optimised the assay using time course gene expression studies with an index of multiple reference genes to validate results (β-actin, GAPDH, HPRT) and the experiments contained within this thesis used GAPDH as a reference gene as previous data had suggested this remains most stable under various tested treatments. Data analysis was performed using the SDS 2.3 Relative quantification software (Applied Biosystems) according to the manufacturer's instructions and the ΔΔCt method of relative quantification (ABI prism 7700 SDS User Bulletin 2-Applied Biosystems). However, relative copy number was also calculated to assess levels of transcripts using the 2-ΔCt method. Cycling conditions were set according to Taqman™ gene expression assays protocol (Applied Biosystems catalogue ref: p/n4333458) in a 10ul final volume containing 5ul dilute cDNA, 4.5ul Taqman™ universal PCR mix 141 with AMPErase (Applied Biosystems) and 0.5ul primer/probe Taqman™ gene expression assay (Applied Biosystems). RT-PCR, no template, inter-run calibrating and positive/negative controls were run routinely in a 384-well optical plate (Applied Biosystems) and optical adhesive film (Applied Biosystems). All reactions were set up in UV irradiated Laminar flow hoods (Labcaire™).

2.2.5 Generation of Transduced PCa cell lines.

In cloning WFDC1/ps20 we wished to achieve two goals, i) to generate a convenient vector for transient expression of ps20 protein species in mammalian cell lines; and ii) to generate retroviral particles encoding WFDC1 which can transduce mammalian

cell lines to generate novel variant cell lines ectopically secreting ps20. In order to serve both these ends we chose to clone the full length and truncated WFDC1 mRNA species expressed in HeLa cells, into the pMIGR1-eGFP (pMIGR1) retroviral plasmid. pMIGR1 serves as both a mammalian and retroviral expression vector and encodes a multiple cloning site (MCS) upstream of enhanced green fluorescent protein (eGFP) separated by an internal ribosome entry site IRES. Genes inserted into the multiple cloning site undergo 5' cap-dependent translation independent of the eGFP gene which is transcribed independently initiated by the IRES element. Consequently the eGFP acts as a reporter of successful retroviral integration and gene expression. The schema for cloning of the WFDC1 cDNAs, generation of plasmids, viral particles and transduction of cells is presented in fig. 2.1.

2.2.5.1 Amplification and Cloning of WFDC1 cDNA

mRNA was extracted form HeLa cells and RT-PCR using WFDC1 specific primers (table 2.4) performed and the resulting product run on a 2% agarose gel. Two WFDC1 cDNAs were amplified, one representing the full length 660bp sequence, and one a truncated variant lacking exon3, a total of 576bp. Both species were excised from the gel and extracted using the gel extraction kit according to the manufacturer's instructions (Qiagen). These species were then amplified by PCR using a Phusion polymerase for improved fidelity and using primers adding Xho1 and EcoRI sequences to the 3' and 5' ends respectively and shown in table 2.4. The products of each reaction were again run out on a 2% agarose gel and the single band in each lane excised and extracted as before. These products were combined in individual aliquots with Xho1 and EcoRI and the relevant buffer in a digest reaction at 37ºC for 2h, as outlined in table 2.2 simultaneously, pMIGR1 was digested with the same restriction endonucleases to linearize the vector and generate the appropriate insertion site for the cleaved WFDC1 cDNAs.

Table 2.4 Primers used to add sticky ends to ps20 cDNAs

primer direction	primer sequence
Fwd (XhoI)	5'-ATATATACTCGAGGCATGCCTTTCCGGC-3'
Rev (EcoRI)	5'-ATATATGAATTCGCTTACTGAAAGTGCTTCTG-3'

Table 2.5 Constituents of endonuclease digest reaction

Either pMIGR1	1µg
or ps20 cDNA	18µl
Xho1	0.5µl
EcoR1	0.5µl
10% BSA	1µl

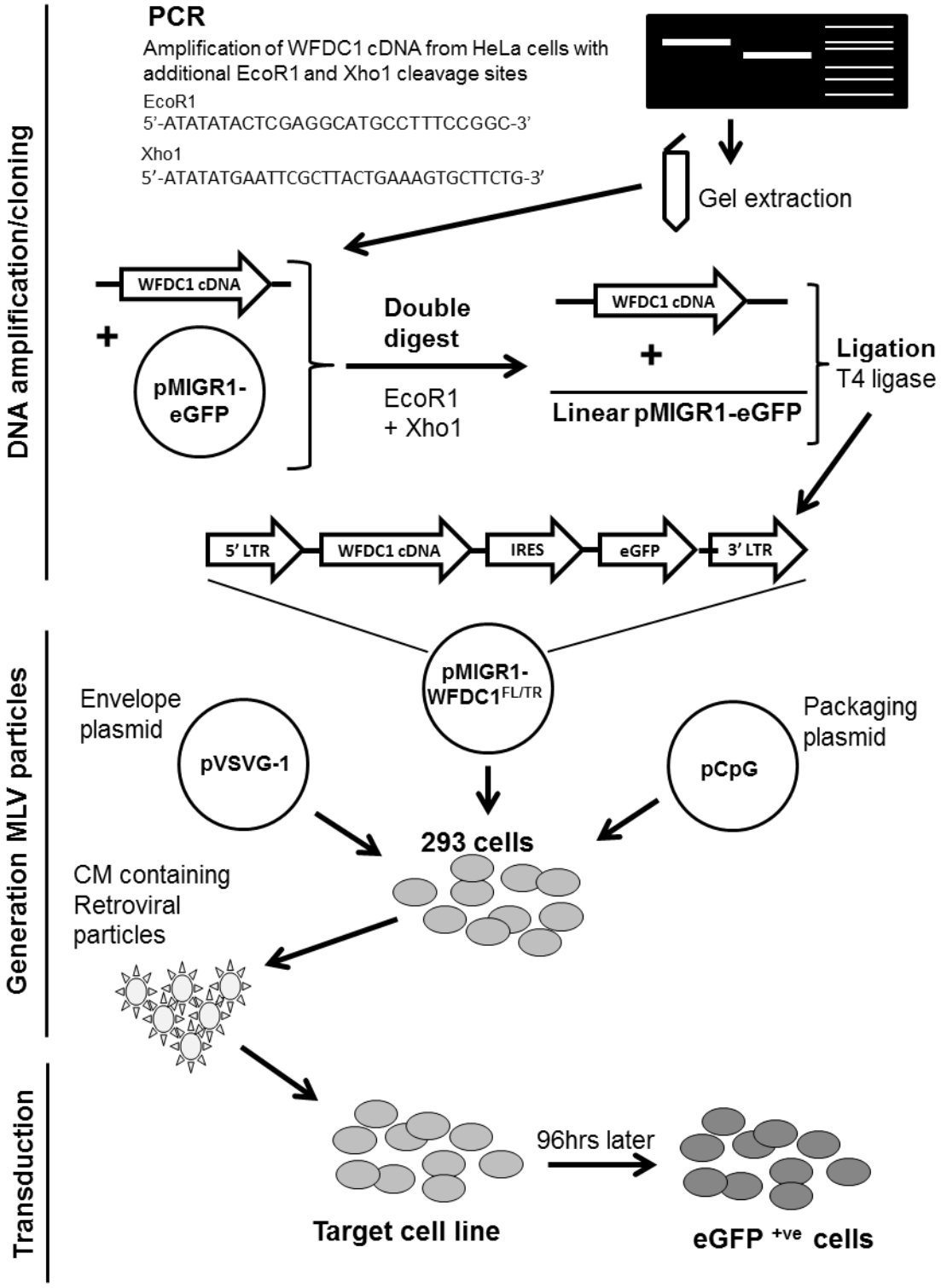

Figure 2.2 Schematic or cloning WFDC1 and generating ps20 expressing cells

The schematic above outlines the sequence of steps undertaken to amplify and clone WFDC1 from HeLa cells, generate infectious MLV virions, and transduce target cells with WFDC1 encoding virus.

Following digestion, the cleaved WFDC1 cDNAs and pMIGR1 were run on a 2% agarose gels, excised, and extracted. Again the nanodrop was used to obtain the amount of digested plasmids and ps20 cDNA obtained from the extraction prior to ligation. In order to insert the ps20 cDNAs into the linear plasmid ligation reactions were then set up as outlined in table 2.6 and incubated at RT for 2h.

Table 2.6 Constituents of ligation reaction

digested pMIGR1	50ng
ps20 cDNA	20ng
T4 ligase	0.5µl
10x T4 ligation buffer	1µl
ddH2O	to 10µl

Subsequently, in each instance 2µl of each ligation reaction was then transformed into competent bacteria and colonies selected by overnight culture on ampicillin containing agar. Colonies were picked at random and grown in 5mls of LB broth. Minipreps were performed and samples were then digested with Xho1 and EcoR1 and run on a gel to identify WFDC1 containing clones. Two were selected, grown in 200mls of LB broth and a maxiprep prepared. A small amount was sent for sequencing using the primers indicated in table 2.3 to confirm the fidelity of the WFDC1 insert.

2.2.5.2 Expression in 293T cells

To confirm that we had generated vectors capable of expressing ps20 we transfected 293T cells with pMIGR1 containing ps20 full length and truncated cDNAs, named $ps20^{FL}$ and $ps20^{TR}$ respectively, or an empty vector (EV) according to the standard transfection protocol described in section 2.2.2.

2.2.5.3 Generation of retroviral particles.

Retroviral particles were produced using 293T cells transfected to express viral components. 293T cells were seeded at $4x10^5$ cells in 6 well plates 16h prior to transfection. The following day each well was transfected with the constituents listed in table 2.7 including either the MIGR1-EV, MIGR1ps20^{FL} or MIGR1ps20^{TR} plasmid. DNA and PEI were added to the optimum medium briefly vortexed and incubated at room temperature for 20 mins. The mixture was then added drop-wise to individual wells containing fresh complete media. After 6h the complete media was changed. Following this, cells were incubated for 48h to express virus which was then collected, clarified by centrifugation, aliquoted and stored at -80ºC.

Table 2.7 Transfection reaction constituents for retroviral particle generation

Optimem	to 100µL
8.91	900ng
MIGR1-EV/ps20	600ng
VSV-G	300ng
PEI	6µg

2.2.5.4 Transduction / Sorting of eGFP$^+$ transduced cells.

Target cells (WPMY-1, PC-3, and DU145) were plated to 50% confluency in 6 well plates. Virus was added 1:1 with complete media. After 48h, media was changed and virus was added again at 1:1 with complete media+10% FCS. After a further 48h cells were viewed under a fluorescence microscope to confirm the expression of eGFP. Cells were then harvested using TrypLE™ as described in section **2.2.1**, washed in complete media, and transferred to FACs tube. Cells were then sorted

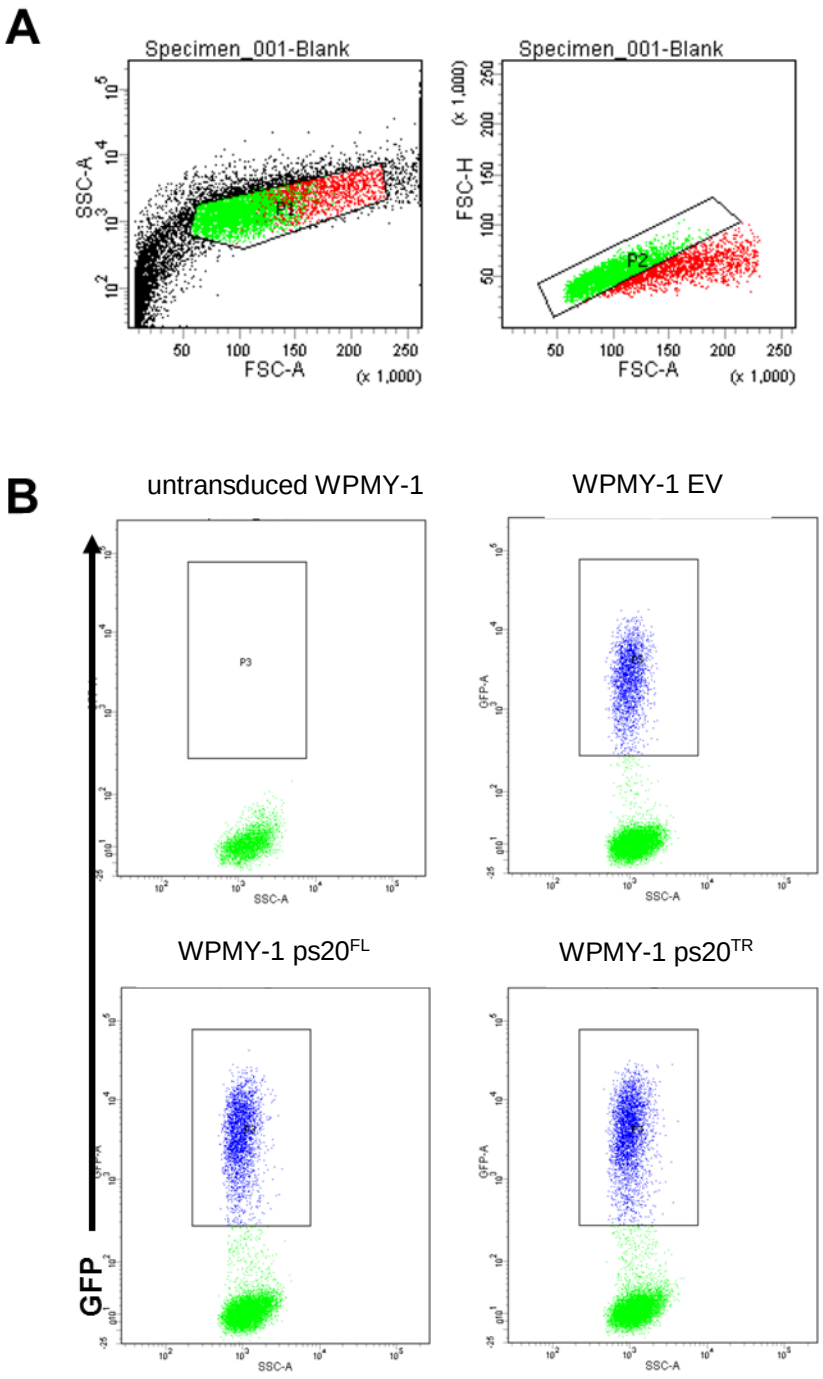

Figure 2.3 Sorting of eGFP+ve transduced cells

Figure shows a representative cell sorting experiment following transduction with ps20 encoding retroviral particles. A) Shows gating for viable cells using forward and side scatter parameters. B) Shows eGFP^{+} transduced populations that were sorted from parental WPMY-1 cells. (Cell sorting was performed by Tom Hayday of the Programme in Infection & Immunity Flow Cytometry Facility.)

for cells expressing high levels of eGFP using a FACS Aria™ (BD Biosciences). 2000 cells were sorted from each condition into a 12 well plate. These cells were then grown out to confluency over 2-3 weeks. Once 80-90% confluent, cells were passage into 10cm culture dishes and expanded again. Cell stocks were made by cryopreservation as described.

2.2.6 Biochemical Assays

2.2.6.1 Ps20 Enzyme Linked Immunosorbant Assay (ELISA)

96-well flat bottom ELISA plates were used for ELISA assays. Three washes with 200µl wash buffer were performed at each wash stage. Plates were coated with anti ps20 rabbit polyclonal antibody 5301(see Section 2.1.4) at 8µg/ml. Ab stock was dissolved in 11 ml PBS and 100µl of Ab solution was dispensed into each well and the plate covered with an adhesive sheet and incubated overnight at 4ºC. All subsequent incubation were conducted at room temperature. The following day contents were ejected into a waste receptacle and the plate blotted by banging on tissue paper to ensure complete removal of excess fluid. Blocking was then performed by placing 200µl blocking buffer to each well followed by incubation for 2h at RT. After washing 100µl of samples were incubated for 2h. After sample incubation, plates were washed. Detection antibody solution was prepared: clone 1G7 pre-conjugated to horseradish peroxide (HRP) was diluted to a concentration of 3.7µg/ml in AB binding buffer. 100µl was added to each well and incubated for 2 h. Plates were then washed and incubated with 150µl of substrate buffer (Sigma fast OPD, Sigma Aldrich) in the dark. Colour development (yellow to orange) was allowed to proceed and the reaction stopped at 30 minutes. Reactions were stopped by addition of 25µl 4M H_2SO_4 to each well. Following agitation for 5secs colourimetric reading was performed at 490nm using a colorimetric plate reader (Biorad, USA). Analysis was performed using Graphpad Prism® 4.

In order to extrapolate the concentrations of ps20 within sample using the ps20 ELISA, in every assay a standard of known concentration was prepared using ps20-GST (Proteintech). Ps20-GST was incubated starting at 50ng/ml with serial ½ dilutions titrated across 8 wells. An average of ps20-GST standard curves from 6

ELISA assays are shown in fig. 2.3. From the standard curve within each ELISA the concentrations of ps20 in samples was calculated using the following equation.

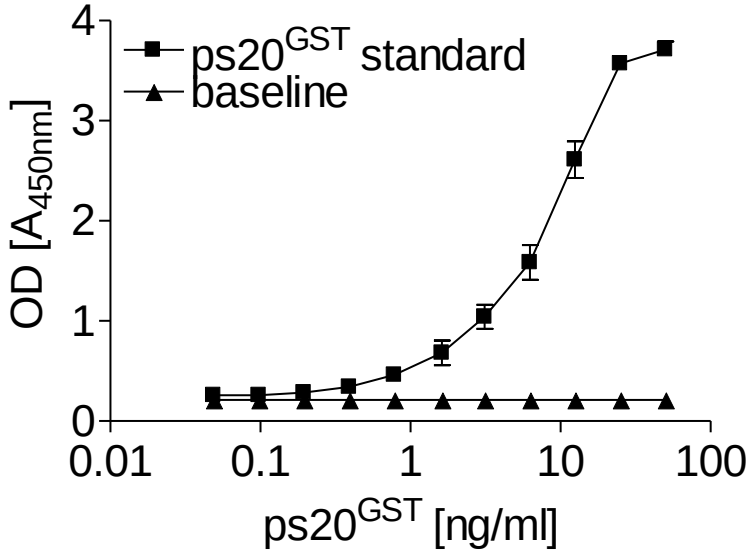

Figure 2.4 ps20-GST Standard curve

Figure shows means and SEM of 6 ps20-GST standard curves taken from separate ELISA assays.

2.2.6.2 ProcartaPlex™ Multiplex Immunoassay (performed by Sangmi Kim)

ProcartaPlex™ Immunoassays use multi-analyte profiling beads to enable the detection and quantitation of multiple protein targets simultaneously in samples such as CM using fluorescent-dyed beads with dual-laser design and digital signal processing using luminex instruments.

All buffers provided were prepared by dilution with recommended volume of ddH_2O. Individual target standards were prepared by 4-fold serial dilution of the standard mix. Antibody magnetic beads were vortexed and 50µL added to each well. 96-well flat

bottom plate was inserted into the hand-held magnetic washer to prevent loss of magnetic beads washed with 150µL of wash buffer. At each step 30secs was left for beads to accumulate on the magnetic surface of the plate. Wash Buffer was removed by inverting the plate/magnetic washer over a sink and blotted on tissue. 50µl of standard or CM was added to each well and the plate was removed from magnetic washer and incubated for 2h with agitation followed by washing as described. Detection antibody mixture was prepared according to the manufacturer's instruction and 25µl added into each well. The plate was then sealed, the magnetic washer removed and the plate incubated for 30 min at RT with agitation. Following washing 50µL of streptavidin-PE solution was added into each well and the plate was again incubated for 30 mins at RT with agitation.

For analysis 120µL of reading buffer was added into each well and the plate shaken for 5 min at RT and the plate analysed using a luminex instrument. Data analysis was performed using ProcartaPlex™ analyst software and standard curve generated using a standard 4PL curve fit algorithm.

2.2.6.3 SDS-PAGE

For electrophoretic separation of proteins the sodium docecyl-sulfate – polyacrylamide-gel electrophoresis (SDS-PAGE) technique was employed. 12% Bis-Tris NuPage™ pre-made gels were used (Invitrogen Life Sciences). Gels were loaded into the XCell SureLock® Mini-Cell gel tank (Novex, Invitrogen Life Technologies) and the tank filled with MOPS SDS loading buffer (Novex, Life Technologies). Samples to be electrophoresed (e.g. recombinant protein, serum free conditioned medium or cell lysates) were diluted to an appropriate concentration in a suitable diluent (e.g PBS or lysis buffer) and then NuPage™ LDS loading buffer was added alongside NuPage™ reducing reagent (Both Life Technologies). These

ingredients were compiled in the following ratio: sample:LDS-buffer:reducing agent – 15:5:2. Samples were then boiled for at least 5 mins at 85^0C and then briefly centrifuged to remove evaporated liquid from the top of the tube. If 15 well gels were used, 12µl of sample were loaded with gel loading tips, if larger combed gels were used an increased amount of sample would be loaded. A 7-177kDa pre-stained protein ladder (New England, Biolabs) was loaded alongside samples. Electrophoresis was at 180V on ice for 1h.

2.2.6.4 Silver Stain

Silver staining for total protein was performed using the SilverXpress® Silver Staining Kit (Invitrogen Life Technologies) which contains a number of premade solutions. The primary reagents contained within these solutions is indicated where advised. Staining was conducted in a plastic lid or tray washed carefully to avoid keratin contamination, and with gentle agitation. At each step solutions were poured into and decanted from the tray after the appropriate incubation time and washes were with 50mls $_{dd}H_2O$. Following electrophoresis, gels were placed in tray and fixed in 50mls 10% Acetic acid, 40% $_{dd}H_2O$, 50% MEOH for 30-60 mins. Gels were then treated with sensitizing solution (containing gluteraldehyde) twice for 5 mins each following by washing twice. Gels were then stained with a 1:1 mixture of solution A (containing silver nitrate) and solution B (Containing ammonium hydroxide & sodium hydroxide) for 10 mins followed by washing twice. Gels were then incubated with developing solution (containing formaldehyde and citric acid). The reaction was stopped after appropriate time with stopper solution for 5 mins (containing citric acid) followed by washing twice. Gels were imaged using a flatbed scanner and presented using PowerPoint™ or windows photo viewer.

2.2.6.5 Western Blotting

Electrophoresed samples were transferred to nitrocellulose membranes (Protran, Whatman, GE Healthcare) using a wet transfer process. To transfer proteins to gel, appropriate sized pieces of membrane and filter paper were cut and pre-soaked in transfer buffer (>5 mins). The gel was carefully extracted from its plastic case and sandwiched appropriately between the membrane with filter paper either side. The sandwich was then loaded into a transfer tank (Biorad) and transferred on ice for 45 mins at 90Vs. Transfer buffer was stored at 4^0C and used repeatedly until current exceeded 400mA when running at 90V (≈10 times). Following transfer, membranes were placed in 50ml falcon tubes and blocked for 30 mins at room temperature on a roller with gentle agitation. Following blocking, primary antibodies were diluted in blocking buffer at the dilution/concentration indicated in table 2.8. Hybridisation was with 5mls of antibody solution for 2h at RT or overnight at 4^0C on a roller with gentle agitation. HRP conjugated secondary antibody was added at 1/2000 in blocking buffer and 5mls of antibody solution was hybridized for either for 2h at RT or overnight at 4^0C. Following hybridisation tubes were emptied and wash buffer added. Washing was with 10mls and it depended on the antibody being used the number of wash steps was altered to give the clearest background to signal ratio following empirical testing (e.g anti-ps20-1G7 = 6 washes, anti-actin-C = 2 washes). Following the appropriate number of wash steps foil was added to tubes to block light, and colourimetric substrate was added (Thermo scientific): 1ml each of reagent A and B were used and incubated on a roller for ≈1 min. Membranes were then transferred to thin transparent PVC sheet and acquired using the Imagequant™ system (GE Healthcare). Images were analysed and presenting using ImageJ software (National Institute of Health, USA).

Table 2.8 Antibody dilutions for western blot

antibody	dilution	concentration
5301	1/1000	5.2µg/ml
651	1/500	3.2µg/ml
650	1/500	3.2µg/ml
1G7	1/1000	3.3µg/ml
actin-c	1/5000	40ng/ml
anti-V5	1/2000	25ng/ml

2.2.6.6 Heparin binding assay

Heparin binding experiments were performed using the Aktä-purifier (GE, Healthcare) fast protein liquid chromatography system. 1ml HiTrap™ Heparin coated columns were washed with >5 Column volumes (CV) of 50mM Tris-HCL buffer (pH7.5). 2mls of 293 generated ps20 CM were then loaded onto the column and further 5 CVs of buffer used to wash away unbound material. A NaCl gradient was then applied to the column over 10 CV taking the NaCl concentration of the buffer from 0M to 1M as 1ml fractions were collected. The flow-through, wash and elution fractions were then subjected to western blotting to detect ps20.

2.2.6.7 Glycosaminoglycan ELISA

Glycosaminoglycan stocks were prepared in ddH_20 at 1mg/ml and subsequently diluted to 25µg/ml and coated overnight onto specially prepared ELISA plates in a volume of 100µl/well. Blocking was for 2h with 1%BSA in PBS. $Ps20^{V5}$ was then titrated onto the plate in doubling dilutions and incubated for 2h prior to washing with

PBS. Subsequently anti-V5-HRP diluted in PBS (1/2000) was incubated for 2h, prior to washing with PBS and incubation with 100µl of TMB ELISA substrate. Reaction was stopped after 15 mins with 50µl H_2SO_4 4M and the plate read with a biorad colourimetric reader at 450nm.

2.2.6.8 Transglutaminase cross-linking assay

Tissue transglutaminase (TG) from guinea pig liver (Sigma Aldrich) was re-solubilised in $_{dd}H_2O$, to a concentration of 2U/ml and stored at -80^{0}C. All experiments were conducted in 1.8ml Eppendorf tubes. Prior to experiments ps20 was dialysed into buffer containing 50mM Tris-HCl pH8 as transglutaminase-mediated transamidation is a calcium dependent reaction and calcium is precipitated out of solution in phosphate containing buffers. Samples of ps20 were prepared according to conditions described in individual experiments. Calcium was then added from a 1M stock of calcium chloride (Sigma Aldrich) to a final concentration of 10mM. DTT (sigma Aldrich) was added from a 1M stock to a final concentration of 5mM. To cross link ps20, TG was added at a final concentration of 0.1U/ml to samples and incubated between 5 mins and 3h at 37^{0}C. Transamination was stopped by adding western blot loading buffer (NuPage™ LDS loading buffer + NuPage™ reducing reagent, as described). Sampled were frozen at -20^{0}C or immediately analysed by electrophoresis and western blotting.

2.2.6.9 Transglutaminase cross-linking ELISA

Fibronectin at 1µl/ml or 1% BSA was coated onto nunc 96 well plates overnight at 4ºC. Blocking was with 1% BSA for 2h at RT. Samples containing 10mM $CaCl_2$, 4mM DTT in pH7.5 50mM TRIS were added to wells. Ps20 was added at 25ng/ml or 5ng/ml

and TG was added at 0.2U/ml. Incubation was at 37ºC for 2h. Plates were washed 3x with 200µl wash buffer as per the regular ps20 ELISA. Detection antibody solution was prepared: clone 1G7 pre-conjugated to HRP was diluted to a concentration of 3.7µg/ml in Ab binding buffer and 100µl was added to each well and incubated for 2h. Plates were then washed 3x and incubated with 150µl of substrate buffer (Sigma fast OPD) in the dark. Colour development (yellow to orange) was allowed to proceed and the reaction stopped at 30 minutes. Reactions were stopped by addition of 25µl 4M H_2SO_4 to each well. Following agitation for 5secs colourimetric reading was performed at 490nm using a colorimetric plate reader (Biorad, USA).

2.2.6.10 Cleavage of ps20 by cathepsin L / B

Cathepsin L or B (both R&D systems) were resolubilised in PBS at a final concentration of 40µg/ml and 10µg/ml respectively, and stored at -20ºC. For individual experiments, proteases were diluted in 50mM MES buffer to working concentrations of 800pg/ml and incubated with a molar excess of 293T purified ps20 in 50mM MES buffer + 4mM DTT for 1 hour at 37^0C according to the specific experimental conditions described. Reactions were stopped by addition of western blot loading buffer and samples were analysed by western blotting as described. For modified ELISA assay, cathepsin L was prepared in 50mM MES+ 4mM DTT and added to ELISA plate following TG crosslinking step for 2h at 37^0C prior to washing and detection as described (the plate was read at 490nm).

2.2.6.11 Ps20 depletion from WPMY-1 CM using antibody conjugated beads.

Antibodies (5B9, 1G7 or IgG1 control) were conjugated to HiTrap NHS-activated columns as described below. Beads were liberated from individual columns using a

scalpel and resuspended in 1ml of 20% ETOH and stored at 4ºC until used. Before use, beads were centrifuged and ETOH aspirated, followed by washing 3 times with 5mls sterile PBS. After washing, beads were resuspended in 1ml of sterile PBS. Depletion of ps20 from WPMY-1 CM was performed by addition of 100µl beads to 1ml of CM with incubation at 4ºC for 1 hour with agitation. Beads were pelleted by centrifugation and CM aspirated and used for cellular assays and the ps20 ELISA to confirm ps20 depletion.

2.2.6 Purification of ps20

2.2.6.1 Preparation of HiTrap™ NHS-activated columns.

HiTrap™ NHS activated columns are sepharose bead based pre-packed columns which provide a matrix for the conjugation for molecules such as antibodies and peptides via primary amines. The sepharose beads are coated with N-hydroxysuccinimide (NHS) ester attached by epichloro-hydrine via a 6-atom spacer arm. The esterification leads to the formation of activated esters, which react rapidly and efficiently with ligands containing amino groups resulting in a very stable amide linkage. In the first instance the isopropanol storage solution is washed out with 1ml of ice cold 1mM HCL solution. Then 1mg of antibody (IG7, 5B9 or Mouse IgG1 control) was injected in the presence of bicarbonate buffer, pH 9, and incubated at RT for 30 mins. The uncoupled ester groups are then inactivated with 5 column volumes of Buffer A (table 2.9), 5 columns of buffer B and a further 5 column volumes of buffer A. The column was left to stand for 30 minutes before the wash was repeated in the order buffer B, Buffer A, Buffer B. The columns were stored in 20% ethanol at 4ºC until use. Where a 5ml column was used, 5mg of antibody was injected.

Table 2.9 Buffers used for HiTrap column conjugation

Buffer A	0.5 M ethanolamine, 0.5 M NaCl, pH 8.3
Buffer B	0.1 M acetate, 0.5 M NaCl, pH 4

2.2.6.2 Purification of ps20 from HeLa cells (performed by eurogentech)

HeLa cells were 'weaned' onto a chemically defined protein media formulation (SFM4CHO utility; Hyclone cat # SH30516.02) and cultured in roller bottles with harvesting at 72h. EDTA (10mM) was added to clarified harvested supernatant which was then concentrated by approximately 10 fold using a tangential cross flow filtration unit (Vivaflow 200, 5kDa MWCO PES). Concentrated, clarified harvests were purified by application to an IG7 affinity matrix (IG7 monoclonal antibody amino coupled to NHS activated Sepharose Fastflow). Binding of ps20 was performed in 25mM Tris HCl/150mM NaCl ph7.2 at a flow rate of 1ml/min. Following sample loading, the resin was washed with 10 column volumes of binding buffer to return to baseline. Elution of ps20 was with 0.1M glycine pH3. Although this elution method worked once the yield was deemed too low on a subsequent purification. More recently 0.2M glycine pH2.0 has been used with a projected better yield. The complete elution peak was collected and neutralised immediately with 1M Tris pH9.

2.2.6.3 Purification of ps20 from transfected 293T and 293F cells.

Batches of 293T and 293F cell CM containing ectopically expressed ps20 were purified using 1G7 activated 1ml or 5ml HiTrap™ columns to produce highly enriched/purified ps20 protein. A number of batches were produced throughout the study and are specifically alluded to in the chapter 3, but the method was the same throughout. The volume of serum free CM was collected from the ps20 expressing

cells, clarified by centrifugation >1000g for 10 mins, and filtered through a 0.2µM filter using either a syringe filter of filtration unit. The filtered CM was then fed onto a PBS washed column at <0.5ml/min at 4ºC. Once loaded, the column was washed with at least 5 volumes of PBS and then eluted with 5 column volumes of 0.2M Glycine buffer pH2.3. Fractions of 1ml (1ml columns) or 5ml (5ml columns) were collected and 5% v/v 1M Tris buffer added to pH buffer the solution. Fractions were then dialysed against 50mM TRIS buffer overnight at 4ºC using snakeskin tubing. Ps20 high fractions were pooled and stored at -80ºC.

2.2.6.5 Expression and purification of ps20^{V5} in drosophila cells (performed by eurogentech)

A batch of ps20 produced from drosophila cells was used for numerous experiments in this thesis. The vector was produced by a previous lab member and the protein expressed and purified by (both as described below). Due to the use of the V5 tag in the proteins detection by western blot, this batch of ps20 heretofore referred to as ps20^{V5}

The Drosophila expression system (Invitrogen) was used to express a V5-His-tagged human ps20 protein in Schneider 2 (S2) cells (Invitrogen) in a copper-inducible manner. The pMT/Bip/V5-His/ps20 vector and pCoHYGRO (Invitrogen) at a ratio of 19:1 were transfected into S2 cells with a CaPO4 transfection kit (Invitrogen) following the manufacturer's protocol. Stably transfected S2-ps20-V5-His cells were selected in complete drosophila expression system medium containing 300 µg/ml of hygromycin B for 3 weeks, and the culture medium was switched stepwise to ultimate insect serum-free medium containing 300 µg/ml of hygromycin B. The stable S2-ps20-V5-His cells were then cultured in suspension. When cell density reached 2 ×

10^6 cells/ml, 500μM CuSO4 was added to induce rps20-V5-His protein expression driven by the Drosophila metallothionein promoter, as confirmed by Western blotting with the anti-V5 Ab. For human rps20-V5-His protein purification, 500 ml of CM from CuSO4-induced S2-ps20-V5-His cells was collected, centrifuged to remove S2 cells, and concentrated 10 times by using the Amicon stirred ultrafiltration cell model 8400 (Millipore, Bedford MA) with a 5-kDa cut-off membrane, followed by dialysis against Tris-HCl buffer (20mM Tris-HCl, 15mM NaCl, pH 7.6) at 4°C. The sample was then loaded slowly onto a Tris-HCl buffer-balanced Ni-nitrilotriacetic acid column. After loading, the column was washed extensively with Tris-HCl buffer with 20mM imidazole and 40mM imidazole. The rps20-V5-His protein was eluted with 20mM Tris-HCl, 150mM NaCl, pH 7.6, with 250 mM imidazole. The protein was then dialyzed against 20 mM Tris-HCl, 150 mM NaCl, pH 7.6, and concentrated to around 1mg/ml by using Amicon Ultra-4 (Millipore). The protein concentration was measured using the Bio-Rad Dc protein assay reagents (Bio-Rad Laboratories, Hercules, CA).

Chapter 3. Purification and cloning of ps20/WFDC1

3.1 Introduction

In the original purification of ps20, published by David Rowley's lab in the mid-nineties, they used litres of conditioned media (CM) generated from rat urogenital-sinus mesenchymal cells and a complex series of cation-exchange, size exclusion, and high pressure liquid chromatography techniques to purify a small amount of ps20 to homogeneity. In so doing they were able to isolate the novel protein species, identify the sequence, and confirm it as the active growth inhibitory molecule in the suppressive CM from the cells they had been studying. They subsequently cloned the mRNAs and used these cDNAs to express and conduct further *in vitro* and *in vivo* studies.

In a collaboration between our lab and David Rowley's a ps20-V5-His tagged protein was generated, purified using a nickel-chelate column, and used to inoculate mice in order to generate a monoclonal antibody to ps20. This antibody, termed 1G7 (table 3.1), has been used in several studies to visualize ps20 by western blotting, and in order to assess expression of ps20 immunohistochemically in mouse and human samples. However, no further published data has emerged using either the untagged rat ps20, or the v5-his tagged ps20 subsequently generated in order to study ps20 function. Indeed, experiments in our lab have suggested this tagged ps20 is not functionally active.

Other studies, including in our own lab have used cellular overexpression of ps20 in order to study its function. Specifically, Madar et al, expressed WFDC1/ps20 in fibroblasts showing reduced growth rates in ps20 expressing cells (Madar et al., 2009), while Lui et al over expressed WFDC1 in melanoma cells (Liu et al., 2009).

Neither lab assess successful overexpression of ps20 at the protein level. To my knowledge, our lab was the first to generate a cell line stably expressing WFDC1/ps20, in order to study the effect of ps20 on the adhesion of T cells and the subsequent effects on the cell-to-cell transmission of HIV virions, Alvarez *et al* constructed a Lentiviral-WFDC1 construct, subsequently transducing Jurkat cells (Alvarez et al., 2008).

In this chapter I present a series of novel tools critical to interrogating ps20 functionality: i) A panel of in house antibodies used within this thesis, ii) I demonstrate a novel technique for purifying ps20 to near homogeneity using immunoaffinity to the 1G7 antibody, iii) I present data showing the cloning of two WFDC1 mRNAs known to be expressed in prostate cancer cells into retroviral vectors co-expressing eGFP as a reporter gene.

3.2 Results

3.2.1 Characterization of anti-ps20 antibodies.

Several antibodies to ps20 have been raised. Figure 3.1A shows the AA sequence of ps20. Underlined are the binding sites of a series of antibodies our lab has raised against the molecule, Listed in table 3.1 Rabbit polyclonal antibodies were previously raised and purified against peptides based on sequences taken from N- and C-terminal regions of the ps20. In addition we use the 1G7 mouse monoclonal raised against a recombinant ps20 molecule as described previously (Alvarez et al., 2008) and used for western blotting and immunohistochemistry. The hybridomas of this mouse antibody were kindly donated to our lab and since then IG7 has been conjugated to horseradish peroxidase for use as the detection antibody in a ps20 ELISA. In addition, we used a mouse monoclonal Ab5B9, raised to the C-terminus peptide by eurogentech. All antibodies used were optimized for use in an anti-ps20 western blot, and shown to bind to ps20 at the predicted molecular weight.

3.2.2 Use of immunoaffinity columns to purify ps20 from conditioned media.

Previously, ps20 was purified by nickel chelate chromatography via a C-terminal HIS tag. However, previous reports have shown that this material was not functional. Our lab also undertook expression of HIS tagged ps20, and previous lab members cloned the WFDC1 full length (FL) mRNA into the pMT-V5-His vector for expression in the SH2 drosophila cell system. Expression and purification of the resulting material yielded variable results. The first small batch was highly pure and is used in Chapter 4 of this thesis in numerous biochemical characterization experiments. However, subsequent attempts to purify the ps20^{V5His} material yielded highly impure material, containing a

Table 3.1 Epitopes of ps20 binding antibodies

Antibody	Animal/class	Raised against	epitope	
650	rabbit/poly	AEEAGAPGGRQPRAD	N-terminal	———
201-254 /3051/651	rabbit/poly	KNVAEPGRGQQKHFQ	C-terminal	- - - - - - -
1G7	mouse/IgG2	Recombinant protein	conformational	.....
5B9	mouse/IgG2	KNVAEPGRGQQKHFQ	C-terminal	-·-·-

A

```
          10          20          30          40
MPLTGVGPGS  CRRQIIRALC  LLLLLLHAGS  AKNIWKRALP
          50          60          70          80
ARLAEKSRAE  EAGAPGGPRQ  PRADRCPPPP  RTLPPGACQA
          90         100         110         120
ARCQADSECP  RHRRCCYNGC  AYACLEAVPP  PPVLDWLVQP
         130         140         150         160
KPRWLGGNGW  LLDGPEEVLQ  AEACSTTEDG  AEPLLCPSGY
         170         180         190         200
ECHILSPGDV  AEGIPNRGQC  VKQRRQADGR  ILRHKLYKEY
         210         220
PEGDSKNVAE  PGRGQQKHFQ
```

B

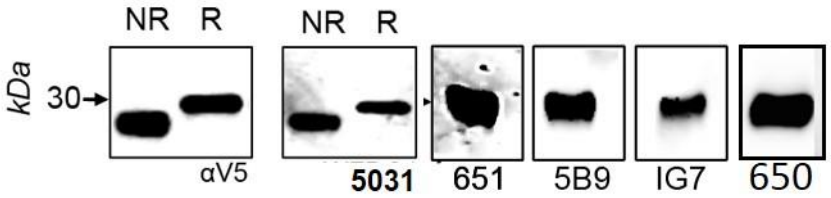

Figure 3.1. Epitopes and specificity of anti-ps20 antibodies A) Emboldened residues highlight the secretion signal peptide sequence and the arrowhead indicates the predicted thrombin cleavage site. B) Western blotting of ps20-V5-His with anti-ps20 antibodies, under reduced and non-reduced (aV5 and 5031), or reduced conditions (651, 5B9, 1G7, 650).

large range of immunoreactive ps20 species, likely representing oligomers of ps20 or stable complexes with other proteins (appendix fig. 8.1 A and B). Because of these difficulties we developed a novel purification system based on immune-affinity purification with anti-ps20 antibodies. Previous work within our lab had shown that 293T cells could be effectively transfected with a pBK-WFDC1 vector and yielded good expression of ps20 as a result. As such we decided to use the freestyle 293F™ expression system, comprising a suspension adapted 293T derived cell line, combined with transient transfection. The schematic shown in fig. 3.2 demonstrates the approach to purification. 293F cells are seeded in conical flasks in specialised serum free media and cells are transfected. 72h later CM is collected, clarified by centrifugation and filtration (0.2µM) and added to a NHS-sepharose column previously conjugated to anti-ps20.

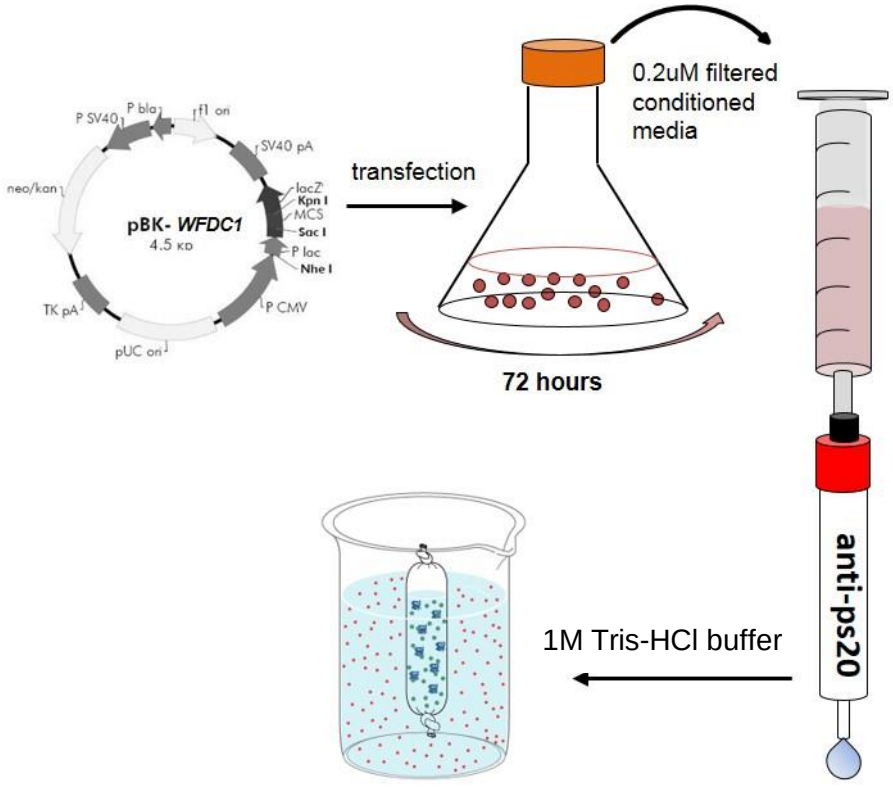

Figure 3.2 Schema for the immunoaffinity purification of ps20.

293 cells are transfected with the pBK-WFDC1 plasmid for 72h. Conditioned media is collected and following clarification, added to an anti-ps20 column. Following elution, material is pH neutralised using 1M Tris-HCl buffer and dialysed overnight into PBS.

In order to optimize the expression of ps20 in the system outlined, we performed a time course transfection of 293F cells using Lipofectamine or PEI on 293F cells cultured in a 30ml vessels (fig 3.3). Surprisingly PEI yielded higher ps20 expression than the more expensive lipofectamine reagent. As such, we decided to use a 72h transfection with PEI to express ps20 in 293F cells for purification.

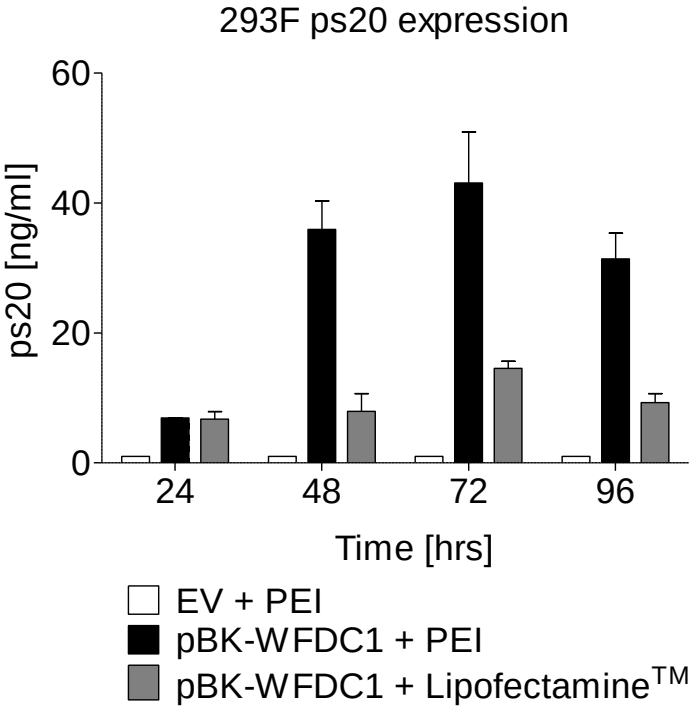

Figure 3.3 Optimisation of 293F™ cell transfection

293F cells were seeded in 24 well plates at $6x10^4$ cell/well. Cells were treated with the indicated formulation of reagent and incubated on a rotation platform for 72h. CM were assayed in the 651-1G7-HRP ELISA as described in materials and methods (the plate was read at 490nm).

3.2.3 Purification of ps20 from conditioned media using anti-ps20 immunoaffinity chromatography.

To test the hypothesis that anti-ps20 immunoglobins conjugated to NHS activated-sepharose columns could generate pure ps20 we prepared two columns. Each

column was conjugated to either 1mg of 1G7 or 5B9 antibody as described in materials and methods. Subsequently, two batches of 90ml of CM was generated as described above using the 293F cells. One batch of CM was absorbed to each column followed by washing, and ps20 was eluted as described in materials and methods. Significant fractions, including the loading material, the flow-through, the wash fraction, and the final eluted material were subjected to SDS-PAGE followed by a silver stain or an anti-ps20 western blot (fig. 3.4A and B). Both experiments results yielded significantly enriched ps20 as demonstrated in table 3.2. However, there appeared to be more non-ps20 species resolved in the eluted fraction in material purified using a 5B9 column (fig 3.4B). Given that the yields were so similar. It was decided that the 1G7 column represented a better tool for purification given the comparable yield and the reduced number of contaminating species present.

Table 3.2 Yield of ps20 purified from immunoaffinity columns

Column:	**5B9**	**1G7**
Conditioned media [ng/ml]	32.456 [1.35nM]	35.198 [1.46nM]
Eluate [ng/ml]	509.245 [21.22nM]	534.481 [22.27nM]
Yield (%)	87.168	84.361

Previous reports have indicated that purified ps20 is functionally active down to a concentration of 7.3nM (Larsen et al., 1998). Consequently, in order to produce a batch of ps20 concentrated enough for functional assays ps20 at least 10x as concentrated (70nM) would be required. In order to generate enough ps20 for functional testing we therefore transfected 20 x 30ml flasks of 293F cells with pBK-WFDC1 and collection the CM. This CM (≈600mls) was absorbed onto a 5ml NHS activated sepharose column conjugated to 1G7. The eluate was collected as before in 5 CVs of elution buffer and following dialysis

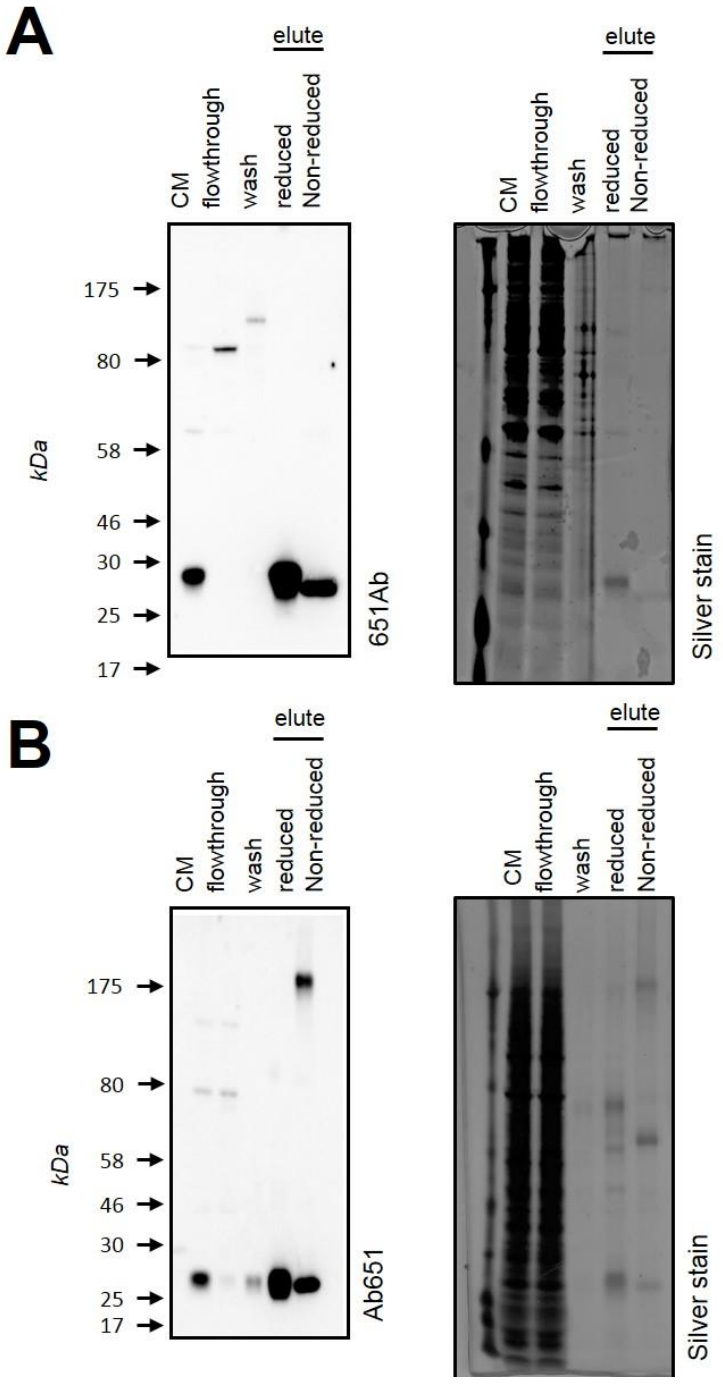

Figure 3.4 Purification of ps20 from CM using1G7 and 5B9 columns.

90mls of clarified CM was loaded onto A) a 1ml 1G7 column or B) a 1ml 5B9 column at 1ml/min flowrate. Columns were washed with 5 column volumes (CV) of PBS and eluted with 5CVs of 0.2M Glycine buffer (pH2.3). Fractions were electrophoresed and silver stained or western blotted as indicated.

concentrated the eluted material 10x using a 3kDa cut-off centrifugal filter (fig. 3.5). The resulting batch of ps20 was called ps20^{293F}.

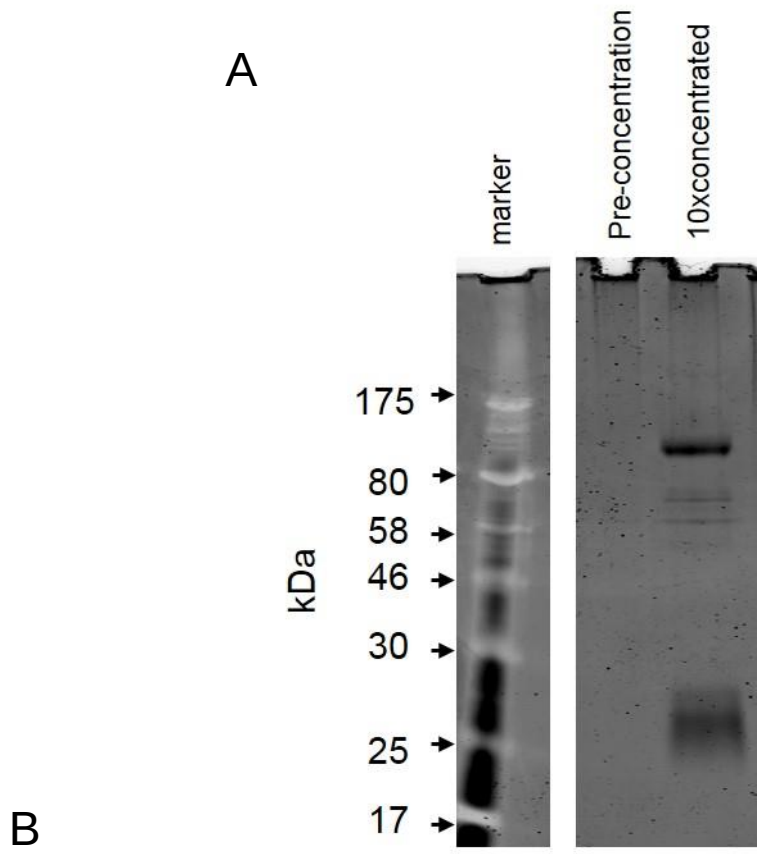

MPLTGVGPGS CRRQIIRALC LLLLLLHAGS AKNIWKRALP ARLAEKSRAE EAGAPGGPRQ
PRADRCPPPP RTLPPGACQA ARCQADSECP RHRRCCYNGC AYACLEAVPP PPVLDWLVQP
KPRWLGGNGW LLDGPEEVLQ AEACSTTEDG AEPLLCPSGY ECHILSPGDV AEGIPNRGQC
VKQRRQADGR ILRHKLYKEY PEGDSKNVAE PGRGQQKHFQ

Figure 3.5 Purification of ps20 from 600mls of 293F CM

A) 600mls of ps20 was absorbed to a 1G7 column at 1ml/min, washed with 5CVs of PBS and eluted with 5CV of elution buffer. Following dialysis, the resulting material was concentrated 10x and subjected to SDS-PAGE analysis and silver stained. B) Amino acid sequence of ps20 showing the coverage obtained by MS analysis of ps20 peptides.

Ps20^{293F} contained significant purified ps20 corresponding to the predicted MW under reduced conditions. However, a significant single contaminating factor was also present. Both bands present in fig. 3.5A were excised and sent for mass-

spectrographic analysis. This analysis confirmed the presence of ps20 with good coverage of the FL molecule within 15aa of the C-terminus and 5aa of the proposed thrombin cleavage site after the N-terminal signal peptide (fig. 3.5B). Sequencing of the contaminating higher molecular weight band showed this to be galectin 3 binding protein (appendix fig. 8.2).

We next calculated the concentration of the resulting ps20 using two methods. Firstly we estimated the concentration using our in house ELISA based on the $ps20^{GST}$ standard presented in materials and methods. The results are presented in Table 3.3. The binding kinetics of $ps20^{293F}$ are clearly different from $ps20^{GST}$, making it difficult to use the $ps20^{GST}$ in order to establish an accurate concentration.

Table 3.3 Results of ELISA quantification of $ps20^{293F}$

ELISA OD	dilution	Concentration [ng/ml]
2.9816	10	311.4
2.1736	100	1445
0.7876	1000	4070
	Average:	**1942.13**

Because the material appeared to contain comparable amounts of galectin 3 Binding protein and ps20 it was decided that generic protein quantification assays, such as bradford staining, would be inappropriate. As such we used a highly pure protein of known concentration as ps20 to compare the profile of ps20 on a stained SDS-PAGE gel. The chosen protein, transforming growth factor β2 (TGFβ2) is also a secreted soluble protein of a similar MW to ps20. Figure 3.6 shows an SDS-PAGE gel stained with a fluorescent lumitein stain. Using a typhoon fluorescent scanner (GE healthcare) we were able to arbitrary densitometry values of the titrated TGFβ2 sample and plot a standard curve. We then titrated $ps20^{293F}$ onto a gel and performed a lumitein stain. The

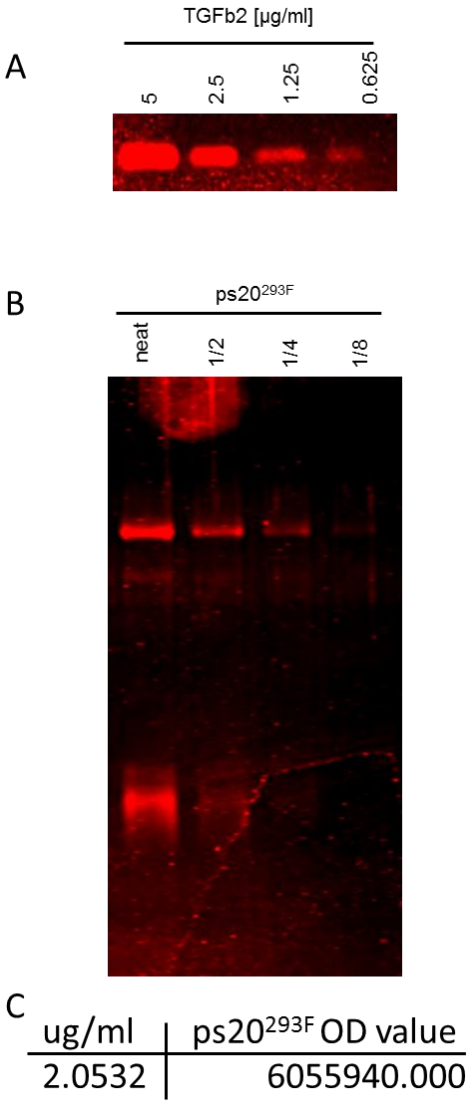

Figure 3.6 Calculation of the concentration of ps20^{293F} using TGFB2 as a standard.
A and B) Indicated concentrations of TGFβ2 (A) and ps20^{293F} (B) were run on SDS-PAGE and lumitein stained. C) The densitometric value of neat ps20^{293F} and the corresponding concentration predicted from non-linear regression analysis.

resulting densitometric analysis allowed us to predict the concentration of ps20^{293F} from the TGFβ2 standard by non-linear regression analysis using prism (fig 3.6B and C). The predicted concentration was shown to be 2.03µg/ml. This was a good match with the estimated concentration taken from the average of the ELISA values shown in table 3.3. As such, we deemed the concentration of ps20^{293F} to be 2µg/ml and it is stated as such where it appears in this thesis.

3.2.3 Cloning of WFDC1 from HeLa cells

In order to undertake a functional characterisation of ps20 I decided to make cell lines stably expressing ps20. To generate these lines we utilised the MIGR1 plasmid (fig. 3.7A) originally generated from murine stem cell virus (Pear et al., 1998). This vector has the advantage of being able to form infectious retroviral particles when co-transfected with the VSVg packaging and Gag/Pol capsid plasmids, or can be directly transfected into mammalian cell lines for transient expression. It also has the eGFP reporter to allow sorting of successfully transduced clones.

We used HeLa cells as the source of WFDC1 mRNA as they has previously reported high expression of both the full length and truncated WFDC1 mRNA species. Sequencing revealed these mRNA species to encode the FL ps20 aa sequence and a 192 aa truncated species lacking exon3, which was previously reported to be expressed at low levels by PC-3 and DU145 cells (Watson et al., 2004b). WFDC1 mRNAs were reverse transcribed and amplified by one-step RT-PCR as described in methods (section 2.2.4.2) and presented in fig. 3.7B.

In order to produce sticky ends for ligation into the EcoR1 and Xho1 sites in MIGR1 we optimized a PCR using a titration of the primers indicated in materials and methods (section 2.2.5.1), shown in fig. 3.7C. Once an optimal concentration for primers had been achieved, we amplified both FL and TR WFDC1 mRNA species (fig. 3.7D). These amplified cDNA species were extracted from the gel and ligated into the digested MIGR1 plasmid. Following transformation of JM109 colonies several were picked at random. Following minipreps to identify successfully transformed clones, two were chosen to be grown up in 100mls of broth for maxi prep.

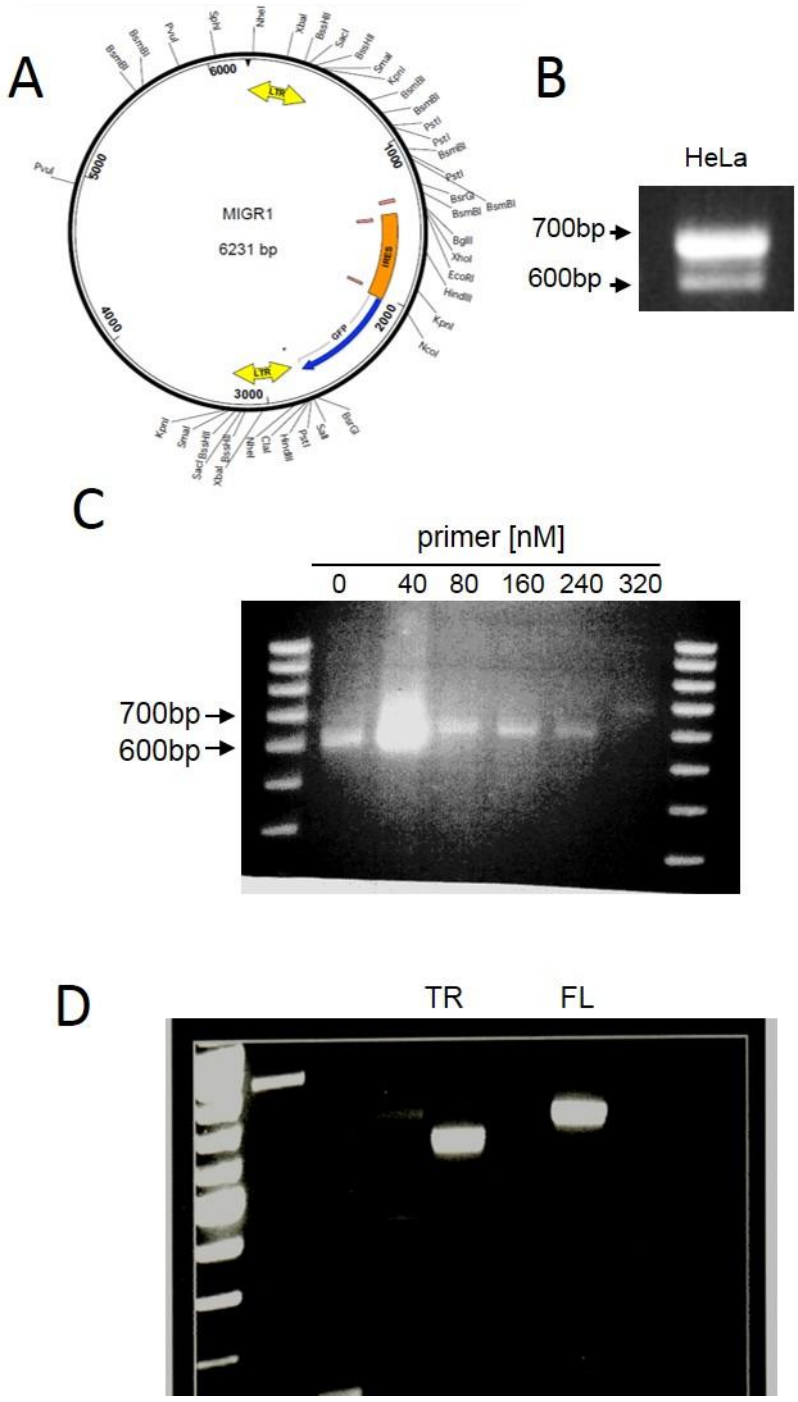

Figure 3.7 Generation of cDNAs for expression of WFDC1 in MIGR1 plasmid. A) Plasmid map of MIGR1 plasmid. B) RT-PCR showing WFDC1 cDNA species amplified from HeLa mRNA run on an agarose gel. C) PCR using EcoR1 and Xho1 WFDC1 primers. D) Amplification of HeLa WFDC1 cDNAs for ligation into MIGR1 plasmid, run on an agarose gel.

Figure 3.8A shows the digestion of resulting maxipreps showing the 576bp and 660bp TR and FL WFDC1 cDNA species respectively. Both plasmids were sent for sequencing as described in materials and methods to confirm fidelity of the WFDC1 inserts. 1µg of each plasmid was transfected into 293T cells in 6 well plates. 48h later images were taken using a fluorescence camera to confirm expression of the MIGR1 eGFP reporter protein (fig. 3.8B). CM was then collected from individual wells and subjected to ps20 ELISA to confirm expression of $ps20^{FL}$ and $ps20^{TR}$ protein species (fig. 3.8C).

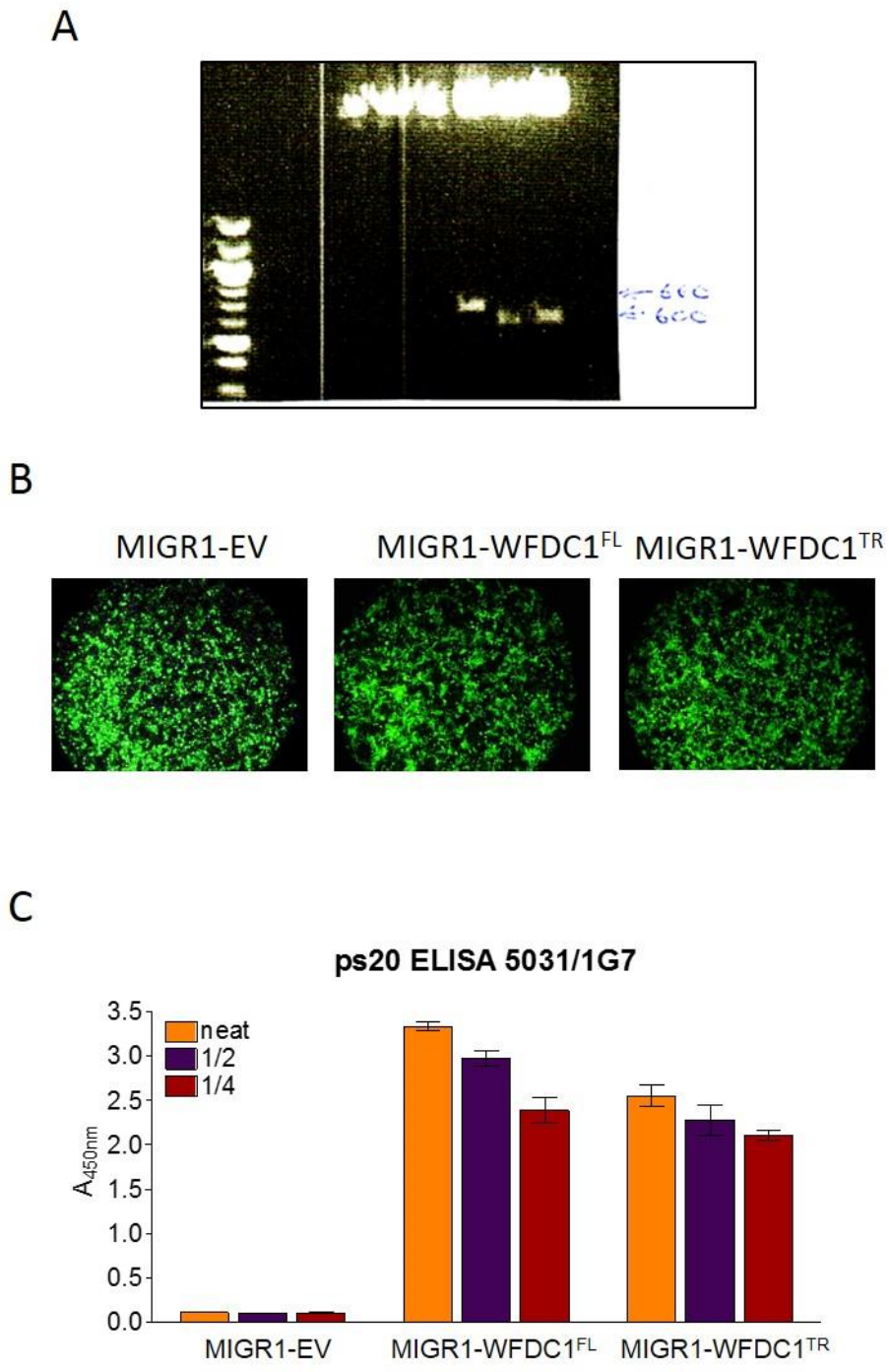

Figure 3.8 Characterisation and expression of MIGR1-WFDC1 plasmids. A) Maxi-preparations of MIGR1-WFDC1^{FL} and MIGR1-WFDC1^{TR} were digested with EcoR1 and Xho1 and run on an agarose gel. B-C) 1µg of MIGR1-WFDC1 plasmids were transiently transfected into 239T cells and assessed for eGFP expression (B) and the CM analysed by ELISA to confirm ps20 expression (C).

3.3 Discussion

To date, the only function of soluble ps20 protein to be identified is as an inhibitor of cellular growth, namely in PC-3 and COS-7 cells. Other proposed functions, such as the regulation of ICAM-1 (Alvarez et al., 2008), regulation of cellular senescence (Madar et al., 2009), induction of angiogenesis (McAlhany et al., 2003) have used cellular models overexpressing ps20 to investigate function. As such, in order to effectively study the role of ps20 *in vitro*, an effective means of obtaining purified ps20, and of producing WFDC1/ps20 overexpressing cell lines is needed.

Herein I have demonstrated that through transfection of 293F cells, ps20 secretion into serum free CM can be induced. Subsequent immunoaffinity chromatography on Ab1G7 and Ab5B9 conjugated media resulted in comparable yields of purified ps20 around 80%. However, 1G7 purification resulted in a more homogenous material, with a sole contaminant identifiable by mass spec (appendix fig. 8.2). This contaminant G3BP was found to present at similar levels to ps20, but addition of recombinant G3BP to PC-3/WPMY-1 proliferation assays resulted in no demonstrable inhibition of cellular growth (appendix fig. 8.3). Given this proliferation assay will be our primary readout of ps20 function in the next chapter we considered the 1G7 technique and the $ps20^{293F}$ purified thereby to be suitable for downstream analysis. The concentration of this protein, determined by a combination of ps20 ELISA and a SDS-PAGE staining with comparison to a TGFβ2 standard, revealed the concentration to be 2µg/ml. Although purification of ps20 to a higher concentration would be more optimal in terms of providing sufficient material for extensive downstream analysis, larger scale production was beyond the scope of this study. Despite this 2µg/ml (83nM) is concentrated enough to treat cells at concentrations comparable to that seen in earlier studies of purified ps20 function, i.e. 7.3nM (Larsen et al., 1998).

Our second approach to studying the function of ps20 was to clone WFDC1 and express ps20 in prostate stromal and PCa cells. There are two WFDC1 isotypes expressed in the prostate. These comprise a FL length transcript encoding a 660aa ps20 molecule. The second is an WFDC1 mRNA species lacking exon3. Notably, exon 3 is the most highly conserved region of ps20 with 100% homology between humans and insects. Both are expressed in HeLa cells, as confirmed by RT-PCR and sequencing using WFDC1 specific primers. It is notable that HeLa cells express high levels of ps20, given its role as a growth inhibitor and potential tumour suppressor protein. HeLa cells are highly proliferative which is in contrast to data presented by Madar *et al* showing WFDC1 is least expressed by the most proliferative cells within a population, suggesting WFDC1 expression is incompatible with high rates of cellular proliferation (Madar et al., 2009). However, no mechanistic understanding of how ps20 mediates its function is yet known, and given the aberrant genetic and functional characteristics of the HeLa cell line (Landry et al., 2013) it is likely an inappropriate model for study of ps20 function. HeLa WFDC1 mRNA was successfully cloned, and inserted into the MIGR1 expression vector. Transfected cells showed high levels of eGFP and ps20 expression. This is the first evidence that the uncharacterised exon 3 splice variant mRNA can be translated and secreted. The MIGR1-WFDC1 expression vectors will be useful tools in studying the function of both full length ps20 and truncated ps20, henceforth referred to as $ps20^{FL}$ and $ps20^{TR}$.

Chapter 4. Biochemical characterisation of ps20

4.1 Introduction

Despite having been first purified 17 years ago, little is known about its biochemical properties of ps20 in the context of the wider WFDC family. In this chapter I attempt to address this issue by examining three important biochemical properties of WAPs: glycosaminoglycan binding; transglutaminase-induced cross-linking and cathepsin L cleavage.

WFDC family members, including SLPI and elafin, lack known cell surface receptors, and no means of signalling has been elucidated for any member. While binding to a number of cell surface proteins has been observed for SLPI (Py et al., 2009) none of these has been linked to cell-intrinsic functionality. Both SLPI and elafin have well documented non-cell-intrinsic extracellular functions, such as protease inhibition and anti-microbial effects (Moreau et al., 2008) which do not rely on protein-cell interactions. However, there is now an abundance of literature demonstrating cellular functions, such as the conditioning of monocytes to inhibit T cell proliferation (Guerrieri et al., 2011) and the regulation by SLPI of MMP expression in ovarian cancer cells (Hoskins et al., 2011). Similarly, knockdown of elafin expression in ovarian cancer cells was shown to reduce the susceptibility to apoptosis induction by chemotherapeutic agents via the caspase-3 pathway, suggesting elafin is regulating this pathway in a cell-intrinsic manner (Wei et al., 2012).

Like SLPI and elafin, ps20 has a number of demonstrated cell-intrinsic functions (Alvarez et al., 2008, Madar et al., 2009, Wilson et al., 2014, Rowley et al., 1995), but

no interacting proteins have been identified and how ps20 interacts with cells to inhibit growth and induce ICAM-1 expression is unknown. Interestingly, both SLPI and elafin are known heparin-binding proteins (HBP) (Fath et al., 1998, Guyot et al., 2005b) and an inspection of the ps20 peptide sequence shows the presence of two 'Cardin and Weintraub' glycosaminoglycan (GAG) binding domains (Imberty et al., 2007). These linear, sulphated disaccharide chains are ubiquitous at the surface of cells and in the ECM where they sequester soluble proteins, facilitate interactions between HBP ligands and cognate signalling receptors (Nakamura et al., 2011), binding all known chemokines, cytokines, growth factors and many proteases and their inhibitors (Handel et al., 2005). There is also now increasing evidence that endocytic uptake of proteins may involve proteoglycans (Kobialka et al., 2009, Favretto et al., 2014, Gump et al., 2010). SLPI has been shown to elicit immune regulatory functions by entering monocytes, translocating to the nucleus and binding DNA. However, the mechanism by which this occurs is unknown (Taggart et al., 2005). More recently the same phenomenon was observed in neurons, where exogenous fluorescein labelled SLPI entered cells and rapidly became localised to the nucleus (Hannila et al., 2013). In lieu of known surface receptors, it remains to be seen if WFDC protein-GAG interactions are involved in the cell-intrinsic functions, especially those which may involve protein internalisation.

In addition to being HBPs, SLPI and elafin have both been shown to interact with transglutaminase 2 (TG), a calcium dependent enzyme responsible for protein-crosslinking of structural polymers and oligomeric protein complexes (Lorand and Conrad, 1984). Indeed, a number of secreted signalling factors are functionally modulated through the TG dependent formation of higher order multimers (Nishimichi et al., 2011, Dierker et al., 2009, Kaartinen et al., 1999). Both SLPI and elafin undergo TG mediated crosslinking to the ECM components fibronectin and elastin (Guyot et al., 2005b, Baranger et al., 2011) which is thought to tether them within the ECM from

where they can perform their protease inhibition and immune-modulatory functions. Another characteristic common to WFDC proteins is susceptibility to cleavage by cathepsins. Elafin's function is dependent on the cleavage of pre-elafin (trappin-2) to the mature elafin form by one of several proteases including Cathepsins-L and -K (Sallenave et al., 1994). Similarly, SLPI has also been shown to be cleaved by cathepsins-B, L and S (Taggart et al., 2001). In contrast to elafin, the cleavage of SLPI by cathepsins was shown to abrogate the protease inhibitory function of the molecule. Cleaved SLPI was found in samples taken from lung epithelia, suggesting this cleavage is a physiologically relevant process (Taggart et al., 2001) and may be a mechanism for regulating extracellular SLPI activity. This posits TG crosslinking and cathepsin cleavage as potential mechanisms for regulating WFDC protein function, though the *in vivo* implications of these processes has not yet been studied.

The interest of our laboratory in studying ps20 was rooted in its potential as a growth inhibitor of PCa cells. However, in order to study ps20 effectively, or to utilize ps20 therapeutically, a far greater understanding of its structure-functional characteristics are required. Herein I present data which demonstrates that ps20 undergoes a high affinity interaction with GAGs and can interact with cell surfaces in a GAG dependent manner. We demonstrate that ps20 growth inhibitory function is regulated by protein cleavage and post-translational processing, and that ps20 interacts with both TG and cathepsins. We propose this crosslinking, and subsequent cleavage as a mechanism for functional regulation/activation within the ECM.

4.2 Results

4.2.1 Ps20 interacts with Glycosaminoglycans (GAGs) at the cell surface.

Secreted signalling molecules including WFDC family proteins SLPI and elafin have a demonstrated affinity for heparin, and GAGs (Imberty et al., 2007, Hoogewerf et al., 1997, Fath et al., 1998, Guyot et al., 2005b). In order to investigate whether the Cardin-Weintraub heparin binding motifs observed in the ps20 amino acid sequence conferred the ability to interact with GAGs, we performed heparin-sepharose affinity chromatography on CM from 293T cells transfected to express ps20 (fig. 4.1). The binding-to and elution of ps20 from a heparin column at between 0.2 and 0.4M NaCl indicated that ps20 is able to bind to heparin. Notably, the concentrated 0.5ml eluted fractions revealed numerous ps20 protein species of different molecular weights (MW).

While physiologically heparin is a heavily sulphated soluble glycosaminoglycan, heparan-sulphate and chondroitin sulphates are cell and ECM associated through their attachment to core proteoglycans (Hamel et al., 2009). As such, we used a modified GAG solid-phase ELISA to assess the *in vitro* binding affinity of recombinant human $ps20^{V5}$ for these GAGs. Binding curves (fig. 4.2A-C) demonstrate the affinity of $ps20^{V5}$ for physiologically relevant glycosaminoglycans, heparan-sulphate, chondroitin sulphate-A, and chondroitin-sulphate-C. Interestingly, ps20 had notably different affinities for different GAG species, with the highest being for heparan-sulphate, and the lowest being the most widely distributed GAG, chondroitin sulphate. Furthermore, all interactions were in the nanomolar range. We then investigated whether ps20 could interact with GAGs present at the cell surface. Fig. 4.2D shows 293T cells treated with $ps20^{V5}$ in the presence of absence of soluble heparin. We show clearly that ps20 is cell associated and that this interaction is interrupted in a

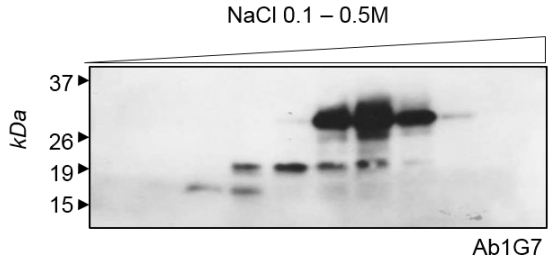

Figure 4.1 Multiple ps20 species bind heparin. 5mls of CM from 293T cells expressing pBK-ps20 loaded onto a 1ml heparin column, washed, and bound protein was eluted with 0-0.5M linear NaCl gradient. Fractions were subjected to western blot with ab1G7.

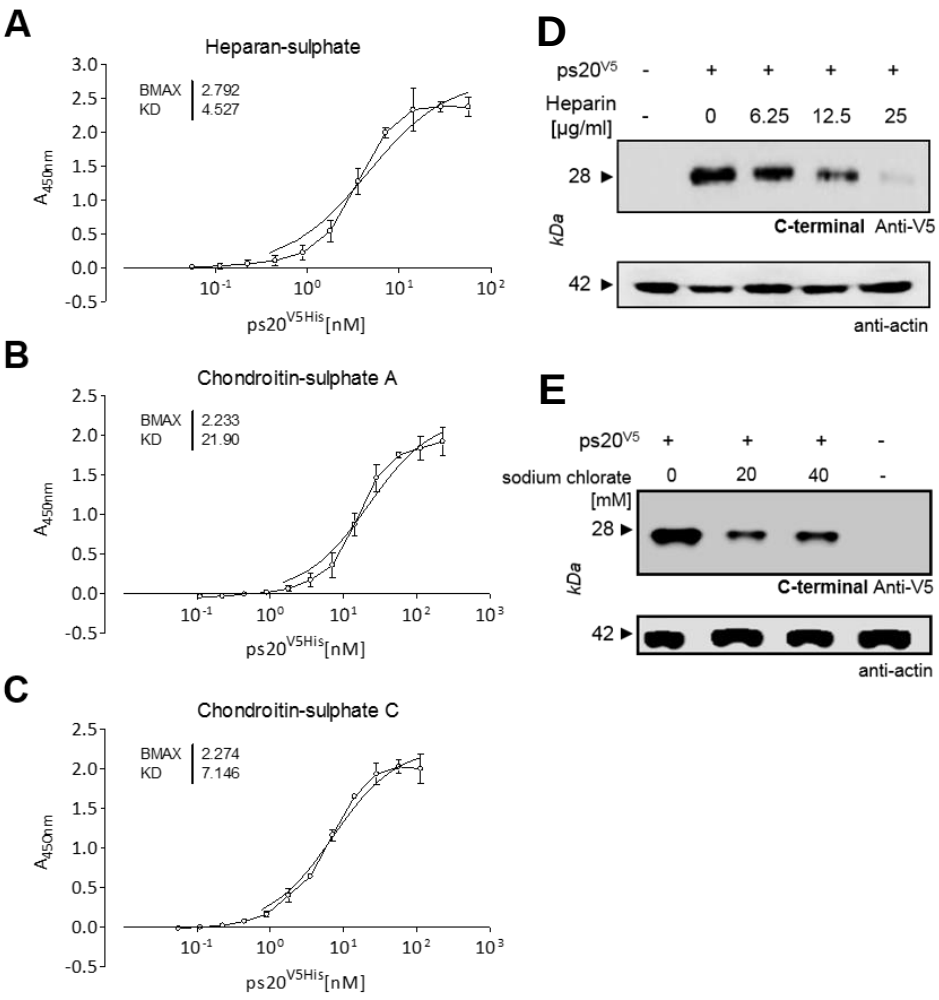

Figure 4.2 Ps20 binds to solid-phase and cell surface glycosaminoglycans. (A-C) rps20^{V5} bound to GAG coated ELISA plate and was detected using anti-V5-HRP. (D-E) rps20V5 [10µg/ml] was absorbed to 293T cells in presence or absence of heparin (D) or following treatment with sodium chlorate (E) before lysates were subjected to WB with anti-V5 or anti-actin.

concentration dependent manner by addition of soluble heparin, indicating that ps20 is undergoing an interaction with cell surface GAGs. To confirm this interaction, we treated cells with sodium chlorate prior to treatment with ps20. Sodium chlorate has been shown to interrupt the coupling of GAG to the protein core of proteoglycans. Fig. 4.2E shows a clear association between $ps20^{V5}$ and untreated cells. However, following treatment with either 20mM or 40mM sodium chlorate this interaction is reduced suggesting this interaction is GAG dependent.

4.2.2 Ps20 undergoes post-translation modification into multiple molecular forms.

Our heparin binding experiments revealed that ps20 is secreted into CM in numerous molecular weight species. Using the $ps20^{293F}$ generated by immunoaffinity purification presented in chapter 3 we interrogated the nature of ps20 species present using ps20 binding antibodies with known binding epitopes. Western blotting with C-and N-terminal antibodies to ps20 revealed one predominant molecular species of ps20 at ≈26kDa, with several minor subspecies resolving at lower MW (fig. 4.3A). The concentration calculated in Chapter 3 is shown again in table 4.1. Interestingly, we observed two immunoreactive minor species at about 22kDa and 16kDa respectively. Functional analysis showed that $ps20^{293F}$ induced a >40% inhibition on WPMY-1 cells while PC-3 cells were inhibited ≈30%. This is in line with growth inhibitory activity seen previously by David Rowley's lab, in which ps20 inhibited the proliferation of PC-3 cells by up to 60% down to a concentration of 7.3nM (Larsen et al., 1998).

In order to compare ps20 secreted from cells transfected with recombinant WFDC1 plasmid with naturally secreted ps20, we purified ps20 from HeLa cell conditioned

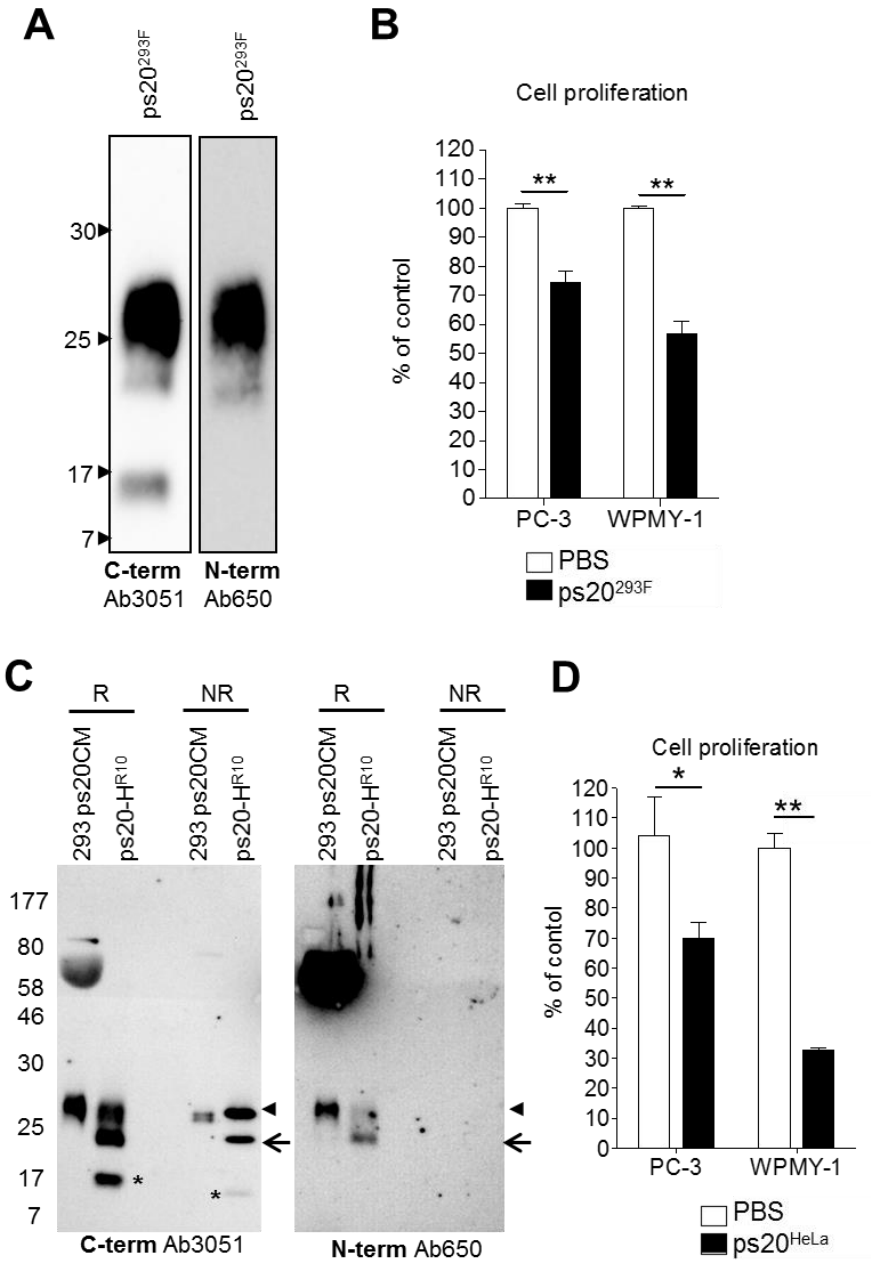

Figure 4.3. **Functional purified ps20 contains multiple immunoreactive species**. (A) ps20^{293F} (diluted 1:100) was subjected to WB with AB3051 and Ab650. (B) PC-3, or WPMY-1 cells were treated with 8.3nM ps20^{293F} and growth assessed by MTS at 72h (C) ps20^{HeLa} and 293T CM were subjected to western blot with the indicated antibodies. Arrowheads indicate the ps20 FL species, arrows the ps20 TR species, and LMW species are indicated with asterisks. (D) PC-3, or WPMY-1 cells were treated with 68pM ps20^{HeLa} and growth assessed by MTS at 72h (the plate was read at 490nm).**P<0.05 **P<0.001 by Student's T test.*

media. Figure 4.3C shows purified native secreted ps20 from a suspension culture of HeLa cells is shown alongside CM from 293T cells transfected to express ps20, used as a positive control (it should be noted that as this CM contained 10% FCS there is a large amount of non-specific immuno-reactivity to serum components at 60-70kDa). Interestingly, multiple ps20 subspecies were again present and were prominent in $ps20^{HeLa}$. The full-length (FL) ps20 molecule (fig. 4.3C, arrowhead) is present, however two lower MW bands (LMW) are prominent. The first at 25kDa recognised by both C- and N-terminal antibodies (fig. 4.3C, arrow) has both N-terminal and C-terminal regions intact. The second at ≈16kDa, is only detected by the C-terminal antibody (fig. 4.3C asterisk), suggesting a product of proteolytic cleavage close to the N-terminus of the molecule. Notably both these ps20 subspecies are comparable to those LMW species visible in the $ps20^{293F}$ material (fig 4.2A). To establish the concentration of the purified ps20, we $ps20^{HeLa}$ using our ps20 ELISA and a ps20-GST standard of known concentration (table 4.1). We then tested $ps20^{HeLa}$ for functional activity. Due to the small amount of material available, a full titration wasn't not possible, however, when added at the highest concentration available $ps20^{HeLa}$ induced potent growth inhibition on PC-3 cells and WPMY-1 cells (Fig. 4.3D) but which was effective at a concentration 2 logs below those observed with $ps20^{293F}$ (fig. 4.2C), or reported previously (Larsen et al., 1998).

Table 4.1 Concentration of immunoaffinity purified ps20 batches

ps20 batch	concentration (from ps20 ELISA)	molar concentration (based on MW of 24kDa)
$ps20^{HeLa}$	15ng/ml	0.68nM
$ps20^{293F}$	2µg/ml	83nM
$ps20^{FL}$	190ng/ml	7.9nM
$ps20^{TR}$	184ng/ml	7.64nM

4.2.3 Ps20 is cleaved by Cathepsin L

Because SLPI and elafin are substrates for proteolytic cleavage by cathepsins we investigated the effect of cathepsins B and L on ps20. $ps20^{FL}$ and $ps20^{TR}$ represent intact ps20 molecules prior to any post-translational cleavage. As such we cloned, expressed (as described in chapter 3) and subsequently purified both FL and TR variants, herein called $ps20^{FL}$ and $ps20^{TR}$ (fig 4.4A). Again the concentrations of these two ps20 batches were discerned by ELISA (table 4.1) and both were tested in WPMY-1 cell growth inhibition assays. Neither were found to have any functional activity (not shown).

In a series of assays to test the effect of cathepsins on ps20 we observed that both $ps20^{FL}$ and $ps20^{TR}$ were cleaved in a concentration dependent manner when incubated with recombinant cathepsin L (fig. 4.4B). A cleavage of 4-6kDa is clearly evident from the shift in electrophoretic mobility in the upper panels, probed with the N-terminal antibody. This cleavage results in a new distinct protein band indicating a discreet cleavage event is taking place. By contrast, the lower panels, probed with the C-terminal antibody, reveal the disappearance of ps20 from the blot with increasing concentrations of cathepsin L. This indicates that cathepsin L is able to efficiently cleave ps20 at a specific point near the C-terminus.

To confirm this, and to test whether native ps20 was subject to cleavage in the same way as recombinant $ps20^{FL}$ and $ps20^{TR}$, material previously purified from HeLa cells was subjected cathepsin L under identical conditions (Figure 4.4C). In this sample both the FL and TR ps20 species can be seen to be cleaved, as evidenced by the electrophoretic shift of both bands in the top panel, probed with

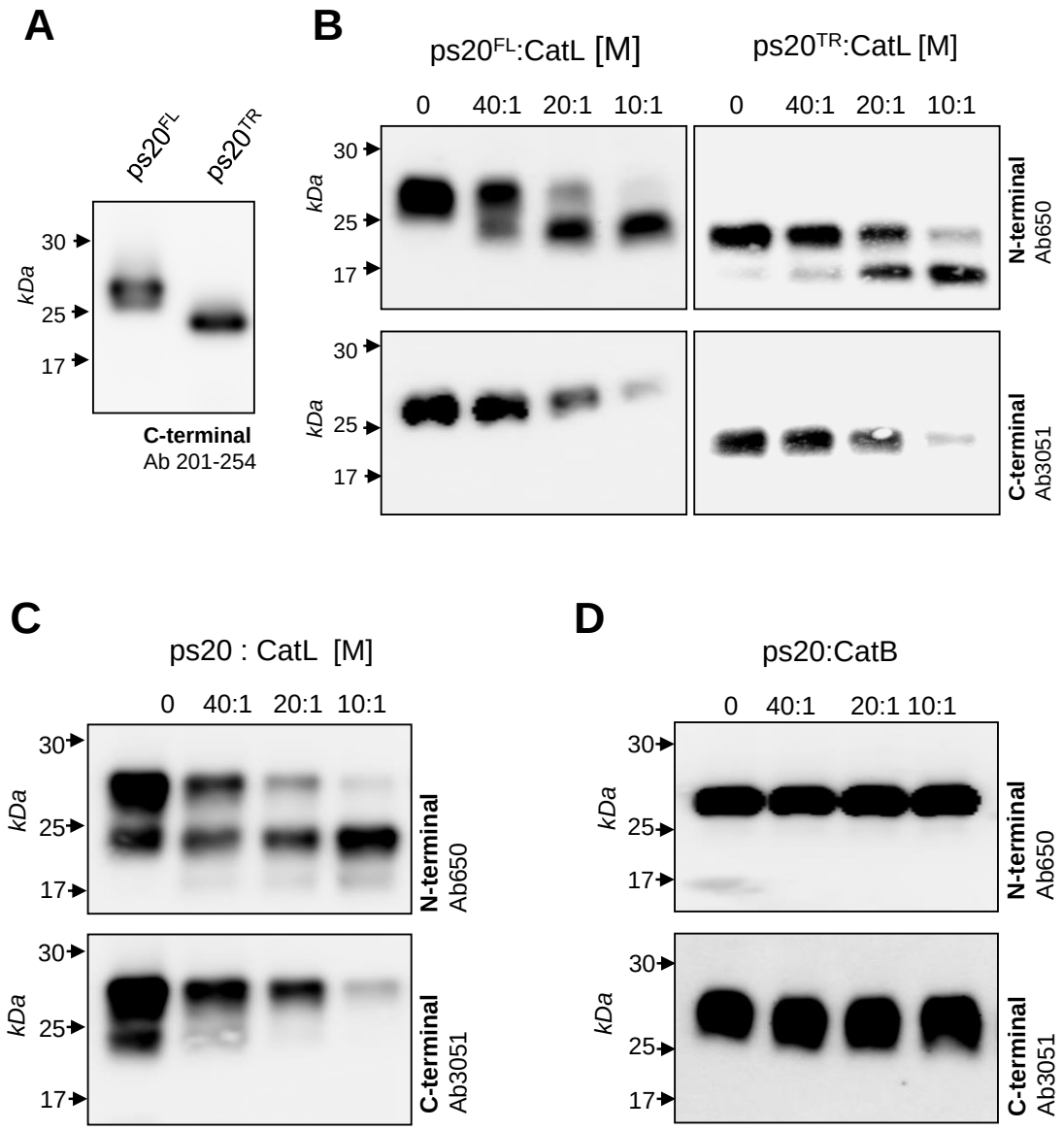

Figure 4.4 ps20^{FL} and ps20^{TR} are substrates for C-terminal cleavage by Cathepsin L but not Cathepsin B. (A) ps20^{FL} and ps20^{TR} were subjected to western blot with Ab201-254. (B) 20ng of ps20^{FL} or ps20^{TR} were incubated with an increasing molar ratio of cathepsin-L for 1h at 37^{0}C. (C) Purified hela-ps20 was subjected to cleavage by an increasing molar ratio of cathepsin-L for 1h at 37^{0}C. (D) Ps20^{FL} was incubated with an increasing molar ratio of cathepsin-B for 1h at 37^{0}C. (B-D) All Samples were electrophoresed on 12% gels and resolved by western blotting with C-terminal anti-ps20 ab5301 or N-terminal anti-ps20 ab650.

the N-terminal antibody, and the disappearance of both bands from the bottom panel probed with the C-terminal antibody. Together these results suggest that ps20 is a substrate for cathepsin L. In contrast, incubation with cathepsin B resulted in no apparent cleavage in $ps20^{FL}$ indicating that ps20 is not a substrate of Cathepsin B (fig.4.4D).

In order to test the functional effects of C-terminal cleavage of ps20 by cathepsin L, we repeated the cathepsin cleavage assay on the highly concentrated batch of $ps20^{293F}$. This batch induced a significant degree of growth suppression especially on WPMY-1 cells (fig. 4.3B), and so was suitable to test if cathepsin L cleavage either enhanced or abrogated ps20 function. $Ps20^{293F}$ was incubated with cathepsin L as described, and subsequently stained for total protein using lumitein (fig. 4.5A). This reveals a clear shift in electrophoretic mobility in the predominant FL ps20 band as well as in a number of LMW bands, suggesting cathepsin L was able to cleave any ps20 species with an intact C-terminus. Interestingly, despite undergoing substantial cleavage no change in growth inhibitory function was observed (fig. 4.5B). Taken together, these experiments indicate that cathepsin L is unlikely to be involved in i) generating functionally active ps20 protein species, or ii) for inactivating the growth inhibitory function of ps20 species.

4.2.4 Ps20 is multimerised by transglutaminase

SLPI and elafin are cross-linked to the ECM, likely as a means of regulating their function *in situ*. We investigated the interaction between ps20 and solid phase of TG in a modified ELISA. $Ps20^{V5}$ bound with high affinity to TG with non-linear regression indicating a K_d of 6.4nM (Fig. 4.6A). We then assessed the ability of TG to catalyse the formation of ps20 HMW multimers. $Ps20^{V5}$ incubated with TG in the presence of calcium formed two or more species of multimer which resolved at i) >100kDa, ii)

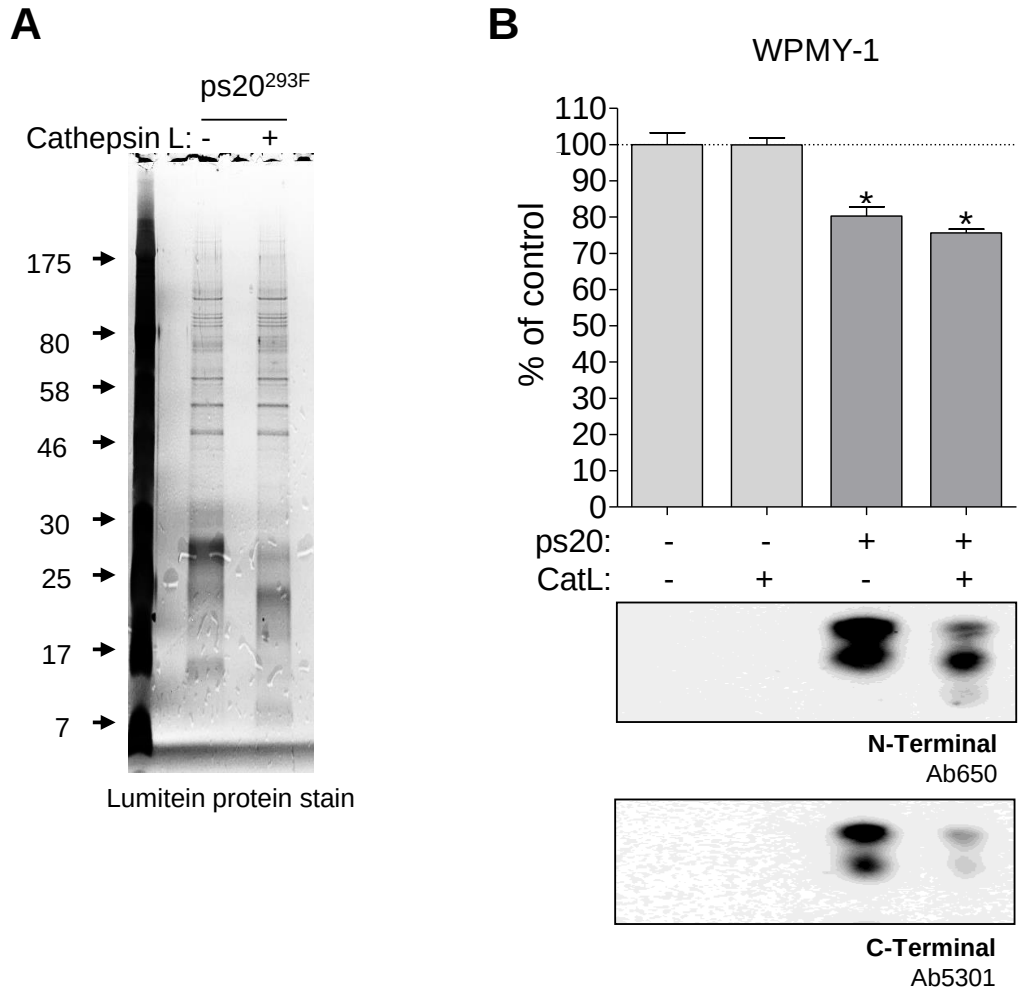

Figure 4.5 Cleavage by cathepsin L fails to abrogate the growth suppressive function of ps20^{293F}. (A) Neat ps20^{293F} was incubated with 200ng/ml Cathepsin L or buffer for 2h at 37^{0}C and subjected to SDS analysis and lumitein stain. (B) 10µl of each ps20 reaction or indicated controls were added to WPMY-1 cells and proliferation was assayed after 72h by addition of MTS (the plate was read at 490nm). The remaining samples were subjected to western blot with the indicated antibody. **p<0.05 relative to the condition without ps20 or Cathepsin L treatment.*

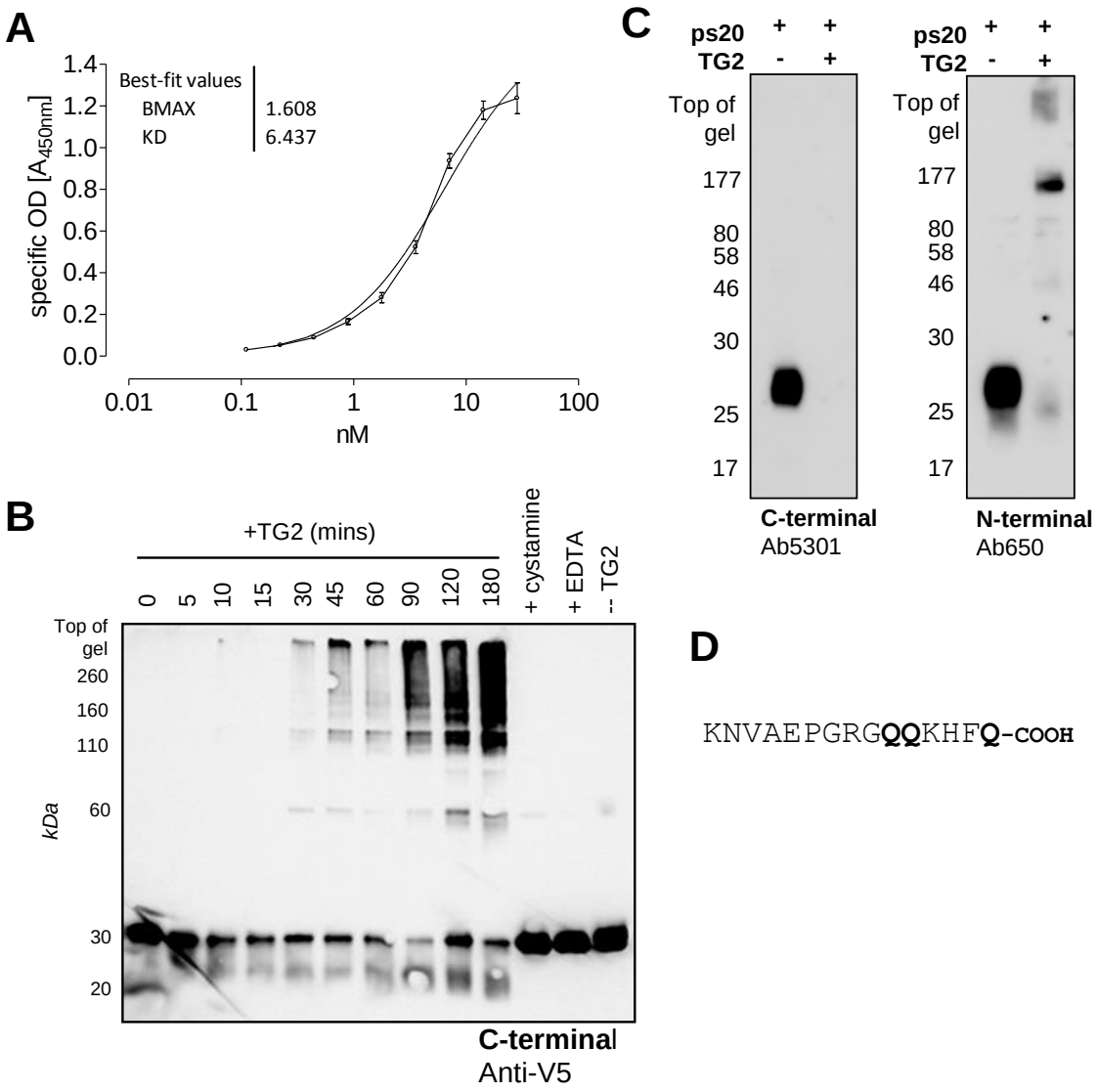

Figure 4.6 ps20 undergoes transglutaminase mediated multimerisation into higher order multimers. (A) ps20^{V5} was titrated in doubling dilutions onto a solid phase of TG. Binding was then detected using anti-V5 conjugated to HRP. Baseline was determined by binding of ps20 to BSA coated wells at each concentration, and subtracted before non-linear regression analysis to determine binding kinetics. Curve shows means/SD of three experiments in duplicate. (B) To induce crosslinking, ps20^{V5} was incubated with 0.2U/ml TG for the indicated time. Controls containing either cystamine, EDTA or without transglutaminase were incubated for 180 mins. Samples were taken into loading buffer containing reducing agents and boiled for 5 mins before SDS-PAGE analysis Western blotting was with anti-V5. (C) ps20^{293F} at 200ng/ml was incubated with 0.2u/ml TG or buffer control for 1h. Samples were taken into loading buffer containing reducing agents and boiled for 5 mins before SDS-PAGE analysis and western blotting with the indicated antibodies. (D) Peptide sequence of the C-terminus of ps20 with the glutamine residues highlighted.

approximately 160kDa, and iii) multimers which were too large to migrate into the gel (Fig. 4.6B). Addition of the competitive TG inhibitor cystamine, or the chelating agent EDTA prevented multimerisation, confirming that this was a TG specific event. Together these data indicate imply that TG is able to cross-link ps20 to irreversibly form stable high order multimers. Given the presence of the C-terminal tags on the $ps20^{V5}$ protein we sought to confirm the TG dependent multimerisation using untagged $ps20^{293F}$. Fig 4.6C right panel shows multimerisation of $ps20^{293F}$ to a predominant ≈150kDa species, and a less distinct species which failed to migrate into the gel, suggesting the presence of higher order multimers. Interestingly, the left panel shows a blot of the same experiment using a ps20 C-terminal antibody which binds the monomeric protein but fails to detect the multimerised forms. The last 15 amino acids of the ps20 peptide (Fig. 4.6D), against which the C-terminal antibody was raised, features three glutamine residues. These are potential substrates for transamination by transglutaminase which we hypothesis is why the C-terminal epitope is obscured by the cross-linking (fig. 4C left panel).

4.2.5 Ps20 becomes cross-linked to fibronectin and is liberated by cathepsin L cleavage.

We then investigated the interaction between ps20 and fibronectin, a component of the ECM known to cross link to SLPI and elafin. TG efficiently catalysed cross-linking to fibronectin in a modified ELISA assay (Fig. 4.7A), with only a small level of binding to fibronectin observed in the absence of TG. In contrast, no interaction was seen between ps20 and BSA either in the presence or absence of TG, suggesting the crosslinking between fibronectin and ps20 catalysed by TG was a specific interaction. In order to assess whether the proposed C-terminal crosslinking of ps20

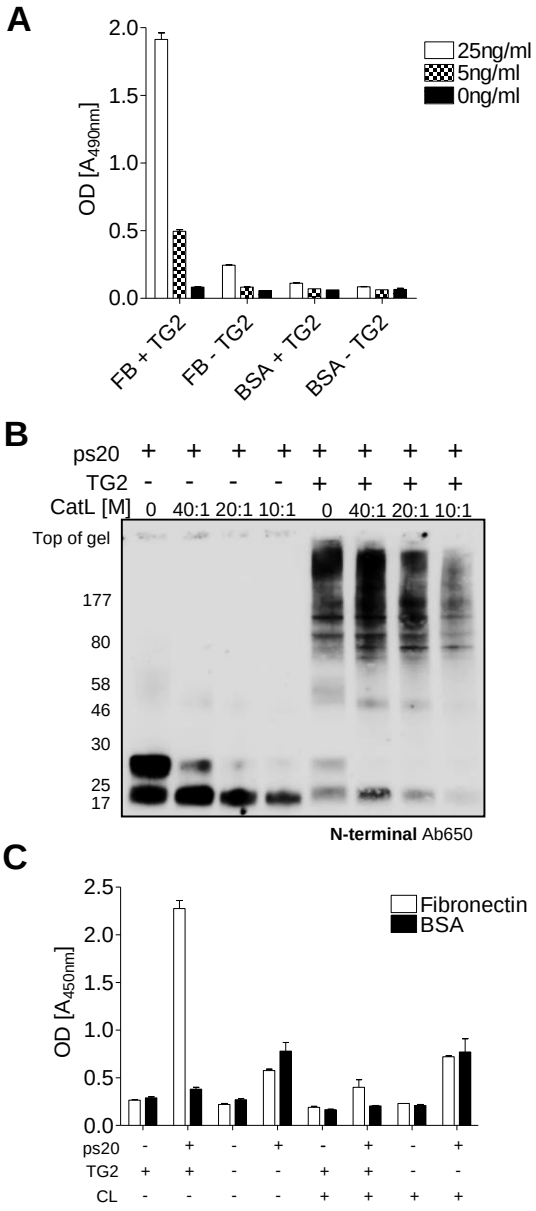

Figure 4.7 ps20 undergoes transglutaminase dependent crosslinking fibronectin and is liberated by cathepsin L cleavage. (A) Ps20 at the indicated concentrations was incubated with solid-phase of fibronectin or BSA and TG at 0.02U/ml for 2h, followed by washing and detection using 1G7-HRP. (B) Purified hela-ps20 was subjected to cleavage by an increasing molar ratio of cathepsin L for 1h at 37^0C then added to buffer containing 10mM $CaCl_2$ +/- 0.02U/ml TG and incubated for a further hour before being subjected to western blot. (C) 25ng/ml $ps20^{FL}$ was incubated with a solid phase of fibronectin or BSA +/- 0.02U/ml TG for 2h. Following washing, MES buffer +/- 400ng/ml cathepsin L was added and incubated for 2h at 37^0C. Cross-linked ps20 was detected with 1G7-HRP.

by TG was abrogated by cathepsin L, we performed a digestion of ps20 at the C-terminus by cathepsin L, followed by an incubation with TG to mediate the formation of HMW multimers (Fig. 4.7B). Multimerisation is far less apparent in ps20 which has been cleaved by cathepsin L, suggesting TG mediated cross-linking involves the poly glutamine motif present at the ps20 C-terminus. We then cross-linked ps20 to fibronectin followed by a digestion using cathepsin L in order to investigate whether cathepsin L cleavage of the C-terminus could liberate the N-terminal portion of the molecule. As before, we observed high levels of ps20 cross-linked to fibronectin in the presence of TG, but far lower with either solid phase BSA or where TG was absent (Fig. 4.7C). Following incubation of crosslinked ps20 with cathepsin L, level of detected ps20 is reduced almost to baseline. This indicates that once cross-linked to fibronectin, ps20 can still be cleaved by cathepsin L at the C-terminus.

4.3 Discussion

Despite being first isolated 20 years ago and being associated with various physiological processes (Larsen et al., 1998, McAlhany et al., 2003, Ressler et al., 2014, Alvarez et al., 2011, Alvarez et al., 2008, Rogers et al., 2012), ps20 remains largely uncharacterised at the protein level. Here we have used SDS-PAGE/western blot and ELISA based assays to characterise ps20 as a Cathepsin L and TG substrate which is present in multiple endogenous molecular species capable of interacting with ECM and cell surface proteoglycans.

We first confirmed that ps20 was a GAG binding factor like family members SLPI and elafin (Guyot et al., 2005b, Fath et al., 1998). GAG containing proteoglycans are important structural and functional components of the ECM (Imberty et al., 2007) as well as being potentially important in mediating cell surface signalling and import/export interactions (Poon and Gariepy, 2007). Our experiments demonstrated a clear interaction between ps20 from 293T CM and heparin, and ps20^{V5} showed a high affinity interaction with HS, CS-A, and CS-C. Furthermore ps20we shown to bind to the cell surface in a GAG dependent manner. This data supports the predicted interaction between ps20 based on the presence of two Cardin-Weintraub heparin binding motifs (Cardin and Weintraub, 1989). To date this is the first ps20 study to have identified possible binding partners or a means of ps20-cellular interaction. GAG binding may have important functional implications for WFDC family proteins; SLPI has previously been shown to become internalized in monocytes and neurons and enter the nucleus (Taggart et al., 2005, Hannila et al., 2013), suggesting the function of SLPI at least, and possibly other WFDC family members may be mediated by the ability to cross the membrane and interact intracellularly. It has been suggested that the cationic nature of SLPI may mediate the observed membrane transduction. Likewise, ps20 is relatively cationic protein, with a predicted isoelectric point of 8.3.

The mechanism by which proteins, cationic or otherwise, cross the cell membrane is still a matter of some debate [26]. There is much evidence from studies with cationic proteins/peptide such as HIV-TAT that cell-surface proteoglycans can mediate macropinocytotic protein/peptide uptake, possibly through interactions with actin and Rac protein (Letoha et al., Lambaerts et al., 2009, Gump et al., 2010). While it was beyond the scope of this study, the interaction shown herein between ps20 and GAG should be the subject of further investigation, whether as a mechanism by which ps20 enters the cell in a manner analogous to SLPI, or as a component of a different signalling mechanism, such as FGF family proteins, which rely on GAG interactions to regulate the binding of their cognate receptors (Coltrini et al., 1993, Kwan et al., 2001, Yang et al., 2008).

Following purification from HeLa and 293F cells CM, multiple immuno-reactive protein species were identified by a panel of anti-ps20 antibodies. These represented monomeric full length, monomeric exon 3 truncated, and various putative cleaved variants lacking either the N- or C-termini. The presence of ps20 species lacking terminal regions of the peptide sequence is strongly suggestive of proteolytic cleavage, especially given that only two discreet WFDC1 mRNA isoforms can be detected in HeLa cells, the full length transcript, and the truncated variant lacking exon 3. Supporting this, the presence of two C- and N-terminal intact protein species indicates the translation and secretion of both known WFDC1 mRNA species is taking place. The presence of ps20 species lacking either N- or C- termini however, suggests that HeLa cells are also expressing proteins that are able to cleave ps20. Interestingly, $ps20^{HeLa}$ had growth suppressive activity comparable to $ps20^{293F}$ at a 2 fold lower concentration. This led us to speculate that it may be one of the cleaved ps20 species that was functionally active. In should be noted that due to the configuration of the antibodies used in the ps20 ELISA, at the C-terminus and WFDC

domain, some LMW ps20 species may not be detectable, meaning the concentration of $ps20^{HeLa}$ generated by ELISA may not be accurate

SLPI and elafin are both substrates of cathepsins (Guyot et al., 2005a, Taggart et al., 2001), cleavage by which respectively inactivates, and activates the protease inhibitory function of these molecules. Herein we show Cathepsin L cleaves both $ps20^{FL}$ and $ps20^{TR}$ at the C-terminus, resulting in a change in MW of ≈4-6kDa, which we predict to result from a cleavage of around 30aa (fig. 4.4B). In contrast, cathepsin B failed to cleave ps20 suggesting that cathepsin L cleavage is a specific reaction and not an artefact of our experimental system. However, cathepsin L cleavage resulted in neither enhancement, nor inhibition of the ability of $ps20^{293F}$ to inhibit WPMY-1 cell proliferation (fig. 4.5B). From this we concluded cathepsin L cleavage is unlikely to be a direct functional regulator of ps20 growth inhibitory activity. In support of this, none of the LMW ps20 products we observed in the functionally active $ps20^{HeLa}$ preparation (Fig. 4.3) appeared to be analogous to the C-terminal cleavage product resulting from incubation of ps20 with cathepsin L. However, we speculated that cathepsin L may have other functional implications (discussed below).

High affinity binding of ps20 to a TG solid-phase, and the TG dependent formation of HMW ps20 multimers demonstrated an interaction between ps20 and TG (fig. 4.5A&B). These multimers were highly stable even following boiling at 90^0C for 20 mins in the presence of 50mM DTT, suggesting the *bona fide* formation of covalent isopeptide bonds. Of interest was the formation of multimers of a specific size. Both $ps20^{V5}$ and $ps20^{293F}$ formed multimers which resolved either at ≈150kDa, or which became lodged in the top of the gel. This indicates that TG dependent ps20 multimerisation is not an *ad hoc* accumulation of ps20 monomers, but the formation of specific multimeric structures. HMW multimers formed by untagged ps20 were only detected with anti-ps20 directed against the N-terminus of the protein, leading us to

hypothesis that the cross-linking utilised one or several of the glutamine residues at the far C-terminal end of the ps20 protein.

Our initial investigation into the crosslinking of ps20 to ECM proteins, utilized a commercially available, set of ECM proteins pre-coated on ELISA strip wells. This assay suggested that ps20 was able to interact with fibronectin, but there was little evidence of interactions with other ECM proteins (appendix fig. 8.4). As such we optimised this assay using ELISA plates coated with soluble fibronectin. These experiments confirmed that ps20 efficiently crosslinks to this ECM protein. We observed that ps20 becomes efficiently cross linked in a TG dependent manner to fibronectin (fig. 4.7A) in line with studies demonstrating that SLPI and elafin become cross linked with fibronectin and retain their protease inhibitory function (Guyot et al., 2005b, Baranger et al., 2011). Ps20 has no known protease inhibitory function, and we were not able to demonstrate a retention of growth inhibitory function by ps20 using this assay system, however, in line with the evidence that ps20 undergoes cross linking through cross-linking of C-terminal glutamine residues, we demonstrated that fibronectin crosslinked-ps20 can be liberated from the solid-phase by C-terminal cleavage by Cathepsin L.

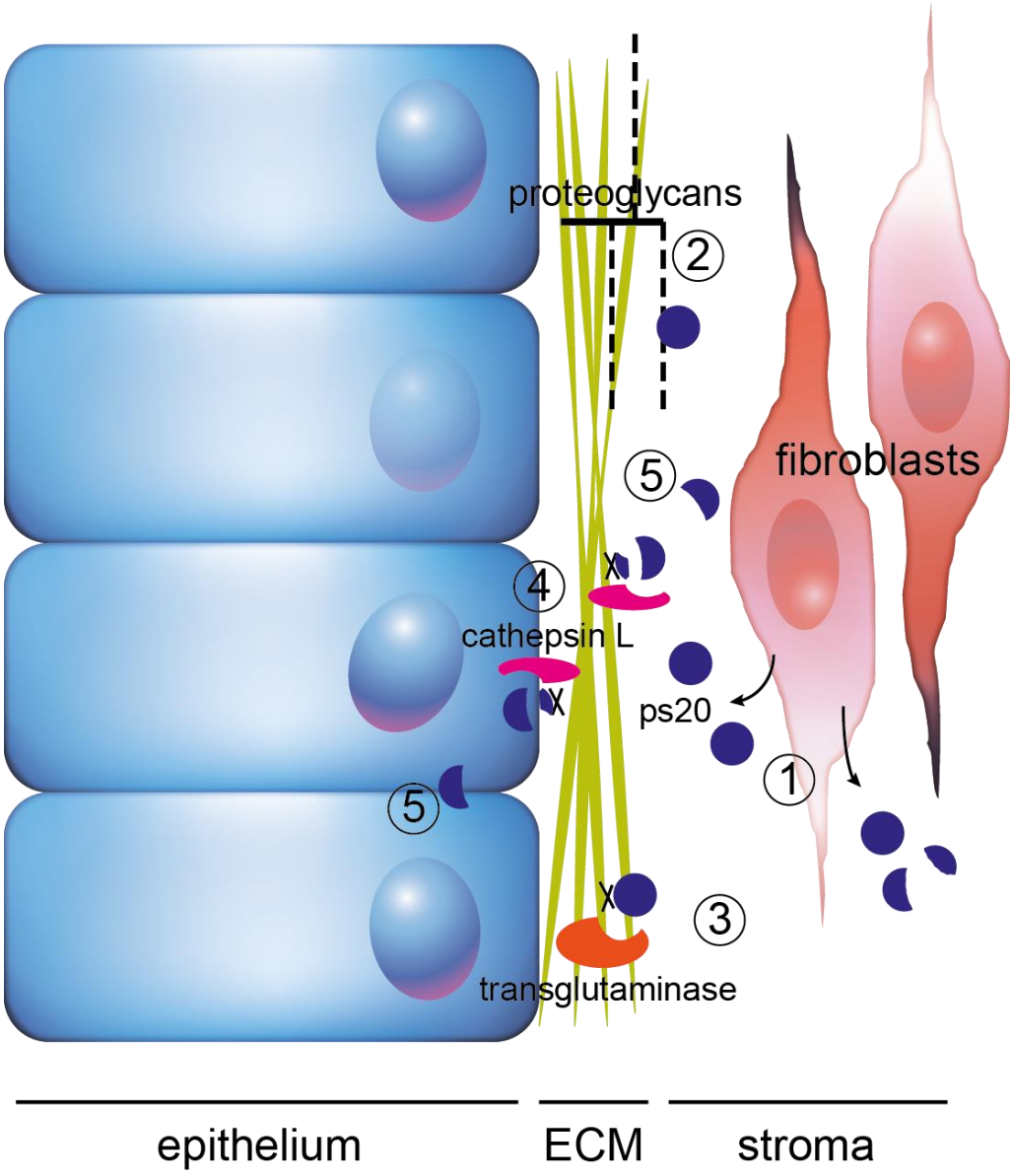

Figure 4.8 Proposed model of the extracellular interactions of ps20. This schematic proposes a model to explain the observed interactions of ps20 in the extracellular environment. Ps20 is secreted from the stroma and cleaved into multiple molecular forms (1). Secreted ps20 interacts with GAGs (2). Ps20 is then cross-linked to extracellular matrix components by TG (3). Soluble ps20 is then made available by cleavage of the cross-linked C-terminus by cathepsins (4). Ps20 is then available to undergo further downstream processing (cleavage/multimerisation) and suppress proliferation of stromal and epithelial cells (5).

Taking these observations together, we propose that TG crosslinking may be part of an apparatus, common to SLPI, elafin and ps20, whereby bio-availability of these proteins is reduced through formation of HMW multimers, or which involves cross-linking of soluble protein to the ECM (fig. 4.8). Our subsequent observation that cathepsin L abrogates formation of HMW ps20 multimers and liberates ps20 from fibronectin cross-linking suggests that in the case of ps20, cathepsin L maybe another component of ps20 regulation. Digestion of ps20 by cathepsin L following cross-linking to fibronectin provides an intuitive mechanism by which ps20 is liberated from its tethers to the ECM and is able to enact its cellular functions (fig. 4.9). This hypothesis is supported by our data showing that ps20 retains functional activity following C-terminal cleavage (fig. 4.6B).

We propose that ps20 is secreted in both FL and TR forms and may be cleaved to a number of smaller protein forms (Fig. 4.8). Different ps20 species can then bind to GAGs, both on the cell surface and within the ECM. Within the ECM, TG is able to cross-link the C-terminus of ps20 to ECM components such as fibronectin, and cathepsin L is able to regulate the bioavailability of ps20 by cleaving the C-terminal fragment from the main protein leaving a function N-terminal ps20 to mediate growth inhibition (fig. 4.7). As we have seen from other studies (Ressler et al., 2014, Alvarez et al., 2011, Alvarez et al., 2008, Rogers et al., 2012), the function of ps20 is likely not limited to cellular growth inhibition, and like other WFDC family proteins there is evidence it mediates pleiotropic functions with a range of growth regulatory and immune effects. The diversity of ps20 species observed in this study suggests that different processing events may produce ps20 species with different functional roles, and these events form part of a larger regulatory apparatus which involved sequestering of ps20 at the ECM through TG cross-linking, and liberation through C-terminal cleavage by Cathepsin L. Future work should seek to characterise the individual forms of ps20 present in the extracellular milieu and elucidate i) the

proteases which generate them, and ii) their individual functions. Any future mechanistic studies of ps20 may benefit from incorporating the role of ps20-GAG binding in any proposed model of ps20-cell interactions. The role of ps20 as an inhibitor of growth and as an immune regulatory protein may be of significant therapeutic application, but its utility may be limited by its complex biochemistry and our limited understanding thereof.

Chapter 5. ps20 as a suppressor of growth in the prostate stroma.

5.1 Introduction

In Prostate cancer (PCa), reciprocal signalling between neoplastic epithelium and the surrounding tissues leads to the emergence of a 'reactive stroma' which co-evolves to support the growth, invasion, immune-suppression and eventual metastasis of the tumour (Barron and Rowley, 2012). In the healthy adult prostate, stromal tissues acting under the influence of androgens secrete the extracellular matrix, which preserves the architecture of the organ; and produce soluble signals to control the growth and differentiation of the epithelial compartment (Cunha et al., 1996, Ressler and Rowley, 2011). Dysregulated stroma occurs during carcinogenesis and supports growth of the tumour by increasing the proliferation of neoplastic cells (Niu and Xia, 2009) and by expressing soluble and membrane bound mediators of immune suppression (Feig et al., 2013). Indeed, it has been shown that experimental elimination of certain stromal compartments is sufficient to induce complete regression of tumours in mice, highlighting the significance of a dysfunctional stroma in tumour growth and survival (Kraman et al., 2010).

In the mid-nineties David Rowley's lab observed that cells from rat urothelial mesenchyme expressed CM that was potently growth suppressive of cell lines isolated from human prostate cancer, namely PC-3 cells (Rowley et al., 1995). Based on this functional activity a novel protein factor was purified from the CM and given the name prostate stromal 20 (ps20) due to its apparent molecular weight of 20kDa (Rowley et al., 1995). The human analogue was soon after identified, cloned and expressed and shown to contain a WFDC domain and given the gene name WFDC1.

The WFDC1 gene locus was subsequently mapped to chromosomal locus 16q24.3, a region whose loss of heterozygosity is specifically associated with progressive prostate cancer (Harkonen et al., 2005, Larsen et al., 2000) where it has been suggested to act as a tumour suppressor gene (Watson et al., 2004a). In experiments investigating the expression of WFDC1/ps20 in human prostate cancer, Rowley *et al* subsequently identified the loss of ps20 from the prostate stromal compartment as a key difference between healthy specimens and the reactive stroma associated with cancerous samples (McAlhany et al., 2004, Ressler and Rowley, 2011). However, a subsequent *in vivo* study showed ps20 expressing xenografts achieved greater size and vascularity than control tumours in mice (McAlhany et al., 2003) suggesting the function of ps20 may be highly tissue specific with context and cell type specific functions which required further investigation.

To date, numerous other studies have identified a loss or reduction in WFDC1 expression in PCa (Watson et al., 2004b) and other cancer types including melanoma (Liu et al., 2008a), lung, brain, bladder and fibrosarcomas (Madar et al., 2009) and reduced WFDC1 expression in cancer associated fibroblasts relative to normal fibroblasts (Madar et al., 2009). Taken together, these observations highlight that understanding the molecular mechanisms by which ps20 regulates cell growth, which has not been examined in detail, is critical to unravelling its function.

In the previous chapter we saw that a complex biochemistry adds numerous levels of complexity to efforts towards elucidating the function of ps20 using exogenously added protein. Consequently, in this chapter we attempt to further investigate the growth suppressive function of ps20 in the prostate through overexpression of two ps20 isoforms in a range of PCa cells lines. Namely, the full length mRNA and the exon 3 truncated splice variant. We aimed to elucidate the mechanisms by which ps20 mediates growth suppressive effects on PCa cells and further elucidate the cell

specific nature of these effects. Herein I present evidence to show that ps20 expression has no effect on the proliferation of PCa cells. However, expression in WPMY-1 prostate stromal cells exhibits paracrine growth suppression of PCa cells through regulation of COX-2 expression.

5.2 Results

5.2.1 Ps20 is secreted in two isoforms

Previous studies have shown WFDC1/ps20 to be down-regulated in numerous cancers (Madar et al., 2009) including prostate cancer (Watson et al., 2004b), suggesting a putative role as a tumour suppressive factor. We used qPCR to assess WFDC1 expression in a number of prostate cancer derived cell lines (PCa) (PC-3, DU145, LNCaP and PNT-2), one prostate stromal cell line (WPMY-1) and HeLa cells, where we have previously observed high levels of ps20 expression (fig. 5.1). We found WFDC1 expression was extremely low in all prostate derived cells. In contrast, expression of SLPI, a WFDC family protein, was 2 -3 logs higher in all cells tested except WPMY-1. HeLa cells had approximately 4 log higher WFDC1 expression than all PCa cells tested. While RT-PCR has revealed WFDC1 transcripts in PC-3 and DU145 cells previously (Watson et al., 2004b), we demonstrate that this expression is very low compared to HeLa, a ps20 secreting cell line. RT-PCR has already revealed expression of two discreet mRNA species in HeLa cells (Chapter 3, fig. 3.7), a full length (660bp) transcript and a truncated (576bp) transcript in which exon3 was absent. Both species are translated and expressed and were cloned for expression for retroviral constructs.

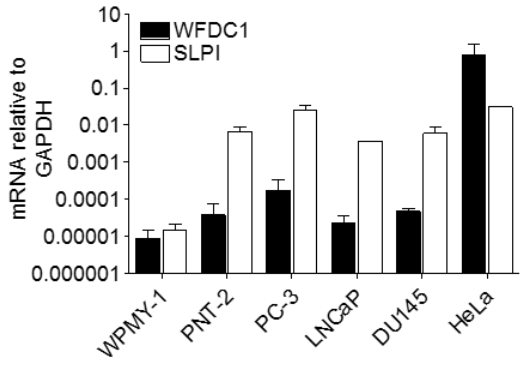

Figure 5.1. Expression WFDC1/ps20 in PCa and HeLa cells. Taqman qPCR was performed on cell lines indicated. RT-PCR generated cDNA was probed for SLPI and WFDC1 copy number and results calculated relative to GAPDH expression.

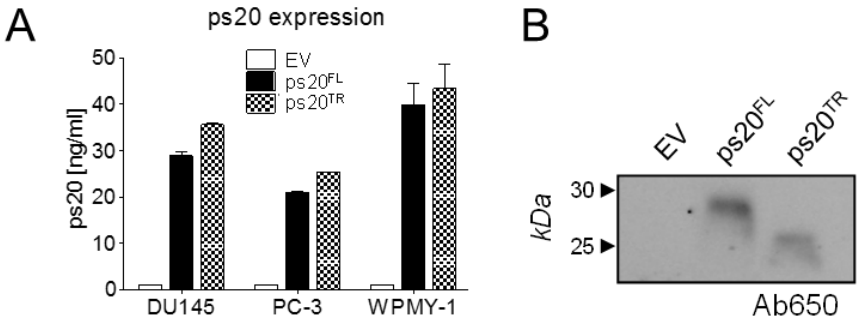

Figure 5.2 Ectopic expression of ps20 in DU145, PC-3 and WPMY-1 cells. (A) CM from transduced PC-3, DU145 and WPMY-1 cells was collected and titrated on a ps20 ELISA and concentration extrapolated by non-linear regression in prism 4. (B) Serum free CM was collected from transduced WPMY-1 cells expressing EV, $ps20^{FL}$ or $ps20^{TR}$, electrophoresed and blotted with N-terminal anti-ps20, 650.

Using these retroviral constructs we transduced PCa and stromal cells (PC-3, DU145 and WPMY-1) with WFDC1 constructs and sorted for eGFP expression cells as described in materials and methods. All ps20 transduced cell lines showed high expression of ps20 in CM as assayed by ps20 ELISA (fig. 5.2A). Both ps20 protein species resolved at the predicted MW when serum free CM was subjected to western blot (fig. 5.2B).

5.2.2 Ectopic expression of ps20 inhibits growth and induces apoptosis in a cell-specific manner.

Ps20 was originally purified from rat urothelial cells as a potent inhibitor of PC-3 cell proliferation (Rowley et al., 1995). Using an MTS based growth assay, we assessed the proliferation of transduced DU145, PC-3 and WPMY-1 cells expressing EV, $ps20^{FL}$ and $ps20^{TR}$. Despite secreting high levels of ps20 no growth inhibition was seen in PC-3 or DU145 cell lines (fig. 5.3A - B). However, in line with a previous report showing growth inhibition in fibroblasts expressing ps20, WPMY-1 stromal cells secreting both $ps20^{FL}$ and $ps20^{TR}$ had reduced proliferation relative to the control EV line (fig. 5.3C). This growth inhibition was confirmed by cell counting of 7 passages of the transduced WPMY-1 cells (fig. 5.3D). We then looked at apoptosis, cell death and the cell cycle to further elucidate the nature of the reduced proliferation associated with ps20 expression. WPMY-1 cells expressing $ps20^{FL}$ had increased levels of apoptosis relative to the EV control, while the $ps20^{TR}$ expressing cells had an intermediate phenotype with levels of apoptosis increased 2-3 fold (fig. 5.3E). The increased levels of apoptosis observed in cells expressing $ps20^{FL}$ and $ps20^{TR}$ were even more pronounced when cultured in serum free media (fig. 5.3F), probably due to absence of growth and survival factors contained in FCS.

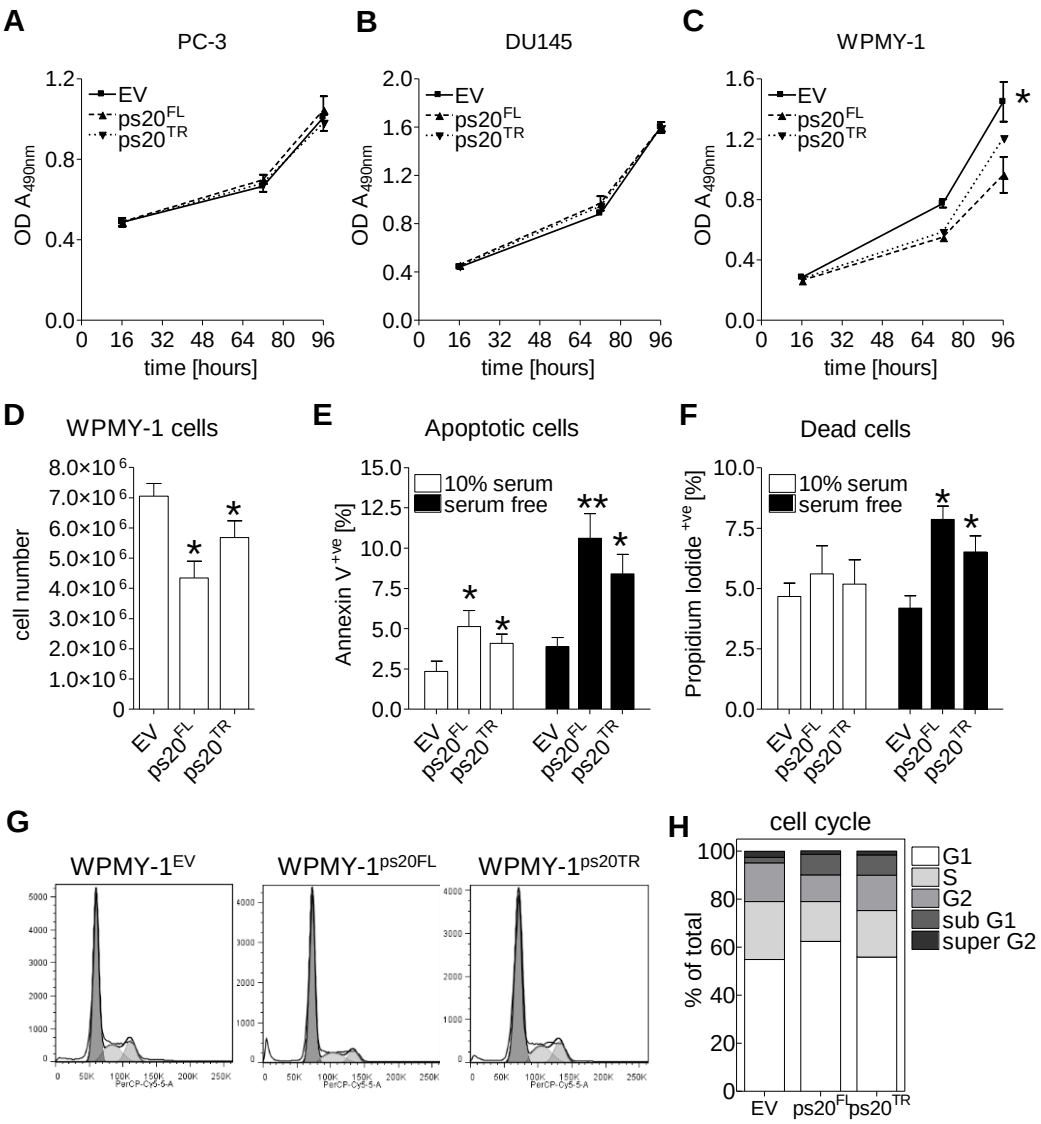

Figure 5.3. Expression of ps20 in prostate stromal cells induces apoptosis and G1 cell cycle arrest. (A-B) PC-3 (A), DU145 (B), or WPMY-1 (C) cells transduced to express $ps20^{FL}$ or $ps20^{TR}$ were seeded in 100µl complete media in 96 well plates. At each respective time point 15µl of MTS reagent was added to respective wells and incubated for 2h and colourimetric readout taken at 490nm. (D) 10^6 transduced WPMY-1 cells were seeded in 75cm^2 flasks and grown for 72h in complete media before counting. Represents 7 passages of cells). (E-F) To investigate apoptosis, $3x10^4$ EV or ps20 transduced WPMY-1 cells were seeded in 24 well plates. At 48h cells were taken and stained with annexin V and PI, to identify (E) apoptotic and (D) dead cells. (G-H) Alternatively the cell cycle of WPMY-1 ps20 transduced cells was analysed by treating cells with RNase A, and staining with PI. Cell cycle staging was elucidated by Watson analysis on FlowJo™. Representative plots are shown in (G) and means of 3 experiments were presented in columns graphs (H). ** p<0.05 and ** p<0.01 Student's T test.*

As indicated in fig. 5.3F the levels of PI positive, or dead cells in each culture condition mirrored the increased levels of apoptosis observed in cells expressing $ps20^{FL}$ or $ps20^{TR}$. Cell cycle analysis of transduced WPMY-1 cell lines indicated that in cells expressing $ps20^{FL}$ a smaller proportion of cells were in G2 and S phase of the cell cycle (fig. 5.3G) suggesting cell-intrinsic expression of ps20 may also function to some extent to restrain cells in G1 phase. In contrast, $ps20^{TR}$ cells had a cell cycle profile comparable to the EV line, suggesting that only $ps20^{FL}$ expression conferred a *bona fide* reduced proliferative rate.

Together these data indicate that the reduced growth rate manifest in ps20 expressing WPMY-1 cells is likely due to an increased propensity to undergo apoptosis and, at least in $ps20^{FL}$ cells, an extended cell cycle. In addition, expression of $ps20^{FL}$ was more biologically active than expression of $ps20^{TR}$.

5.2.3 CM from WPMY-1 cells expressing ps20 has broad growth inhibitory effects.

Previous studies showed ps20 to be highly expressed in the healthy prostate stroma (McAlhany et al., 2004, McAlhany et al., 2003). Given the reported propensity for ps20 expression to be reduced or switched off within the context of tumours, we hypothesised that stromal ps20 may be a paracrine regulator of growth and a barrier to the development of prostate neoplasms. To assay the effect of ps20 expression in WPMY-1 cells in paracrine, CM was collected from WPMY-1 cells expressing EV, $ps20^{FL}$ or $ps20^{TR}$ and titrated onto PCa cells in culture. WPMY-1 CM from ps20 expressing cells was potently growth inhibitory on metastatic (PC-3/DU145), androgen sensitive (LNCaP) and primary (PNT-2) PCa cell lines (fig. 5.4 A - D). Media conditioned for 72h also inhibited growth when added back onto WPMY-1 cells

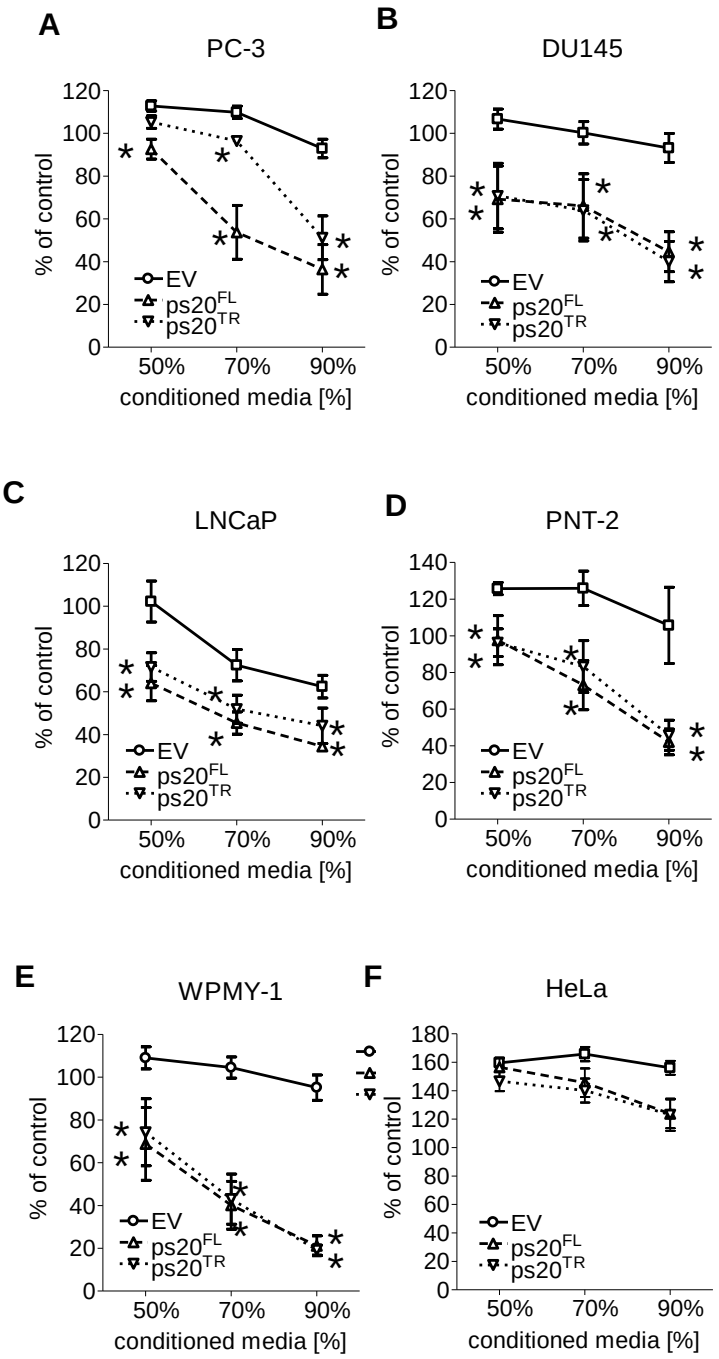

Figure 5.4. CM from WPMY-1 cells expressing ps20 potently inhibits growth of PCa cells. (A-F) CM taken from transduced WPMY-1 following 72h in culture was titrated onto PC-3 (A), DU145 (B), LNCaP (C), PNT-2 (D), WPMY-1 (E), and HeLa (F) cells, and cultures where grown for 96h. Growth was assayed following addition of MTS reagent (the plate was read at 490nm). Following background subtraction ODs were plotted as a percentage of cells from each cell line grown in complete media only. Each plot represents at least two separate experiments with different batches of CM. **p<0.05 relative to EV control at same dose by Student's T test.*

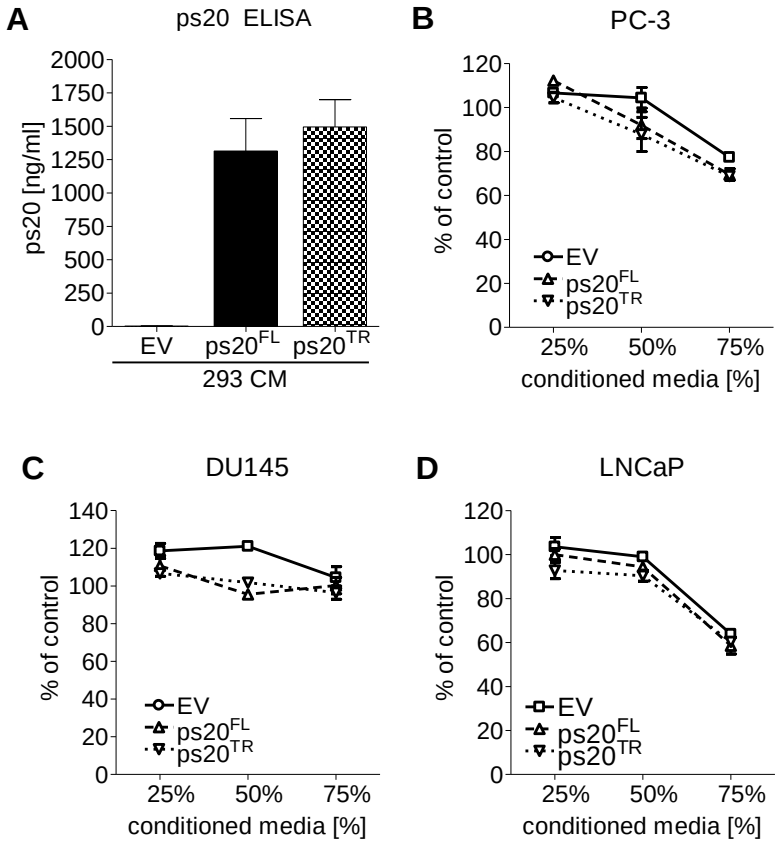

Figure 5.5 Conditioned media from ps20 expressing 293T cells does not suppress PCa cell growth. (A) 293T cells were transiently transfected with constructs encoding $ps20^{FL}$ or $ps20^{TR}$ or an EV control. The resulting CM was collected, clarified and assayed by ELISA. (B-D) CM was then titrated onto PCa cells. Growth of PC-3 (B), DU145 (C), and LNCaP (D) following 96h in culture was ascertained by addition of MTS reagent (the plate was read at 490nm) and plotted relative to cells grown in complete media alone.

(fig. 5.4E). In all cases this effect titrated when a lower concentration of CM was offered relative to CM from EV transduced WPMY-1 cells. However, ps20 transduced WPMY-1 CM did not suppress HeLa cell proliferation and conversely a slight growth enhancement was noted. Interestingly, despite having a ps20 concentration two logs higher than transduced WPMY-1 lines (fig. 5.5A), we failed to observe any specific growth suppression of PCa cell lines treated with CM from 293T cells expressing ps20 species (fig 5.5B-C), suggesting that i) ps20 is not directly inducing the growth suppression, and ii) that the growth inhibitory effect of ps20 expression is producer cell-type specific.

5.2.4 CM from WPMY-1 cells expressing ps20 induces growth suppression through the induction of apoptosis.

Having seen that CM collected from WPMY-1 cells transduced to express both $ps20^{FL}$ and $ps20^{TR}$ suppresses proliferation of PCa cells, we sought to elucidate whether this was related to cellular death or inhibition of cell division. Using a standard measurement of apoptosis we assayed cells for expression of annexin V at the cell surface following treatment with WPMY-1 cell CM. Figure 5.6A-B demonstrates an increase in apoptosis in DU145 and PC-3 cells respectively following treatment with CM from ps20 transduced WPMY-1 cells. This data suggests that the growth inhibitory phenotype observed is due to a paracrine induced increase in apoptosis. We next looked at the effects on the cell cycle of cells treated with WPMY-1 CM. Again we assayed DU145 and PC-3 cells and used PI staining to assess the percentage of cells at different stages on of the cell cycle. WPMY-1 CM treatment had little or no effect on the cell cycle in either cell line. Taken together, data from fig. 5.6 and fig. 5.7 suggests that ps20 expressing WPMY-1 cells is able to induce apoptosis through a paracrine mechanism without impacting the progression of cells through the cell cycle.

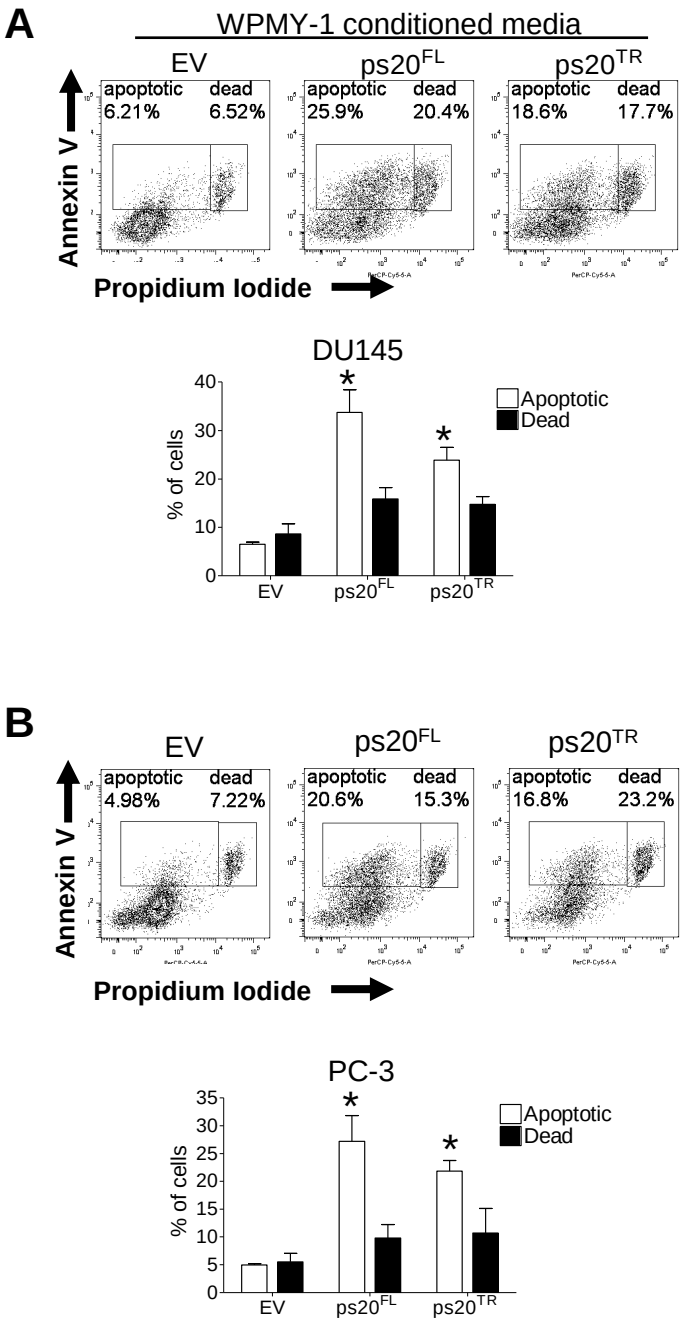

Figure 5.6 Conditioned media from WPMY-1 cells expressing ps20 induces apoptosis in PCa cells. DU145 (A) or PC3 (B) cells were seeded at 3x103 cells in 24 well plates and cultured in WPMY-1 CM for 48h before harvesting. Cells were stained with PI and annexin V. Representative plots are shown and graphs are means and SEMs of 3 experiments with 3 different batches of CM. **p<0.05 from EV control, Student's T test.*

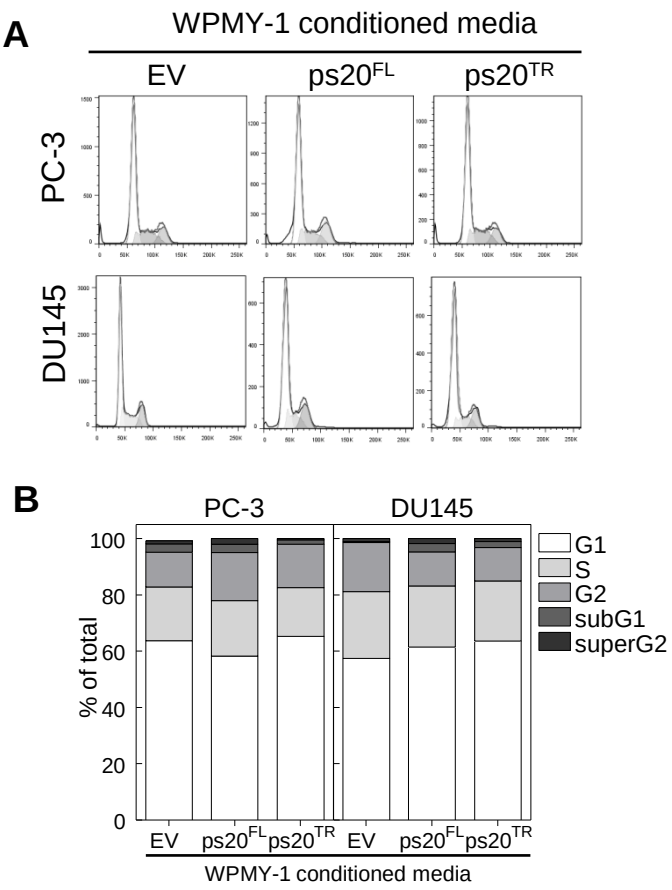

Figure 5.7 CM from WPMY-1 expressing ps20 does not impact entry to the cell cycle. (A-B) DU145 or PC3 cells were seeded at $3x10^3$ cells in 24 well plates and cultured in WPMY-1 CM for 48h before harvesting. Cells were analysed by PI staining and FACS. (A) Shows representative plots and (B) shows means of cell cycle staging over 3 experiments.

5.2.5 Ps20 does not mediate growth suppression directly.

Given that CM from 293T cells expressing ps20 was unable to specifically suppress the proliferation of PCa cell lines, we hypothesised that the suppressive effects of WPMY CM are mediated indirectly. To verify this possibility, we used beads coated with anti-ps20 antibody to deplete ps20 from the WPMY-1 CM. CM from $ps20^{FL}$ and $ps20^{TR}$ expressing WPMY-1 cells was successfully depleted to near background level (fig. 5.8A) whereas this did not have any demonstrable effect on the ability of ps20 transduced WPMY-1 CM to inhibit proliferation (Figure 5.8B). These data indicate that the growth suppressive paracrine phenotype effects of ps20 is likely mediated by a secondary factor that is regulated by ps20.

To determine the nature of the suppressive factor, and to exclude the possibility that the WPMY-1 cells were not mediating paracrine growth suppression by depleting the CM of vital nutrients, we treated PC-3 and DU145 cells to transduced WPMY-1 CM which had been boiled for 20 minutes. Data in fig. 5.8C-D shows that boiling completely abrogates the growth suppressive phenotype conferred by ps20 expressing cells, suggesting that the suppressive effect is mediated by a soluble factor which can be denatured by heat, such as a protein or lipid (fig. 5.8C and D).

5.2.6 Ps20 expression regulates expression of numerous growth inhibitory factors including COX-2.

Given the potent paracrine growth suppressive activity exhibited by transduced WPMY-1 cells we sought to identify the differences in gene expression in WPMY-1 cells expressing ps20 species relative to EV controls. To this end we performed a global differential transcriptome analysis of two passages each of $WPMY\text{-}1^{EV}$,

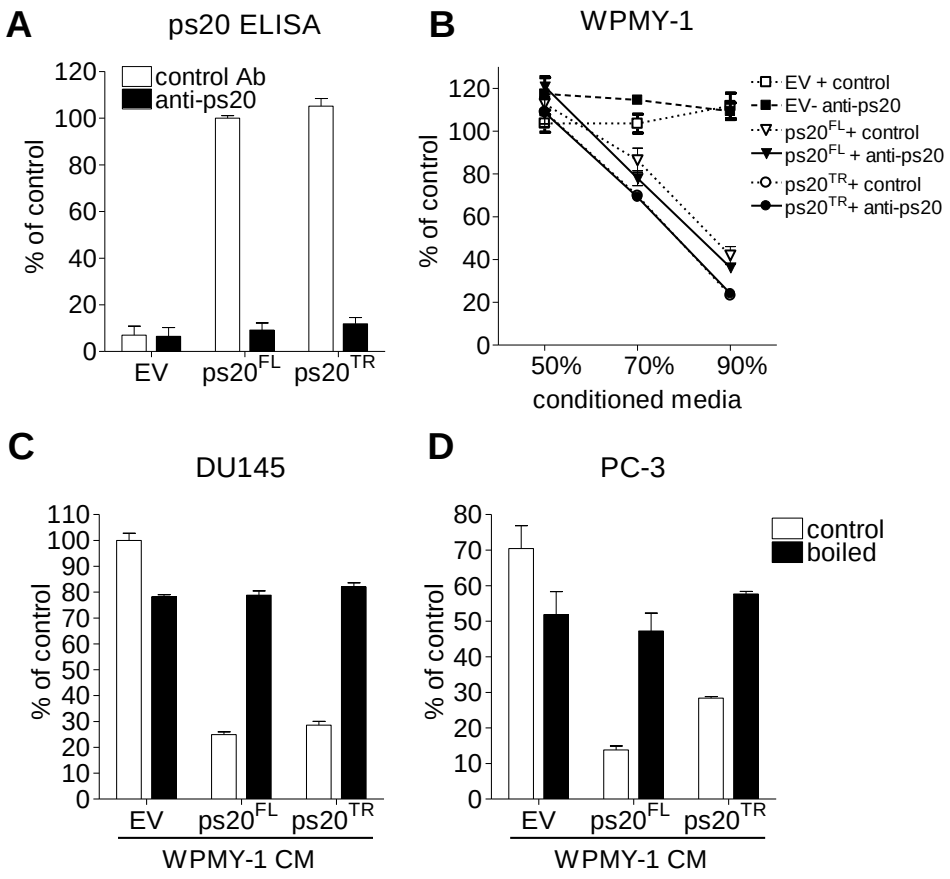

Figure 5.8 Suppression of PCa cell growth by WPMY-1 CM is not mediated directly by ps20. (A & B) CM from transduced WPMY-1 cells was incubated overnight with beads conjugated to anti-ps20 ab1G7 or an isotype. Following centrifugation to pellet beads, CM was assayed by ps20 ELISA (A) or was titrated onto WPMY-1 cells and cultured for 96h (B) followed by MTS assay (readout was at 490nm). (C-D) WPMY-1 CM was subjected to 20 mins boiling at 95ºC before addition to either DU145 (C) or PC-3 (D) cells for 96h. (B-D) Growth of cells was measured using the MTS reagent and plate read at 490nm.

WPMY1-ps20^{FL} and WPMY-1-ps20^{TR} cells. The results showed significant overlap in both upregulated and down regulated transcripts between ps20^{FL} and ps20^{TR} cells (fig. 5.9A-C) and subsequent pathway analysis revealed that ps20 altered the expression of a number of cytokine/chemokine pathways, metabolic pathways, and cell adhesion pathways (fig. 5.9D).

To further investigate changes in the secretory profile of ps20 transduced WPMY-1 cells, we mined the data specifically for differentially expressed growth inhibitory factors (table 5.1). Those upregulated in both ps20^{FL} and ps20^{TR} expressing WPMY-1 cells are indicated with an asterisk. Factors of interest with known anti-proliferative effects that were upregulated were SerpinF1 (Pigment epithelium-derived factor) (Becerra and Notario, 2013) and IL-32 (Joosten et al., 2013). IL-8, on the other hand can stimulate the growth of prostate cancer epithelium (Waugh and Wilson, 2008). Lastly, we observed a 5.29, and 3.86 fold increase in the expression of PTGS2 in WPMY-1-ps20^{FL} and WPMY-1-ps20^{TR} respectively. PTGS2 encodes cyclooxygenase-2 (COX-2), an enzyme responsible to metabolising arachidonic acid into PGH_2, which has diverse roles in the control of cellular growth, including inhibiting proliferation and the induction of apoptosis (Chaffer et al., 2006). COX-2 is not secreted, but rather associated with the nuclear envelop and endoplasmic reticulum. However, COX-2 is the rate limiting enzyme in a pathway which results in the formation of numerous growth inhibitory secreted prostanoids (Otto and Smith, 1994, Morita et al., 1995).

The expression of the four above noted genes was verified by qRT-PCR. Using cDNA generated from 3 passages of transduced WPMY-1 cell lines we confirmed up-regulation of COX-2, SerpinF1, IL-8 and IL-32 mRNAs in WPMY-1 cells expressing ps20^{FL} and ps20^{TR}. In all cases up-regulation was observed to a lesser

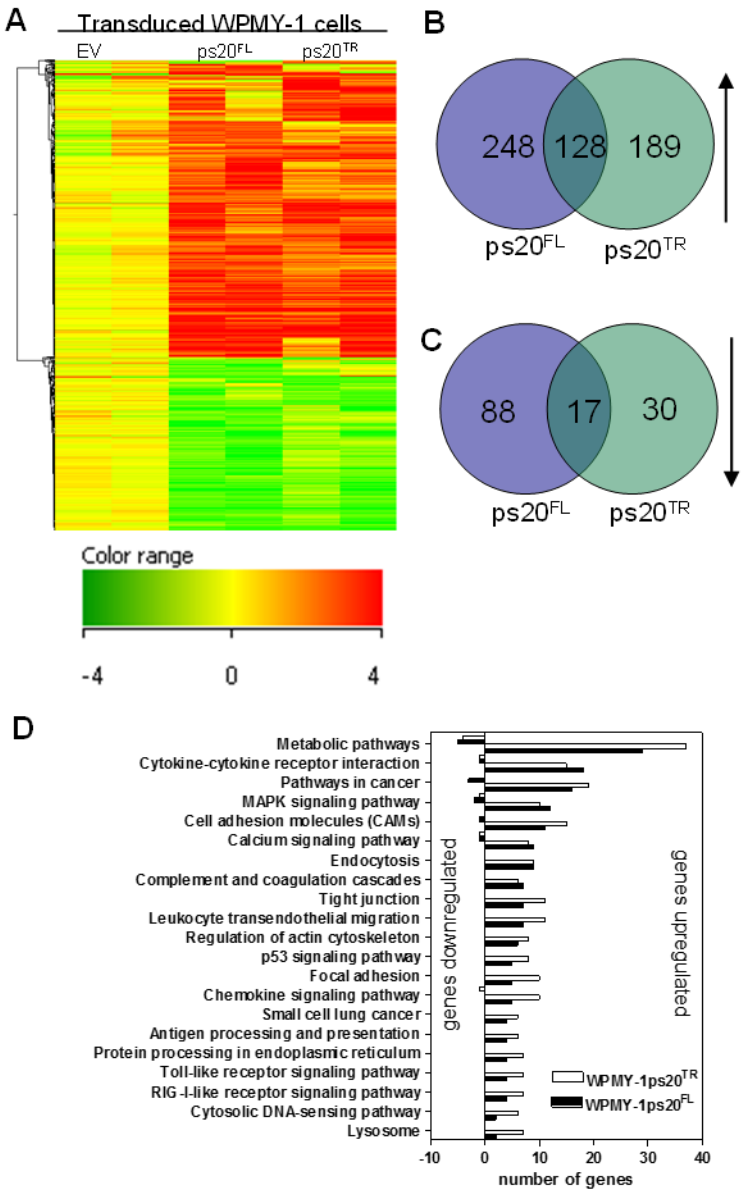

Figure 5.9 Transcriptome analysis of ps20 expression WPMY-1 cells. (A-D) WPMY-1 cells transduced to express EV, ps20^{FL} or ps20^{TR} were subjected to a full transcriptome analysis as described. In materials and methods (A) Heat-map depicting differential gene regulation (log_2) in WPMY-1 cells transduced to express EV, ps20^{FL} or ps20^{TR} according to the colour scheme shown and based on the mean of the EV replicates. (B-C) Venn diagrams depict the overlapping expression profiles of ps20^{FL} and ps20^{TR} WPMY-1 cells showing upregulated genes (B), and down-regulated genes (C). (D) Pathway analysis showing the number of genes up/down-regulated from specific cellular pathways in WPMY-1 cells expressing ps20^{FL} or ps20^{TR} relative to EV controls.

Table 5.1 Secreted factors differentially expressed in ps20^{FL} and ps20^{TR} WPMY-1 cells

	WPMY-ps20^{FL}		WPMY-ps20^{TR}	
Gene	**log2 fc**	**p value**	**log2 fc**	**p value**
PTGS2*	+ 5.29	0.01	+ 3.86	0.01
CXCL11	+ 4.51	0.03	-	-
CXCL6*	+ 3.78	0.01	+ 4.22	0.01
CSF3	-	-	+ 3.76	0.04
CCL5	+ 3.66	0.03	-	-
IL4I1	-	-	+ 3.56	0.00
C3	+ 3.51	0.03	+ 3.07	0.00
CXCL2	+ 3.25	0.04	-	-
IL8*	+ 3.00	0.01	+ 2.99	0.01
SERPINC1	-	-	+ 2.84	0.05
SERPINF1*	+ 2.72	0.00	+ 2.72	0.00
SERPING1	+ 2.72	0.05	-	-
IL33	+ 2.57	0.00	-	-
IL11	-	-	+ 2.32	0.01
IL32	+ 2.28	0.01	-	-
LIF	-	-	+ 2.06	0.04
SERPINB9	-	-	+ 2.06	0.04
CXCL14	- 2.95	0.02	-	
FGF1	- 3.60	0.03	-	

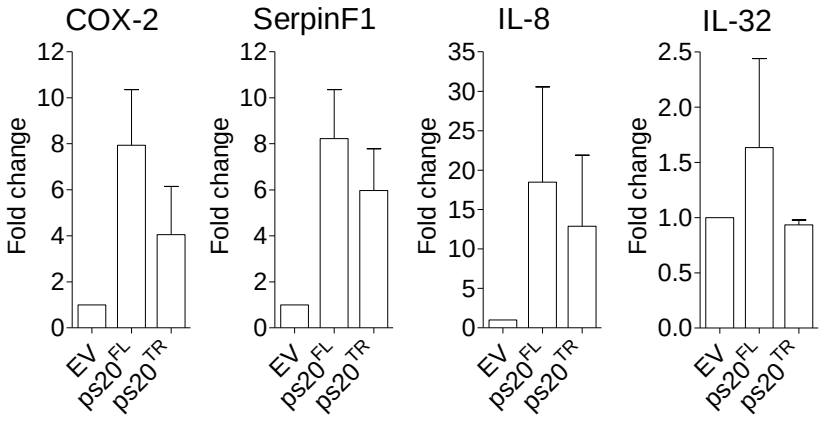

Figure 5.10 qPCR quantification of target mRNA species in ps20 expressing WPMY-1 cells. To assess expression of putative ps20-regulated targets cDNA was generated by RT-PCR from WPMY-1 cells expressing EV, ps20^{FL} or ps20^{TR} and subjected to SYBR green qPCR for the targets indicated. Relative copy numbers were calculated based on GAPDH expression.

extent in the $ps20^{TR}$ expressing cells than on those expressing $ps20^{FL}$ (fig. 5.10). This observation mirrors the intermediate growth suppressive phenotype observed in $ps20^{TR}$ expressing WPMY-1 cells relative to those cells expressing $ps20^{FL}$, suggesting that the truncated ps20 molecule may be functionally equivalent to the full length molecule, but with different kinetics.

5.2.7 Neutralisation of IL-6, IL-32 and TGFβ fails to abrogate growth suppression.

We confirmed by qPCR that both SerpinF1, IL-32 were upregulated in ps20 expressing cells. In order to test if either of these factors were responsible for the suppression of PCa cell growth elicited by WPMY-1 CM we performed a series of neutralisation assays. In addition, we assayed for TGFβ dependent suppression, given the established importance of this factor as a regulator of growth and apoptosis in the prostate. Antibodies that had been previously reported to neutralize the functional effects of their respective targets were chosen and incubated with cells at a concentration at least 2 fold above the reported IC_{50} (fig. 5.11A - C). In each case the antibodies failed to have any effect on the growth suppression induced by incubation of PC-3 cells with ps20 expressing WPMY-1 CM.

5.2.8 WPMY-1 cells cultured in the presence of COX-2 inhibitor do not produce growth suppressive conditioned media.

COX-2 is an enzyme which catalyses the conversion of arachidonic acid to prostaglandin H_2 ($PG\text{-}H_2$). COX-2 is the rate limiting enzyme in a pathway which leads to the generation of downstream prostanoids including Prostaglandin (PG) D_2

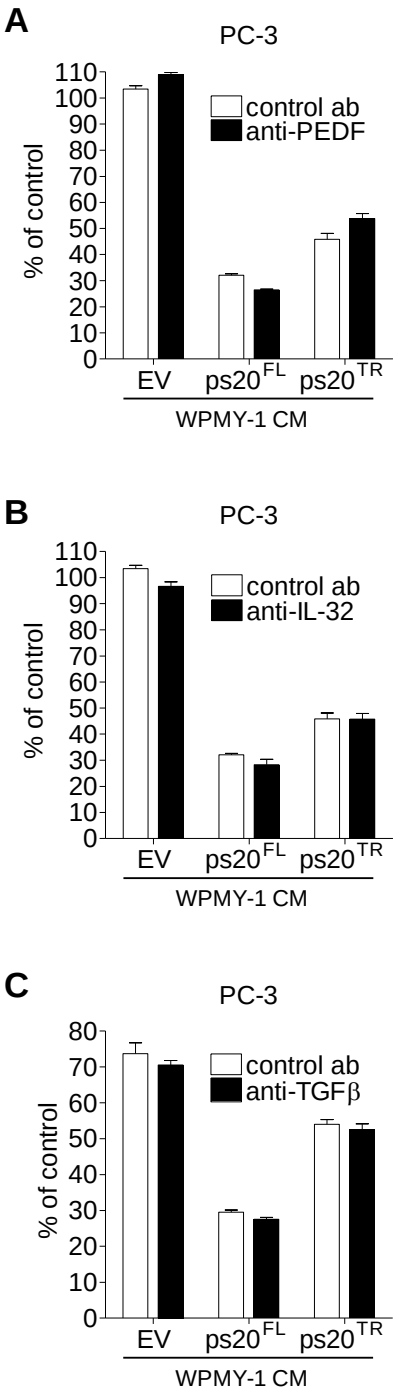

Figure 5.11. Neutralisation of secreted factors has no effect on WPMY-1 conditioned media mediated growth suppression. (A-C) PC-3 cells were cultured for 96h in 90% transduced WPMY-1 CM in the presence of neutralizing antibody to SerpinF1 (PEDF) [10g/ml](A), IL-32 [5g/ml](B), and TGFβ [20g/ml](C), or an isotype matched control antibody. Growth was measured by addition of MTS reagent and plate read at 490nm.

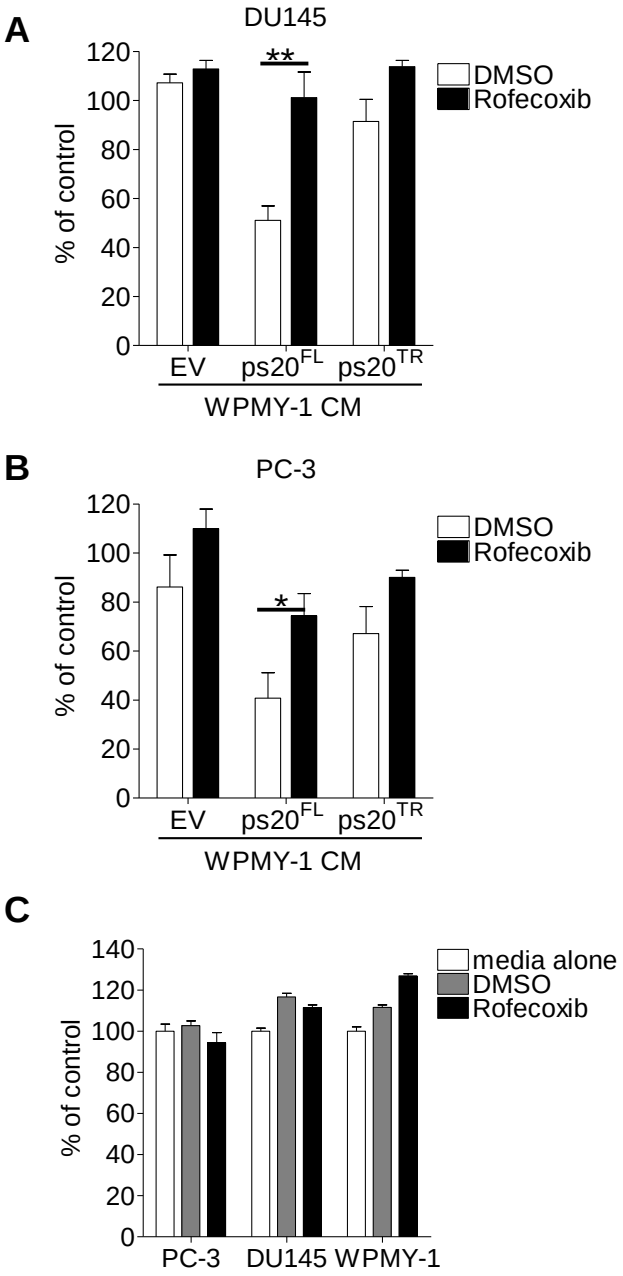

Figure 5.12 Inhibition of COX-2 abrogates ps20 dependent growth suppression of PCa cells. Transduced WPMY-1 cells were seeded in 12 wells plates and cultured for 72h in the presence of 50μM Rofecoxib or the same volume of DMSO. CM was then added to DU145 cells (A, 70% CM) or PC-3 cells (B, 9% CM) respectively. Cells were cultured for 96h and readouts taken by addition of MTS reagent (the plate was read at 490nm). Data of plotted as a percentage of cells grown in only in complete media only. Data is the Mean and SEM of 3 independent experiments with different batches of CM. PC-3, DU145 or WPMY-1 cells were treated with complete media, DMSO, or 50μM Rofecoxib for 96h prior to addition of MTS reagent to assay growth (the plate was read at 490nm) (C). **p<0.05, **p<0.01 Student's T test*

and 15d-PGJ_2. 15d-PGJ_2 is present in the prostate and seminal fluid (Jowsey et al., 2003, Tokugawa et al., 1998) and prostate stromal derived 15d-PGJ_2 has been shown to inhibit the growth and induce apoptosis of prostate cancer cells (Kim et al., 2005, Nakamura et al., 2013). We used a COX-2 inhibitor, rofecoxib, to produce WPMY-1 CM in which the COX-2 pathway was inhibited. Fig. 5.12 shows PC-3 and DU145 cells cultured in ps20 transduced WPMY-1 CM produced in the presence of rofecoxib, or DMSO. We show that ps20 transduced WPMY-1 CM is no longer highly suppressive when cultured in the presence of the COX-2 inhibitor. When added to DU145 cells suppression is relieved to the level observed with WPMY-1-EV control CM, while on PC-3 cells the abrogation of suppression was less complete, but still pronounced. This strongly suggests that activation of the prostaglandin pathway by COX-2 is responsible for ps20 driven growth suppression exhibited by ps20 expressing WPMY-1 CM. To control for non-specific effects on cell growth we cultured PC-3, WPMY-1 and DU145 cells in complete media alone, with or without Rofecoxib or the same volume of DMSO (fig. 5.12C). Both DMSO and Rofecoxib, demonstrated a slight increase in cell proliferation, especially when added to WPMY-1 cells, presumably due to inhibition of background COX-2 activity. There was no growth suppression observed in any cell line tested, indicating that the addition of rofecoxib or DMSO had no toxic effect on any of the cells lines tested.

5.3 Discussion

We sought to characterize, express and functionally elucidate the role of stromally derived ps20 in prostate cancer through a series of *in vitro* assays. We found no significant expression of ps20 in any prostate cancer cell line tested, nor in WPMY-1 prostate stromal cells in line with the study by Madar *et al* that found WFDC1 is absent or down-regulated in tumours and in highly proliferative and cancer-associated cells (Madar et al., 2009). Despite their highly proliferative nature we previously observed expression and secretion of two isoforms of ps20 in HeLa cells, which corresponded to those previously identified in PCa lines by others (Watson et al., 2004b).

It has been repeatedly observed that ps20 is present in healthy stroma *in vivo* (McAlhany et al., 2004) and fibroblasts derived from non-cancerous tissue *ex-vivo* (Madar et al., 2009) but is lost or decreased in tumour associated and cancerous samples (Madar et al., 2009) suggesting a potential tumour-suppressive function. To investigate this we reconstituted expression of both FL and TR ps20 species in WPMY-1 cells, an SV-40 immortalised prostate stromal cell line, exhibiting features of fibroblasts and myofibroblasts (Webber et al., 1999) and in both PC-3 and DU145 PCa lines. In contrast to studies investigating the role of rat-ps20 (Hung, 2005, Larsen et al., 1998, Rowley et al., 1995), we failed to observe ps20 dependent growth inhibition of either PC-3, or indeed in DU145 cells, suggesting that human and rat ps20 may have different functions, or that soluble ps20 requires specific biochemical processing to induce direct growth inhibition, in line with data presented in chapter 3. We did however observe growth inhibition of WPMY-1 stromal cells expressing both $ps20^{FL}$ and $ps20^{TR}$. Likewise, ps20 expressing WPMY-1 cells showed a reduced proportion of cells in G2/S phase of the cell cycle and an increased proportion of cells undergoing apoptosis, suggesting ps20 secretion can confer an anti-proliferative and pro-apoptotic phenotype in an autocrine fashion on specific cell types. Again, the

producer and/or the target cell may be significant with regard to the direct growth inhibition by secretion of ps20.

We then sought to model the expression of ps20 in healthy prostate stroma through the expression and collection of CM from ps20 or EV expressing WPMY-1 cells. A series of experiments showed potent growth inhibition of numerous PCa cell lines by WPMY-1 cell CM expressing ps20, with the exception of HeLa cells. Assessment of apoptosis levels on PC-3 and DU145 cells treated with ps20 containing WPMY-1 CM revealed that WPMY-1 cells expressing ps20 confer through paracrine mechanisms a potent pro-apoptotic phenotype. In contrast, the cell cycle of treated cells was largely unaffected, suggesting that cell-cycle blockade is not involved in the growth suppressive phenotype conferred in paracrine by WPMY-1 cells expressing ps20.

Subsequent depletion of ps20 from the highly suppressive WPMY-1 CM strongly suggested that this growth inhibitory and pro-apoptotic phenotype was mediated indirectly, likely through ps20 dependent regulation of one or more paracrine effector molecules in WPMY-1 cells. In chapter 4, I presented data showing the growth inhibition of PCa cells by ps20 purified both from HeLa and 293F cells. This would seem to disagree with the data herein that WPMY-1 CM containing ps20 does not suppress growth in a ps20 dependent manner. As demonstrated in fig. 5.2, ps20 expressed by transduced WPMY-1 cells does not appear to be cleaved or processed in a manner analogous to that observed in the material purified from HeLa cells in the previous chapter (fig 4.3). The concentration of ps20 in WMPY-1 cell CM is in a similar range to that ps20 purified from HeLa cells. As such, I would argue that this data supports the previous conclusion that without post translational processing steps not yet elucidated which result in the presence of LMW protein species, FL or indeed TR ps20 does not efficiently suppress cellular growth. This is further supported by data suggesting that 293T CM from cells expressing $ps20^{FL}$ and $ps20^{TR}$ did not suppress

PCa growth, even given the high concentration of ps20 (>1.25µg/ml)(fig. 5.5). Together then this data supports the fact that CM from WPMY-1 cells expressing ps20 mediate growth suppression indirectly. This hypothesis was supported by the fact that the growth suppression by WPMY-1 CM containing ps20 could be abrogated following heat treatment.

Towards elucidating how ps20 was able to regulate growth indirectly we performed a transcriptome analysis to assess differential regulation of downstream protein factors. Microarray analysis of transduced WPMY-1 cell lines identified numerous secreted targets upregulated in WPMY-1 cells expressing ps20 species, which were subsequently confirmed using qPCR analysis. Despite various published studies suggesting that IL-32 and SerpinF1 are capable of mediating growth suppression and/or the induction of apoptosis the use of neutralising antibodies in growth inhibition assays failed to abrogate the suppressive effects of the ps20 transduced WPMY-1 CM. We then sought to investigate whether the up-regulation of PTGS2 in ps20 expressing WPMY-1 cells may be mediating the growth suppression. We added rofecoxib, a highly specific inhibitor of COX-2 to the EV, $ps20^{FL}$ and $ps20^{TR}$ expressing WPMY-1 cells for 72h prior to the collection of CM. WPMY-1 CM produced in the presence of this inhibitor was significantly less growth suppressive than that cultured in the presence of DMSO, on both the PC-3 and DU145 cells, abrogating suppression to the levels seen with the WPMY-1-EV cells.

PTGS2 encodes COX-2, the rate limiting enzyme of the arachidonic acid pathway, and catalyses production of numerous prostanoids. COX-2 initially converts arachidonic acid to PGH_2 before further enzymes then catalyse the formation of downstream prostanoids, many of which are known to have potent effects of cellular growth. Of pertinence to our findings, lipocalin-type prostaglandin D synthase (L-PGDS), is responsible for the conversion of PGH_2 into PGD_2. Expression of L-PGDS

is restricted to specific tissues, including the heart, brain, adipose tissue and notably the prostate (Jowsey et al., 2003). In line with this, significant amounts of PGD_2 are found in the seminal fluid, and at least one study has confirmed expression of L-PGDS at high levels in prostate tissue (Tokugawa et al., 1998). PGD_2 is spontaneously dehydrated into 15-deoxy-D12–14- PGJ_2 the endogenous ligand of the peroxisome proliferator-activated receptor γ (PPARγ), an intracellular molecule responsible involved in numerous cellular processes including the inhibition of cell growth. Indeed, PGJ_2 has been shown in increase apoptosis in ERα positive breast cancer cells (Yaacob et al., 2013), vascular epithelial cells (Haslmayer et al., 2002) and osteoblastic cells (Lee et al., 2008) via it's interaction with the PPARγ receptor. Two studies to date have shown PGJ_2 to be a potent inhibitor of prostate cancer cell proliferation. The first, demonstrated PGJ_2 resulted in significantly reduced proliferation of PC-3, DU145 and to a lesser extent LNCaP cells (Nagata et al., 2008). A second study showed a similar pattern of proliferation inhibition by $PGj_{2,}$ with LNCaP cells showing reduced PGJ_2 dependent growth abrogation relative to PC-2 and DU145 cells. This study also demonstrated that PGJ_2 was able to induce apoptosis in PC-3 cells, though this was not investigated on either DU145 or LNCaP cells (Chaffer et al., 2006).

We hypothesis then that where ps20 is expressed in the healthy prostate stroma, it acts to induce COX-2 expression and regulate the formation of growth suppressive and pro-apoptotic prostanoids, and by doing so, places a restraint on epithelial growth and prevents emergence of neoplastic tissue. We propose that the loss of ps20 expression in tumours demonstrated previously (McAlhany et al., 2004, Watson et al., 2004b, Madar et al., 2009) is driven by selective pressure on the tumour to escape this mechanism of growth suppression. Further experiments are required to confirm the exact mechanism of COX-2 dependent suppression induced by ps20 expression, and to elucidate how ps20 expression is regulated, and the mechanisms by which it

is turned off. Understanding of the role of ps20 in prostate tissue homeostasis will better clarify how the situation in disease, where ps20 is absent, differs from that of a healthy prostate, and how this biology can be manipulated therapeutically.

Chapter 6. ps20 as a suppressor of T cell immunity in the prostate stroma.

6.1 Introduction

Tumours are surrounded and enmeshed by a reactive stromal compartment, composed of various cell types including fibroblasts and immune cells (Barron and Rowley, 2012). Reciprocal interactions between the stroma and tumour tissue cause the tissues to co-evolve resulting in a stroma which secretes growth factors and cytokines to support the growth of the tumour, and which manipulates the immune response to its advantage (Barron and Rowley, 2012). In chapter 2 we demonstrated that the expression of ps20 in prostate stromal WPMY-1 cells up-regulates PTGS2 and induces a potent paracrine growth suppression of prostate cancer cell lines dependent on COX-2 activity. Ps20 has been previously demonstrated to inhibit proliferation of PC-3 cells (Hung, 2005, Larsen et al., 1998, Rowley et al., 1995), but data presented in chapter 4 suggests that this may require specific post-translational events and/or concentrations of ps20 in the µg/ml range that are unlikely to be achieved within the prostate micro-environment. However, a number of studies have demonstrated a reduced ps20 expression in prostate cancer (Watson et al., 2004b, Madar et al., 2009), especially in the stroma (McAlhany et al., 2004), suggesting that tumours may switch off ps20 expression in order to remove a barrier to further growth.

Given the evidence from this thesis and elsewhere that ps20 can mediate both direct and indirect growth inhibition of PCa cells, there is a logical rational for investigating its potential for therapeutic use. Focally targeted tumour therapies utilise local delivery of growth suppressive and immune activating agents into the tumours to antagonise tumour growth and activate locally suppressive anti-tumour immunity (Galustian et al., 2011, Patel et al., 2006). The development of membrane-localising

or ‘cytotopic’ peptide technology enables locally delivered molecules to become anchored to cell-membranes serving to i) increase the local concentration of the therapeutic agent, and ii) prevent global distribution of the agent via the blood and lymphatics, and the deleterious effects this may manifest (Bowles et al., 2007). Our lab is committed to investigating agents which may be candidates for inclusion in locally administered cytotopic therapy in the prostate. Despite our failure to elucidate completely the processing events that result in expression of a functionally active ps20 molecule, the experiments presented in chapter 4 suggest ps20 is able to induce a potent growth inhibitory phenotype on the tumour stroma, and could be a candidate for inclusion in such a therapeutic regimen.

However, previous researches into fellow WFDC family proteins SLPI and elafin have demonstrated pleiotropic immunomodulatory functions, impacting both the adaptive and the innate immune responses. And as we have seen WFDC protein expression is frequently dysregulated in cancers, though no studies to date have established a direct link of the immunomodulatory effects of the these proteins with their pro- or anti-tumourigenic effects. Even so, it may be the case that expression of WFDC family proteins in health or disease may have implications within the tumour microenvironment. In line with this, SLPI treated monocytes were shown to inhibit the proliferation of CD4 T cel (Guerrieri et al., 2011). Similarly, increases in elafin expression during the inflammatory response in the lung has been linked with an augmented T_H1 response (Tremblay et al., 1996). Both SLPI and elafin have been shown to regulate activation of the NFκB pathway, which regulates the expression of multiple immune modulating cytokines and chemokines (Bingle and Vyakarnam, 2008). As such, despite not sharing protease inhibitory or anti-microbial function, it is tempting to speculate that ps20 has a similar immunomodulatory role, albeit specific to the tissues in which ps20 is expressed, notably the prostate.

Three recent studies have already provided evidence that ps20 may elicit significant immune functions. Two studies have shown altered anti-viral response in mice which lack ps20. Experimentally infected ps20 null mice showed increased mouse hepatitis virus-1 (MHV-1) viral titres, relative to control mice (Rogers et al., 2012). In contrast, in an experimental model of influenza, ps20 null infected mice again had significantly lower viral titres than control animals (Ressler et al., 2014). Both studies imply therefore that ps20 can manipulate innate anti-viral responses, though with disparate effects. Interestingly, these two studies observed similarly disparate features with relation to the migration of immune cells. In the MHV infection model, ps20 null mice demonstrated increased neutrophil infiltration in the lungs, and elevated levels of CXCL1 and CXCL2, both chemotactic for neutrophils (Bozic et al., 1994). In contrast, infection with the influenza virus resulted in elevated migration of MΦ into the lungs in ps20 null mice (Ressler et al., 2014). Both sets of contrasting results imply that ps20 has broad immune regulatory properties that are highly context specific. In both model systems ps20 served to regulate infiltration of immune cells into the lung, suggesting that the effect of ps20 expression in the lung is broadly anti-inflammatory and mediated at least in part by the regulation of chemokines. However, a third recent study demonstrated the up regulation of IL-8 expression in cells transfected to express WFDC1 (Wilson et al., 2014). IL-8 is potently chemotactic for neutrophils and has been shown to be pro-tumourigenic. So while this study again implicates ps20 in the regulation of chemokines, the increase in IL-8 is in contrast with the results showing reduced neutrophil influx, which migrate toward IL-8 gradients (Ribeiro et al., 1991). Again these results imply that ps20 function is likely cell- and tissue-type specific.

Given the importance of neutrophils and MΦ in tumourigenic processes (Panni et al., 2013, Gregory and Houghton, 2011) it seems intuitive that ps20 expression in the prostate may have immune modulatory properties that could impact the outcome of

tumourigenic processes, either in modulating the inflammatory processes thought to precede the development of neoplastic cell growth, or at a later stage in the tumourigenic process. Our lab has previously observed a correlation between T cell phenotypes and WFDC1 expression in T cell clones, and we hypothesis that ps20 expression may restrain T_H1 type activation of T cells, including the secretion of IFNγ and proliferation in a similar way to the inhibition of T cells response by SLPI (Guerrieri et al., 2011). In the previous chapter we developed an *in vitro* model of ps20 expression in the prostate stroma whereby ps20 secretion is transgenically induced in prostate WPMY-1 stromal fibroblasts. In addition we observed that numerous immune factors e.g. IL-6 and IL-8, were upregulated in WPMY-1 cells expressing ps20 (Table 4.1).

In this chapter we will further interrogate that system to investigate the paracrine effect of ps20 expression in prostate stromal cells on T cell responses and phenotypes *in vitro*. From these experiments we hope to learn whether ps20 is able to elicit direct or indirect effects on T cells. These experiments will help us i) to establish the potential role for ps20 in regulating adaptive immunity in the prostate in health, and ii) will help us to extrapolate the potential impact of ps20 as a component of a localised cytotopic therapy on anti-tumour immunity.

6.2 Results

6.2.1 ps20 expression by WPMY-1 cells suppresses anti-CD3/28 induced T cell proliferation.

As we saw in chapter 4, the expression of COX-2, a rate limiting enzyme of the prostanoid pathway was highly upregulated in WPMY-1 cells expressing ps20 isoforms. We found WPMY-1 CM suppressed growth of PCa cells in a COX-2 dependent matter. COX-2 has been shown to regulate formation of numerous growth and immune regulating prostanoids and has been shown to affect T cell proliferation and cytokine expression (Schiffmann et al., 2014, Sha et al., 2013). We assayed the proliferation of CD4 T cells treated with CM from WPMY-1 cells expressing ps20 (fig 6.1A). Cells from two separate donors showed significant proliferation upon treatment with anti-CD3/28 beads (fig 6.1B-C). This was suppressed in a dose dependent manner in CD4 T cells treated with ps20 expressing WPMY-1 cell CM. Indeed, at 75% CM proliferation of cells treated with ps20 CM was abrogated almost completely. Moreover, the effects of $ps20^{FL}$ and $ps20^{TR}$ CM were comparable. Notably, there was a degree of non-specific growth suppression, with cells showing moderately reduced proliferation in the presence of increasing concentrations of EV CM. However, the data indicate a clear ps20-expression dependent suppression of anti-CD3/28 induced CD4 T cell proliferation.

In order to establish if the ps20 dependent suppression of T cell proliferation affected CD8 T cells in the same way as observed on CD4 T cells, we performed a series of assays using whole PBMCs. Cells were treated with WPMY-1 CM as before and anti-CD3/28 stimulated. Following 6 days of proliferation staining for T cell

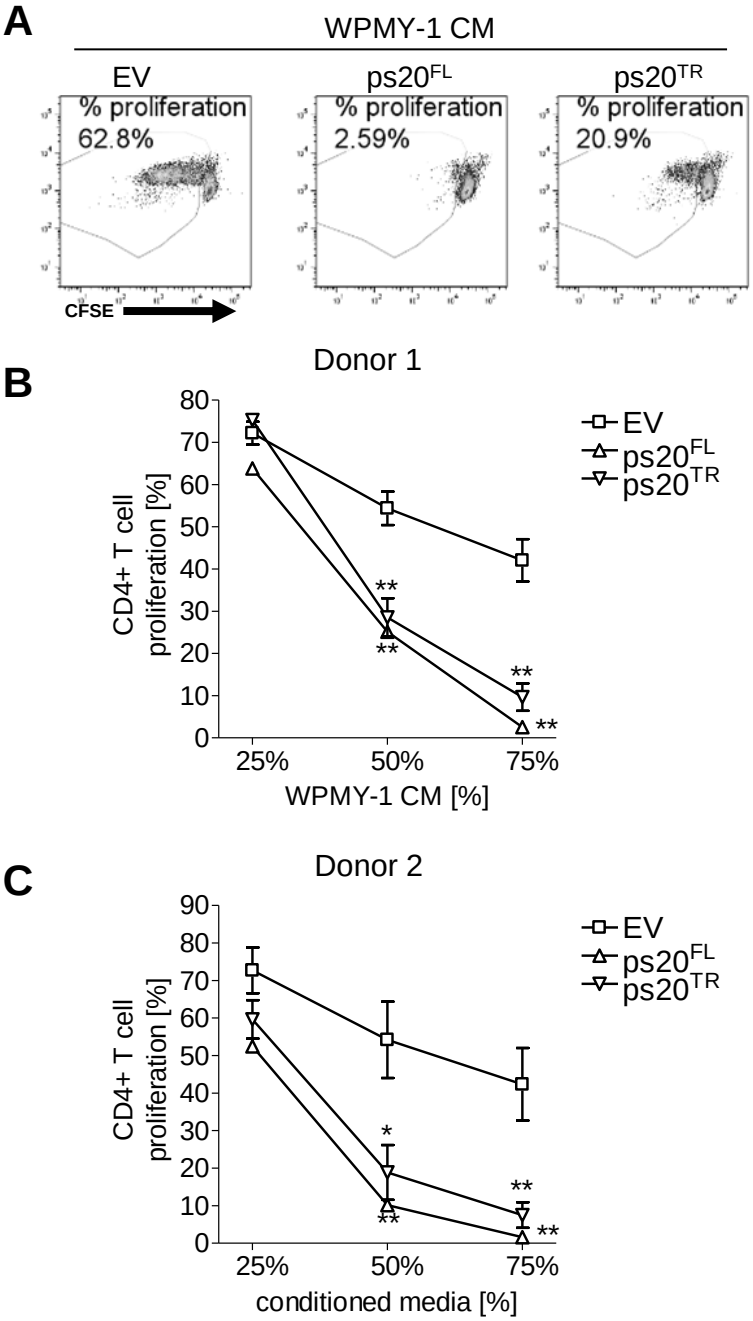

Figure 6.1 Ps20 expressing WPMY-1 cell conditioned media inhibits CD4 T cell proliferation. (A-C) CD4 positive T cells were negatively isolated, stained with CFSE, and incubated with a titration of WPMY-1 EV, ps20^{FL} or ps20^{TR} CM followed by stimulation with anti-CD3/28 beads. Proliferation was measured 6 days later through CFSE dilution by FACS. (A) Representative plots of T cell suppression at by 75% CM. (B) and (C) show data using three separate batches of WPMY-1 CM respectively. **p<0.05 **p<0.01 relative to EV control at same dose, Student's T test.*

markers CD3 and CD8 was used to assess the proliferation of both CD4 and CD8 T cell populations. Figure 6.2A shows an example of the staining regimen, indicating the gating of CD3+ cells into CD8+ and CD8- respectively, thereby delineating between CD4 and CD8 subsets of T lymphocyte. Subsequent analysis shows dilution of the efluor605 dye indicating cells had undergone significant cell division. As before, cells treated with CM from WPMY-1 cells expressing ps20 showed reduced suppression relative to EV treated counterparts. This effect was comparable both for CD4 and CD8 T cells (fig 6.2B-C), suggesting the effect was not specific to either population. Notably, the suppression of 25% $ps20^{TR}$ CM was not has pronounced in the PBMC assay, compared to the suppression of purified CD4 T cells (fig 6.1B-C), though suppression by $ps20^{FL}$ showed comparable dynamics.

6.2.2 ps20 expression by WPMY-1 cells suppresses IL-7/15 induced T cell proliferation.

Using anti-CD3/28 beads to stimulate T cells is an experimental analogue of TCR engagement simultaneous with the second activating signal, by activated APCs. Physiologically this mechanism induces clonal expansion of T cells in response to antigen restricted stimulation. However, within tissues and in the circulation T cells are also subject to stimulation with cytokines such as IL-7 and IL-15 which induce proliferation without antigen restricted activation (Tan et al., 2001). This stimulation is referred to as homeostatic proliferation.

In order to investigate if ps20 can regulate the suppression of homeostatic proliferation of T cells, we stimulated PBMCs with IL-15 and IL-7 following treatment with 50% WPMY-1 CM (fig 6.3). We saw a significant levels of proliferation in both CD4 and CD8 T cells, though with notably different dynamics than seen with

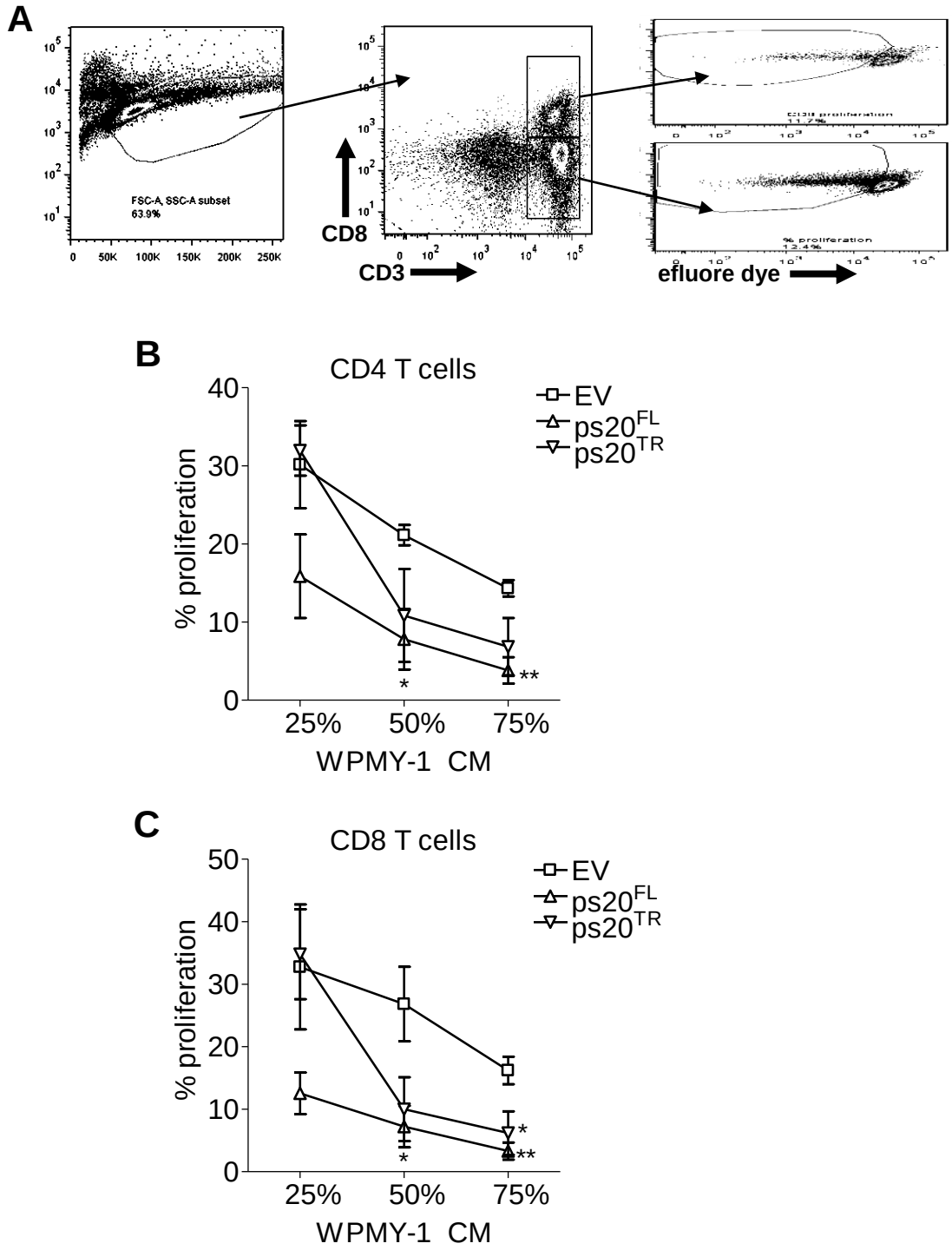

Figure 6.2 Ps20 WPMY-1 conditioned media inhibits CD4 and CD8 T cell proliferation. Whole PBMCs were isolated, and incubated with a titration of WPMY-1 EV, ps20FL or ps20TR CM followed by stimulation with anti-CD3/28 beads. Proliferation was measured 6 days later by efluore670 dye dilution by FACS. A) Shows representative plots of suppression at by 75% CM. (B) and (C) show data using three separate batches of WPMY-1 CM in two separate donors. **p<0.05, **p<0.01*

anti-CD3/28 stimulation, with cells undergoing 2-4 distinct cycles of division when treated with EV CM (fig 6.3A). However, as was seen with anti-CD3/28 proliferation, incubation with $ps20^{FL}$ or $ps20^{TR}$ expressing WPMY-1 CM completely abrogated proliferation of both CD4 and CD8 T cells, suggesting that ps20 is able to induce WPMY-1 cells to express a broadly anti-proliferative phenotype (fig 6.3B-C).

6.2.3 Inhibition of T cell proliferation is caused by G0/G1 arrest.

In order to further elucidate the nature of ps20 expressing WPMY-1 cell CM suppression of T cell proliferation, we used PI staining of purified T cells to investigate the effect on the cell cycle of anti-CD3/28 stimulated CD4 T cells. As shown in fig. 6.4 a significant proportion of T cells treated with WPMY-1 EV CM were in the G2 phase of the cell cycle 48h following treatment, indicating that these cells were undergoing division. In contrast, cells treated with CM from WPMY-1 expressing either $ps20^{FL}$ or $ps20^{TR}$ remained in the G0/G1 phase of the cell cycle, with almost no dividing cells in evidence. This indicates that ps20 is inducing a stromal phentype which prevents cell cycling in T cells.

6.2.4 ps20 does not directly inhibit T cell proliferation

In chapter 5, using immuneaffinity depletion, I demonstrated that niether $ps20^{FL}$ and $ps20^{TR}$ were able to directly inhibit growth in PCa, but instead expression of either molecule in WPMY-1 induces a phenotype which includes the induction of COX-2 alongside numerous growth factors and cytokines. This supported data presented in chapter 4 that processing of ps20 is required to produce active growth inhbitory ps20 protein species.

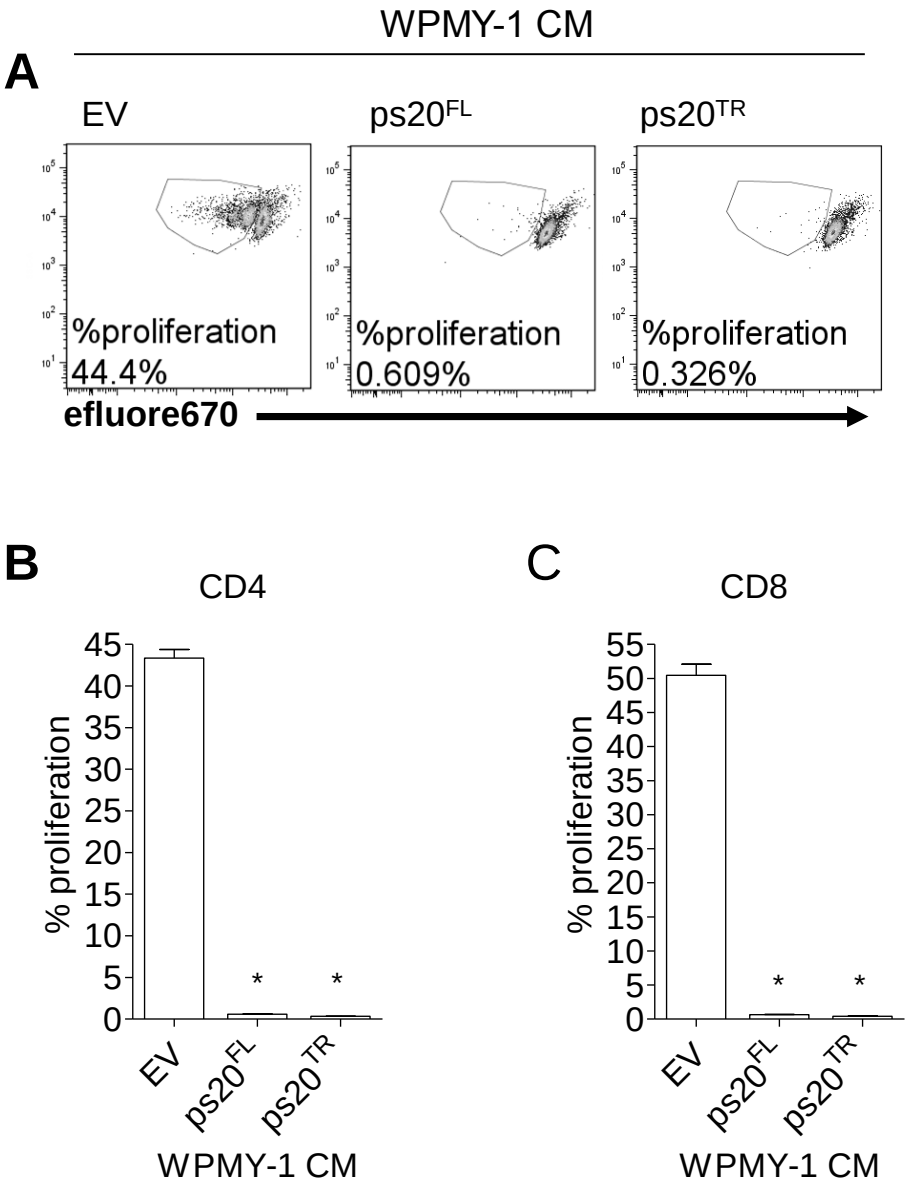

Figure 6.3 Ps20 transduced WPMY-1 conditioned media inhibits IL-7/-15 induced T cell proliferation. (A-B) Whole PBMCs were isolated and incubated with 50% WPMY-1 EV, ps20^{FL} or ps20^{TR} CM followed by stimulation with IL-7 and IL-15. Proliferation was measured 6 days later through efluore dye dilution, by FACS. (A) Representative plots of CD4 T cell proliferation. (B-C) Means of CD4 (A) and CD8 (C) proliferation from 2 batches of CM. **p<0.05 by Student's T test.*

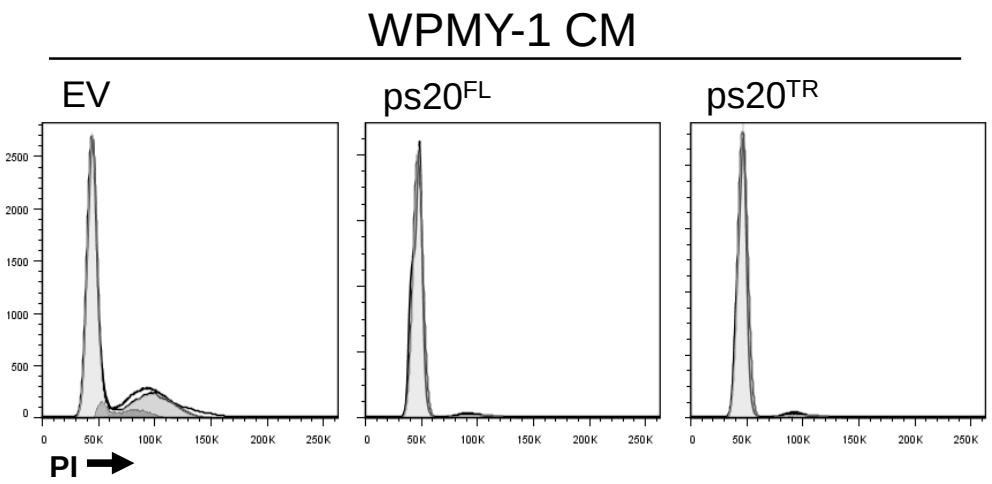

Figure 6.4 Ps20 transduced WPMY-1 CM restrains cells in phase G1/G0 of the cell cycle. CD4 T cells were isolated and stimulated with anti-CD3/28 beads in the presence of 50% WPMY-1 CM. 72h later cells were stained with PI and acquired by FACS.

.

Here we investigated if depletion of ps20 from WPMY-1 CM abrogated the suppressive effect on T cell proliferation. As shown in fig. 6.5A, depletion using anti-ps20 5B9 conjugated beads removed a significant amount of the ps20 from the CM as determined by the reduced signal in the ELISA assay. However, ps20 depletion had no discernible impact on the level of suppression observed following treatment of T cells with depleted versus non-depleted CM (fig 6.5B). Consequently, ps20 appears to have little of no effect directly on the proliferation of T cells, sugesting that as is the case with PCa proliferation, ps20 is inducing a secondary phenotype responsible for the observed T cell suppression.

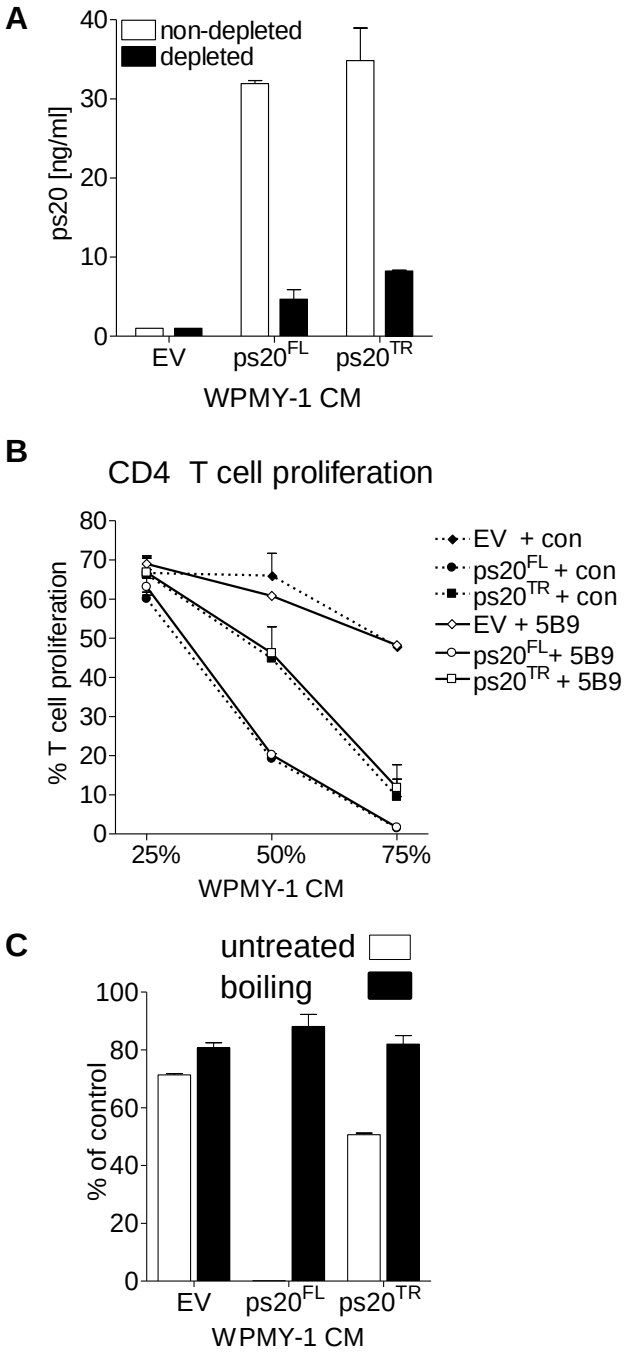

Figure 6.5 ps20 does not inhibit T cell proliferation directly. (A) CM from transduced WPMY-1 cells was incubated overnight with beads conjugated to anti-ps20 ab5B9 or with CM sepharose as a control. ps20 or control depleted CM was assayed by ps20 ELISA. (B-C) Ps20 depleted or control CM (B) or CM which had been boiled for 20 mins (C) was then added to CFSE labelled CD4 T cells, stimulated with anti-CD3/28 and cultured for 6 days followed before measuring proliferation by FACS.

We then investigated if boiling of CM abrogated the suppresive phenotype. WPMY-1 CM from cells expressing EV, $ps20^{FL}$ or $ps20^{TR}$ was boiled for 20mins, and added to T cells, prior to stimulation with anti-CD3/28 beads. While boiling did induce a slight increase in the percentage of proliferating cells treated with EV CM (fig 6.5C), it completely abrogated the specific growth suppression accociated with WPMY-1 CM collected from ps20 expressing cells, suggesting a labile soluble mediator was responsible for growth suppressive phenotype.

6.2.5 IFNγ expression is not abrogated by ps20 expressing WPMY-1 cell CM

Having observed that ps20 induces a WPMY-1 cells to express CM which suppresses the proliferation of T cells, we investigated the effect of WPMY-1 CM on the expression of T_H1 cytokines in T cells. IFNγ is a T_H1 cell associated cytokine which is secreted by activated T cells and has been shown to be critical in the elicitation of successful anti-tumour response (Heusinkveld et al., 2011). It has anti-tumourigenic properties and is an important component of an active T_H1 and CTL response. Similarly, IL-2 is expressed by activated T cells and is responsible for inducing and maintaining T cell production (Ashwell et al., 1986).

We assessed the IFNγ and IL-2 expression in T cells following WPMY-1 CM treatment. Cells were stimulated or for 48h with anti-CD3/28 beads and analysed by intracellular cytokine staining. Interestingly both CD4 and CD8 T cells treated with WPMY-1 CM showed increased secretion of IFNγ relative to cells treated with media alone (fig 6.6A). There was slightly reduced secretion of IFNγ in cell treated with CM from ps20 expressing WPMY-1 cells but the difference was marginal (6.6B).

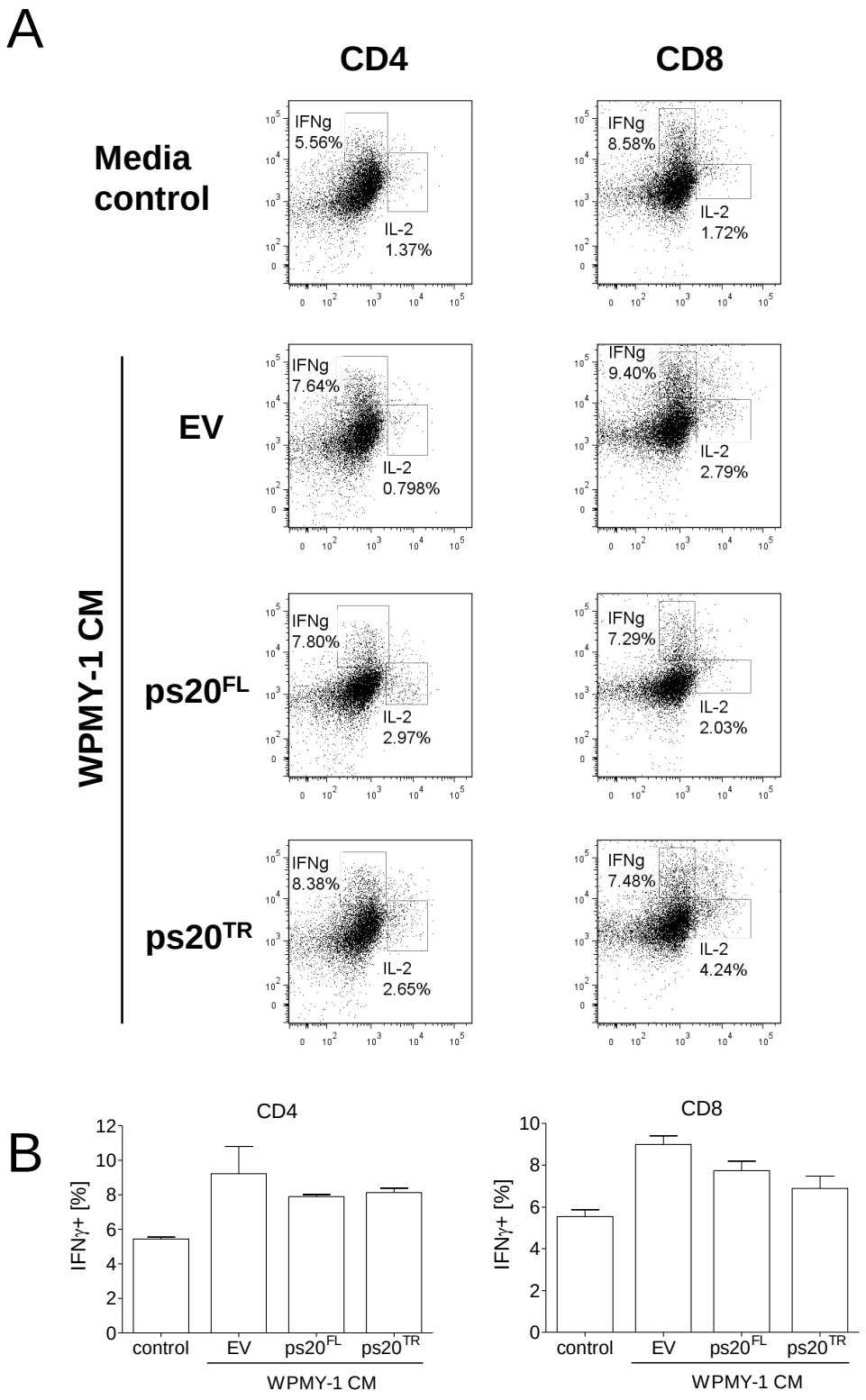

Figure 6.6 WPMY-1 CM does not inhibit IFNγ and IL-2 production in T cells. PBMCs were treated with CM and stimulated with anti-CD3/28 beads for 48 h. Cells were stained for T cell markers and cytokines and analysed by FACS as described. A) Shows representative plots and B) shows means and SEM of 2 experiments.

With respect to IL-2 secretion, a negligible population of T cells secreted IL-2 following activation and it would not have been reliable to quantify the differences between IL-2 expression given such small percentages of IL-2 expressing cells regardless of conditions (6.6A). Together then, this data suggests that WPMY-1 cell CM enhances IFNγ expression from cells, but ps20 expression has no specific inhibitory effect on the secretion of either IFNγ or IL-2.

6.2.6 Expression of T cell activation markers is unaffected by WPMY-1 CM.

Following activation of T cells, surface molecules are upregulated whose measurement serves as a metric of cellular activation. Two such molecules which are highly expressed in a transient manner in the hours following stimulation of activation of T cells are CD69, and CD25. CD69 acts to retain cells in lymph nodes and CD25 is the IL-2Rα component of the IL-2 receptor. In order to further investigate the inhibitory phenotype conferred upon T cells following treatment with CM from ps20 expressing WPMY-1 cells, we assessed the expression of these key T cell activation markers on cells treated with CM from WPMY-1 cells expressing ps20 (fig 6.7). We observed high levels of induction of CD69 and CD25 in both CD4 and CD8 cells relative to un-stimulated controls (fig 6.7 A&B). In both CD4 and CD8 T cells treated with CM, marginally higher numbers of CD25 induction was observed in cells treated with CM from WPMY-1 cells expressing ps20. However, when looking at CD69 expression, no apparent difference was observed in cells treated with different WPMY-1 CM. Consequently, we suggest that WPMY-1 CM from cells expressing ps20 is not inducing T cell suppression through a mechanism which involves inhibition of T cell activation.

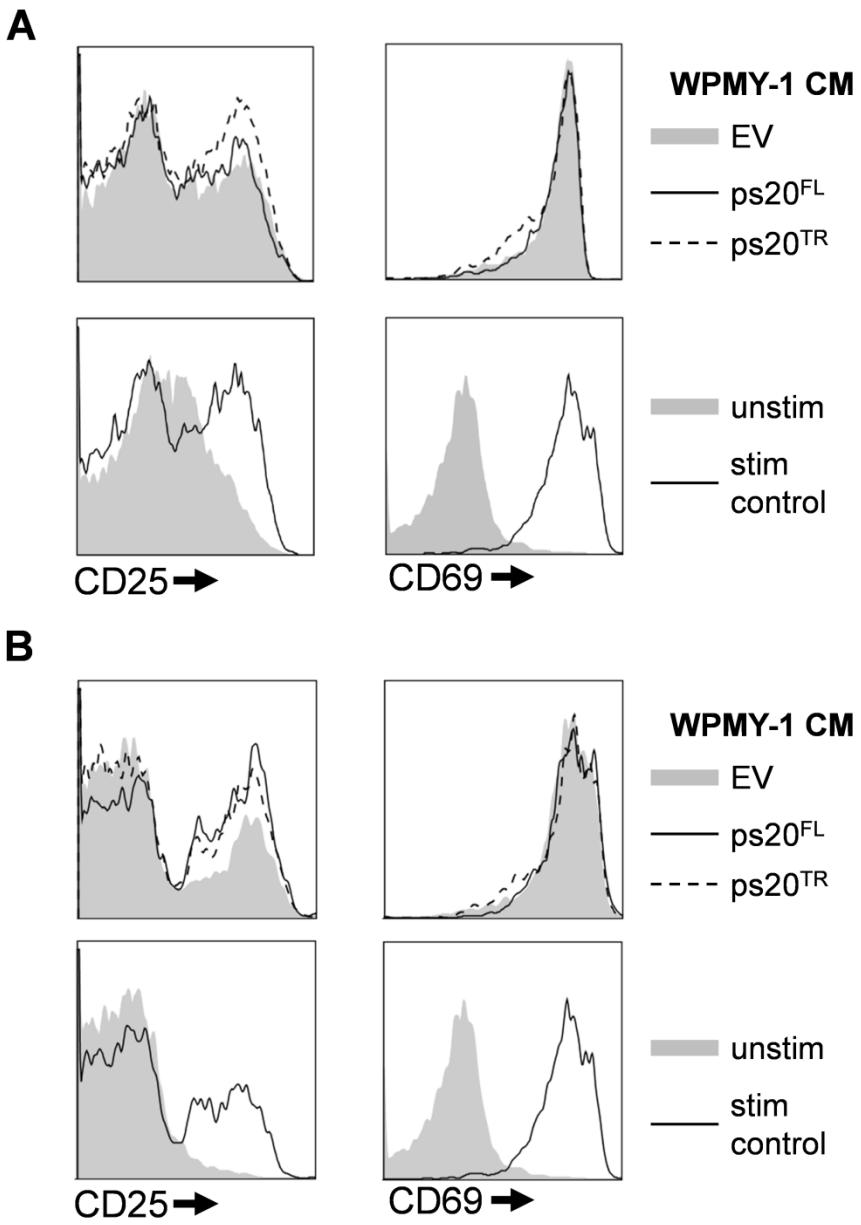

Figure 6.7 WPMY-1 CM treatment does not inhibit T cell activation. PBMCs were treated with 50% CM and stimulated with anti-CD3/28 beads. At 16h following stimulation cells were harvested and stained for T cell activation markers. A) CD4 T cells, B) CD8 T cells. Data representative of 2 experiments.

6.2.7 Inhibition of COX-2 abrogates ps20 dependent growth suppressive effect.

In chapter 2 we saw that the suppressive effect of ps20-expressing WPMY-1 cells of PCa could be abrogated through the inhibition of COX-2. Herein we have observed a similar growth suppressive phenotype on T cells leading us to ask if this is again dependent upon COX-2 up-regulation. In fig. 6.8 CD4 T cells are cultured in CM from WPMY-1 cells grown in the presence or absence or either DMSO or rofecoxib. As can be seen, WPMY-1 CM is suppressive relative to media controls, but WPMY-1 CM from ps20 expressing cells is notably more suppressive, especially from $ps20^{FL}$ expressing cells, where proliferation is completely abrogated. T cells treated with rofecoxib proliferated marginally better than cells treated with DMSO alone, indicating a small amount of non-specific growth enhancement. In all conditions CM generated in the presence of rofecoxib is less suppressive than the DMSO control. However, addition of the inhibitor to cells treated with either $ps20^{FL}$ or $ps20^{TR}$ WPMY-1 CM reduced growth suppression to levels observed with the WPMY-1 EV CM, suggesting a specific effect. However, suppression mediated by EV WPMY1 CM was also dramatically reduced, suggesting COX-2 is active in these cells, albeit to a lesser extent than in WPMY-1 cells expressing ps20.

6.2.8 WPMY-1 expression of ps20 regulates expression of growth factors and cytokines

In the previous chapter we saw how the transgenic expression of two ps20 isoforms in WPMY-1 prostate stromal cells induced a potent phenotype change in those cells; regulating a number of cellular and secreted factors, including PTGS2, which led to the COX-2 dependent suppression of PCa cell growth. COX-2 again appears

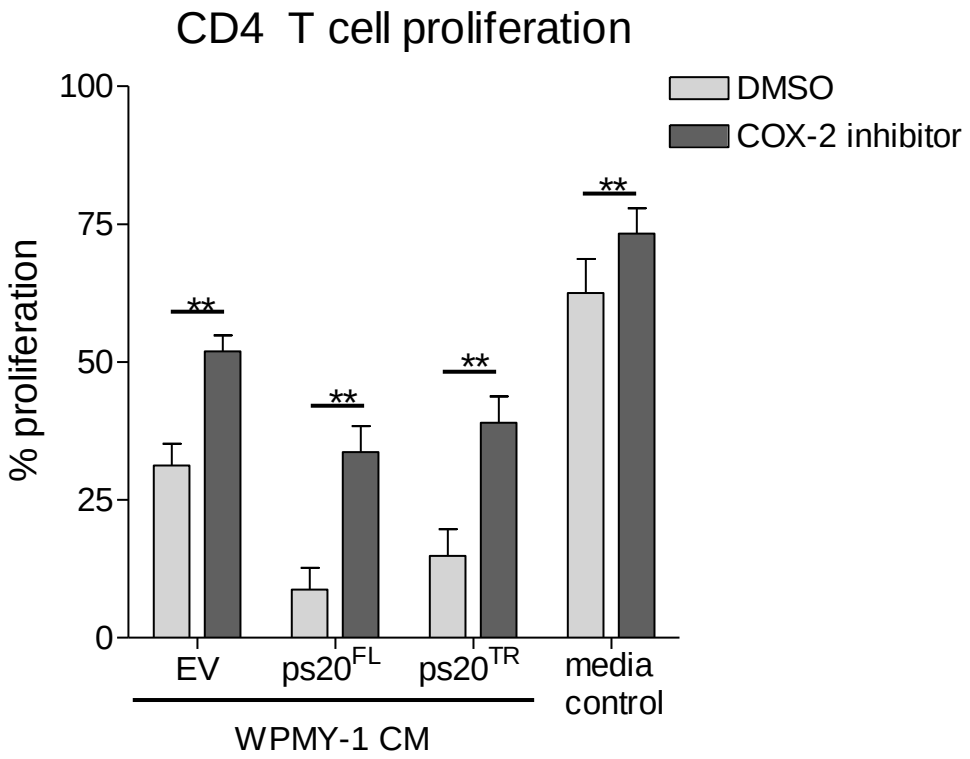

Figure 6.8 Suppression of CD4 T cell proliferation by WPMY-1 CM is COX-2 dependent. Transduced WPMY-1 cells were seeded in 12 wells plates and cultured for 72h in the presence of 50μM Rofecoxib or the same volume of DMSO. CM was then added to purified T cells at 50%CM to 50%x-vivo™ media. Cells were stimulated with anti-CD3/28 and harvested 7 days later. Data shows means and SEMs of two separate experiments in duplicate with different batches of CM. ***p<0.01 Student's T test.*

to be responsible for inhibition of T cell proliferation, though the levels of suppression indicate that this phenotype is only partially dependent on COX-2. To further investigate the change in phenotype induced following the expression of ps20, we assayed 5 batches of CM secreted by transduced WPMY-1 cells using a commercially available multiplex ELISA which quantifies the concentrations of 45 growth factors, cytokines and chemokines (see materials and methods section).

In fig. 6.10, I present data showing secreted factors which underwent differential regulation in WPMY-1 cells, or which were highly expressed but whose expression did not appear to be affected by ps20. WPMY-1 cells expressing $ps20^{FL}$ and $ps20^{TR}$ showed increased expression of GM-CSF, LIF, IP-10, IL-6, FGF-2, VEGF, IL-8, SDF-1 and RANTES. However only IL-2 up-regulation was significant in both $ps20^{FL}$ and $ps20^{TR}$ WPMY-1 cells, while IL-8, GM-CSF up-regulation reached significance only in $ps20^{TR}$ WPMY-1 CM. Interestingly numerous growth factors were regulated by ps20 expression in WPMY-1 cells such as fibroblast growth factor-2 (FGF-2) and platelet growth factor-1 (PIGF-1) though only the latter reached significance. We also observed minor increases in levels of vascular endothelial growth factor-1 (VEGF), and two members of the neurotropin family, beta-nerve growth factor (bNGF) and brain derived neurotropic factor (BDNF) in ps20 expressing WPMY-1 CM.

WPMY-1 cells also showed significant expression of numerous secreted whose expression was not affected, such as hepatocyte growth factor (HGF), GROα and MIP-1α, indicating that a global increase in secretion was not taking place, but rather the enhanced expression of a number of specific factors.

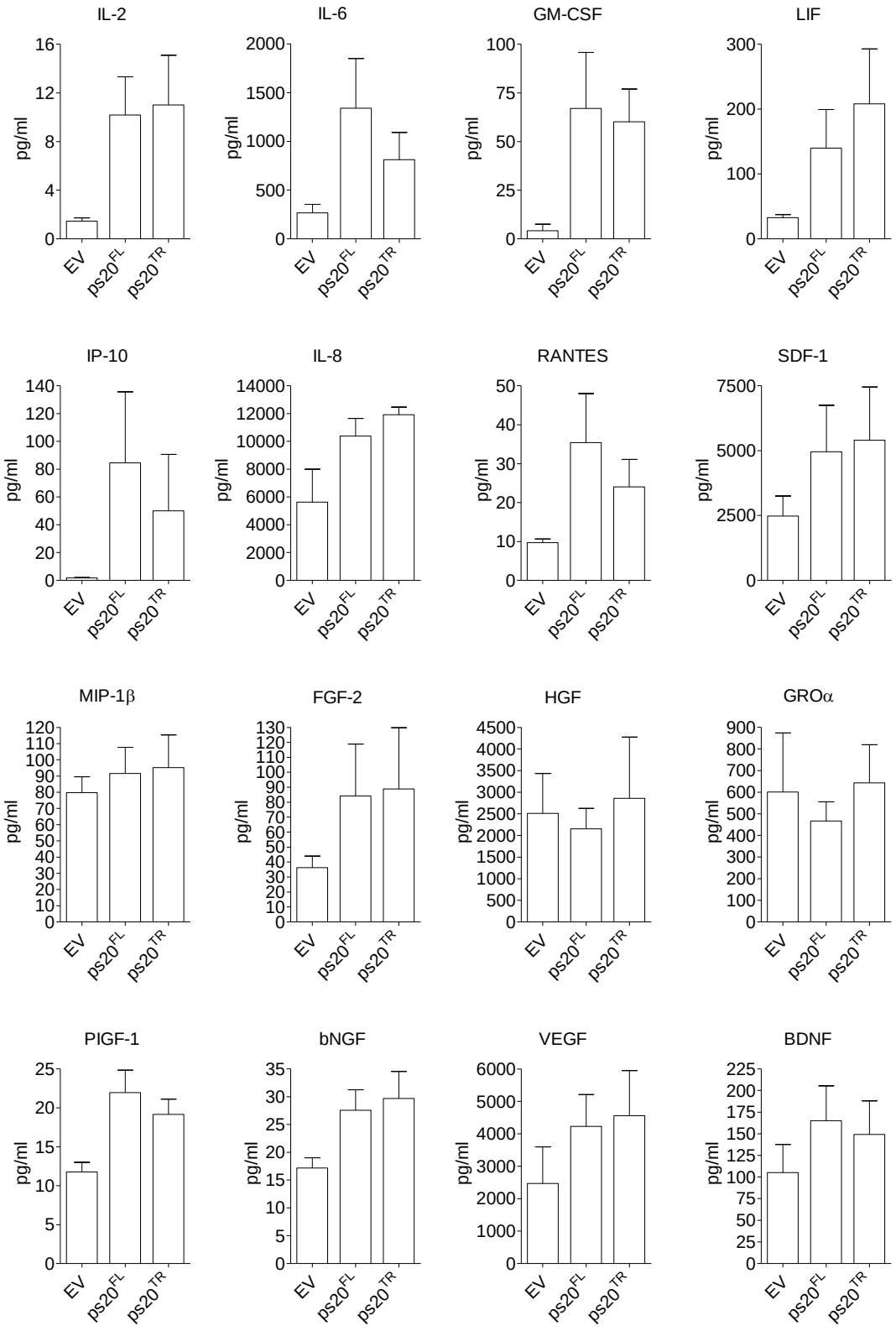

Figure 5.9 ps20 regulates expression of growth factors and cytokines in WPMY-1 cells. CM from WPMY-1 cells cultured for 72h was analysed by a multiplex ELISA. Data shows means and SEMs of 5 separate batches of CM. (This data was generated by Sangmi Kim using CM generated by the author.)

6.3 Discussion

Herein we have demonstrated for the first time, that ps20 expression in prostate stromal cells induces the expression of a potently T cell suppressive phenotype capable of severely abrogating proliferation in response to both anti-CD3/28 bead stimulation, and IL-7/ IL-15 stimulation. Interestingly, the suppression of proliferation was comparable in both CD4 and CD8 cells, and acted upon purified CD4 T cells with similar dynamics as upon PBMC cultures subsequently stained for CD4 and CD8 T cell populations, indicating that ps20 transduced WPMY-1 CM is capable of suppressing T cell proliferation directly without the presence of other cells such as monocytes. This is notable given that SLPI has been shown to inhibit CD4 T cell proliferation through conditioning of monocytes. This suppression was specific to CD4 T cells, having no effect on CD8 cells (Guerrieri et al., 2011).

We have shown that ps20 is indirectly capable of regulating T cell division in response to stimulation with IL-7/15 (fig 6.3). The cytokines IL-7 and IL-15 share the common gamma (γ) chain receptor component with IL-2 and are known to induce T cell proliferation (Tan et al., 2001). T cell division in response to these proliferative cytokines has been called homeostatic proliferation and represents a mechanism for the persistence of memory T cells, and a means of immune reconstitution following immune-depletion, for example following chemotherapy (Martin et al., 2013). While these cytokines are probably not expressed at high level within the prostate (Olurinde et al., 2011) they have been shown to skew the T cell populations towards memory effector phenotypes for both CD4 and CD8 cell types and induce functionality beneficial to anti-tumour immunity (Kaiser et al., 2013). Stimulation with IL-7 and IL-15 has been shown to reduce T cell anergy following activation (Lu et al., 2002) and confer resistance to T cell suppression by Tregs (Perna et al., 2013). As such, both cytokines are translational targets for localized tumour therapy including in enhancing

activity of T cell - chimeric-antigen-receptor (CAR) based therapies (Xu et al., 2014). Indeed our group is investigating the use of locally delivered IL-15 to induce expansion of CD8 effector cells and target tumour cell killing (Galustian et al., 2011). Given these insights, the observation that ps20 expression induces a microenvironment which suppresses the proliferative response of T cells to these cytokines indicates that its expression within prostate tumours would likely be detrimental to anti-tumour immunity, favouring the growth of the tumour. It also suggests that the expression of ps20 in the healthy prostate stroma may have intrinsic modulatory function, perhaps involved in limiting T cell activation and proliferation within prostate tissue, perhaps as a means of limiting auto-immune activity.

In chapter 5 I described the induction of a pro-apoptotic phenotype in WPMY-1 cell CM following expression of ps20. In this chapter, however we have observed that unlike the effects on PCa cells in chapter 5, ps20 expressing WPMY-1 cell CM added to T cells was able to completely inhibit entry into S/G2 phase of the cell cycle. In addition, T cells used in these experiments were analysed by FACS which involved gating on viable cell populations. Consequently, no effect on increased cell death was observed on T cells. Together these data suggest that the pro-apoptotic phenotype observed on PCa cells is distinct from the anti-proliferative phenotype described in this chapter, on T cells, suggesting that ps20 has pleiotropic functions and acts in a cell specific manner.

In order to assess whether the T cell suppressive phenotype exhibited by WPMY-1 cells expressing ps20 was directly mediated by ps20 expression, we again depleted the CM of ps20. This had no discernible effect on the proliferation of T cells. However boiling of WPMY-1 cell CM showed complete abrogation of T cell suppression, again indicating that ps20 is not directly mediating the suppressive phenotype and is instead inducing expression of a labile soluble mediator. Boiling of functional CM also

served to rule out one potential T cell suppressive mechanism. Stromal tissues, including mesenchymal stem cells have been shown to suppress T cell proliferation by up-regulating IDO, which depletes tryptophan from the CM (Reading et al., 2013b, Reading et al., 2013a, Haniffa et al., 2007). However, tryptophan levels within CM would be unaffected by boiling, suggesting the suppressive effects are unlikely mediated by the presence expression of IDO and the subsequent depletion of tryptophan from the CM, and are fact mediated by a labile factor capable of acting directly upon T cells.

In order to gain mechanistic sights into the means of T cell suppression elicited by ps20 expressing WPMY-1 cell CM we investigated the expression of key T cell activation markers. We chose to investigate expression of CD69, and CD25 both of which become highly and transiently expressed following activation of T cells (Testi et al., 1989, Cerdan et al., 1992). Both were unchanged by CM treatment indicating that the suppression of T cells by ps20 expressing WPMY-1 cells was not occurring at the level of T cells activation, which supports the evidence that the ability to produce IFNγ upon activation remained unchanged. CD25 is the cluster of differentiation nomenclature for IL-2Rα, a component of the heterotrimeric IL-2 receptor, allowing us to rule out another mechanism of suppression. Unchanged CD25 expression also suggests that T cells are not being suppressed because of their inability to respond to IL-2, at least not at the receptor level.

Following work in the previous chapter that demonstrated up-regulation of PTGS2 in ps20 expressing WPMY-1 cells, we sought to investigate if the suppression of T cells we have observed is dependent on COX-2 activity. As with our experiments addressing PCa cell growth in chapter 5, we observed herein that inhibition of COX-2 in WPMY-1 cell cultures increased proliferation in CD4 T cells treated with ps20-expressing WPMY-1 cell CM. However, this suppression was not complete and there

was a notable level of proliferation enhancement in control conditions, namely in T cells treated with the COX2 inhibitor but not-treated with CM, and in WPMY-1 EV CM treated T cells (fig 6.8). This makes it highly likely that COX-2 is a component of the T cell suppressive effect, but is also suggestive that there may be other mechanisms involved. There is prior *in vivo* evidence that COX-2 is a component of tumour associated T cell responses. Namely, it was recently found that antigen specific immunity was blunted in mouse tumours expressing COX-2 (Gobel et al., 2014). However, without further characterising the suppression of T cells in our culture systems, or the presence of individual prostanoids within ps20 containing WPMY-1 CM we are unable to conclude precisely how the COX-2 dependent suppression is being mediated here.

To speculate on how COX-2 activity may be mediating T cell suppression, There are numerous examples of PGE_2, a prostanoid downstream of COX-2 and PGE synthase (PGES) enzymes, inducing an immune suppressive/tolerogenic environment within tumours, positing this molecule as a potential mechanism (Sharma et al., 2003, Obermajer et al., 2011). Indeed, PGE_2, has been shown to have context dependent T cell suppressive activity; DU145 spheroids in 3D culture were shown to suppress IFNγ expression in CD4 and CD8 T cells in a PGE_2 dependent manner(Sha et al., 2013) which is in contrast to our data showing that WPMY-1 CM has little effect on the expression of IFNγ. However there are numerous instances of other prostanoids downstream of COX-2 capable of mediating immune suppressive phenotypes. For example, PGJ_2 has been shown to inhibit NFκB activation (Uchida and Shibata, 2008), which while unlikely to elicit robust suppression of T cell proliferation as has been observed in this study, could contribute to a suppressive phenotype by restricting expression of numerous T cell derived factors which contribute to a T_H1 inducing milieu. We have found no evidence in the literature that PGE_2 or any of the prostanoids downstream of COX-2 are able to mediate direct functional effects on T

cells, and more experiments will be required to dissect the mechanisms by which the COX-2-dependent component of the suppressive phenotype we have described in this chapter is impacting T cell function.

Towards elucidating the mechanism by which T cells proliferation is supressed, we observed a number of factors to be upregulated in the CM of ps20 expressing WPMY-1 cells (fig. 6.9). We performed extensive literature searches to elucidate precedence of any of these upregulated factors in the suppression of T cells. VEGF was the only factor other than COX-2 we found which has been shown to have a direct anti-proliferative on T cells, acting through CD47 to inhibit CD3 and IL-2 induced proliferation in a dose dependent manner (Ziogas et al., 2012). It would be interesting to see if neutralisation or depletion of VEGF from WPMY-1 CM would synergise with COX-2 inhibition to restore T cell proliferation. Interestingly, the change in expression of a number of cytokines key to the regulation of T cell phenotype invokes further questions about the potential mechanism of ps20 dependent WPMY-1 CM suppression of T cell proliferation. IL-6, GM-CSF, and VEGF were all seen to be upregulated and are notable for their association with a T_H17 type phenotype. The induction of a non-T_H1 T cell phenotype is one potential mechanism to explain the failure of T cells to proliferate in response to either anti-CD3/28 or IL-7/15 stimulation. T_H17 cells are not activated efficiently following anti-CD3/28 stimulation. However, without further experiments to better define the immune phenotype of T cells treated with ps20 expressing WPMY-1 cell CM it is impossible to accurately predict the mechanism by which proliferation is being suppressed. Further elucidation of the immune phenotype could be obtained by assessing the expression of T cell transcription factors. It is quite possible that the changes in the cytokine milieu secreted from WPMY-1 cells caused by ps20 expression could induce expression of a Treg or T_H17 phenotypes respectively (Taflin et al., 2011). Assessment of T bet expression alongside induction of either FoxP3 or RORγt, would help to elucidate

what if any changes in immuno-phenotypes were being induced in T cells by ps20-expressing WPMY-1 CM.

Another factor we observed to be upregulated in ps20 expressing WPMY-1 CM was leukaemia inhibitory factor (LIF). LIF is an IL-6 family cytokine which signals through the LIF-Receptor, composed of glycoprotein (GP) 130 and 190 subunits (Metcalfe, 2011). Interestingly, LIF has been a shown to be an inducer of FoxP3 expression in activated T cells, conferring a Treg phenotype (Gao et al., 2009), and is a potent inducer of an immuno-tolerogenic phenotype (Metcalfe, 2011). In addition, it has been shown to compete with IL-6 over the induction of T_H17 versus Treg cells (Gao et al., 2009, Thompson et al., 2010). As presented in fig. 6.9, IL-6 was also upregulated by ps20 expression in WPMY-1 cells. It is possible that in regulating the expression of LIF and IL-6 ps20 transduced WPMY-1 cells are inducing either T_H17 and/or Treg cell phenotypes. As mentioned, neither of these T cell populations will proliferate efficiently in response to anti-CD3/28 beads providing a rational for the data presented herein (Annunziato et al., 2007). Increased Treg frequency likely would suppress proliferation of FoxP3 negative cells, further reducing the proliferative response of T cells within the culture. It will be important to further investigate the regulation of both IL-6 and LIF by ps20 and examine their role if any in the suppressive function of WPMY-1 cell CM.

We observed an up-regulation of numerous chemokines in CM from ps20 expressing WPMY-1 cells (fig 6.9). With respect to the function of ps20 within the healthy prostate stroma, the regulation of chemokines may be significant. Chemokines are generally accepted to be responsible for regulating the migration of immune cells into and out of tissues, including the migration of T cells. Furthermore, there are two previously published reports of ps20 regulating the expression of IL-8 (Wilson et al., 2014) and CXCL1/CXCL2 respectively (Rogers et al., 2012) demonstrating that ps20 is a

molecule capable of influencing the chemokine milieu within tissues. Both RANTES (CCL5), IL-8 and IP-10 (CXCL10) were upregulated in ps20 expressing WPMY-1 cells, while there was notably little change in levels of MIP-1β or GROα. RANTES is a potent T cell chemotactic factor (Schall et al., 1990), while IL-8 is potently chemotactic for neutrophils (Ward and Newman, 1969). In addition, IP-10 has been shown to be chemotactic for monocytes, T cells, and NK cells, and is considered broadly pro-inflammatory and angiostatic (Ahmadi et al., 2013). It is likely therefore that where ps20 is expressed within the prostate stroma it contributes to the regulation of specific chemokines. This implies a potential role for ps20 in shaping the compliment of infiltrating leukocytes and lymphocytes in the prostate in health and in disease. Whether this function would have significant implication on the development or progression of prostate neoplasms where ps20 expression is switched off remains to be seen. Future work should seek to further explore the range of chemokines regulated by ps20 in stromal and other cell types and how this affects immune cell migration within tissues where ps20 is expressed. In the case of the prostate, it would be interestingly to compare the immune phenotype of infiltrating immune cells, especially T cell in prostates from ps20 null and ps20 replete mice.

Chapter 7. General Discussion and Future work

7.1 General Discussion

In this thesis, I set out to investigate the role of WFDC1/ps20 in the context of prostate cancer (PCa). Previous work had indicated that ps20 has potent growth suppressive function on PCa cells (Larsen et al., 1998, Rowley et al., 1995) and our interest in studying ps20 was as a potential growth inhibitor for use in a cocktail of locally delivered therapeutics. Indeed, previous studies have employed WFDC family proteins therapeutically highlighting their translational potential (Zani et al., 2011, Shaw and Wiedow, 2011). However, in addition to therapeutically useful growth inhibitory properties, ps20, like SLPI and elafin, may have immunomodulatory functions (Ressler et al., 2014, Rogers et al., 2012). By understanding the relevance of these immunomodulatory functions within the prostate where ps20 is expressed, would allow us to anticipate the potentially deleterious effects that therapeutic delivery of ps20 to a prostate tumour would have on anti-tumour immunity. As such we set out to study the biochemistry, growth inhibitory, and immune regulatory functions of ps20 so as to close some of the gaps in our understanding of the functionality of this molecule.

In chapter 3 I demonstrate that functional ps20 can be purified to near homogeneity by immune-affinity to anti-ps20 IgG. Unfortunately, due to the work being done externally as part of collaboration (Work performed by myself supervised by Dr Simon Jeff's, Imperial College London) we were not able to upscale the production of this near pure $ps20^{293F}$ material in order to manufacture large quantities. Still, enough was obtained for functional experiments and numerous downstream biochemical characterisation assays. In Chapter 4, I present data describing the complexity of biochemical processing of ps20. I show conclusively that ps20 is able to interact with

fibronectin, transglutaminase and GAGs, and that cathepsin L is one means by which ps20 is post-translationally processed. However, data within this chapter also reveal the presence of multiple functional molecular forms of ps20. Indeed, in terms of growth inhibition of PC-3 cells, smaller, cleaved species of ps20 appeared to have far greater activity than highly-pure FL ps20. It is predictable, therefore, that the post-translational processes which produce cleaved or oligomerised ps20 species do so to specific, ill understood functional ends. These processes and the nature of the species of ps20 they produce will require further elucidation. Previous work has shown that WFDC proteins are cleaved physiologically; specifically cleaved forms of SLPI were found in bronchial lavage fluid from human samples, suggesting that cleavage of that nature does take place in vivo. Towards understanding the physiological relevance of individual ps20 protein species, it will be important to elucidate which species are present in the prostate, what processes they are associated with; and how they come about following secretion of the full length and/or truncated ps20 species.

Based on the data presented in this thesis, we propose that ps20 has at least two mechanisms of activity. The first, which likely relies on ps20 cleavage, leading to generation of a growth inhibitory protein fragments, can be assumed to rely on the induction of ps20 expression, combined with the induction of the relevant protease to generate the active fragments. The second mechanism then, gleaned from data presented in chapter 4, is through the regulation of PTGS2/COX-2 expression. COX-2 is an inducible enzyme, and the rate-limiting step in the prostanoid pathway. Our data, including a transcriptome analysis of ps20-expressing WPMY-1 cells, and subsequent qPCR confirmation of ps20 dependent COX-2 up-regulation, suggest ps20 is regulating this expression. However, PTGS2 was amongst 248 genes (fig 5.8) leaving open the possibility the COX-2 up-regulation is further downstream and induced by a secondary factor. Indeed, COX-2 being a pleiotropic inflammatory

mediator, the PTSG2 gene has been shown to be transcriptionally regulated by numerous pathways and transcription factors, including NFκB, SP-1, ETS-1 and AP-1 and its promoter possesses numerous other regulatory elements (Appleby et al., 1994). Both SLPI and elafin, have been shown to regulate transcription factor activation (Drannik et al., 2012, Taggart et al., 2005) leaving room for speculation that ps20 may play a part in the regulation of a transcription factors which in-turn regulate PTGS2/COX-2 expression. Further experiments will be required to examine the nature and dynamics of ps20 dependent PTGS2 induction in WPMY-1 and other cell types.

The function of COX-2 has features which fit with previous paradigms of ps20 function within the prostate. COX-2 is upstream of numerous prostanoids with disparate functions. As such, COX-2 function within tissues specifically relies on the regulation of downstream enzymes, such as mPGES-1 and prostaglandin D synthase, which determine the ultimate physiological effect of local arachidonic acid metabolism. Interestingly, a recent meta-analysis of COX-2 expression and polymorphisms in PCa concluded that while there was no association of PCa with any known COX-2 polymorphisms, and there was no correlation of COX-2 expression with gleason score of tumour, COX-2 expression was shown to be overexpressed in progressive and metastatic PCa (Shao et al., 2012). Given that ps20 expression is reduced or absent in PCa this would appear to be contradictory to our data presented herein, were it not for the previous work from David Rowley's lab showing the concomitant down-regulation of ps20 in the prostate stroma with ps20 over-expression in the epithelial tissues of the cancerous prostate (McAlhany et al., 2004). Moreover, increased expression in epithelial tissue was significantly correlated with reduced survival (McAlhany et al., 2004). Of pertinence to this observation is the fact that the expression of PGDS is associated with stromal tissues, whereas mPGES-1 is known to be expressed in PCa (Finetti et al., 2015). PGDS catalyses the formation of the

pro-apoptotic and anti-inflammatory PGD_2, which undergoes rearrangement to become PGJ_2 (Ho et al., 2008, Koppal et al., 2000, Nakamura et al., 2013, Uchida and Shibata, 2008), whereas conversely, mPGES-1 and other PGE_2 synthases catalyse formation of the PGE_2 which is broadly pro-inflammatory. As such, it seems reasonable to suggest that stromally expressed ps20 may regulate pro-apoptotic, anti-inflammatory COX-2 activity. It remains to be seen if ps20 is also a regulator of COX-2 in epithelial tissues, which if this is the case, may have entirely disparate effects. This will be important to clarify, because the ps20 dependent overexpression of COX-2 in epithelial/cancerous tissues could induce different prostanoids downstream of COX-2 than in stromal tissue. This would provide a mechanistic rational for three key observations made previously, i) that ps20 is down-regulated in the prostate stroma during cancer (Orr et al., 2012, McAlhany et al., 2004), ii) that ps20 becomes associated with the epithelia during advanced prostate cancer (McAlhany et al., 2004), and iii) that ps20 expression in PC-3 xenografts induces angiogenesis and facilitates tumour growth (McAlhany et al., 2003). With reference to the last point, PGE_2 is a well-known mediator of angiogenic processes, including in PCa (Cao and Prescott, 2002, Jain et al., 2008, Wang et al., 2005b).

Our data presented herein showing the COX-2 dependent induction of apoptosis of PCa cells leads us to suggest that the expression of ps20 in the prostate stroma is incompatible with tumour growth. Consequently, we posit, as others have done (Ressler and Rowley, 2011), that tumours need to invoke changes in the stroma which switch off ps20 expression, allowing outgrowth of neoplastic tissues. However, we also observed in work presented in chapter 6, that ps20-induced stromal COX-2 expression also reduces T cell proliferation. There would seem then to be a trade-off within the co-evolution of the stromal compartment with the developing tumour. The T cell suppression conferred by ps20 up-regulation of COX-2 is presumably less deleterious to the growth of the tumour than the more direct effect on cellular growth

and apoptosis. Given that most T cell activation and proliferation takes place in secondary immune sites such as lymph nodes, it is perhaps understandable that the type of T cell inhibition conferred by ps20 expression in the stroma may not in fact be advantageous to the tumour, which can instead invoke myriad suppression mechanisms to abrogate any such anti-tumour immune response (Arnold et al., 2014, Kraman et al., 2010, Young et al., 1996). However, the effect of ps20-dependent immune suppression becomes pertinent when considered therapeutically. The exact mechanism by which stromal ps20/COX-2 is able to suppress activated T cell responses therefore requires further elucidation. Understanding how broad the suppression is, and whether it acts upon other immune cell types such as MΦ, DCs, and especially NK cells, will be important in elucidating how therapeutic ps20 may affect any active immunity within tumours. Understanding of these effects with regard to the ps20 dependent regulation of chemokines observed herein and elsewhere (Wilson et al., 2014, Rogers et al., 2012), as well the effects on suppression of homeostatic T cell proliferation observed herein will increase our understanding of prostate immunity in health, of which little is known.

Principally, it should be considered that ps20 is a molecule present and active in the prostate stroma, and may be a component of the regulatory apparatus defining immune homeostatic processes within the healthy organ. This could be especially pertinent if the loss of ps20 acts as a suppressor of inflammation of the prostate, which would provide an etiological link between the loss of ps20 expression and tumour causing inflammation in the prostate.

7.2 Future work

7.2.1 Chapters 3 and 4

The first objective of this study was to purify ps20. We developed a protocol which allowed simple and rapid purification of ps20 from serum free CM using immune-affinity and the anti ps20 1G7 antibody. However, one disadvantage to using this protocol is the unpredictability of the protein's response to treatment with low pH buffer. Despite being neutralized in TRIS buffer rapidly following elution, it is predictable that some degree of protein unfolding, or mis-folding may take place during this process. The extent of this damage is also impossible to assess without suitable functional standards and controls being available, as they are not for ps20. A modification of this technique which does not require elution in denaturing buffer involves elution with a peptide of high affinity to the antibody column. While no such peptide has yet been elucidated for the 1G7 Ab, other ps20 antibodies, namely the monoclonal C-terminal 5B9 AB, were raised to a specific peptide. A suitable next step in attempts to optimize an immune affinity protocol for ps20 purification could utilise a 5B9 conjugated antibody column, and would employ competitive binding elution using an ab specific peptide rather than low pH glycine buffer. This way, a lack of functionality with the resulting protein preparation could not be attributed to denaturing by low pH elution.

A subsequent goal was to elucidate the interaction between ps20 and GAGs. While we demonstrated a high affinity interaction, we were unable to follow this through to demonstrate a functional consequence of such an interaction. Numerous proteins have been shown to be functionally dependent of protein GAG interacts and in the case of ps20, treating cells such as PC-3 or WPMY-1 with ps20 in the presence or absence of competing glycosaminoglycans would have indicated whether ps20-GAG interactions were required for ps20 dependent inhibition of proliferation. Alternatively, treatment with sodium chlorate to inhibit glycosylation of surface proteoglycans would also have serviced this end. Further insights into the nature of the ps20-GAG interaction could have been revealed using fluorophore conjugated ps20 as was

utilised in the study of SLPI internalisation. The limiting factor in these experiments is the availability of highly pure, functional ps20.

An additional oversight of this project, was the failure to sequence the LMW species of ps20, despite resolving them using silver staining on a gel (fig. 4.5A). Indeed, numerous likely ps20 fragments could be predicted by their similarly increased electrophoretic mobility following treatment with cathepsin L. I had excised and destained these ps20 from the gel and they were ready to be sent for mass-spectrographic analysis. However, it was decided it would have been an inefficient use of funds to sequence numerous ps20 species and those generated by controls, unless it was demonstrated that cathepsin L cleavage has a specific functional ramification. I believe this was the incorrect decision for two reasons; i), a direct functional consequence of cathepsin L may have been found further into the investigation, perhaps as a results of cloning, and expressing specific fragments shown to result from such a cleavage; ii) sequencing would have allowed us to identify the exact nature of at least two LMW ps20 species, which share proclivity to cathepsin L cleavage, but which do not result from it. This additional information would have allowed us to steer the investigation towards elucidation of the function of ps20 subspecies, rather than trying to elucidate how they come about.

Regarding the use of cellular assays to investigate ps20 function, future work could use various cellular assays to investigate the functional consequence ps20 cross-linking to fibronectin. Many cell types adhere to fibronectin and will migrate on a fibronectin solid-phase in culture. Given previous indications that ps20 may induce cellular migration (McAlhany et al., 2003), a simple migration assay using cells seeded on fibronectin coated plates in the presence or absence of cross-linked ps20 would begin to interrogate the functional consequence of the fibronectin-ps20 interaction. It would also be interesting to see if ps20 retained growth inhibitory

function when cross-linked to fibronectin, for which the same basic experimental set-up could be used. However, the ability of cathepsin L to release the ps20 N-terminal region from the ps20-fibronectin conjugate adds complexity to such an investigation. Cells overexpressing secreted cathepsin L would be a useful tool in investigating this phenotype further, again utilising fibronectin coated culture plates in the presence or absence of cross-linked ps20 to investigate if the presence of increased levels of cathepsin L had functional effect on the ps20 dependent phenotype being investigated.

All future work involving purified ps20 should take into account the prevailing lack of consensus on what constitutes a functional ps20 molecule. Work presented in this thesis proposes that unmodified FL ps20 is unlikely to be the most active growth inhibitory species, and that a post-translational cleavage or some other post-translational modification produces a molecule with increased growth inhibitory function. The primary aim of future work pertaining to elucidate the function of ps20 using purified protein should first elucidate decisively which ps20 species are functional and which are not, and base the production and purification strategy around the results.

7.2.2 Chapters 5 and 6

Our first observation was that while ps20 expression in WPMY-1 cells reduced proliferation, this effect was not noted in PC-3 or DU145 cells. I have already discussed the possible reasons for the absence of this phenotype. However, ps20 may have been inducing other cellular changes, beside proliferation rates, that went unnoticed. Transcriptomic data was not obtained for either the PC-3 or DU145 transduced cells, and so ps20-induced changes in expression profiles were never ascertained. This information would have been useful i) as a point of comparison with

the WPMY-1 cells where a potent growth inhibitory phenotype was observed, and ii) in order to note general changes in signalling within the cells which would have provided insights into ps20 function. There are numerous generic cellular assays that can be undertaken to investigate changes in phenotype which were not explored in this project. Firstly, adhesion assays may have uncovered ps20 dependent changes in expression of adhesion molecules. This would be especially pertinent in light of the two studies which observed ps20 dependent increases in expression of ICAM-1 in T cells. Secondly, changes in cellular migration may also have been investigated. The use of simple wound closure assays, or a more 3D set-up, such as migration through a transwell or into a substrate such as Matrigel™ would have allowed us to observe if ps20 mediates effects on cellular phenotypes other than on proliferation via COX-2 expression. Study of cellular adhesion and migration are both pertinent to tumour biology. Surface expression of adhesion molecules holds cells together, both by allowing tethering of cells to each other, and to the ECM. Changes in expression of key families of adhesion factors such the cadherens (involved in tight junctions) and integrins (involved cell-to-cell and ECM-to-cell signalling) can have profound effects of cell shape and motility, and changes in patterns of adherence and cell motility contribute to greater levels of tumour invasion and subsequent metastasis (Mol et al., 2007). To date there is no evidence that ps20 plays a role in either of these events, but the enhanced growth of ps20 expressing PC-3 xenografts in mice provides sufficient rational for performing experiments to investigate potential change in these phenotypes.

Questions also remain regarding the nature the COX-2 dependent phenotypes induced by ps20 induction in WPMY-1 cells. COX-2 is upstream of numerous prostanoids, each with different, often pleiotropic, functions. As discussed in the previous section, a prominent candidate for a pro-apoptotic effects downstream of COX-2 expression is PGJ-2. Increases in this prostanoid can now be detected by a

commercially available ELISA. However, numerous other factors may be responsible for the effect. Ideally, proteomic analysis of ps20 expressing WPMY-1 CM would be performed to establish the levels of different prostanoids present, however, all the growth suppressive CM used in experiments presented within this thesis contained 10% FCS, which would drastically obscure or invalidate data obtained through currently available mass-spec techniques. An obvious solution would be to generate growth suppressive media in serum free conditions. My attempts to do this were unsuccessful and the ps20 dependent suppressive phenotype was never observed in media developed without sera. This may be because i) WPMY-1 cells do not grow well in serum free media, ii) albumin is required for the spontaneous conversation of PGD_2 to PGJ_2 (Shibata et al., 2002), which remains our prime candidate for the suppressive phenotype observed. Experiments could be performed to find a suitable serum free media in which the growth suppressive phenotype of ps20 expressing WPMY-1 could be replicated. This would facilitate downstream analysis of the CM for identification of active factors downstream of ps20 expression.

Another question which arises from work in chapter 5 and 6, is how ps20 is able to regulate PTGS2/COX-2 expression. Given the complete lack of functional data on the mechanism of action of ps20 in the literature, and the additional questions of what constitutes functional ps20 raised in the fourth chapter of this thesis, this would likely prove a difficult area of investigation. None-the-less, our data demonstrate that WPMY-1 cells expressing ps20 have higher levels of PTGS2 expression. However, this regulation may be direct or indirect. Increased PTGS2 expression may be regulated downstream of other secreted or indeed non-secreted factors induced by ps20. In order to dissect the dynamics of PTGS2 upregulation in response to ps20, in lieu of reliably functional soluble ps20, transfection studies should be performed to assess how rapidly following ps20 expression PTGS2 is induced, using qPCR as readout of PTGS2 induction. Alternatively, PTGS2 promoter reporter plasmids (e.g

using luciferase) could help to elucidate the dynamics and mechanisms of ps20 dependent PTGS2 regulation.

More broadly, it remains to be seen whether COX-2 is a general mechanism of ps20 function, or whether it is specific to the WPMY-1 model employed throughout this thesis. Given that the expression of ps20 is not limited to prostate tissue, future work aimed at elucidating ps20 function should employ cells from other tissues where ps20 expression has been recorded, most notably the lung. Using numerous cell lines, alongside, where available, primary cells, would increase the power of results, allowing a more reliable assessment of whether COX-2 regulation is a common feature of ps20 function or is restricted to prostrate stromal tissue. Primary prostate cells are notoriously difficult to grow, and few studies utilise them, but given the unanimous reports of ps20 down-regulation in cancers derived from that tissue, their use may be key to unravelling the mysteries of ps20 function.

7.2.3 WFDC1 in senescence: Loss of function vs Gain of function.

In this thesis, we have used gain of function techniques to investigate a model of ps20 expression in prostate tumours and stromal tissue. However, the benefits of these types of assays in elucidating protein function are difficult to predict. For example within tissues, regulation of ps20 expression may be very tightly controlled, and its function may be limited to highly specific spatiotemporal scenarios. As such, a better understanding of how ps20 functions may be garnered from cells which have intrinsically high levels of ps20. So far, no study to date has described high levels of ps20 expression in cells *in vitro*, with the exception of HeLa cells. Thus, the question remains, which physiologically relevant cell types express ps20 at high levels, and what stimulus induces this? The Rowley lab showed induction of WFDC1 RNA in stromal cells in response to TGFβ, but our attempts to induce ps20 expression in

stromal and numerous other cell types have never shown any observable increase in expression. The best insight to date, then, as to how WFDC1 can be regulated physiologically has come from studies investigating senescent cells. Madar *et al,* showed significantly increased WFDC1 expression in two fibroblast cell lines grown to replicative senescence (RS) (Madar et al., 2009). At least one other study has published supplemental data showing WFDC1 up-regulation in transcriptome array data from cells grown to RS and we were able to confirm expression of WFDC1 in these senescent cells by qPCR (appendix fig. 8.5) (Nelson et al., 2014). Interestingly, the same phenomenon is not observed in cells induced to senescence by overexpression of oncogenes (oncogene induced senescence (OIS) (Nelson et al., 2014). In line with this, our data taken from the microarray data presented in chapter 5 and the multiplex ELISA data shown in chapter 6, show that in WPMY-1 cells transduced to express ps20, numerous secreted factors are upregulated. The combination of factors affected, including IL-6, IL-8, and numerous chemokines are all factors induced in cells grown to replicative senescence, and have become collectively known as the senescence associated secretory phenotype (Coppe et al., 2010). Therefore, one hypothesis that emerges from this is that WFDC1 is involved either i) in the regulation of replicative senescence, or ii) that WFDC1 is upregulated during replicative senescence and is a regulator of the SASP. Unfortunately, we were unable to use our WPMY-1 cells to study this phenotype given they are immortalised, unable to undergo senescence, and therefore an inappropriate model of that particular physiological event. Our attempts to culture primary fibroblasts to senescence made it clear that the study of replicative senescence was beyond the remit of this project. By the time we had established the similarity between the ps20 induced secretory phenotype and the SASP, there was simply not enough time available to culture cells long enough to reach replicative senescence, which can take between 6 months to 1 year for slow growing cells. However, it is likely that at least one of the roles of WFDC1/ps20 is involved in senescence. As such, future work

should seek to investigate this. The use of shRNA knockdown or the CRISPR/Cas9 system to suppress WFDC1 expression would allow the role of WFDC1 in RS to be dissected.

Chapter 8. Appendix

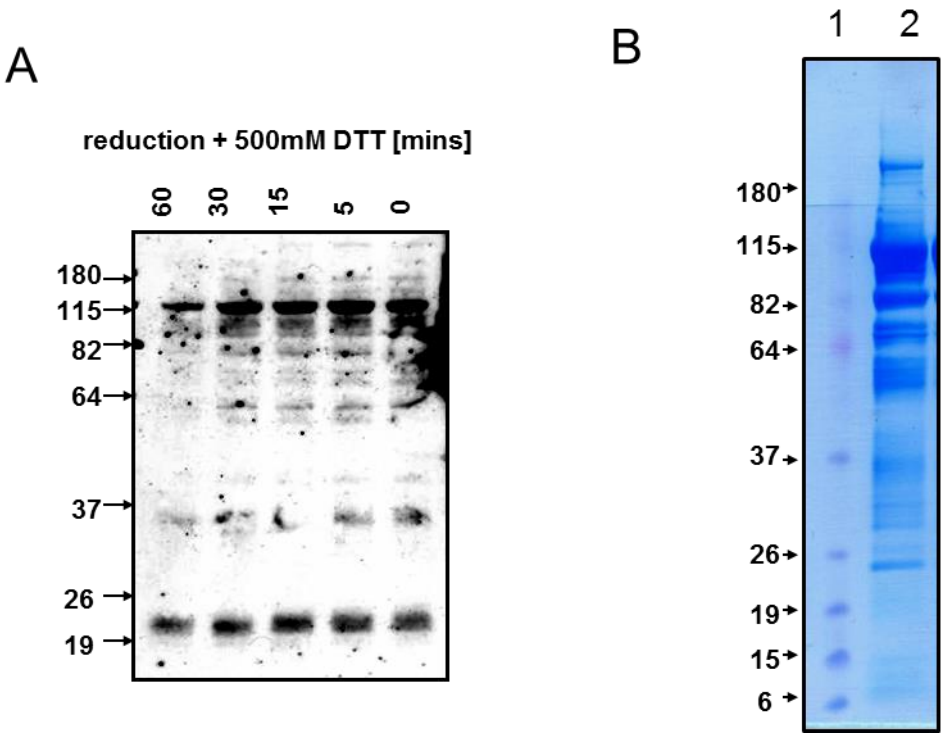

Figure 8.1 purified rps20 contains non-labile oligomers and higher MW contaminants. (A) anti-V5 western blot of rps20^{V5} boiled for indicated time in 500mM DTT. (B) rps20^{V5} was analysed by SDS-PAGE and stained with coomassie blue, lane 1 ladder, lane 2, 20µg of rps20^{V5}.

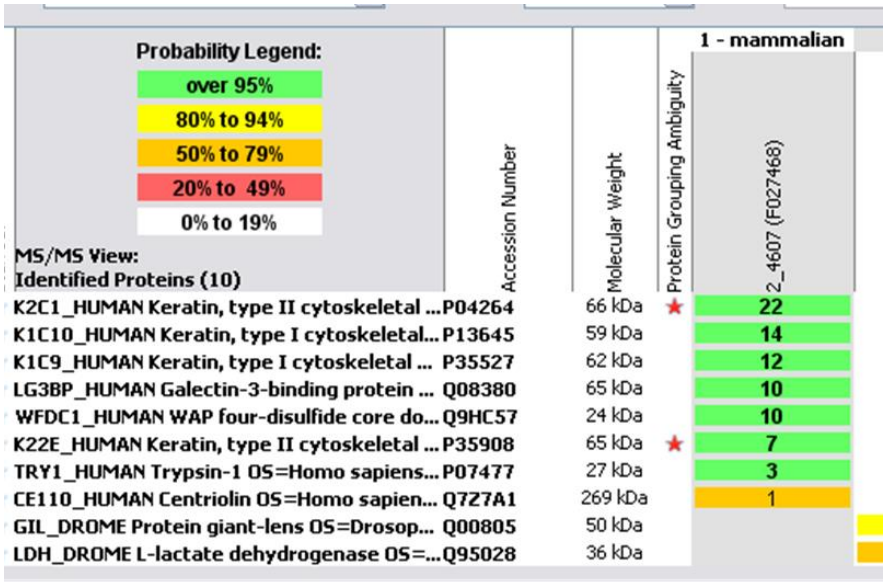

Figure 8.2 Contaminating factors in 293F generated ps20 purification

Screenshot from scaffold programme showing results of MS analysis of 293F ps20 material. The only protein factor besides WFDC1 (ps20) identified was G3BP and numerous keratins. Keratins are frequently detected in sample dues to contamination from skin, hair in dust etc. Tryspin appears as it was the protease used to digest the sample.

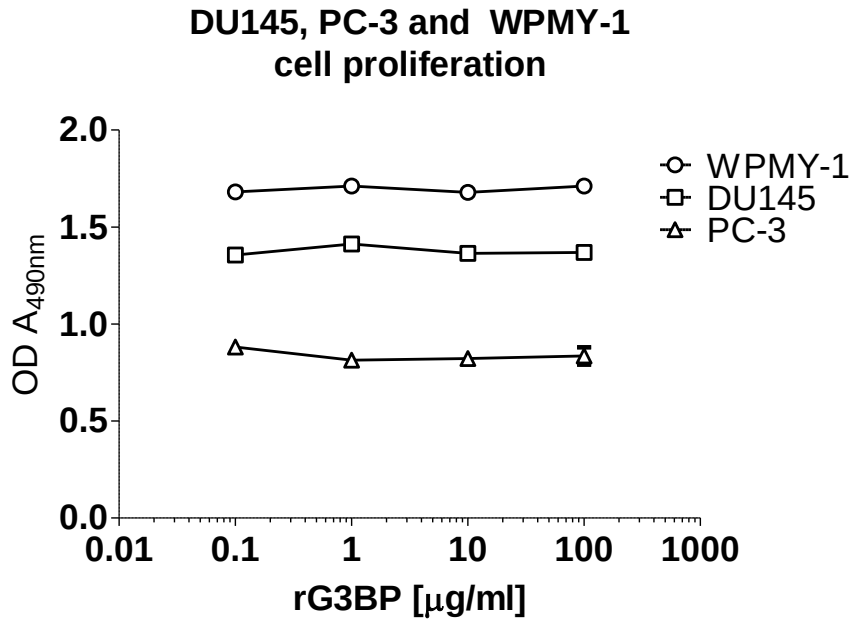

Figure 8.3 Galectin 3 binding protein does not inhibit cell proliferation.

DU145, PC-3 and WPMY-1 cells were seeded at 2000 cells per well and treated with the indicated concentration of G3BP in complete media for 96h. Proliferation was assayed by MTS reagent and read at 490nm.

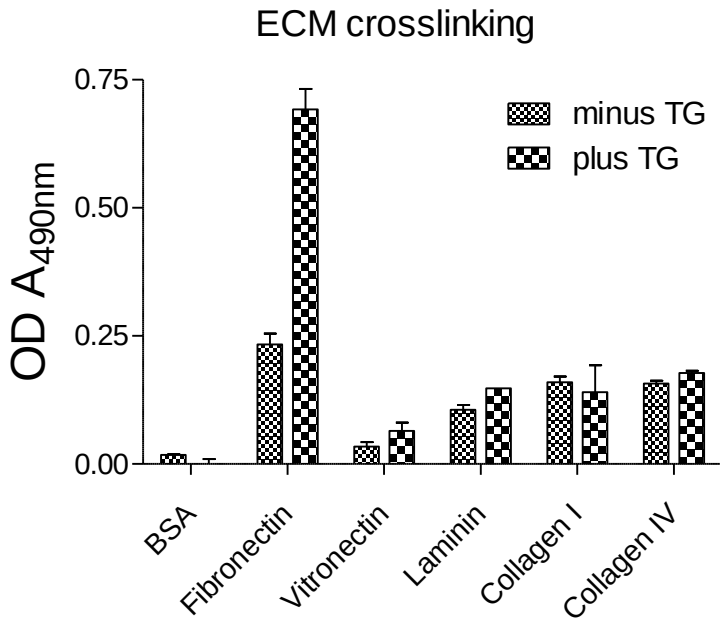

Figure 8.4 Crosslinking of ps20 to pre-prepared ECM solid-phases

25ng/ml ps20 was incubated on pre-prepared ECM plates. 0.02U/ml TG was added for 2h, followed by washing and detection using 1G7-HRP. Absorption was measured at 490nm.

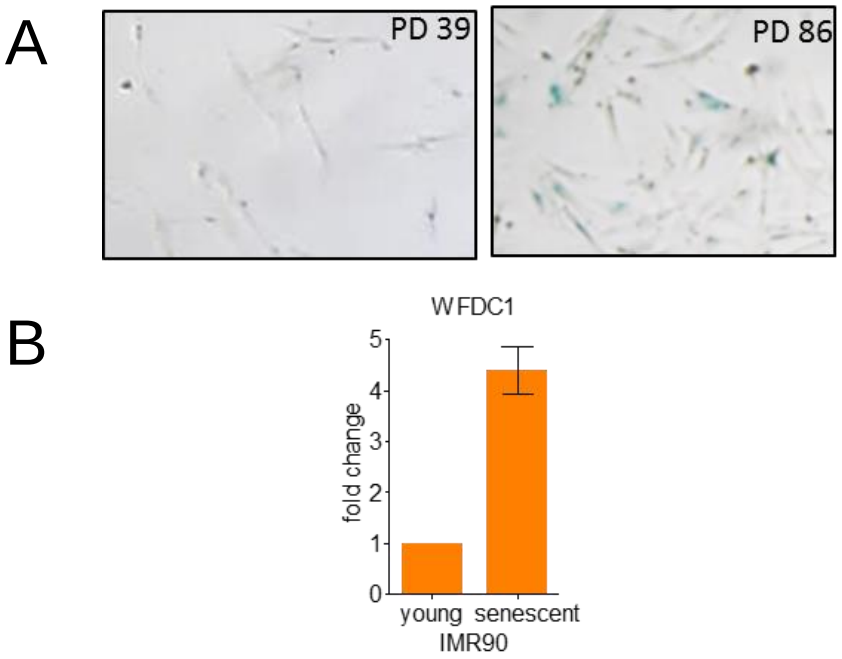

Figure 8.5 WFDC1 expression increases as cells reach replicative senescence

A) IMR90 fibroblasts cultured for the indicated number of population doublings were x-gal stained, and photographed using a light microscope. Blue cells are x-gal positive. B) Young (PD36) and senescent (PD86) IMR90 cells were harvested and WFDC1 expression measured by qPCR.

References

http://info.cancerresearchuk.org.

ABBASI, A. R., KHALAJ, M., TSUJI, T., TANAHARA, M., UCHIDA, K., SUGIMOTO, Y. & KUNIEDA, T. 2009. A mutation of the WFDC1 gene is responsible for multiple ocular defects in cattle. *Genomics,* 94**,** 55-62.

AHMADI, Z., ARABABADI, M. K. & HASSANSHAHI, G. 2013. CXCL10 activities, biological structure, and source along with its significant role played in pathophysiology of type I diabetes mellitus. *Inflammation,* 36**,** 364-71.

ALIZADEH, D., KATSANIS, E. & LARMONIER, N. 2013. The multifaceted role of Th17 lymphocytes and their associated cytokines in cancer. *Clin Dev Immunol,* 2013**,** 957878.

ALKEMADE, H. A., VAN VLIJMEN-WILLEMS, I. M., VAN HAELST, U. J., VAN DE KERKHOF, P. C. & SCHALKWIJK, J. 1994. Demonstration of skin-derived antileukoproteinase (SKALP) and its target enzyme human leukocyte elastase in squamous cell carcinoma. *J Pathol,* 174**,** 121-9.

ALVAREZ, R., READING, J., KING, D. F., HAYES, M., EASTERBROOK, P., FARZANEH, F., RESSLER, S., YANG, F., ROWLEY, D. & VYAKARNAM, A. 2008. WFDC1/ps20 is a novel innate immunomodulatory signature protein of human immunodeficiency virus (HIV)-permissive CD4+ CD45RO+ memory T cells that promotes infection by upregulating CD54 integrin expression and is elevated in HIV type 1 infection. *J Virol,* 82**,** 471-86.

ALVAREZ, R. A., THORBORN, G., READING, J. L., REDDY, S. K. & VYAKARNAM, A. 2011. WFDC1 expression identifies memory CD4 T-lymphocytes rendered vulnerable to cell-cell HIV-1 transfer by promoting intercellular adhesive junctions. *Retrovirology,* 8**,** 29.

AMESHIMA, S., ISHIZAKI, T., DEMURA, Y., IMAMURA, Y., MIYAMORI, I. & MITSUHASHI, H. 2000. Increased secretory leukoprotease inhibitor in patients with nonsmall cell lung carcinoma. *Cancer,* 89**,** 1448-56.

AMIANO, N., REITERI, R. M., COSTA, M. J., TATEOSIAN, N. & CHULUYAN, H. E. 2011. Immunotherapy with SLPI over-expressing mammary tumor cells decreases tumor growth. *Cancer Immunol Immunother,* 60**,** 895-900.

AMIANO, N. O., COSTA, M. J., REITERI, R. M., PAYES, C., GUERRIERI, D., TATEOSIAN, N. L., SANCHEZ, M., MAFFIA, P. C., DIAMENT, M., KARAS, R., ORQUEDA, A., RIZZO, M., ALANIZ, L., MAZZOLINI, G., KLEIN, S., SALLENAVE, J. M. & CHULUYAN, H. E. 2012. Antitumor effect of SLPI on mammary but not colon tumor growth. *J Cell Physiol*.

ANDERSEN, R. S., THRUE, C. A., JUNKER, N., LYNGAA, R., DONIA, M., ELLEBAEK, E., SVANE, I. M., SCHUMACHER, T. N., THOR STRATEN, P. & HADRUP, S. R. 2012. Dissection of T-cell antigen specificity in human melanoma. *Cancer Res,* 72**,** 1642-50.

ANNUNZIATO, F., COSMI, L., SANTARLASCI, V., MAGGI, L., LIOTTA, F., MAZZINGHI, B., PARENTE, E., FILI, L., FERRI, S., FROSALI, F., GIUDICI, F., ROMAGNANI, P., PARRONCHI, P., TONELLI, F., MAGGI, E. & ROMAGNANI, S. 2007. Phenotypic and functional features of human Th17 cells. *J Exp Med,* 204**,** 1849-61.

AO, M., WILLIAMS, K., BHOWMICK, N. A. & HAYWARD, S. W. 2006. Transforming growth factor-beta promotes invasion in tumorigenic but not in nontumorigenic human prostatic epithelial cells. *Cancer Res,* 66**,** 8007-16.

APOSTOLOU, I., SARUKHAN, A., KLEIN, L. & VON BOEHMER, H. 2002. Origin of regulatory T cells with known specificity for antigen. *Nat Immunol,* 3**,** 756-63.

APPLEBY, S. B., RISTIMAKI, A., NEILSON, K., NARKO, K. & HLA, T. 1994. Structure of the human cyclo-oxygenase-2 gene. *Biochem J,* 302 (Pt 3)**,** 723-7.

ARNOLD, J. N., MAGIERA, L., KRAMAN, M. & FEARON, D. T. 2014. Tumoral immune suppression by macrophages expressing fibroblast activation protein-alpha and heme oxygenase-1. *Cancer Immunol Res,* 2**,** 121-6.

ARRUVITO, L., PAYASLIAN, F., BAZ, P., PODHORZER, A., BILLORDO, A., PANDOLFI, J., SEMENIUK, G., ARRIBALZAGA, E. & FAINBOIM, L. 2014. Identification and Clinical Relevance of Naturally Occurring Human CD8+HLA-DR+ Regulatory T Cells. *J Immunol*.

ASHWELL, J. D., ROBB, R. J. & MALEK, T. R. 1986. Proliferation of T lymphocytes in response to interleukin 2 varies with their state of activation. *J Immunol,* 137**,** 2572-8.

BARANGER, K., ZANI, M. L., LABAS, V., DALLET-CHOISY, S. & MOREAU, T. 2011. Secretory leukocyte protease inhibitor (SLPI) is, like its homologue trappin-2 (pre-elafin), a transglutaminase substrate. *PLoS One,* 6**,** e20976.

BARRON, D. A. & ROWLEY, D. R. 2012. The reactive stroma microenvironment and prostate cancer progression. *Endocr Relat Cancer,* 19**,** R187-204.

BECERRA, S. P. & NOTARIO, V. 2013. The effects of PEDF on cancer biology: mechanisms of action and therapeutic potential. *Nat Rev Cancer,* 13**,** 258-71.

BELLADONNA, M. L., VOLPI, C., BIANCHI, R., VACCA, C., ORABONA, C., PALLOTTA, M. T., BOON, L., GIZZI, S., FIORETTI, M. C., GROHMANN, U. & PUCCETTI, P. 2008. Cutting edge: Autocrine TGF-beta sustains default tolerogenesis by IDO-competent dendritic cells. *J Immunol,* 181**,** 5194-8.

BERKE, G. 1994. The binding and lysis of target cells by cytotoxic lymphocytes: molecular and cellular aspects. *Annu Rev Immunol,* 12**,** 735-73.

BERNARDINI, G., GISMONDI, A. & SANTONI, A. 2012. Chemokines and NK cells: regulators of development, trafficking and functions. *Immunol Lett,* 145**,** 39-46.

BERTUCCI, F., FINETTI, P., ROUGEMONT, J., CHARAFE-JAUFFRET, E., NASSER, V., LORIOD, B., CAMERLO, J., TAGETT, R., TARPIN, C., HOUVENAEGHEL, G., NGUYEN, C., MARANINCHI, D., JACQUEMIER, J., HOULGATTE, R., BIRNBAUM, D. & VIENS, P. 2004. Gene expression profiling for molecular characterization of inflammatory breast cancer and prediction of response to chemotherapy. *Cancer Res,* 64**,** 8558-65.

BILD, A. H., YAO, G., CHANG, J. T., WANG, Q., POTTI, A., CHASSE, D., JOSHI, M. B., HARPOLE, D., LANCASTER, J. M., BERCHUCK, A., OLSON, J. A., JR., MARKS, J. R., DRESSMAN, H. K., WEST, M. & NEVINS, J. R. 2006. Oncogenic pathway signatures in human cancers as a guide to targeted therapies. *Nature,* 439**,** 353-7.

BINGLE, C. D. & VYAKARNAM, A. 2008. Novel innate immune functions of the whey acidic protein family. *Trends Immunol,* 29**,** 444-53.

BINGLE, L., CROSS, S. S., HIGH, A. S., WALLACE, W. A., RASSL, D., YUAN, G., HELLSTROM, I., CAMPOS, M. A. & BINGLE, C. D. 2006. WFDC2 (HE4): a potential role in the innate immunity of the oral cavity and respiratory tract and the development of adenocarcinomas of the lung. *Respir Res,* 7**,** 61.

BLAVERI, E., SIMKO, J. P., KORKOLA, J. E., BREWER, J. L., BAEHNER, F., MEHTA, K., DEVRIES, S., KOPPIE, T., PEJAVAR, S., CARROLL, P. & WALDMAN, F. M. 2005. Bladder cancer outcome and subtype classification by gene expression. *Clin Cancer Res,* 11**,** 4044-55.

BOUCHARD, D., MORISSET, D., BOURBONNAIS, Y. & TREMBLAY, G. M. 2006. Proteins with whey-acidic-protein motifs and cancer. *Lancet Oncol,* 7**,** 167-74.

BOWLES, C. E., WILKINSON, I., SMITH, R. A., MOIR, A. J., MONTGOMERY, H. & ROSS, R. J. 2007. Membrane reinsertion of a myristoyl-peptidyl anchored extracellular domain growth hormone receptor. *Endocrinology,* 148**,** 824-30.

BOZIC, C. R., GERARD, N. P., VON UEXKULL-GULDENBAND, C., KOLAKOWSKI, L. F., JR., CONKLYN, M. J., BRESLOW, R., SHOWELL, H. J. & GERARD, C. 1994. The murine interleukin 8 type B receptor homologue and its ligands. Expression and biological characterization. *J Biol Chem,* 269**,** 29355-8.

BUBENDORF, L., KONONEN, J., KOIVISTO, P., SCHRAML, P., MOCH, H., GASSER, T. C., WILLI, N., MIHATSCH, M. J., SAUTER, G. & KALLIONIEMI, O. P. 1999. Survey of gene amplifications during prostate cancer progression by high-throughout fluorescence in situ hybridization on tissue microarrays. *Cancer Res,* 59**,** 803-6.

CAO, Y. & PRESCOTT, S. M. 2002. Many actions of cyclooxygenase-2 in cellular dynamics and in cancer. *J Cell Physiol,* 190**,** 279-86.

CARDIN, A. D. & WEINTRAUB, H. J. 1989. Molecular modeling of protein-glycosaminoglycan interactions. *Arteriosclerosis,* 9**,** 21-32.

CARUSO, J. A., HUNT, K. K. & KEYOMARSI, K. 2010. The neutrophil elastase inhibitor elafin triggers rb-mediated growth arrest and caspase-dependent apoptosis in breast cancer. *Cancer Res,* 70**,** 7125-36.

CARVER, B. S., TRAN, J., CHEN, Z., CARRACEDO-PEREZ, A., ALIMONTI, A., NARDELLA, C., GOPALAN, A., SCARDINO, P. T., CORDON-CARDO, C., GERALD, W. & PANDOLFI, P. P. 2009. ETS rearrangements and prostate cancer initiation. *Nature,* 457**,** E1; discussion E2-3.

CERDAN, C., MARTIN, Y., COURCOUL, M., BRAILLY, H., MAWAS, C., BIRG, F. & OLIVE, D. 1992. Prolonged IL-2 receptor alpha/CD25 expression after T cell activation via the adhesion molecules CD2 and CD28. Demonstration of combined transcriptional and post-transcriptional regulation. *J Immunol,* 149**,** 2255-61.

CHAFFER, C. L., THOMAS, D. M., THOMPSON, E. W. & WILLIAMS, E. D. 2006. PPARgamma-independent induction of growth arrest and apoptosis in prostate and bladder carcinoma. *BMC Cancer,* 6**,** 53.

CHENG, W. L., WANG, C. S., HUANG, Y. H., LIANG, Y., LIN, P. Y., HSUEH, C., WU, Y. C., CHEN, W. J., YU, C. J., LIN, S. R. & LIN, K. H. 2008. Overexpression of a secretory leukocyte protease inhibitor in human gastric cancer. *Int J Cancer,* 123**,** 1787-96.

CIMINO, D., FUSO, L., SFILIGOI, C., BIGLIA, N., PONZONE, R., MAGGIOROTTO, F., RUSSO, G., CICATIELLO, L., WEISZ, A., TAVERNA, D., SISMONDI, P. & DE BORTOLI, M. 2008. Identification of new genes associated with breast cancer progression by gene expression analysis of predefined sets of neoplastic tissues. *Int J Cancer,* 123**,** 1327-38.

CLAUSS, A., LILJA, H. & LUNDWALL, A. 2005. The evolution of a genetic locus encoding small serine proteinase inhibitors. *Biochem Biophys Res Commun,* 333**,** 383-9.

CLAUSS, A., NG, V., LIU, J., PIAO, H., RUSSO, M., VENA, N., SHENG, Q., HIRSCH, M. S., BONOME, T., MATULONIS, U., LIGON, A. H., BIRRER, M. J. & DRAPKIN, R. 2010. Overexpression of elafin in ovarian carcinoma is driven by genomic gains and activation of the nuclear factor kappaB pathway and is associated with poor overall survival. *Neoplasia,* 12**,** 161-72.

COLTRINI, D., RUSNATI, M., ZOPPETTI, G., ORESTE, P., ISACCHI, A., CACCIA, P., BERGONZONI, L. & PRESTA, M. 1993. Biochemical bases of the interaction of human basic fibroblast growth factor with glycosaminoglycans. New insights from trypsin digestion studies. *Eur J Biochem,* 214**,** 51-8.

COPPE, J. P., DESPREZ, P. Y., KRTOLICA, A. & CAMPISI, J. 2010. The senescence-associated secretory phenotype: the dark side of tumor suppression. *Annu Rev Pathol,* 5**,** 99-118.

CUNHA, G. R., COOKE, P. S. & KURITA, T. 2004. Role of stromal-epithelial interactions in hormonal responses. *Arch Histol Cytol,* 67**,** 417-34.

CUNHA, G. R., HAYWARD, S. W., DAHIYA, R. & FOSTER, B. A. 1996. Smooth muscle-epithelial interactions in normal and neoplastic prostatic development. *Acta Anat (Basel),* 155**,** 63-72.

DE MARZO, A. M., PLATZ, E. A., SUTCLIFFE, S., XU, J., GRONBERG, H., DRAKE, C. G., NAKAI, Y., ISAACS, W. B. & NELSON, W. G. 2007. Inflammation in prostate carcinogenesis. *Nat Rev Cancer,* 7**,** 256-69.

DERHOVANESSIAN, E., ADAMS, V., HAHNEL, K., GROEGER, A., PANDHA, H., WARD, S. & PAWELEC, G. 2009. Pretreatment frequency of circulating IL-17+ CD4+ T-cells, but not Tregs, correlates with clinical response to whole-cell vaccination in prostate cancer patients. *Int J Cancer,* 125**,** 1372-9.

DEVOOGDT, N., HASSANZADEH GHASSABEH, G., ZHANG, J., BRYS, L., DE BAETSELIER, P. & REVETS, H. 2003. Secretory leukocyte protease inhibitor promotes the tumorigenic and metastatic potential of cancer cells. *Proc Natl Acad Sci U S A,* 100**,** 5778-82.

DEVOOGDT, N., RASOOL, N., HOSKINS, E., SIMPKINS, F., TCHABO, N. & KOHN, E. C. 2009. Overexpression of protease inhibitor-dead secretory leukocyte protease inhibitor causes more aggressive ovarian cancer in vitro and in vivo. *Cancer Sci,* 100**,** 434-40.

DEVOOGDT, N., REVETS, H., GHASSABEH, G. H. & DE BAETSELIER, P. 2004. Secretory leukocyte protease inhibitor in cancer development. *Ann N Y Acad Sci,* 1028**,** 380-9.

DEVOOGDT, N., REVETS, H., KINDT, A., LIU, Y. Q., DE BAETSELIER, P. & GHASSABEH, G. H. 2006. The tumor-promoting effect of TNF-alpha involves the induction of secretory leukocyte protease inhibitor. *J Immunol,* 177**,** 8046-52.

DIERKER, T., DREIER, R., MIGONE, M., HAMER, S. & GROBE, K. 2009. Heparan sulfate and transglutaminase activity are required for the formation of covalently cross-linked hedgehog oligomers. *J Biol Chem,* 284**,** 32562-71.

DING, Z., WU, C. J., CHU, G. C., XIAO, Y., HO, D., ZHANG, J., PERRY, S. R., LABROT, E. S., WU, X., LIS, R., HOSHIDA, Y., HILLER, D., HU, B., JIANG, S., ZHENG, H., STEGH, A. H., SCOTT, K. L., SIGNORETTI, S., BARDEESY, N., WANG, Y. A., HILL, D. E., GOLUB, T. R., STAMPFER, M. J., WONG, W. H., LODA, M., MUCCI, L., CHIN, L. & DEPINHO, R. A. 2011. SMAD4-dependent barrier constrains prostate cancer growth and metastatic progression. *Nature,* 470**,** 269-73.

DONKOR, M. K., SARKAR, A., SAVAGE, P. A., FRANKLIN, R. A., JOHNSON, L. K., JUNGBLUTH, A. A., ALLISON, J. P. & LI, M. O. 2011. T cell surveillance of oncogene-induced prostate cancer is impeded by T cell-derived TGF-beta1 cytokine. *Immunity,* 35**,** 123-34.

DOYLE, S. L. & O'NEILL, L. A. 2006. Toll-like receptors: from the discovery of NFkappaB to new insights into transcriptional regulations in innate immunity. *Biochem Pharmacol,* 72**,** 1102-13.

DRANNIK, A. G., NAG, K., YAO, X. D., HENRICK, B. M., SALLENAVE, J. M. & ROSENTHAL, K. L. 2012. Trappin-2/elafin modulate innate immune responses of human endometrial epithelial cells to PolyI:C. *PLoS One,* 7**,** e35866.

DUNN, G. P., BRUCE, A. T., IKEDA, H., OLD, L. J. & SCHREIBER, R. D. 2002. Cancer immunoediting: from immunosurveillance to tumor escape. *Nat Immunol,* 3**,** 991-8.

DUNN, G. P., OLD, L. J. & SCHREIBER, R. D. 2004. The immunobiology of cancer immunosurveillance and immunoediting. *Immunity,* 21**,** 137-48.

EISENBARTH, S. C. & FLAVELL, R. A. 2009. Innate instruction of adaptive immunity revisited: the inflammasome. *EMBO Mol Med,* 1**,** 92-8.

EL SHEIKH, S. S., ROMANSKA, H. M., ABEL, P., DOMIN, J. & LALANI EL, N. 2008. Predictive value of PTEN and AR coexpression of sustained responsiveness to hormonal therapy in prostate cancer--a pilot study. *Neoplasia,* 10**,** 949-53.

EMES, R. D., GOODSTADT, L., WINTER, E. E. & PONTING, C. P. 2003. Comparison of the genomes of human and mouse lays the foundation of genome zoology. *Hum Mol Genet,* 12**,** 701-9.

EPSTEIN, J. I. 2009. Precursor lesions to prostatic adenocarcinoma. *Virchows Arch,* 454**,** 1-16.

FATH, M. A., WU, X., HILEMAN, R. E., LINHARDT, R. J., KASHEM, M. A., NELSON, R. M., WRIGHT, C. D. & ABRAHAM, W. M. 1998. Interaction of secretory leukocyte protease inhibitor with heparin inhibits proteases involved in asthma. *J Biol Chem,* 273**,** 13563-9.

FAVRETTO, M. E., WALLBRECHER, R., SCHMIDT, S., VAN DE PUTTE, R. & BROCK, R. 2014. Glycosaminoglycans in the cellular uptake of drug delivery vectors - bystanders or active players? *J Control Release,* 180**,** 81-90.

FEIG, C., JONES, J. O., KRAMAN, M., WELLS, R. J., DEONARINE, A., CHAN, D. S., CONNELL, C. M., ROBERTS, E. W., ZHAO, Q., CABALLERO, O. L., TEICHMANN, S. A., JANOWITZ, T., JODRELL, D. I., TUVESON, D. A. & FEARON, D. T. 2013. Targeting CXCL12 from FAP-expressing carcinoma-associated fibroblasts synergizes with anti-PD-L1 immunotherapy in pancreatic cancer. *Proc Natl Acad Sci U S A,* 110**,** 20212-7.

FERLAY, J., SOERJOMATARAM, I., DIKSHIT, R., ESER, S., MATHERS, C., REBELO, M., PARKIN, D. M., FORMAN, D. & BRAY, F. 2015. Cancer incidence and mortality worldwide: sources, methods and major patterns in GLOBOCAN 2012. *Int J Cancer,* 136**,** E359-86.

FINETTI, F., TERZUOLI, E., GIACHETTI, A., SANTI, R., VILLARI, D., HANAKA, H., RADMARK, O., ZICHE, M. & DONNINI, S. 2015. mPGES-1 in prostate cancer controls stemness and amplifies epidermal growth factor receptor-driven oncogenicity. *Endocr Relat Cancer,* 22**,** 665-78.

FLEMING, D. C., KING, A. E., WILLIAMS, A. R., CRITCHLEY, H. O. & KELLY, R. W. 2003. Hormonal contraception can suppress natural antimicrobial gene transcription in human endometrium. *Fertil Steril,* 79**,** 856-63.

GABRILOVICH, D. I., CHEN, H. L., GIRGIS, K. R., CUNNINGHAM, H. T., MENY, G. M., NADAF, S., KAVANAUGH, D. & CARBONE, D. P. 1996. Production of vascular endothelial growth factor by human tumors inhibits the functional maturation of dendritic cells. *Nat Med,* 2**,** 1096-103.

GALON, J., COSTES, A., SANCHEZ-CABO, F., KIRILOVSKY, A., MLECNIK, B., LAGORCE-PAGES, C., TOSOLINI, M., CAMUS, M., BERGER, A., WIND, P., ZINZINDOHOUE, F., BRUNEVAL, P., CUGNENC, P. H., TRAJANOSKI, Z., FRIDMAN, W. H. & PAGES, F. 2006. Type, density, and location of immune cells within human colorectal tumors predict clinical outcome. *Science,* 313**,** 1960-4.

GALUSTIAN, C., VYAKARNAM, A., ELHAGE, O., HICKMAN, O., DASGUPTA, P. & SMITH, R. A. 2011. Immunotherapy of prostate cancer: identification of new treatments and targets for therapy, and role of WAP domain-containing proteins. *Biochem Soc Trans,* 39**,** 1433-6.

GANSS, R. & HANAHAN, D. 1998. Tumor microenvironment can restrict the effectiveness of activated antitumor lymphocytes. *Cancer Res,* 58**,** 4673-81.

GAO, W., THOMPSON, L., ZHOU, Q., PUTHETI, P., FAHMY, T. M., STROM, T. B. & METCALFE, S. M. 2009. Treg versus Th17 lymphocyte lineages are cross-regulated by LIF versus IL-6. *Cell Cycle,* 8**,** 1444-50.

GETNET, D., MARIS, C. H., HIPKISS, E. L., GROSSO, J. F., HARRIS, T. J., YEN, H. R., BRUNO, T. C., WADA, S., ADLER, A., GEORGANTAS, R. W., JIE, C., GOLDBERG, M. V., PARDOLL, D. M. & DRAKE, C. G. 2009. Tumor recognition and self-recognition induce distinct transcriptional profiles in antigen-specific CD4 T cells. *J Immunol,* 182**,** 4675-85.

GHIRINGHELLI, F., APETOH, L., TESNIERE, A., AYMERIC, L., MA, Y., ORTIZ, C., VERMAELEN, K., PANARETAKIS, T., MIGNOT, G., ULLRICH, E., PERFETTINI, J. L., SCHLEMMER, F., TASDEMIR, E., UHL, M., GENIN, P., CIVAS, A., RYFFEL, B., KANELLOPOULOS, J., TSCHOPP, J., ANDRE, F., LIDEREAU, R., MCLAUGHLIN, N. M., HAYNES, N. M., SMYTH, M. J., KROEMER, G. & ZITVOGEL, L. 2009. Activation of the NLRP3 inflammasome

in dendritic cells induces IL-1beta-dependent adaptive immunity against tumors. *Nat Med,* 15**,** 1170-8.

GOBEL, C., BREITENBUECHER, F., KALKAVAN, H., HAHNEL, P. S., KASPER, S., HOFFARTH, S., MERCHES, K., SCHILD, H., LANG, K. S. & SCHULER, M. 2014. Functional expression cloning identifies COX-2 as a suppressor of antigen-specific cancer immunity. *Cell Death Dis,* 5**,** e1568.

GOLDSTEIN, A. S., HUANG, J., GUO, C., GARRAWAY, I. P. & WITTE, O. N. 2010. Identification of a cell of origin for human prostate cancer. *Science,* 329**,** 568-71.

GOTTLIEB, B., BEITEL, L. K., WU, J. H. & TRIFIRO, M. 2004. The androgen receptor gene mutations database (ARDB): 2004 update. *Hum Mutat,* 23**,** 527-33.

GRATIAS, S., RIEDER, H., ULLMANN, R., KLEIN-HITPASS, L., SCHNEIDER, S., BOLONI, R., KAPPLER, M. & LOHMANN, D. R. 2007. Allelic loss in a minimal region on chromosome 16q24 is associated with vitreous seeding of retinoblastoma. *Cancer Res,* 67**,** 408-16.

GREGORY, A. D. & HOUGHTON, A. M. 2011. Tumor-associated neutrophils: new targets for cancer therapy. *Cancer Res,* 71**,** 2411-6.

GUERRA, N., TAN, Y. X., JONCKER, N. T., CHOY, A., GALLARDO, F., XIONG, N., KNOBLAUGH, S., CADO, D., GREENBERG, N. M. & RAULET, D. H. 2008. NKG2D-deficient mice are defective in tumor surveillance in models of spontaneous malignancy. *Immunity,* 28**,** 571-80.

GUERRIERI, D., TATEOSIAN, N. L., MAFFIA, P. C., REITERI, R. M., AMIANO, N. O., COSTA, M. J., VILLALONGA, X., SANCHEZ, M. L., ESTEIN, S. M., GARCIA, V. E., SALLENAVE, J. M. & CHULUYAN, H. E. 2011. Serine leucocyte proteinase inhibitor-treated monocyte inhibits human CD4(+) lymphocyte proliferation. *Immunology,* 133**,** 434-41.

GUMP, J. M., JUNE, R. K. & DOWDY, S. F. 2010. Revised role of glycosaminoglycans in TAT protein transduction domain-mediated cellular transduction. *J Biol Chem,* 285**,** 1500-7.

GUYOT, N., ZANI, M. L., BERGER, P., DALLET-CHOISY, S. & MOREAU, T. 2005a. Proteolytic susceptibility of the serine protease inhibitor trappin-2 (pre-elafin): evidence for tryptase-mediated generation of elafin. *Biol Chem,* 386**,** 391-9.

GUYOT, N., ZANI, M. L., MAUREL, M. C., DALLET-CHOISY, S. & MOREAU, T. 2005b. Elafin and its precursor trappin-2 still inhibit neutrophil serine proteinases when they are covalently bound to extracellular matrix proteins by tissue transglutaminase. *Biochemistry,* 44**,** 15610-8.

HADASCHIK, B., SU, Y., HUTER, E., GE, Y., HOHENFELLNER, M. & BECKHOVE, P. 2012. Antigen specific T-cell responses against tumor antigens are controlled by regulatory T cells in patients with prostate cancer. *J Urol,* 187**,** 1458-65.

HAJDU, S. I. 2011. A note from history: landmarks in history of cancer, part 1. *Cancer,* 117**,** 1097-102.

HAMEED, O. & HUMPHREY, P. A. 2005. Immunohistochemistry in diagnostic surgical pathology of the prostate. *Semin Diagn Pathol,* 22**,** 88-104.

HAMEL, D. J., SIELAFF, I., PROUDFOOT, A. E. & HANDEL, T. M. 2009. Chapter 4. Interactions of chemokines with glycosaminoglycans. *Methods Enzymol,* 461**,** 71-102.

HANDEL, T. M., JOHNSON, Z., CROWN, S. E., LAU, E. K. & PROUDFOOT, A. E. 2005. Regulation of protein function by glycosaminoglycans--as exemplified by chemokines. *Annu Rev Biochem,* 74**,** 385-410.

HANIFFA, M. A., WANG, X. N., HOLTICK, U., RAE, M., ISAACS, J. D., DICKINSON, A. M., HILKENS, C. M. & COLLIN, M. P. 2007. Adult human fibroblasts are potent immunoregulatory cells and functionally equivalent to mesenchymal stem cells. *J Immunol,* 179**,** 1595-604.

HANNELIEN, V., KAREL, G., JO, V. D. & SOFIE, S. 2012. The role of CXC chemokines in the transition of chronic inflammation to esophageal and gastric cancer. *Biochim Biophys Acta,* 1825**,** 117-29.

HANNILA, S. S., SIDDIQ, M. M., CARMEL, J. B., HOU, J., CHAUDHRY, N., BRADLEY, P. M., HILAIRE, M., RICHMAN, E. L., HART, R. P. & FILBIN, M. T. 2013. Secretory leukocyte protease inhibitor reverses inhibition by CNS myelin, promotes regeneration in the optic nerve, and suppresses expression of the transforming growth factor-beta signaling protein Smad2. *J Neurosci,* 33**,** 5138-51.

HARKONEN, P., KYLLONEN, A. P., NORDLING, S. & VIHKO, P. 2005. Loss of heterozygosity in chromosomal region 16q24.3 associated with progression of prostate cancer. *Prostate,* 62**,** 267-74.

HARRINGTON, L. E., HATTON, R. D., MANGAN, P. R., TURNER, H., MURPHY, T. L., MURPHY, K. M. & WEAVER, C. T. 2005. Interleukin 17-producing CD4+ effector T cells develop via a lineage distinct from the T helper type 1 and 2 lineages. *Nat Immunol,* 6**,** 1123-32.

HASLMAYER, P., THALHAMMER, T., JAGER, W., AUST, S., STEINER, G., ENSINGER, C. & OBRIST, P. 2002. The peroxisome proliferator-activated receptor gamma ligand 15-deoxy-Delta12,14-prostaglandin J2 induces vascular endothelial growth factor in the hormone-independent prostate cancer cell line PC 3 and the urinary bladder carcinoma cell line 5637. *Int J Oncol,* 21**,** 915-20.

HAVRILESKY, L. J., WHITEHEAD, C. M., RUBATT, J. M., CHEEK, R. L., GROELKE, J., HE, Q., MALINOWSKI, D. P., FISCHER, T. J. & BERCHUCK, A. 2008. Evaluation of biomarker panels for early stage ovarian cancer detection and monitoring for disease recurrence. *Gynecol Oncol,* 110**,** 374-82.

HAYASHI, T., IMAI, K., MORISHITA, Y., HAYASHI, I., KUSUNOKI, Y. & NAKACHI, K. 2006. Identification of the NKG2D haplotypes associated with natural cytotoxic activity of peripheral blood lymphocytes and cancer immunosurveillance. *Cancer Res,* 66**,** 563-70.

HEINLEIN, C. A. & CHANG, C. 2002a. Androgen receptor (AR) coregulators: an overview. *Endocr Rev,* 23**,** 175-200.

HEINLEIN, C. A. & CHANG, C. 2002b. The roles of androgen receptors and androgen-binding proteins in nongenomic androgen actions. *Mol Endocrinol,* 16**,** 2181-7.

HEUSINKVELD, M., DE VOS VAN STEENWIJK, P. J., GOEDEMANS, R., RAMWADHDOEBE, T. H., GORTER, A., WELTERS, M. J., VAN HALL, T. & VAN DER BURG, S. H. 2011. M2 macrophages induced by prostaglandin E2 and IL-6 from cervical carcinoma are switched to activated M1 macrophages by CD4+ Th1 cells. *J Immunol,* 187**,** 1157-65.

HILL, R., SONG, Y., CARDIFF, R. D. & VAN DYKE, T. 2005. Selective evolution of stromal mesenchyme with p53 loss in response to epithelial tumorigenesis. *Cell,* 123**,** 1001-11.

HINDLEY, J. P., FERREIRA, C., JONES, E., LAUDER, S. N., LADELL, K., WYNN, K. K., BETTS, G. J., SINGH, Y., PRICE, D. A., GODKIN, A. J., DYSON, J. & GALLIMORE, A. 2011. Analysis of the T-cell receptor repertoires of tumor-infiltrating conventional and regulatory T cells reveals no evidence for conversion in carcinogen-induced tumors. *Cancer Res,* 71**,** 736-46.

HO, T. C., CHEN, S. L., YANG, Y. C., CHEN, C. Y., FENG, F. P., HSIEH, J. W., CHENG, H. C. & TSAO, Y. P. 2008. 15-deoxy-Delta(12,14)-prostaglandin J2 induces vascular endothelial cell apoptosis through the sequential activation of MAPKS and p53. *J Biol Chem,* 283**,** 30273-88.

HOOGEWERF, A. J., KUSCHERT, G. S., PROUDFOOT, A. E., BORLAT, F., CLARK-LEWIS, I., POWER, C. A. & WELLS, T. N. 1997. Glycosaminoglycans mediate cell surface oligomerization of chemokines. *Biochemistry,* 36**,** 13570-8.

HOROSZEWICZ, J. S., LEONG, S. S., CHU, T. M., WAJSMAN, Z. L., FRIEDMAN, M., PAPSIDERO, L., KIM, U., CHAI, L. S., KAKATI, S., ARYA, S. K. & SANDBERG, A. A. 1980. The LNCaP cell line--a new model for studies on human prostatic carcinoma. *Prog Clin Biol Res,* 37**,** 115-32.

HOSKINS, E., RODRIGUEZ-CANALES, J., HEWITT, S. M., ELMASRI, W., HAN, J., HAN, S., DAVIDSON, B. & KOHN, E. C. 2011. Paracrine SLPI secretion upregulates MMP-9 transcription and secretion in ovarian cancer cells. *Gynecol Oncol,* 122**,** 656-62.

HOUGH, C. D., CHO, K. R., ZONDERMAN, A. B., SCHWARTZ, D. R. & MORIN, P. J. 2001. Coordinately up-regulated genes in ovarian cancer. *Cancer Res,* 61**,** 3869-76.

HU, R., DUNN, T. A., WEI, S., ISHARWAL, S., VELTRI, R. W., HUMPHREYS, E., HAN, M., PARTIN, A. W., VESSELLA, R. L., ISAACS, W. B., BOVA, G. S. & LUO, J. 2009. Ligand-independent androgen receptor variants derived from splicing of cryptic exons signify hormone-refractory prostate cancer. *Cancer Res,* 69**,** 16-22.

HU, Y., SUN, H., DRAKE, J., KITTRELL, F., ABBA, M. C., DENG, L., GADDIS, S., SAHIN, A., BAGGERLY, K., MEDINA, D. & ALDAZ, C. M. 2004. From mice to humans: identification of commonly deregulated genes in mammary cancer via comparative SAGE studies. *Cancer Res,* 64**,** 7748-55.

HUANG, C., TANG, H., ZHANG, W., SHE, X., LIAO, Q., LI, X., WU, M. & LI, G. 2012. Integrated analysis of multiple gene expression profiling datasets revealed novel gene signatures and molecular markers in nasopharyngeal carcinoma. *Cancer Epidemiol Biomarkers Prev,* 21**,** 166-75.

HUNG, H. 2005. Suppression of ps20 expression in the rat uterus by tamoxifen and estrogens. *Endocrinology,* 146**,** 2388-96.

HURLE, B., SWANSON, W. & GREEN, E. D. 2007. Comparative sequence analyses reveal rapid and divergent evolutionary changes of the WFDC locus in the primate lineage. *Genome Res,* 17**,** 276-86.

HURWITZ, A. A., FOSTER, B. A., ALLISON, J. P., GREENBERG, N. M. & KWON, E. D. 2001. The TRAMP mouse as a model for prostate cancer. *Curr Protoc Immunol,* Chapter 20**,** Unit 20 5.

IACOBUZIO-DONAHUE, C. A., ASHFAQ, R., MAITRA, A., ADSAY, N. V., SHEN-ONG, G. L., BERG, K., HOLLINGSWORTH, M. A., CAMERON, J. L., YEO, C. J., KERN, S. E., GOGGINS, M. & HRUBAN, R. H. 2003. Highly expressed genes in pancreatic ductal adenocarcinomas: a comprehensive characterization and comparison of the transcription profiles obtained from three major technologies. *Cancer Res,* 63**,** 8614-22.

IKUTA, Y., OKUGAWA, T., FURUGEN, R., NAGATA, Y., TAKAHASHI, Y., WANG, L., IKEDA, H., WATANABE, M., IMAI, S. & SHIKU, H. 2000. A HER2/NEU-derived peptide, a K(d)-restricted murine tumor rejection antigen, induces HER2-specific HLA-A2402-restricted CD8(+) cytotoxic T lymphocytes. *Int J Cancer,* 87**,** 553-8.

IMAI, K., MATSUYAMA, S., MIYAKE, S., SUGA, K. & NAKACHI, K. 2000. Natural cytotoxic activity of peripheral-blood lymphocytes and cancer incidence: an 11-year follow-up study of a general population. *Lancet,* 356**,** 1795-9.

IMBERTY, A., LORTAT-JACOB, H. & PEREZ, S. 2007. Structural view of glycosaminoglycan-protein interactions. *Carbohydr Res,* 342**,** 430-9.

IQBAL, S. M., BALL, T. B., LEVINSON, P., MARANAN, L., JAOKO, W., WACHIHI, C., PAK, B. J., PODUST, V. N., BROLIDEN, K., HIRBOD, T., KAUL, R. & PLUMMER, F. A. 2009. Elevated elafin/trappin-2 in the female genital tract is associated with protection against HIV acquisition. *AIDS,* 23**,** 1669-77.

ISRAELI, O., GOLDRING-AVIRAM, A., RIENSTEIN, S., BEN-BARUCH, G., KORACH, J., GOLDMAN, B. & FRIEDMAN, E. 2005. In silico chromosomal clustering of genes displaying altered expression patterns in ovarian cancer. *Cancer Genet Cytogenet,* 160**,** 35-42.

JACOB, F., GOLDSTEIN, D. R., FINK, D. & HEINZELMANN-SCHWARZ, V. 2009. Proteogenomic studies in epithelial ovarian cancer: established knowledge and future needs. *Biomark Med,* 3**,** 743-56.

JAEGER, J., KOCZAN, D., THIESEN, H. J., IBRAHIM, S. M., GROSS, G., SPANG, R. & KUNZ, M. 2007. Gene expression signatures for tumor progression, tumor subtype, and tumor thickness in laser-microdissected melanoma tissues. *Clin Cancer Res,* 13**,** 806-15.

JAIN, S., CHAKRABORTY, G., RAJA, R., KALE, S. & KUNDU, G. C. 2008. Prostaglandin E2 regulates tumor angiogenesis in prostate cancer. *Cancer Res,* 68**,** 7750-9.

JIN, F., NATHAN, C. F., RADZIOCH, D. & DING, A. 1998. Lipopolysaccharide-related stimuli induce expression of the secretory leukocyte protease inhibitor, a macrophage-derived lipopolysaccharide inhibitor. *Infect Immun,* 66**,** 2447-52.

JOOSTEN, L. A., HEINHUIS, B., NETEA, M. G. & DINARELLO, C. A. 2013. Novel insights into the biology of interleukin-32. *Cell Mol Life Sci,* 70**,** 3883-92.

JORDAN, M. S., BOESTEANU, A., REED, A. J., PETRONE, A. L., HOLENBECK, A. E., LERMAN, M. A., NAJI, A. & CATON, A. J. 2001. Thymic selection of CD4+CD25+ regulatory T cells induced by an agonist self-peptide. *Nat Immunol,* 2**,** 301-6.

JOWSEY, I. R., MURDOCK, P. R., MOORE, G. B., MURPHY, G. J., SMITH, S. A. & HAYES, J. D. 2003. Prostaglandin D2 synthase enzymes and PPARgamma are co-expressed in mouse 3T3-L1 adipocytes and human tissues. *Prostaglandins Other Lipid Mediat,* 70**,** 267-84.

JUKKOLA, T., LAHTI, L., NASERKE, T., WURST, W. & PARTANEN, J. 2006. FGF regulated gene-expression and neuronal differentiation in the developing midbrain-hindbrain region. *Dev Biol,* 297**,** 141-57.

KAARTINEN, M. T., PIRHONEN, A., LINNALA-KANKKUNEN, A. & MAENPAA, P. H. 1999. Cross-linking of osteopontin by tissue transglutaminase increases its collagen binding properties. *J Biol Chem,* 274**,** 1729-35.

KAIGHN, M. E., NARAYAN, K. S., OHNUKI, Y., LECHNER, J. F. & JONES, L. W. 1979. Establishment and characterization of a human prostatic carcinoma cell line (PC-3). *Invest Urol,* 17**,** 16-23.

KAISER, A. D., GADIOT, J., GUISLAIN, A. & BLANK, C. U. 2013. Mimicking homeostatic proliferation in vitro generates T cells with high anti-tumor function in non-lymphopenic hosts. *Cancer Immunol Immunother,* 62**,** 503-15.

KATOH, M. 2005. WNT/PCP signaling pathway and human cancer (review). *Oncol Rep,* 14**,** 1583-8.

KIM, J., YANG, P., SURAOKAR, M., SABICHI, A. L., LLANSA, N. D., MENDOZA, G., SUBBARAYAN, V., LOGOTHETIS, C. J., NEWMAN, R. A., LIPPMAN, S. M. & MENTER, D. G. 2005. Suppression of prostate tumor cell growth by stromal cell prostaglandin D synthase-derived products. *Cancer Res,* 65**,** 6189-98.

KINIWA, Y., MIYAHARA, Y., WANG, H. Y., PENG, W., PENG, G., WHEELER, T. M., THOMPSON, T. C., OLD, L. J. & WANG, R. F. 2007. CD8+ Foxp3+ regulatory T cells mediate immunosuppression in prostate cancer. *Clin Cancer Res,* 13**,** 6947-58.

KLUGER, H. M., CHELOUCHE LEV, D., KLUGER, Y., MCCARTHY, M. M., KIRIAKOVA, G., CAMP, R. L., RIMM, D. L. & PRICE, J. E. 2005. Using a xenograft model of human breast cancer metastasis to find genes associated with clinically aggressive disease. *Cancer Res,* 65**,** 5578-87.

KOBIALKA, S., BEURET, N., BEN-TEKAYA, H. & SPIESS, M. 2009. Glycosaminoglycan chains affect exocytic and endocytic protein traffic. *Traffic,* 10**,** 1845-55.

KOEBEL, C. M., VERMI, W., SWANN, J. B., ZERAFA, N., RODIG, S. J., OLD, L. J., SMYTH, M. J. & SCHREIBER, R. D. 2007. Adaptive immunity maintains occult cancer in an equilibrium state. *Nature,* 450**,** 903-7.

KOENEN, H. J., SMEETS, R. L., VINK, P. M., VAN RIJSSEN, E., BOOTS, A. M. & JOOSTEN, I. 2008. Human CD25highFoxp3pos regulatory T cells differentiate into IL-17-producing cells. *Blood,* 112**,** 2340-52.

KOPPAL, T., PETROVA, T. V. & VAN ELDIK, L. J. 2000. Cyclopentenone prostaglandin 15-deoxy-Delta(12,14)-prostaglandin J(2) acts as a general inhibitor of inflammatory responses in activated BV-2 microglial cells. *Brain Res,* 867**,** 115-21.

KRAMAN, M., BAMBROUGH, P. J., ARNOLD, J. N., ROBERTS, E. W., MAGIERA, L., JONES, J. O., GOPINATHAN, A., TUVESON, D. A. & FEARON, D. T. 2010. Suppression of antitumor immunity by stromal cells expressing fibroblast activation protein-alpha. *Science,* 330**,** 827-30.

KRYCZEK, I., BANERJEE, M., CHENG, P., VATAN, L., SZELIGA, W., WEI, S., HUANG, E., FINLAYSON, E., SIMEONE, D., WELLING, T. H., CHANG, A., COUKOS, G., LIU, R. & ZOU, W. 2009. Phenotype, distribution, generation, and functional and clinical relevance of Th17 cells in the human tumor environments. *Blood,* 114**,** 1141-9.

KWAN, C. P., VENKATARAMAN, G., SHRIVER, Z., RAMAN, R., LIU, D., QI, Y., VARTICOVSKI, L. & SASISEKHARAN, R. 2001. Probing fibroblast growth factor dimerization and role of heparin-like glycosaminoglycans in modulating dimerization and signaling. *J Biol Chem,* 276**,** 23421-9.

LAI, K. P., YAMASHITA, S., HUANG, C. K., YEH, S. & CHANG, C. 2012. Loss of stromal androgen receptor leads to suppressed prostate tumourigenesis via modulation of pro-inflammatory cytokines/chemokines. *EMBO Mol Med,* 4**,** 791-807.

LAMBAERTS, K., WILCOX-ADELMAN, S. A. & ZIMMERMANN, P. 2009. The signaling mechanisms of syndecan heparan sulfate proteoglycans. *Curr Opin Cell Biol,* 21**,** 662-9.

LANDRY, J. J., PYL, P. T., RAUSCH, T., ZICHNER, T., TEKKEDIL, M. M., STUTZ, A. M., JAUCH, A., AIYAR, R. S., PAU, G., DELHOMME, N., GAGNEUR, J., KORBEL, J. O., HUBER, W. & STEINMETZ, L. M. 2013. The genomic and transcriptomic landscape of a HeLa cell line. *G3 (Bethesda),* 3**,** 1213-24.

LARRAMENDY, M. L., LUSHNIKOVA, T., BJORKQVIST, A. M., WISTUBA, II, VIRMANI, A. K., SHIVAPURKAR, N., GAZDAR, A. F. & KNUUTILA, S. 2000. Comparative genomic hybridization reveals complex genetic changes in primary breast cancer tumors and their cell lines. *Cancer Genet Cytogenet,* 119**,** 132-8.

LARSEN, M., RESSLER, S. J., GERDES, M. J., LU, B., BYRON, M., LAWRENCE, J. B. & ROWLEY, D. R. 2000. The WFDC1 gene encoding ps20 localizes to 16q24, a region of LOH in multiple cancers. *Mamm Genome,* 11**,** 767-73.

LARSEN, M., RESSLER, S. J., LU, B., GERDES, M. J., MCBRIDE, L., DANG, T. D. & ROWLEY, D. R. 1998. Molecular cloning and expression of ps20 growth inhibitor. A novel WAP-type "four-disulfide core" domain protein expressed in smooth muscle. *J Biol Chem,* 273**,** 4574-84.

LARSEN, S. K., MUNIR, S., WOETMANN, A., FROSIG, T. M., ODUM, N., SVANE, I. M., BECKER, J. C. & ANDERSEN, M. H. 2013. Functional characterization of Foxp3-specific spontaneous immune responses. *Leukemia,* 27**,** 2332-40.

LEE, C. H., AKIN-OLUGBADE, O. & KIRSCHENBAUM, A. 2011. Overview of prostate anatomy, histology, and pathology. *Endocrinol Metab Clin North Am,* 40**,** 565-75, viii-ix.

LEE, S. J., KIM, M. S., PARK, J. Y., WOO, J. S. & KIM, Y. K. 2008. 15-Deoxy-delta 12,14-prostaglandin J2 induces apoptosis via JNK-mediated mitochondrial pathway in osteoblastic cells. *Toxicology,* 248**,** 121-9.

LETOHA, T., KELLER-PINTER, A., KUSZ, E., KOLOZSI, C., BOZSO, Z., TOTH, G., VIZLER, C., OLAH, Z. & SZILAK, L. Cell-penetrating peptide exploited syndecans. *Biochim Biophys Acta*.

LI, Y., BASANG, Z., DING, H., LU, Z., NING, T., WEI, H., CAI, H. & KE, Y. 2011. Latexin expression is downregulated in human gastric carcinomas and exhibits tumor suppressor potential. *BMC Cancer,* 11**,** 121.

LI, Y. & SARKAR, F. H. 2002. Gene expression profiles of genistein-treated PC3 prostate cancer cells. *J Nutr,* 132**,** 3623-31.

LIANG, G., GONZALES, F. A., JONES, P. A., ORNTOFT, T. F. & THYKJAER, T. 2002. Analysis of gene induction in human fibroblasts and bladder cancer cells exposed to the methylation inhibitor 5-aza-2'-deoxycytidine. *Cancer Res,* 62**,** 961-6.

LIN, C., YANG, L., TANASA, B., HUTT, K., JU, B. G., OHGI, K., ZHANG, J., ROSE, D. W., FU, X. D., GLASS, C. K. & ROSENFELD, M. G. 2009. Nuclear receptor-induced chromosomal proximity and DNA breaks underlie specific translocations in cancer. *Cell,* 139**,** 1069-83.

LIU, S., HOWELL, P., REN, S., FODSTAD, O., ZHANG, G., SAMANT, R., SHEVDE, L., XI, Y., PANNELL, L. K. & RIKER, A. I. 2009. Expression and functional analysis of the WAP four disulfide core domain 1 gene in human melanoma. *Clin Exp Metastasis,* 26**,** 739-49.

LIU, S., REN, S., HOWELL, P., FODSTAD, O. & RIKER, A. I. 2008a. Identification of novel epigenetically modified genes in human melanoma via promoter methylation gene profiling. *Pigment Cell Melanoma Res,* 21**,** 545-58.

LIU, W., XIE, C. C., ZHU, Y., LI, T., SUN, J., CHENG, Y., EWING, C. M., DALRYMPLE, S., TURNER, A. R., ISAACS, J. T., CHANG, B. L., ZHENG, S. L., ISAACS, W. B. & XU, J. 2008b. Homozygous deletions and recurrent amplifications implicate new genes involved in prostate cancer. *Neoplasia,* 10**,** 897-907.

LO, W. L. & ALLEN, P. M. 2014. Self-peptides in TCR repertoire selection and peripheral T cell function. *Curr Top Microbiol Immunol,* 373**,** 49-67.

LONG, E. O., KIM, H. S., LIU, D., PETERSON, M. E. & RAJAGOPALAN, S. 2013. Controlling natural killer cell responses: integration of signals for activation and inhibition. *Annu Rev Immunol,* 31**,** 227-58.

LORAND, L. & CONRAD, S. M. 1984. Transglutaminases. *Mol Cell Biochem,* 58**,** 9-35.

LU, J., GIUNTOLI, R. L., 2ND, OMIYA, R., KOBAYASHI, H., KENNEDY, R. & CELIS, E. 2002. Interleukin 15 promotes antigen-independent in vitro expansion and long-term survival of antitumor cytotoxic T lymphocytes. *Clin Cancer Res,* 8**,** 3877-84.

MADAR, S., BROSH, R., BUGANIM, Y., EZRA, O., GOLDSTEIN, I., SOLOMON, H., KOGAN, I., GOLDFINGER, N., KLOCKER, H. & ROTTER, V. 2009. Modulated expression of WFDC1 during carcinogenesis and cellular senescence. *Carcinogenesis,* 30**,** 20-7.

MALCHOW, S., LEVENTHAL, D. S., NISHI, S., FISCHER, B. I., SHEN, L., PANER, G. P., AMIT, A. S., KANG, C., GEDDES, J. E., ALLISON, J. P., SOCCI, N. D. & SAVAGE, P. A. 2013. Aire-dependent thymic development of tumor-associated regulatory T cells. *Science,* 339**,** 1219-24.

MARTIN, C. E., FRIMPONG-BOATENG, K., SPASOVA, D. S., STONE, J. C. & SURH, C. D. 2013. Homeostatic proliferation of mature T cells. *Methods Mol Biol,* 979**,** 81-106.

MARTINS, W. K., ESTEVES, G. H., ALMEIDA, O. M., REZZE, G. G., LANDMAN, G., MARQUES, S. M., CARVALHO, A. F., LF, L. R., DUPRAT, J. P. & STOLF, B. S. 2011. Gene network analyses point to the importance of human tissue kallikreins in melanoma progression. *BMC Med Genomics,* 4**,** 76.

MASSAGUE, J. 2008. TGFbeta in Cancer. *Cell,* 134**,** 215-30.

MCALHANY, S. J., AYALA, G. E., FROLOV, A., RESSLER, S. J., WHEELER, T. M., WATSON, J. E., COLLINS, C. & ROWLEY, D. R. 2004. Decreased stromal expression and increased epithelial expression of WFDC1/ps20 in prostate cancer is associated with reduced recurrence-free survival. *Prostate,* 61**,** 182-91.

MCALHANY, S. J., RESSLER, S. J., LARSEN, M., TUXHORN, J. A., YANG, F., DANG, T. D. & ROWLEY, D. R. 2003. Promotion of angiogenesis by ps20 in the differential reactive stroma prostate cancer xenograft model. *Cancer Res,* 63**,** 5859-65.

METCALFE, S. M. 2011. LIF in the regulation of T-cell fate and as a potential therapeutic. *Genes Immun,* 12**,** 157-68.

MEYER, C., SEVKO, A., RAMACHER, M., BAZHIN, A. V., FALK, C. S., OSEN, W., BORRELLO, I., KATO, M., SCHADENDORF, D., BANIYASH, M. & UMANSKY, V. 2011. Chronic inflammation promotes myeloid-derived suppressor cell activation blocking antitumor immunity in transgenic mouse melanoma model. *Proc Natl Acad Sci U S A,* 108**,** 17111-6.

MIYAHARA, Y., ODUNSI, K., CHEN, W., PENG, G., MATSUZAKI, J. & WANG, R. F. 2008. Generation and regulation of human CD4+ IL-17-producing T cells in ovarian cancer. *Proc Natl Acad Sci U S A,* 105**,** 15505-10.

MOL, A. J., GELDOF, A. A., MEIJER, G. A., VAN DER POEL, H. G. & VAN MOORSELAAR, R. J. 2007. New experimental markers for early detection of high-risk prostate cancer: role of cell-cell adhesion and cell migration. *J Cancer Res Clin Oncol,* 133**,** 687-95.

MOREAU, T., BARANGER, K., DADE, S., DALLET-CHOISY, S., GUYOT, N. & ZANI, M. L. 2008. Multifaceted roles of human elafin and secretory leukocyte proteinase inhibitor (SLPI), two serine protease inhibitors of the chelonianin family. *Biochimie,* 90**,** 284-95.

MORITA, I., SCHINDLER, M., REGIER, M. K., OTTO, J. C., HORI, T., DEWITT, D. L. & SMITH, W. L. 1995. Different intracellular locations for prostaglandin endoperoxide H synthase-1 and -2. *J Biol Chem,* 270**,** 10902-8.

MUNIR, S., ANDERSEN, G. H., MET, O., DONIA, M., FROSIG, T. M., LARSEN, S. K., KLAUSEN, T. W., SVANE, I. M. & ANDERSEN, M. H. 2013a. HLA-restricted CTL that are specific for the immune checkpoint ligand PD-L1 occur with high frequency in cancer patients. *Cancer Res,* 73**,** 1764-76.

MUNIR, S., ANDERSEN, G. H., WOETMANN, A., ODUM, N., BECKER, J. C. & ANDERSEN, M. H. 2013b. Cutaneous T cell lymphoma cells are targets for immune checkpoint ligand PD-L1-specific, cytotoxic T cells. *Leukemia,* 27**,** 2251-3.

NAGATA, D., YOSHIHIRO, H., NAKANISHI, M., NARUYAMA, H., OKADA, S., ANDO, R., TOZAWA, K. & KOHRI, K. 2008. Peroxisome proliferator-activated receptor-gamma and growth inhibition by its ligands in prostate cancer. *Cancer Detect Prev,* 32**,** 259-66.

NAKAMURA, M., TSUMURA, H., SATOH, T., MATSUMOTO, K., MARUYAMA, H., MAJIMA, M. & KITASATO, H. 2013. Tumor apoptosis in prostate cancer by PGD(2) and its metabolite 15d-PGJ(2) in murine model. *Biomed Pharmacother,* 67**,** 66-71.

NAKAMURA, M., UEHARA, Y., ASADA, M., HONDA, E., NAGAI, N., KIMATA, K., SUZUKI, M. & IMAMURA, T. 2011. Sulfated glycosaminoglycans are required for specific and sensitive fibroblast growth factor (FGF) 19 signaling via FGF receptor 4 and betaKlotho. *J Biol Chem,* 286**,** 26418-23.

NELSON, D. M., MCBRYAN, T., JEYAPALAN, J. C., SEDIVY, J. M. & ADAMS, P. D. 2014. A comparison of oncogene-induced senescence and replicative senescence: implications for tumor suppression and aging. *Age (Dordr),* 36**,** 9637.

NISHIMICHI, N., HAYASHITA-KINOH, H., CHEN, C., MATSUDA, H., SHEPPARD, D. & YOKOSAKI, Y. 2011. Osteopontin undergoes polymerization in vivo and gains chemotactic activity for neutrophils mediated by integrin alpha9beta1. *J Biol Chem,* 286**,** 11170-8.

NIU, Y. N. & XIA, S. J. 2009. Stroma-epithelium crosstalk in prostate cancer. *Asian J Androl,* 11**,** 28-35.

NUKIWA, T., SUZUKI, T., FUKUHARA, T. & KIKUCHI, T. 2008. Secretory leukocyte peptidase inhibitor and lung cancer. *Cancer Sci,* 99**,** 849-55.

NUMASAKI, M., FUKUSHI, J., ONO, M., NARULA, S. K., ZAVODNY, P. J., KUDO, T., ROBBINS, P. D., TAHARA, H. & LOTZE, M. T. 2003. Interleukin-17 promotes angiogenesis and tumor growth. *Blood,* 101**,** 2620-7.

O'SULLIVAN, T., SADDAWI-KONEFKA, R., VERMI, W., KOEBEL, C. M., ARTHUR, C., WHITE, J. M., UPPALURI, R., ANDREWS, D. M., NGIOW, S. F., TENG, M. W., SMYTH, M. J., SCHREIBER, R. D. & BUI, J. D. 2012. Cancer immunoediting by the innate immune system in the absence of adaptive immunity. *J Exp Med,* 209**,** 1869-82.

OBERMAJER, N., MUTHUSWAMY, R., LESNOCK, J., EDWARDS, R. P. & KALINSKI, P. 2011. Positive feedback between PGE2 and COX2 redirects the differentiation of human dendritic cells toward stable myeloid-derived suppressor cells. *Blood,* 118**,** 5498-505.

OLSON, B. M., JANKOWSKA-GAN, E., BECKER, J. T., VIGNALI, D. A., BURLINGHAM, W. J. & MCNEEL, D. G. 2012. Human prostate tumor antigen-specific CD8+ regulatory T cells are inhibited by CTLA-4 or IL-35 blockade. *J Immunol,* 189**,** 5590-601.

OLURINDE, M. O., SHEN, C. H., DRAKE, A., BAI, A. & CHEN, J. 2011. Persistence of tumor-infiltrating CD8 T cells is tumor-dependent but antigen-independent. *Cell Mol Immunol,* 8**,** 415-23.

ORR, B., RIDDICK, A. C., STEWART, G. D., ANDERSON, R. A., FRANCO, O. E., HAYWARD, S. W. & THOMSON, A. A. 2012. Identification of stromally expressed molecules in the prostate by tag-profiling of cancer-associated fibroblasts, normal fibroblasts and fetal prostate. *Oncogene,* 31**,** 1130-42.

OTTO, J. C. & SMITH, W. L. 1994. The orientation of prostaglandin endoperoxide synthases-1 and -2 in the endoplasmic reticulum. *J Biol Chem,* 269**,** 19868-75.

PANNI, R. Z., LINEHAN, D. C. & DENARDO, D. G. 2013. Targeting tumor-infiltrating macrophages to combat cancer. *Immunotherapy,* 5**,** 1075-87.

PARK, H., LI, Z., YANG, X. O., CHANG, S. H., NURIEVA, R., WANG, Y. H., WANG, Y., HOOD, L., ZHU, Z., TIAN, Q. & DONG, C. 2005. A distinct lineage of CD4 T cells regulates tissue inflammation by producing interleukin 17. *Nat Immunol,* 6**,** 1133-41.

PATEL, H., SMITH, R. A., SACKS, S. H. & ZHOU, W. 2006. Therapeutic strategy with a membrane-localizing complement regulator to increase the number of usable donor organs after prolonged cold storage. *J Am Soc Nephrol,* 17**,** 1102-11.

PEAR, W. S., MILLER, J. P., XU, L., PUI, J. C., SOFFER, B., QUACKENBUSH, R. C., PENDERGAST, A. M., BRONSON, R., ASTER, J. C., SCOTT, M. L. & BALTIMORE, D. 1998. Efficient and rapid induction of a chronic myelogenous leukemia-like myeloproliferative disease in mice receiving P210 bcr/abl-transduced bone marrow. *Blood,* 92**,** 3780-92.

PERNA, S. K., DE ANGELIS, B., PAGLIARA, D., HASAN, S. T., ZHANG, L., MAHENDRAVADA, A., HESLOP, H. E., BRENNER, M. K., ROONEY, C. M., DOTTI, G. & SAVOLDO, B. 2013. Interleukin 15 provides relief to CTLs from regulatory T cell-mediated inhibition: implications for adoptive T cell-based therapies for lymphoma. *Clin Cancer Res,* 19**,** 106-17.

POON, G. M. & GARIEPY, J. 2007. Cell-surface proteoglycans as molecular portals for cationic peptide and polymer entry into cells. *Biochem Soc Trans,* 35**,** 788-93.

POWELL, D. W., MIFFLIN, R. C., VALENTICH, J. D., CROWE, S. E., SAADA, J. I. & WEST, A. B. 1999. Myofibroblasts. I. Paracrine cells important in health and disease. *Am J Physiol,* 277**,** C1-9.

PRENDERGAST, G. C., SMITH, C., THOMAS, S., MANDIK-NAYAK, L., LAURY-KLEINTOP, L., METZ, R. & MULLER, A. J. 2014. Indoleamine 2,3-dioxygenase pathways of pathogenic inflammation and immune escape in cancer. *Cancer Immunol Immunother,* 63**,** 721-35.

PY, B., BASMACIOGULLARI, S., BOUCHET, J., ZARKA, M., MOURA, I. C., BENHAMOU, M., MONTEIRO, R. C., HOCINI, H., MADRID, R. & BENICHOU,

S. 2009. The phospholipid scramblases 1 and 4 are cellular receptors for the secretory leukocyte protease inhibitor and interact with CD4 at the plasma membrane. *PLoS One,* 4**,** e5006.

QIN, J., WU, S. P., CREIGHTON, C. J., DAI, F., XIE, X., CHENG, C. M., FROLOV, A., AYALA, G., LIN, X., FENG, X. H., ITTMANN, M. M., TSAI, S. J., TSAI, M. J. & TSAI, S. Y. 2013. COUP-TFII inhibits TGF-beta-induced growth barrier to promote prostate tumorigenesis. *Nature,* 493**,** 236-40.

RAJAKUMAR, A., CHU, T., HANDLEY, D. E., BUNCE, K. D., BURKE, B., HUBEL, C. A., JEYABALAN, A. & PETERS, D. G. 2011. Maternal gene expression profiling during pregnancy and preeclampsia in human peripheral blood mononuclear cells. *Placenta,* 32**,** 70-8.

RAPHAEL, I., NALAWADE, S., EAGAR, T. N. & FORSTHUBER, T. G. 2014. T cell subsets and their signature cytokines in autoimmune and inflammatory diseases. *Cytokine*.

RASOOL, N., LAROCHELLE, W., ZHONG, H., ARA, G., COHEN, J. & KOHN, E. C. 2010. Secretory leukocyte protease inhibitor antagonizes paclitaxel in ovarian cancer cells. *Clin Cancer Res,* 16**,** 600-9.

READING, J. L., SABBAH, S., BUSCH, S. & TREE, T. I. 2013a. Mesenchymal stromal cells as a means of controlling pathological T-cell responses in allogeneic islet transplantation. *Curr Opin Organ Transplant,* 18**,** 59-64.

READING, J. L., YANG, J. H., SABBAH, S., SKOWERA, A., KNIGHT, R. R., PINXTEREN, J., VAES, B., ALLSOPP, T., TING, A. E., BUSCH, S., RABER, A., DEANS, R. & TREE, T. I. 2013b. Clinical-grade multipotent adult progenitor cells durably control pathogenic T cell responses in human models of transplantation and autoimmunity. *J Immunol,* 190**,** 4542-52.

REID, A. H., ATTARD, G., AMBROISINE, L., FISHER, G., KOVACS, G., BREWER, D., CLARK, J., FLOHR, P., EDWARDS, S., BERNEY, D. M., FOSTER, C. S., FLETCHER, A., GERALD, W. L., MOLLER, H., REUTER, V. E., SCARDINO, P. T., CUZICK, J., DE BONO, J. S. & COOPER, C. S. 2010. Molecular characterisation of ERG, ETV1 and PTEN gene loci identifies patients at low and high risk of death from prostate cancer. *Br J Cancer,* 102**,** 678-84.

REIN, D. T., BREIDENBACH, M., NETTELBECK, D. M., KAWAKAMI, Y., SIEGAL, G. P., HUH, W. K., WANG, M., HEMMINKI, A., BAUERSCHMITZ, G. J., YAMAMOTO, M., ADACHI, Y., TAKAYAMA, K., DALL, P. & CURIEL, D. T. 2004. Evaluation of tissue-specific promoters in carcinomas of the cervix uteri. *J Gene Med,* 6**,** 1281-9.

REIS E SOUSA, C. 2001. Dendritic cells as sensors of infection. *Immunity,* 14**,** 495-8.

RESSLER, S. J., DANG, T. D., WU, S. M., TSE, D. Y., GILBERT, B. E., VYAKARNAM, A., YANG, F., SCHAUER, I. G., BARRON, D. A. & ROWLEY, D. R. 2014. WFDC1 Is a Key Modulator of Inflammatory and Wound Repair Responses. *Am J Pathol*.

RESSLER, S. J. & ROWLEY, D. R. 2011. The WFDC1 gene: role in wound response and tissue homoeostasis. *Biochem Soc Trans,* 39**,** 1455-9.

RIBEIRO, R. A., FLORES, C. A., CUNHA, F. Q. & FERREIRA, S. H. 1991. IL-8 causes in vivo neutrophil migration by a cell-dependent mechanism. *Immunology,* 73**,** 472-7.

RIZZUTO, G. A., MERGHOUB, T., HIRSCHHORN-CYMERMAN, D., LIU, C., LESOKHIN, A. M., SAHAWNEH, D., ZHONG, H., PANAGEAS, K. S., PERALES, M. A., ALTAN-BONNET, G., WOLCHOK, J. D. & HOUGHTON, A. N. 2009. Self-antigen-specific CD8+ T cell precursor frequency determines the quality of the antitumor immune response. *J Exp Med,* 206**,** 849-66.

ROBINSON, P. A., MARKHAM, A. F., SCHALKWIJK, J. & HIGH, A. S. 1996. Increased elafin expression in cystic, dysplastic and neoplastic oral tissues. *J Oral Pathol Med,* 25**,** 135-9.

ROGERS, E., WANG, B. X., CUI, Z., ROWLEY, D. R., RESSLER, S. J., VYAKARNAM, A. & FISH, E. N. 2012. WFDC1/ps20: A host factor that influences the neutrophil response to murine hepatitis virus (MHV) 1 infection. *Antiviral Res*.

ROGHANIAN, A., WILLIAMS, S. E., SHELDRAKE, T. A., BROWN, T. I., OBERHEIM, K., XING, Z., HOWIE, S. E. & SALLENAVE, J. M. 2006. The antimicrobial/elastase inhibitor elafin regulates lung dendritic cells and adaptive immunity. *Am J Respir Cell Mol Biol,* 34**,** 634-42.

ROWLEY, D. R., DANG, T. D., LARSEN, M., GERDES, M. J., MCBRIDE, L. & LU, B. 1995. Purification of a novel protein (ps20) from urogenital sinus mesenchymal cells with growth inhibitory properties in vitro. *J Biol Chem,* 270**,** 22058-65.

RYU, B., JONES, J., BLADES, N. J., PARMIGIANI, G., HOLLINGSWORTH, M. A., HRUBAN, R. H. & KERN, S. E. 2002. Relationships and differentially expressed genes among pancreatic cancers examined by large-scale serial analysis of gene expression. *Cancer Res,* 62**,** 819-26.

SAFFROY, R., RIOU, P., SOLER, G., AZOULAY, D., EMILE, J. F., DEBUIRE, B. & LEMOINE, A. 2002. Analysis of alterations of WFDC1, a new putative tumour suppressor gene, in hepatocellular carcinoma. *Eur J Hum Genet,* 10**,** 239-44.

SAIDI, A., JAVERZAT, S., BELLAHCENE, A., DE VOS, J., BELLO, L., CASTRONOVO, V., DEPREZ, M., LOISEAU, H., BIKFALVI, A. & HAGEDORN, M. 2008. Experimental anti-angiogenesis causes upregulation of genes associated with poor survival in glioblastoma. *Int J Cancer,* 122**,** 2187-98.

SALLENAVE, J. M. 2010. Secretory leukocyte protease inhibitor and elafin/trappin-2: versatile mucosal antimicrobials and regulators of immunity. *Am J Respir Cell Mol Biol,* 42**,** 635-43.

SALLENAVE, J. M., SHULMANN, J., CROSSLEY, J., JORDANA, M. & GAULDIE, J. 1994. Regulation of secretory leukocyte proteinase inhibitor (SLPI) and elastase-specific inhibitor (ESI/elafin) in human airway epithelial cells by cytokines and neutrophilic enzymes. *Am J Respir Cell Mol Biol,* 11**,** 733-41.

SALLENAVE, J. M. & SILVA, A. 1993. Characterization and gene sequence of the precursor of elafin, an elastase-specific inhibitor in bronchial secretions. *Am J Respir Cell Mol Biol,* 8**,** 439-45.

SAMSOM, J. N., VAN DER MAREL, A. P., VAN BERKEL, L. A., VAN HELVOORT, J. M., SIMONS-OOSTERHUIS, Y., JANSEN, W., GREUTER, M., NELISSEN, R. L., MEEUWISSE, C. M., NIEUWENHUIS, E. E., MEBIUS, R. E. & KRAAL, G. 2007. Secretory leukoprotease inhibitor in mucosal lymph node dendritic cells regulates the threshold for mucosal tolerance. *J Immunol,* 179**,** 6588-95.

SAVAGE, P., COWBURN, P., CLAYTON, A., MAN, S., LAWSON, T., OGG, G., LEMOINE, N., MCMICHAEL, A. & EPENETOS, A. 2002. Anti-viral cytotoxic T cells inhibit the growth of cancer cells with antibody targeted HLA class I/peptide complexes in SCID mice. *Int J Cancer,* 98**,** 561-6.

SAVAGE, P. A., LEVENTHAL, D. S. & MALCHOW, S. 2014. Shaping the repertoire of tumor-infiltrating effector and regulatory T cells. *Immunol Rev,* 259**,** 245-58.

SAVAGE, P. A., VOSSELLER, K., KANG, C., LARIMORE, K., RIEDEL, E., WOJNOONSKI, K., JUNGBLUTH, A. A. & ALLISON, J. P. 2008. Recognition of a ubiquitous self antigen by prostate cancer-infiltrating CD8+ T lymphocytes. *Science,* 319**,** 215-20.

SCHALKWIJK, J., VAN VLIJMEN, I. M., ALKEMADE, J. A. & DE JONGH, G. J. 1993. Immunohistochemical localization of SKALP/elafin in psoriatic epidermis. *J Invest Dermatol,* 100**,** 390-3.

SCHALKWIJK, J., WIEDOW, O. & HIROSE, S. 1999. The trappin gene family: proteins defined by an N-terminal transglutaminase substrate domain and a C-terminal four-disulphide core. *Biochem J,* 340 (Pt 3)**,** 569-77.

SCHALL, T. J., BACON, K., TOY, K. J. & GOEDDEL, D. V. 1990. Selective attraction of monocytes and T lymphocytes of the memory phenotype by cytokine RANTES. *Nature,* 347**,** 669-71.

SCHERER, W. F., SYVERTON, J. T. & GEY, G. O. 1953. Studies on the propagation in vitro of poliomyelitis viruses. IV. Viral multiplication in a stable strain of human malignant epithelial cells (strain HeLa) derived from an epidermoid carcinoma of the cervix. *J Exp Med,* 97**,** 695-710.

SCHIFFMANN, S., WEIGERT, A., MANNICH, J., EBERLE, M., BIROD, K., HAUSSLER, A., FERREIROS, N., SCHREIBER, Y., KUNKEL, H., GREZ, M., WEICHAND, B., BRUNE, B., PFEILSCHIFTER, W., NUSING, R., NIEDERBERGER, E., GROSCH, S., SCHOLICH, K. & GEISSLINGER, G. 2014. PGE2/EP4 signaling in peripheral immune cells promotes development of experimental autoimmune encephalomyelitis. *Biochem Pharmacol,* 87**,** 625-35.

SCHWARTZ, D. R., KARDIA, S. L., SHEDDEN, K. A., KUICK, R., MICHAILIDIS, G., TAYLOR, J. M., MISEK, D. E., WU, R., ZHAI, Y., DARRAH, D. M., REED, H., ELLENSON, L. H., GIORDANO, T. J., FEARON, E. R., HANASH, S. M. & CHO, K. R. 2002. Gene expression in ovarian cancer reflects both morphology and biological behavior, distinguishing clear cell from other poor-prognosis ovarian carcinomas. *Cancer Res,* 62**,** 4722-9.

SEUNG, L. P., ROWLEY, D. A., DUBEY, P. & SCHREIBER, H. 1995. Synergy between T-cell immunity and inhibition of paracrine stimulation causes tumor rejection. *Proc Natl Acad Sci U S A,* 92**,** 6254-8.

SFANOS, K. S., BRUNO, T. C., MARIS, C. H., XU, L., THOBURN, C. J., DEMARZO, A. M., MEEKER, A. K., ISAACS, W. B. & DRAKE, C. G. 2008. Phenotypic analysis of prostate-infiltrating lymphocytes reveals TH17 and Treg skewing. *Clin Cancer Res,* 14**,** 3254-61.

SHA, W., OLESCH, C., HANAKA, H., RADMARK, O., WEIGERT, A. & BRUNE, B. 2013. Necrosis in DU145 prostate cancer spheroids induces COX-2/mPGES-1-derived PGE2 to promote tumor growth and to inhibit T cell activation. *Int J Cancer,* 133**,** 1578-88.

SHAFER-WEAVER, K. A., ANDERSON, M. J., STAGLIANO, K., MALYGUINE, A., GREENBERG, N. M. & HURWITZ, A. A. 2009. Cutting Edge: Tumor-specific CD8+ T cells infiltrating prostatic tumors are induced to become suppressor cells. *J Immunol,* 183**,** 4848-52.

SHAFI, A. A., YEN, A. E. & WEIGEL, N. L. 2013. Androgen receptors in hormone-dependent and castration-resistant prostate cancer. *Pharmacol Ther,* 140**,** 223-38.

SHANKARAN, V., IKEDA, H., BRUCE, A. T., WHITE, J. M., SWANSON, P. E., OLD, L. J. & SCHREIBER, R. D. 2001. IFNgamma and lymphocytes prevent primary tumour development and shape tumour immunogenicity. *Nature,* 410**,** 1107-11.

SHAO, N., FENG, N., WANG, Y., MI, Y., LI, T. & HUA, L. 2012. Systematic review and meta-analysis of COX-2 expression and polymorphisms in prostate cancer. *Mol Biol Rep,* 39**,** 10997-1004.

SHARMA, S., STOLINA, M., YANG, S. C., BARATELLI, F., LIN, J. F., ATIANZAR, K., LUO, J., ZHU, L., LIN, Y., HUANG, M., DOHADWALA, M., BATRA, R. K. & DUBINETT, S. M. 2003. Tumor cyclooxygenase 2-dependent suppression of dendritic cell function. *Clin Cancer Res,* 9**,** 961-8.

SHAW, L. & WIEDOW, O. 2011. Therapeutic potential of human elafin. *Biochem Soc Trans,* 39**,** 1450-4.

SHIBATA, T., KONDO, M., OSAWA, T., SHIBATA, N., KOBAYASHI, M. & UCHIDA, K. 2002. 15-deoxy-delta 12,14-prostaglandin J2. A prostaglandin D2 metabolite generated during inflammatory processes. *J Biol Chem,* 277**,** 10459-66.

SIEGEL, P. M. & MASSAGUE, J. 2003. Cytostatic and apoptotic actions of TGF-beta in homeostasis and cancer. *Nat Rev Cancer,* 3**,** 807-21.

SIMPKINS, F. A., DEVOOGDT, N. M., RASOOL, N., TCHABO, N. E., ALEJANDRO, E. U., KAMRAVA, M. M. & KOHN, E. C. 2008. The alarm anti-protease, secretory leukocyte protease inhibitor, is a proliferation and survival factor for ovarian cancer cells. *Carcinogenesis,* 29**,** 466-72.

SIMPSON, A. J., CUNNINGHAM, G. A., PORTEOUS, D. J., HASLETT, C. & SALLENAVE, J. M. 2001a. Regulation of adenovirus-mediated elafin transgene expression by bacterial lipopolysaccharide. *Hum Gene Ther,* 12**,** 1395-406.

SIMPSON, A. J., WALLACE, W. A., MARSDEN, M. E., GOVAN, J. R., PORTEOUS, D. J., HASLETT, C. & SALLENAVE, J. M. 2001b. Adenoviral augmentation of elafin protects the lung against acute injury mediated by activated neutrophils and bacterial infection. *J Immunol,* 167**,** 1778-86.

SMITH, B. A., KENNEDY, W. J., HARNDEN, P., SELBY, P. J., TREJDOSIEWICZ, L. K. & SOUTHGATE, J. 2001. Identification of genes involved in human urothelial cell-matrix interactions: implications for the progression pathways of malignant urothelium. *Cancer Res,* 61**,** 1678-85.

SMITH, V. J. 2011. Phylogeny of whey acidic protein (WAP) four-disulfide core proteins and their role in lower vertebrates and invertebrates. *Biochem Soc Trans,* 39**,** 1403-8.

SORENSEN, R. B., HADRUP, S. R., SVANE, I. M., HJORTSO, M. C., THOR STRATEN, P. & ANDERSEN, M. H. 2011a. Indoleamine 2,3-dioxygenase specific, cytotoxic T cells as immune regulators. *Blood,* 117**,** 2200-10.

SORENSEN, R. B., KOLLGAARD, T., ANDERSEN, R. S., VAN DEN BERG, J. H., SVANE, I. M., STRATEN, P. & ANDERSEN, M. H. 2011b. Spontaneous cytotoxic T-Cell reactivity against indoleamine 2,3-dioxygenase-2. *Cancer Res,* 71**,** 2038-44.

SRIURANPONG, V., MUTIRANGURA, A., GILLESPIE, J. W., PATEL, V., AMORNPHIMOLTHAM, P., MOLINOLO, A. A., KEREKHANJANARONG, V., SUPANAKORN, S., SUPIYAPHUN, P., RANGDAENG, S., VORAVUD, N. & GUTKIND, J. S. 2004. Global gene expression profile of nasopharyngeal carcinoma by laser capture microdissection and complementary DNA microarrays. *Clin Cancer Res,* 10**,** 4944-58.

STOVER, D. G., BIERIE, B. & MOSES, H. L. 2007. A delicate balance: TGF-beta and the tumor microenvironment. *J Cell Biochem,* 101**,** 851-61.

SU, A. I., COOKE, M. P., CHING, K. A., HAKAK, Y., WALKER, J. R., WILTSHIRE, T., ORTH, A. P., VEGA, R. G., SAPINOSO, L. M., MOQRICH, A., PATAPOUTIAN, A., HAMPTON, G. M., SCHULTZ, P. G. & HOGENESCH, J. B. 2002. Large-scale analysis of the human and mouse transcriptomes. *Proc Natl Acad Sci U S A,* 99**,** 4465-70.

SU, X., YE, J., HSUEH, E. C., ZHANG, Y., HOFT, D. F. & PENG, G. 2010. Tumor microenvironments direct the recruitment and expansion of human Th17 cells. *J Immunol,* 184**,** 1630-41.

SUGINO, T., YAMAGUCHI, T., OGURA, G., KUSAKABE, T., GOODISON, S., HOMMA, Y. & SUZUKI, T. 2007. The secretory leukocyte protease inhibitor (SLPI) suppresses cancer cell invasion but promotes blood-borne metastasis via an invasion-independent pathway. *J Pathol,* 212**,** 152-60.

TABORDA, N. A., CATANO, J. C., DELGADO, J. C., RUGELES, M. T. & MONTOYA, C. J. 2012. Higher SLPI expression, lower immune activation, and increased frequency of immune cells in a cohort of Colombian HIV-1 controllers. *J Acquir Immune Defic Syndr,* 60**,** 12-9.

TAFLIN, C., FAVIER, B., BAUDHUIN, J., SAVENAY, A., HEMON, P., BENSUSSAN, A., CHARRON, D., GLOTZ, D. & MOONEY, N. 2011. Human endothelial cells generate Th17 and regulatory T cells under inflammatory conditions. *Proc Natl Acad Sci U S A,* 108**,** 2891-6.

TAGGART, C. C., CRYAN, S. A., WELDON, S., GIBBONS, A., GREENE, C. M., KELLY, E., LOW, T. B., O'NEILL S, J. & MCELVANEY, N. G. 2005. Secretory leucoprotease inhibitor binds to NF-kappaB binding sites in monocytes and inhibits p65 binding. *J Exp Med,* 202**,** 1659-68.

TAGGART, C. C., LOWE, G. J., GREENE, C. M., MULGREW, A. T., O'NEILL, S. J., LEVINE, R. L. & MCELVANEY, N. G. 2001. Cathepsin B, L, and S cleave and inactivate secretory leucoprotease inhibitor. *J Biol Chem,* 276**,** 33345-52.

TAHA, A. S., FACCENDA, E., ANGERSON, W. J., BALSITIS, M. & KELLY, R. W. 2005. Gastric epithelial anti-microbial peptides--histological correlation and influence of anatomical site and peptic ulcer disease. *Dig Liver Dis,* 37**,** 51-6.

TAN, J. T., DUDL, E., LEROY, E., MURRAY, R., SPRENT, J., WEINBERG, K. I. & SURH, C. D. 2001. IL-7 is critical for homeostatic proliferation and survival of naive T cells. *Proc Natl Acad Sci U S A,* 98**,** 8732-7.

TANNER, M. M., GRENMAN, S., KOUL, A., JOHANNSSON, O., MELTZER, P., PEJOVIC, T., BORG, A. & ISOLA, J. J. 2000. Frequent amplification of chromosomal region 20q12-q13 in ovarian cancer. *Clin Cancer Res,* 6**,** 1833-9.

TARTOUR, E., FOSSIEZ, F., JOYEUX, I., GALINHA, A., GEY, A., CLARET, E., SASTRE-GARAU, X., COUTURIER, J., MOSSERI, V., VIVES, V., BANCHEREAU, J., FRIDMAN, W. H., WIJDENES, J., LEBECQUE, S. & SAUTES-FRIDMAN, C. 1999. Interleukin 17, a T-cell-derived cytokine, promotes tumorigenicity of human cervical tumors in nude mice. *Cancer Res,* 59**,** 3698-704.

TAYLOR, B. S., SCHULTZ, N., HIERONYMUS, H., GOPALAN, A., XIAO, Y., CARVER, B. S., ARORA, V. K., KAUSHIK, P., CERAMI, E., REVA, B., ANTIPIN, Y., MITSIADES, N., LANDERS, T., DOLGALEV, I., MAJOR, J. E., WILSON, M., SOCCI, N. D., LASH, A. E., HEGUY, A., EASTHAM, J. A., SCHER, H. I., REUTER, V. E., SCARDINO, P. T., SANDER, C., SAWYERS, C. L. & GERALD, W. L. 2010. Integrative genomic profiling of human prostate cancer. *Cancer Cell,* 18**,** 11-22.

TESTI, R., PHILLIPS, J. H. & LANIER, L. L. 1989. T cell activation via Leu-23 (CD69). *J Immunol,* 143**,** 1123-8.

THOMPSON, L. H., WHISTON, R. A., RAKHIMOV, Y., TACCIOLI, C., LIU, C. G., CROCE, C. & METCALFE, S. M. 2010. A LIF/Nanog axis is revealed in T lymphocytes that lack MARCH-7, a RINGv E3 ligase that regulates the LIF-receptor. *Cell Cycle,* 9**,** 4213-21.

THOMPSON, M., LAPOINTE, J., CHOI, Y. L., ONG, D. E., HIGGINS, J. P., BROOKS, J. D. & POLLACK, J. R. 2008. Identification of candidate prostate cancer genes through comparative expression-profiling of seminal vesicle. *Prostate,* 68**,** 1248-56.

TIAN, X., SHIGEMASA, K., HIRATA, E., GU, L., UEBABA, Y., NAGAI, N., O'BRIEN, T. J. & OHAMA, K. 2004. Expression of human kallikrein 7 (hK7/SCCE) and its inhibitor antileukoprotease (ALP/SLPI) in uterine endocervical glands and in cervical adenocarcinomas. *Oncol Rep,* 12**,** 1001-6.

TOKUGAWA, Y., KUNISHIGE, I., KUBOTA, Y., SHIMOYA, K., NOBUNAGA, T., KIMURA, T., SAJI, F., MURATA, Y., EGUCHI, N., ODA, H., URADE, Y. & HAYAISHI, O. 1998. Lipocalin-type prostaglandin D synthase in human male reproductive organs and seminal plasma. *Biol Reprod,* 58**,** 600-7.

TOMLINS, S. A., LAXMAN, B., DHANASEKARAN, S. M., HELGESON, B. E., CAO, X., MORRIS, D. S., MENON, A., JING, X., CAO, Q., HAN, B., YU, J., WANG, L., MONTIE, J. E., RUBIN, M. A., PIENTA, K. J., ROULSTON, D., SHAH, R. B., VARAMBALLY, S., MEHRA, R. & CHINNAIYAN, A. M. 2007. Distinct classes of chromosomal rearrangements create oncogenic ETS gene fusions in prostate cancer. *Nature,* 448**,** 595-9.

TOMLINS, S. A., RHODES, D. R., PERNER, S., DHANASEKARAN, S. M., MEHRA, R., SUN, X. W., VARAMBALLY, S., CAO, X., TCHINDA, J., KUEFER, R., LEE, C., MONTIE, J. E., SHAH, R. B., PIENTA, K. J., RUBIN, M. A. & CHINNAIYAN, A. M. 2005. Recurrent fusion of TMPRSS2 and ETS transcription factor genes in prostate cancer. *Science,* 310**,** 644-8.

TREMBLAY, G. M., SALLENAVE, J. M., ISRAEL-ASSAYAG, E., CORMIER, Y. & GAULDIE, J. 1996. Elafin/elastase-specific inhibitor in bronchoalveolar lavage of normal subjects and farmer's lung. *Am J Respir Crit Care Med,* 154**,** 1092-8.

TSE, K. P., WU, C. S., HSUEH, C., CHANG, K. P., HAO, S. P., CHANG, Y. S. & TSANG, N. M. 2012. The relationship between secretory leukocyte protease inhibitor expression and Epstein-Barr virus status among patients with nasopharyngeal carcinoma. *Anticancer Res,* 32**,** 1299-307.

TSUKISHIRO, S., SUZUMORI, N., NISHIKAWA, H., ARAKAWA, A. & SUZUMORI, K. 2005. Use of serum secretory leukocyte protease inhibitor levels in patients to improve specificity of ovarian cancer diagnosis. *Gynecol Oncol,* 96**,** 516-9.

TURK, V., STOKA, V., VASILJEVA, O., RENKO, M., SUN, T., TURK, B. & TURK, D. 2012. Cysteine cathepsins: from structure, function and regulation to new frontiers. *Biochim Biophys Acta,* 1824**,** 68-88.

TUXHORN, J. A., AYALA, G. E. & ROWLEY, D. R. 2001. Reactive stroma in prostate cancer progression. *J Urol,* 166**,** 2472-83.

TUXHORN, J. A., AYALA, G. E., SMITH, M. J., SMITH, V. C., DANG, T. D. & ROWLEY, D. R. 2002. Reactive stroma in human prostate cancer: induction of myofibroblast phenotype and extracellular matrix remodeling. *Clin Cancer Res,* 8**,** 2912-23.

UCHIDA, K. & SHIBATA, T. 2008. 15-Deoxy-Delta(12,14)-prostaglandin J2: an electrophilic trigger of cellular responses. *Chem Res Toxicol,* 21**,** 138-44.

VALENCIA, T., KIM, J. Y., ABU-BAKER, S., MOSCAT-PARDOS, J., AHN, C. S., REINA-CAMPOS, M., DURAN, A., CASTILLA, E. A., METALLO, C. M., DIAZ-MECO, M. T. & MOSCAT, J. 2014. Metabolic reprogramming of stromal fibroblasts through p62-mTORC1 signaling promotes inflammation and tumorigenesis. *Cancer Cell,* 26**,** 121-35.

VAN ROOIJ, N., VAN BUUREN, M. M., PHILIPS, D., VELDS, A., TOEBES, M., HEEMSKERK, B., VAN DIJK, L. J., BEHJATI, S., HILKMANN, H., EL ATMIOUI, D., NIEUWLAND, M., STRATTON, M. R., KERKHOVEN, R. M., KESMIR, C., HAANEN, J. B., KVISTBORG, P. & SCHUMACHER, T. N. 2013. Tumor exome analysis reveals neoantigen-specific T-cell reactivity in an ipilimumab-responsive melanoma. *J Clin Oncol,* 31**,** e439-42.

VIGNERON, N., STROOBANT, V., VAN DEN EYNDE, B. J. & VAN DER BRUGGEN, P. 2013. Database of T cell-defined human tumor antigens: the 2013 update. *Cancer Immun,* 13**,** 15.

WANG, H. Y., PENG, G., GUO, Z., SHEVACH, E. M. & WANG, R. F. 2005a. Recognition of a new ARTC1 peptide ligand uniquely expressed in tumor cells by antigen-specific CD4+ regulatory T cells. *J Immunol,* 174**,** 2661-70.

WANG, N., THURAISINGAM, T., FALLAVOLLITA, L., DING, A., RADZIOCH, D. & BRODT, P. 2006a. The secretory leukocyte protease inhibitor is a type 1 insulin-like growth factor receptor-regulated protein that protects against liver metastasis by attenuating the host proinflammatory response. *Cancer Res,* 66**,** 3062-70.

WANG, R. F., PENG, G. & WANG, H. Y. 2006b. Regulatory T cells and Toll-like receptors in tumor immunity. *Semin Immunol,* 18**,** 136-42.

WANG, S., GAO, J., LEI, Q., ROZENGURT, N., PRITCHARD, C., JIAO, J., THOMAS, G. V., LI, G., ROY-BURMAN, P., NELSON, P. S., LIU, X. & WU, H. 2003. Prostate-specific deletion of the murine Pten tumor suppressor gene leads to metastatic prostate cancer. *Cancer Cell,* 4**,** 209-21.

WANG, W., BERGH, A. & DAMBER, J. E. 2005b. Cyclooxygenase-2 expression correlates with local chronic inflammation and tumor neovascularization in human prostate cancer. *Clin Cancer Res,* 11**,** 3250-6.

WARD, P. A. & NEWMAN, L. J. 1969. A neutrophil chemotactic factor from human C'5. *J Immunol,* 102**,** 93-9.

WATSON, J. E., DOGGETT, N. A., ALBERTSON, D. G., ANDAYA, A., CHINNAIYAN, A., VAN DEKKEN, H., GINZINGER, D., HAQQ, C., JAMES, K., KAMKAR, S.,

KOWBEL, D., PINKEL, D., SCHMITT, L., SIMKO, J. P., VOLIK, S., WEINBERG, V. K., PARIS, P. L. & COLLINS, C. 2004a. Integration of high-resolution array comparative genomic hybridization analysis of chromosome 16q with expression array data refines common regions of loss at 16q23-qter and identifies underlying candidate tumor suppressor genes in prostate cancer. *Oncogene,* 23**,** 3487-94.

WATSON, J. E., KAMKAR, S., JAMES, K., KOWBEL, D., ANDAYA, A., PARIS, P. L., SIMKO, J., CARROLL, P., MCALHANY, S., ROWLEY, D. & COLLINS, C. 2004b. Molecular analysis of WFDC1/ps20 gene in prostate cancer. *Prostate,* 61**,** 192-9.

WAUGH, D. J. & WILSON, C. 2008. The interleukin-8 pathway in cancer. *Clin Cancer Res,* 14**,** 6735-41.

WEBBER, M. M., TRAKUL, N., THRAVES, P. S., BELLO-DEOCAMPO, D., CHU, W. W., STORTO, P. D., HUARD, T. K., RHIM, J. S. & WILLIAMS, D. E. 1999. A human prostatic stromal myofibroblast cell line WPMY-1: a model for stromal-epithelial interactions in prostatic neoplasia. *Carcinogenesis,* 20**,** 1185-92.

WEI, H., HELLSTROM, K. E. & HELLSTROM, I. 2012. Elafin selectively regulates the sensitivity of ovarian cancer cells to genotoxic drug-induced apoptosis. *Gynecol Oncol,* 125**,** 727-33.

WESTDORP, H., SKOLD, A. E., SNIJER, B. A., FRANIK, S., MULDER, S. F., MAJOR, P. P., FOLEY, R., GERRITSEN, W. R. & DE VRIES, I. J. 2014. Immunotherapy for prostate cancer: lessons from responses to tumor-associated antigens. *Front Immunol,* 5**,** 191.

WESTIN, U., NYSTROM, M., LJUNGCRANTZ, I., ERIKSSON, B. & OHLSSON, K. 2002. The presence of elafin, SLPI, IL1-RA and STNFalpha RI in head and neck squamous cell carcinomas and their relation to the degree of tumour differentiation. *Mediators Inflamm,* 11**,** 7-12.

WILKINSON, T. S., DHALIWAL, K., HAMILTON, T. W., LIPKA, A. F., FARRELL, L., DAVIDSON, D. J., DUFFIN, R., MORRIS, A. C., HASLETT, C., GOVAN, J. R., GREGORY, C. D., SALLENAVE, J. M. & SIMPSON, A. J. 2009. Trappin-2 promotes early clearance of Pseudomonas aeruginosa through CD14-dependent macrophage activation and neutrophil recruitment. *Am J Pathol,* 174**,** 1338-46.

WILKINSON, T. S., ROGHANIAN, A., SIMPSON, A. J. & SALLENAVE, J. M. 2011. WAP domain proteins as modulators of mucosal immunity. *Biochem Soc Trans,* 39**,** 1409-15.

WILLIAMS, S. E., BROWN, T. I., ROGHANIAN, A. & SALLENAVE, J. M. 2006. SLPI and elafin: one glove, many fingers. *Clin Sci (Lond),* 110**,** 21-35.

WILLIMSKY, G. & BLANKENSTEIN, T. 2005. Sporadic immunogenic tumours avoid destruction by inducing T-cell tolerance. *Nature,* 437**,** 141-6.

WILLIMSKY, G., CZEH, M., LODDENKEMPER, C., GELLERMANN, J., SCHMIDT, K., WUST, P., STEIN, H. & BLANKENSTEIN, T. 2008. Immunogenicity of premalignant lesions is the primary cause of general cytotoxic T lymphocyte unresponsiveness. *J Exp Med,* 205**,** 1687-700.

WILSON, B. J., SAAB, K. R., MA, J., SCHATTON, T., PUTZ, P., ZHAN, Q., MURPHY, G. F., GASSER, M., WAAGA-GASSER, A. M., FRANK, N. Y. & FRANK, M. H. 2014. ABCB5 maintains melanoma-initiating cells through a proinflammatory cytokine signaling circuit. *Cancer Res,* 74**,** 4196-207.

WILSON, N. J., BONIFACE, K., CHAN, J. R., MCKENZIE, B. S., BLUMENSCHEIN, W. M., MATTSON, J. D., BASHAM, B., SMITH, K., CHEN, T., MOREL, F., LECRON, J. C., KASTELEIN, R. A., CUA, D. J., MCCLANAHAN, T. K., BOWMAN, E. P. & DE WAAL MALEFYT, R. 2007. Development, cytokine profile and function of human interleukin 17-producing helper T cells. *Nat Immunol,* 8**,** 950-7.

WOO, E. Y., CHU, C. S., GOLETZ, T. J., SCHLIENGER, K., YEH, H., COUKOS, G., RUBIN, S. C., KAISER, L. R. & JUNE, C. H. 2001. Regulatory CD4(+)CD25(+)

T cells in tumors from patients with early-stage non-small cell lung cancer and late-stage ovarian cancer. *Cancer Res,* 61**,** 4766-72.

XU, W., HE, B., CHIU, A., CHADBURN, A., SHAN, M., BULDYS, M., DING, A., KNOWLES, D. M., SANTINI, P. A. & CERUTTI, A. 2007. Epithelial cells trigger frontline immunoglobulin class switching through a pathway regulated by the inhibitor SLPI. *Nat Immunol,* 8**,** 294-303.

XU, Y., ZHANG, M., RAMOS, C. A., DURETT, A., LIU, E., DAKHOVA, O., LIU, H., CREIGHTON, C. J., GEE, A. P., HESLOP, H. E., ROONEY, C. M., SAVOLDO, B. & DOTTI, G. 2014. Closely related T-memory stem cells correlate with in vivo expansion of CAR.CD19-T cells and are preserved by IL-7 and IL-15. *Blood,* 123**,** 3750-9.

YAACOB, N. S., NASIR, R. & NORAZMI, M. N. 2013. Influence of 17beta-estradiol on 15-deoxy-delta12,14 prostaglandin J2 -induced apoptosis in MCF-7 and MDA-MB-231 cells. *Asian Pac J Cancer Prev,* 14**,** 6761-7.

YANG, F., STRAND, D. W. & ROWLEY, D. R. 2008. Fibroblast growth factor-2 mediates transforming growth factor-beta action in prostate cancer reactive stroma. *Oncogene,* 27**,** 450-9.

YANG, L., PANG, Y. & MOSES, H. L. 2010. TGF-beta and immune cells: an important regulatory axis in the tumor microenvironment and progression. *Trends Immunol,* 31**,** 220-7.

YE, J., LIVERGOOD, R. S. & PENG, G. 2013. The role and regulation of human Th17 cells in tumor immunity. *Am J Pathol,* 182**,** 10-20.

YEE, C., SAVAGE, P. A., LEE, P. P., DAVIS, M. M. & GREENBERG, P. D. 1999. Isolation of high avidity melanoma-reactive CTL from heterogeneous populations using peptide-MHC tetramers. *J Immunol,* 162**,** 2227-34.

YIGIT, R., MASSUGER, L. F., FIGDOR, C. G. & TORENSMA, R. 2010. Ovarian cancer creates a suppressive microenvironment to escape immune elimination. *Gynecol Oncol,* 117**,** 366-72.

YOSHIDA, N., EGAMI, H., YAMASHITA, J., TAKAI, E., TAMORI, Y., FUJINO, N., KITAOKA, M., SCHALKWIJK, J. & OGAWA, M. 2002. Immunohistochemical expression of SKALP/elafin in squamous cell carcinoma of human lung. *Oncol Rep,* 9**,** 495-501.

YOUNG, M. R., WRIGHT, M. A., MATTHEWS, J. P., MALIK, I. & PRECHEL, M. 1996. Suppression of T cell proliferation by tumor-induced granulocyte-macrophage progenitor cells producing transforming growth factor-beta and nitric oxide. *J Immunol,* 156**,** 1916-22.

YU, K. S., JO, J. Y., KIM, S. J., LEE, Y., BAE, J. H., CHUNG, Y. H. & KOH, S. S. 2011. Epigenetic regulation of the transcription factor Foxa2 directs differential elafin expression in melanocytes and melanoma cells. *Biochem Biophys Res Commun,* 408**,** 160-6.

YU, K. S., LEE, Y., KIM, C. M., PARK, E. C., CHOI, J., LIM, D. S., CHUNG, Y. H. & KOH, S. S. 2010. The protease inhibitor, elafin, induces p53-dependent apoptosis in human melanoma cells. *Int J Cancer,* 127**,** 1308-20.

YU, P., LEE, Y., LIU, W., KRAUSZ, T., CHONG, A., SCHREIBER, H. & FU, Y. X. 2005. Intratumor depletion of CD4+ cells unmasks tumor immunogenicity leading to the rejection of late-stage tumors. *J Exp Med,* 201**,** 779-91.

YU, P., STEEL, J. C., ZHANG, M., MORRIS, J. C., WAITZ, R., FASSO, M., ALLISON, J. P. & WALDMANN, T. A. 2012. Simultaneous inhibition of two regulatory T-cell subsets enhanced Interleukin-15 efficacy in a prostate tumor model. *Proc Natl Acad Sci U S A,* 109**,** 6187-92.

YU, S. Q., LAI, K. P., XIA, S. J., CHANG, H. C., CHANG, C. & YEH, S. 2009. The diverse and contrasting effects of using human prostate cancer cell lines to study androgen receptor roles in prostate cancer. *Asian J Androl,* 11**,** 39-48.

ZANI, M. L., TANGA, A., SAIDI, A., SERRANO, H., DALLET-CHOISY, S., BARANGER, K. & MOREAU, T. 2011. SLPI and trappin-2 as therapeutic agents to target

airway serine proteases in inflammatory lung diseases: current and future directions. *Biochem Soc Trans,* 39**,** 1441-6.

ZHANG, D., SIMMEN, R. C., MICHEL, F. J., ZHAO, G., VALE-CRUZ, D. & SIMMEN, F. A. 2002. Secretory leukocyte protease inhibitor mediates proliferation of human endometrial epithelial cells by positive and negative regulation of growth-associated genes. *J Biol Chem,* 277**,** 29999-30009.

ZHANG, M., ZOU, Z., MAASS, N. & SAGER, R. 1995. Differential expression of elafin in human normal mammary epithelial cells and carcinomas is regulated at the transcriptional level. *Cancer Res,* 55**,** 2537-41.

ZHANG, Q., YANG, X. J., KUNDU, S. D., PINS, M., JAVONOVIC, B., MEYER, R., KIM, S. J., GREENBERG, N. M., KUZEL, T., MEAGHER, R., GUO, Y. & LEE, C. 2006. Blockade of transforming growth factor-{beta} signaling in tumor-reactive CD8(+) T cells activates the antitumor immune response cycle. *Mol Cancer Ther,* 5**,** 1733-43.

ZHU, J., NATHAN, C., JIN, W., SIM, D., ASHCROFT, G. S., WAHL, S. M., LACOMIS, L., ERDJUMENT-BROMAGE, H., TEMPST, P., WRIGHT, C. D. & DING, A. 2002. Conversion of proepithelin to epithelins: roles of SLPI and elastase in host defense and wound repair. *Cell,* 111**,** 867-78.

ZIOGAS, A. C., GAVALAS, N. G., TSIATAS, M., TSITSILONIS, O., POLITI, E., TERPOS, E., RODOLAKIS, A., VLAHOS, G., THOMAKOS, N., HAIDOPOULOS, D., ANTSAKLIS, A., DIMOPOULOS, M. A. & BAMIAS, A. 2012. VEGF directly suppresses activation of T cells from ovarian cancer patients and healthy individuals via VEGF receptor Type 2. *Int J Cancer,* 130**,** 857-64.

ZOU, W., MACHELON, V., COULOMB-L'HERMIN, A., BORVAK, J., NOME, F., ISAEVA, T., WEI, S., KRZYSIEK, R., DURAND-GASSELIN, I., GORDON, A., PUSTILNIK, T., CURIEL, D. T., GALANAUD, P., CAPRON, F., EMILIE, D. & CURIEL, T. J. 2001. Stromal-derived factor-1 in human tumors recruits and alters the function of plasmacytoid precursor dendritic cells. *Nat Med,* 7**,** 1339-46.

ZWIRNER, N. W. & DOMAICA, C. I. 2010. Cytokine regulation of natural killer cell effector functions. *Biofactors,* 36**,** 274-88.